Studies Towards Enhanced Fastness of Ink Jet Dyes

David John Benstead

A thesis submitted for the degree of

Doctor of Philosophy

University of Edinburgh

September 2005

For My Parents

Abstract

A series of magenta azo dyes for use in inkjet printers have been synthesised in order to study the effects of substituted arylhydrazide substituents on their light and ozone fastness. Large-scale syntheses were successfully adapted to the laboratory and arylhydrazides were coupled to an existing azo dye *via* a cyanuric chloride coupling reaction in good yield and purity.

Improved methodologies were developed for the synthesis of a series *N*-methylhydrazides, *N,N'*-dimethylhydrazides and *N'*-isopropylhydrazides. *N*-methylhydrazides were synthesised by reaction of methylhydrazine with an appropriate acid chloride. Improvements in yield, purity and ease of work-up were made over existing methods. *N,N'*-dimethylhydrazides were synthesised from *N*-methylhydrazides, avoiding the use of the carcinogenic dimethylhydrazine employed in previous syntheses. Synthesis was *via* a reductive amination strategy employing previously unreported *N*-methyl, *N'*-methylidene arylhydrazides, followed by reduction with sodium cyanoborohydride. *N'*-isopropylhydrazides were also prepared *via* reductive amination, following condensation of commercially available hydrazides with propanone, again followed by reduction with sodium borohydride. The newly synthesises dyes were tested at Avecia (Blackley) for light and ozone fastness according to standard protocols. The *N*-methylhydrazide series of dyes showed slightly improved ozone fastness, light fastness was essentially unchanged across the range of dyes.

Solution ozonolysis experiments were carried out on simple dye systems, such as 1-phenylazo-2-naphthol and 1-phenylazo-4-naphthol. In order to study the effects of

azo / hydrazone tautomerism, some of the "locked" tautomers of these compounds were synthesised by methylation of the appropriate functional group. The rates of ozonolysis were studied and attempts were made to determine the breakdown pathway of the dyes by LC-MS experiments. It was shown that the main intermediate formed was naphthoquinone. Solution ozonolysis was also performed on some of the more complex hydrazide substituted dyes previously synthesised and the rates of ozonolysis determined.

Acknowledgements

I would like to thank first and foremost Dr Alison Hulme and Professor Hamish McNab for their invaluable support and advice throughout my PhD, especially the time they took out to check, pass comment and give advice on this document. I would also like to thank Dr Paul Wight of Avecia (Blackley) for his help and advice during my time in Manchester. I thank also all those who made my time there an enjoyable one, particularly Rachael, Sarfraz, Neil, Tomas, Martin and everyone else.

I thank my parents and family for their love and invaluable support, without which this thesis could not have been written.

My gratitude goes to John Miller and Stuart Wharton for their training on the running of NMR spectra, Stuart Johnstone for his glassware blowing skills, Stuart Mains for his help in various pieces of fabrication and Robert Smith for LC-MS training and advice.

Thanks to all those in the Hulme and McNab groups, past and present, who have helped me, humoured me, kept it Scotch and kept me sane.

Last but not least, thank you Tina, without whom the last year would have been a darker place.

Abbreviations

AcOH	acetic acid
ANSI	American National Standards Institute
Aq.	aqueous
COSY	COrrelation SpectroscopY
Da	Daltons
DCM	dichloromethane
DME	dimethyl ethylene glycol
DMF	*N,N*-dimethylformamide
DMAP	4-dimethylaminopyridine
DMSO	dimethylsulfoxide
nOe	nuclear Overhauser effect
NOESY	Nuclear Overhauser Effect SpectroscopY
EI	Electron Impact mass spectrometry
ESI	ElectroSpray Ionisation mass spectrometry
Et_3N	triethylamine
EtOAc	ethyl acetate
Eq.	equivalents
FAB	Fast Atom Bombardment mass spectrometry
HPLC	High Performance Liquid Chromatography
HRMS	High Resolution Mass Spectrometry
HSQC	Heteronuclear Single-Quantum Coherence
Hz	Hertz
i.d.	internal diameter
IPA	iso-propyl alcohol
IR	Infra Red
M	mol dm^{-3}
Me	methyl
m.p.	melting point
NMR	Nuclear Magnetic Resonance
o.d.	outer diameter

PEEK	PolyEtherEtherKetone
ppm	parts per million
R_f	retention factor
RT	room temperature
R_t	HPLC retention time
S	Siemens
sat.	saturated
T.l.c.	thin layer chromatography
w/v	percentage weight by volume
w/w	percentage weight by weight

Table of Contents

1 Introduction

1.1 Ink jet technology

From beginnings in the latter part of the 19th century, when Lord Rayleigh first investigated hydrodynamics and the process by which a liquid stream breaks up into droplets,[1] ink jet printing has now been described as the leading non-impact printing technology of today.[2]

Ink jet printing has largely replaced impact printing technologies, such as typewriters, daisy wheel and dot matrix printers, in the home and office markets.[3] This is largely due to its simplicity, cost-effectiveness and the ability to produce full-colour, high quality prints. The only serious commercial rival to ink jet printing is the laser printer, which is most suited to printing text and is much less flexible and more costly.

Ink jet printing is also employed in a wide range of commercial applications, utilising its unique ability to print on uneven or rough surfaces, from printing directly onto packaging on the production line to printing colour filters used in flat screen displays.[3]

There are now two main classes of ink jet printing technology, continuous and drop-on-demand (DOD). The fundamental difference between the two is that in continuous ink jet a constant stream of ink droplets is produced; in DOD a droplet of ink is only formed of it is required to make the image. Continuous technology, in its most basic form, is simpler than DOD, however DOD has marked advantages. Today, the majority of activity in ink jet printing is in DOD methods.[4]

1.1.1 Continuous Ink jet Technology

The first practical device based on Rayleigh's theories was the Mingograph, developed by Siemens in 1951.[5] This continuous ink jet system was developed as a chart recorder for analogue signals, and was unable to print characters or images. In 1965,[6] Sweet demonstrated that by applying a pressure wave to an ink reservoir containing an orifice, a stream of ink droplets of uniform size and spacing could be formed. These droplets could then be provided with an electronic charge and deflected in an electromagnetic field to form the desired character.

At around the same time, Hertz independently developed a similar continuous ink jet system based on ink deflection methods.[7] This system had the additional ability to modulate ink-flow, allowing it to produce grey-scale prints. This was achieved by controlling the number of drops used to form each pixel, thereby allowing darker or lighter shades of grey to be printed.

Continuous ink jet printers fall into two main types, binary- and multiple-deflection devices. In binary-deflection printers, only certain drops are charged, and the charged ink is directed through an electrostatic field onto the medium. Uncharged ink is allowed to fall into the gutter channel (Figure 1.1).

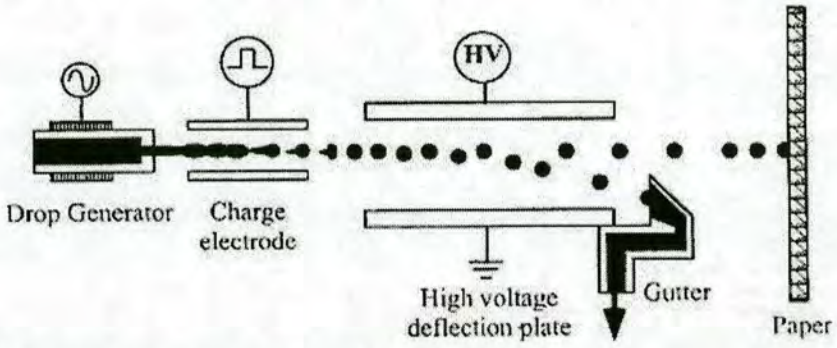

Figure 1.1 Binary Deflection Technology[4]

In multiple-deflection systems, all drops are provided with a varying charge and deflected onto the paper at different levels, allowing a swathe of drops to be printed from a single head. Uncharged drops are again passed into a gutter (Figure 1.2).

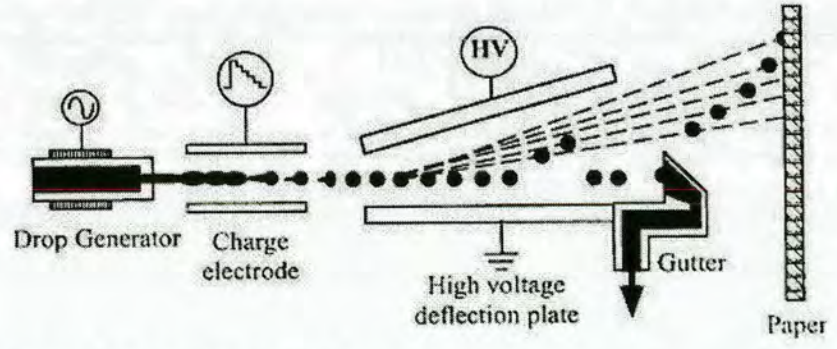

Figure 1.2 Multiple Deflection Technology [4]

Although continuous ink jet technology is effective, the wasted ink impacts on the economy of the system. This is easily overcome by recycling the unused ink,

however this creates problems such as solvent evaporation. Other problems include the need to charge and deflect the ink in a controlled manner, and also the distance the ink must travel before striking the medium. Today, continuous ink jet technology is generally employed in commercial systems, such as printing onto packaging or in very large format printing, where precision printing is not required.

1.1.2 Drop-on-Demand Ink jet Technology

DOD printing technology differs from continuous ink jet in that an ink droplet is only formed if it is required to make the image, thus eliminating ink wastage. The ink is ejected from the printhead directly onto the page, bypassing the need for charging / deflection hardware and ink recirculation. The printhead is also positioned as close to the printing media as possible, meaning the ink drop has less distance to travel than in continuous methods.

Of the four major DOD technologies that currently exist (thermal, piezoelectric, acoustic and electrostatic) thermal and piezoelectric are by far the most important.[4] The first example of a DOD system was piezoelectric, developed in 1972.[8] This system was based on a piezoelectric crystal contained in an ink chamber (Figure 1.3). When a voltage is applied to the crystal, causing it to deform, the resultant pressure wave expels the ink from the chamber through an orifice.

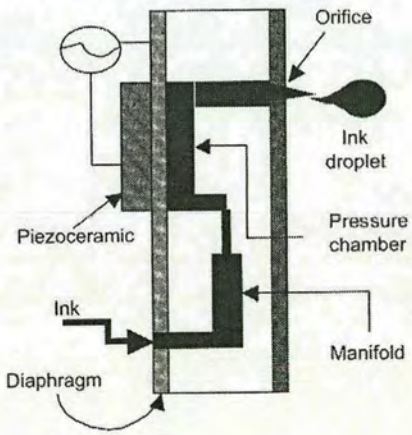

Figure 1.3 Piezoelectric DOD [9]

The second type of DOD system was developed by Canon in 1979.[10] It was reportedly discovered by accident when a researcher brought a soldering iron into contact with a syringe of ink. The resultant bubble in the syringe forced a drop of ink from the needle. From this observation, Bubble Jet technology was developed. At around the same time, Hewlett-Packard was also developing a DOD system based on heat, the Thermal Ink jet system (Figure 1.4).

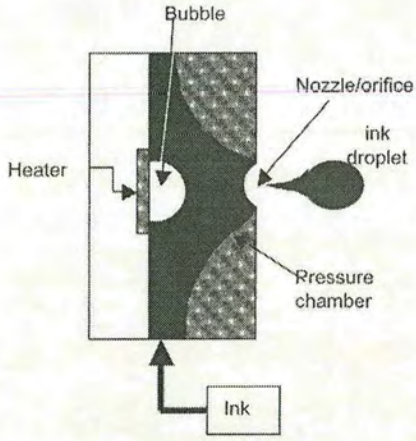

Figure 1.4 Thermal DOD [9]

A short pulse of current (<5 μs) applied to a thin film resistor heats the aqueous ink to form a small bubble. As the bubble expands, exerting pressure in the chamber, a super-fine droplet of ink is ejected from the nozzle. A vacuum is formed when the bubble collapses, drawing more ink into the chamber (Figure 1.5).[3, 11]

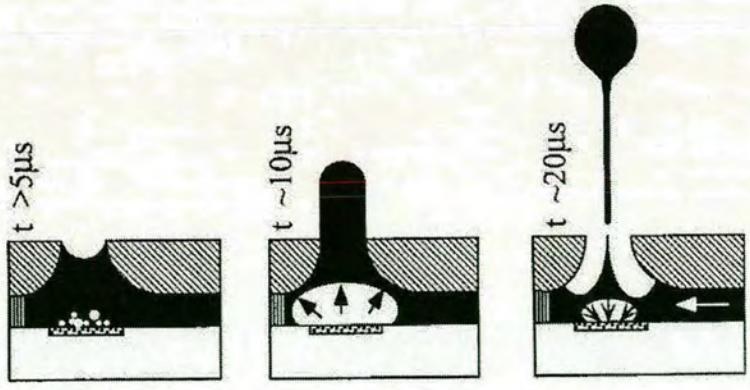

Figure 1.5 Formation of a bubble in thermal DOD systems [3]

The bubble of steam can quickly condense, allowing the entire process to be completed within ~100 μs in a highly repeatable manner. The image shown in Figure 1.6 was made by illuminating droplets formed in this way with an LED that was pulsed at the droplet generation frequency. The exposure time of the camera was ~1 s, so that the image represents thousands of drops superimposed on each other. The extremely clear image of the droplets demonstrates the repeatability of the process.[12]

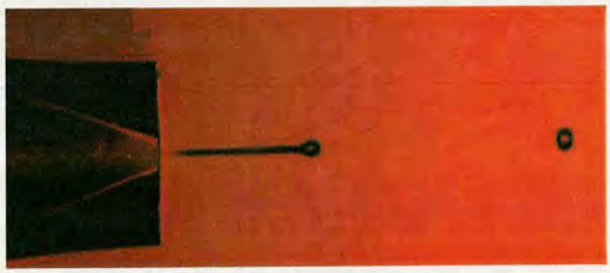

Figure 1.6 DOD device generating drops at 4 kHz [12]

1.2 Developments

Although the principles behind ink jet printing have changed little over the years, the pace of development has increased markedly. These developments have been concerned with many aspects of the process. Electronics and machining advances have improved printhead design, allowing much smaller droplets of ink to be used, improving resolution. The medium onto which the image is printed has also been the subject of much scrutiny, with the development of paper coatings improving image quality (*e.g.* organic polymers, such as polyvinyl alcohol and inorganic oxides, such as SiO_2 and TiO_2). The majority of research has, perhaps, been focussed on the ink itself. An indication of this can be found in the worldwide patent records.[13] A CAS SciFinder search reveals that in the year 1974 just 6 patents relating to ink jet inks were filed. This had increased to 133 in the year 1984, and to 669 in the year 2001.

One of the main reasons behind this surge in research is the home computer. Ink jet technology is extremely competitive when compared with its rivals (such as laser printing) both in terms of cost-effectiveness and versatility. With the advent of digital photography, the need for accurate reprographics has become paramount.

Modern digital cameras are capable of capturing high quality images, and are able to rival traditional wet-film photography in terms of image definition. This has resulted in the need for technologies that can reproduce this image in hard copy with accuracy comparable to silver halide prints. This has been made possible by the development of inks used in printing.

1.3 Inks in Ink jet Printing

The three most common inks in ink jet printing are aqueous, solvent and hot-melt inks.[9, 14] DOD printers generally use aqueous inks, whereas continuous printers tend to employ solvent or hot-melt inks.[9]

1.3.1 Aqueous Inks

The anionic dyes which are mainly used in DOD printing were originally sourced from existing industries such as food and textile dying. These dyes tended to be highly water soluble, and so most early ink jet inks were water based. Aqueous inks also have the advantage that the solvent is safe and cheap. Water does have disadvantages, however, in that it can promote the growth of bacteria and fungi, and cause corrosion.[9, 14] These problems can be minimised by the use of additives, such as corrosion inhibitors and bactericides, and will be discussed later in this chapter.

1.3.2 Solvent Inks

Solvent inks are used in preference to aqueous inks when printing on hydrophobic substrates such as plastics or metals, or where fast drying times are required. There are relatively few solvent-soluble colourants, and so the use of solvent inks is limited. The main application of solvent inks is in large character printing in an industrial environment, where only one colour is required, usually black. Common solvents are ketones, such as methyl ethyl ketone (MEK).[9] These are often highly flammable and so there has been a shift towards less hazardous alcohol-based inks. There are also toxicity problems with some ink solvents. Generally speaking, solvent-based inks fulfil the criteria for industrial applications, but have little use in the home or office market.

1.3.3 Hot-melt Inks

Hot-melt inks are solid at ambient temperatures. In a thermal DOD system, when they are heated in the ink chamber they become liquid and are ejected from the print head. Typical melting points for hot-melt inks are in the range of 60-125 °C. A series of aryl sulphonamide inks has been patented by Howtek,[15] whilst Exxon[16, 17] has patented a range of fatty (C_{18} - C_{24}) alcohols and carboxylic acids. Hot-melt inks have the potential to produce extremely good quality results, but are still limited in application.

This project is concerned with dyes used in aqueous inks, specifically magenta anionic azo compounds. The properties of these inks, the origins of their colour and their structures will form the remainder of this introduction.

1.4 Properties of Aqueous Inks

1.4.1 Aqueous Ink Formulation

Aqueous inks used in ink jet printing are formed from many components, all of which are required for an ink to perform well (Table 1.1).

Component	% Composition
Dye	~ 3 – 6 %
Water	~ 70 – 80 %
Humectant	~ 5 – 10 %
Surfactant	~ 1 %
Penetrant	~ 2 – 10 %

Table 1.1 Composition of a typical ink jet printing ink

Azo dyes are typically used in magenta inks in ink jet printing, as they are capable of great structural and chromogenic diversity. The other important classes of ink jet colourant are the phthalocyanines and anthroquinones. Anthroquinone dyes can give a range of hues, however they are most important as purple, blue or green dyes since they complement the yellow, orange and red hues available from azo dyes.[18]

As has been mentioned, aqueous solvent is well suited to ink jet applications. It is, however, not without drawbacks. It promotes corrosion, which can reduce the lifespan of the printer and cause insoluble metal salts to precipitate, blocking printhead nozzles; it is therefore important to use a pure dye and a pH that is compatible with the other ink additives and the print head. Chelating agents can be added to the ink to prevent the formation of precipitates. The pH is also important for dye solubility and stability. Sulfonic acid groups are generally used to confer water solubility to a dye in aqueous inks. They are generally superior to the carboxylic acid functionality in this respect and are usually present not as the free acid, but as a metal salt. Sodium is the conventional counterion in ink jet printing, although some dyes are used as the lithium, ammonium or potassium salt. Humectants are added to control water evaporation from the ink, preventing the ink from drying out and the dye crystallizing or crusting. They are water miscible, high boiling compounds such as diethylene glycol or *N*-methylpyrrolidone.[19] These cosolvents also affect the viscosity and specific gravity of the ink, which must be controlled for stable drop formation, as well as helping prevent bacterial growth.
The use of surfactants / penetrants lowers the surface tension of the ink droplet, allowing rapid penetration of the ink into the medium. An example of a penetrant would be pentane-1,5-diol and a surfactant Surfynol 465.[3]

1.4.2 Physical Properties

Physical properties such as viscosity, specific gravity and surface tension determine how the ink drops form as they are ejected from the print head. These are important so that the drop maintains its shape both in flight, and on impact with the paper, leading to well a defined print area.[9] They also determine the rate of ejection from the print head *i.e.* if the ink viscosity is too high it will be harder to release it from the nozzle.

1.4.3 Printing Properties

The medium onto which an image is printed plays a large role in the quality of the image, and it is possible to tailor an ink to suit a particular medium. The medium will affect the optical density of a dye, as well as influence other printing phenomena such as feathering and bleeding.[3] Feathering is where the ink runs in the fibre of the

page by capillary action. Bleeding is when the drop spreads on the surface of the paper and is controlled by the surface tension of the formulation. Inks with a low surface tension, known as penetrating inks, quickly diffuse into the paper with little lateral spread. This is important where different colours are printed adjacent to one another, where bleeding would blur the boundary between the colour blocks. Non-penetrating inks, *i.e.* those with a higher surface tension, do not diffuse into the paper, and are therefore prone to bleeding. They have a higher optical density however, and are used to print text, where colour-to-colour bleed is not an issue, but intense black characters are. The spreading must be uniform to ensure there is no distortion of the text. Also, with penetrating inks, care must be taken to ensure that the ink does not "strike-through" the paper.[9] Modern papers for ink jet images are often coated with a dye receiving layer. The two main types are swellable polymer and inorganic oxide coated papers. Swellable polymer papers are coated with organic polymers such as PVA and give glossy prints. The dye diffuses into the polymer as it is swelled by the ink, as the ink dries the dye is encapsulated within the receiving layer. Inorganic oxide papers, for example coated with SiO_2 or TiO_2, hold the ink within the porous structure of the oxide particle. They give good colour definition and a matte finish to the print.

1.5 Structure and Synthesis of Azo Dyes

Although there are many ways of synthesising azo compounds, commercial azo dyes are produced almost without exception by the azo coupling reaction.[3] This is a two-step reaction sequence in which an aromatic amine is diazotised (the diazo component) and reacted with an activated aromatic system (the coupling component). Common coupling components for the synthesis of useful azo dyes are shown in Figure 1.7 (H-acid **1**, J-acid **2**, γ-acid **3**). The positions indicated show the sites of azo coupling when the reacion is carried out under acidic or alkaline conditions.

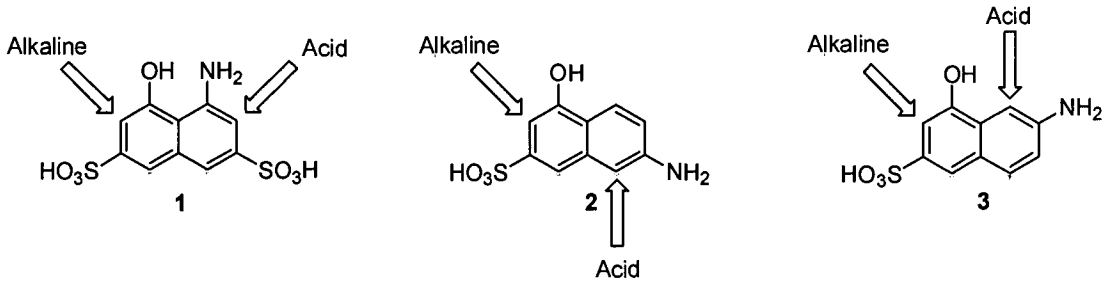

Figure 1.7 pH control of azo coupling regioselectivity

Azo dyes containing a single azo group are known as monoazo dyes, those containing two are known as disazo dyes, those with three trisazo dyes etc. Azo dyes rarely contain more than four azo groups.[20] The ability to control regioselectivity is particularly useful for the synthesis of unsymmetrical dis- and trisazo compounds *e.g.* acid black I **4**, derived from H-acid **1** (Figure 1.8).[21]

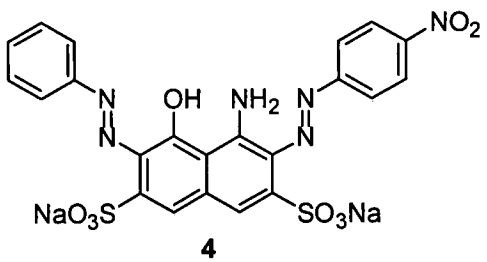

Figure 1.8 Acid black I

1.5.1 Azo/Hydrazone Tautomerism

Azo dyes in which the azo component is *ortho* or *para* to a phenol can exist in two tautomeric forms, the azo form or the hydrazone form. This was realised in 1884 by Zincke and Binderwald following the observation that the diazo coupling between aniline **5** and 1-naphthol **6** gave rise to the same product (4-phenylazo-2-naphthol **9**) as the condensation reaction between phenyl hydrazine **7** and 1,4-naphthoquinone **8** (Scheme 1.1).[22] It was therefore suggested that a tautomeric equilibrium between the azo and hydrazone products must exist.[23]

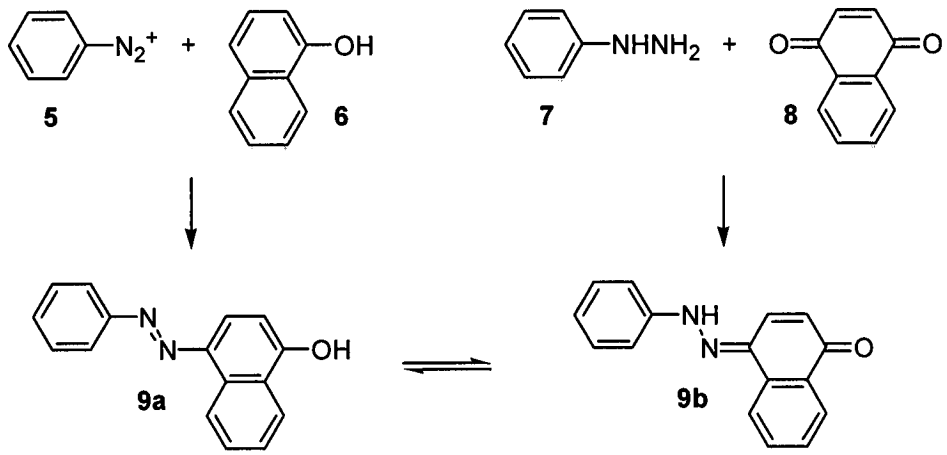

Scheme 1.1

The same azo / hydrazone tautomeric equilibria are present in 1-phenylazo-2-naphthol **10** and 2-phenylazo-1-naphthol **11**. 2-Phenylazo-3-naphthol **12** and 6-phenylazo-1-naphthol **13** exist only as azo structures, as the hydrazone tautomer requires complete disruption of aromaticity (Figure 1.9).

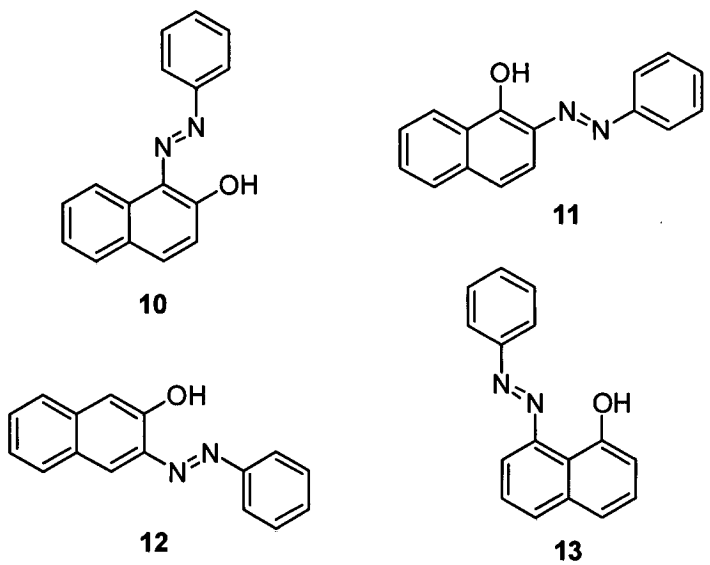

Figure 1.9 Phenylazonaphthols

The properties of a dye, including colour and fastness, vary depending on which tautomer predominates. The position of the tautomeric equilibrium is dependent on

many things, including solvent, pH and dye substitution. More polar solvents, such as water, formamide and acetic acid, favour the hydrazone form, whereas less polar solvents, such as pyridine, alcohols and hydrocarbons, favour the azo form.[24] If the dye has an *ortho* substituent in the phenyl ring capable of intramolecular hydrogen bonding then the hydrazone form will predominate, to the extent that tautomerism is often insensitive to changes in pH or solvent. This makes *ortho*-substituted azo dyes highly attractive as commercial colourants, as their properties are generally stable and predictable.[21]

1.6 Dyes and Colour

1.6.1 The Origin of Colour in Dyes

A molecule will appear to be coloured if it absorbs electromagnetic radiation in the visible range (~ 400 – 700 nm). This absorption promotes an electron from the ground state (HOMO), to a higher, unoccupied orbital (LUMO). The energy difference between these two orbitals determines the colour, and depends on the structure of the molecule.[21] Structurally, dyes are conjugated systems that consist of a chromophore and auxochromes *e.g.* acid red 4 (**14**).

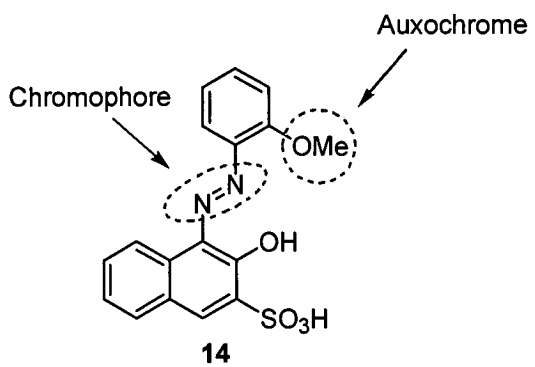

14

Figure 1.10 **Acid red 4, showing examples of a chromophore and auxochrome**

A chromophore is a group that has an absorbance in the UV or visible range of the electromagnetic spectrum. Often the chromophore absorbs in the UV region, and the

compound appears weakly coloured. An example of this is the azo group, but could also include nitro, methine or carbonyl groups. To shift the absorption band into the visible region an auxochrome is employed. These functional groups are conjugatively linked to the chromophore and influence the colour of the compound by affecting the energy transition responsible. They are generally groups containing oxygen, nitrogen or a halogen; common examples are the amino and hydroxy groups. The shift observed is termed bathochromic if it causes the absorbance to shift to a longer wavelength (known as a red shift) or hypsochromic if it causes the absorbance to shift to a shorter wavelength (known as a blue shift).

1.6.2 Dye Structure and Colour Correlation

The chromophore / auxochrome theory on the colour of dyes was proposed in 1876,[25] where it was thought the chromophore was principally responsible for the colour, and the auxochrome provided an "enhancement". The terms still find use today, although their roles have been more rigorously defined. Two important refinements to the theory were made, one by Hewitt and Mitchell in 1907, which recognised the role of conjugation in the colour of a dye, and the other in 1928 by Dilthey and Wizinger,[26] that chromophores are commonly electron-withdrawing groups and auxochromes are electron-donating groups.

It was observed that a bathochromic shift could be induced by increasing either the electron-withdrawing power of the chromophore; the electron donating-power of the auxochrome; or the length of conjugation. From these observations came the donor / acceptor model of a dye **15** (Figure 1.11).

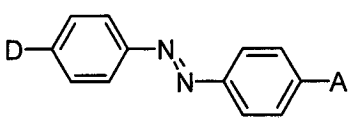

15

Figure 1.11 **Donor / acceptor model of a chromogen**

Most azo dyes are based on this structure, and the principle can be applied to many chromophores, including azo, carbonyl, methine and nitro. By increasing the strength of the donor (electron-donating, D) or acceptor (electron-withdrawing, A) a

bathochromic shift can be effected.[21] These principles are demonstrated in a more advanced description of the colour properties of a dye, the valence bond approach.

1.6.3 The Valence Bond Approach to Colour

The valence bond, or resonance, approach to colour proposes that the lowest energy canonical forms of a molecule (for instance resonance within a phenyl ring) and the higher energy forms (*e.g.* charge-separated states) approximate the ground state and first photoexcited state of the molecule respectively. The energy difference between these states predicts that the colour will vary as the energy gap varies, in accordance with Planck's relationship ($\Delta E = hc / \lambda$), where the energy gap has an inverse relationship to wavelength of light absorbed. Thus, a decrease in the difference in energy levels will produce a bathochromic shift of the λ_{max}, demonstrated in the following series of azobenzene derivatives (Table 1.2):

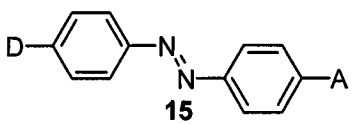

15

Compound	A	D	λ_{max} / nm in EtOH
16	H	H	320
17	NO_2	H	332
18	H	NH_2	385
19	H	NMe_2	407
20	H	NEt_2	415
21	NO_2	NEt_2	486

Table 1.2 Absorbances of some azobenzenes[21]

Azobenzene **16** is weakly coloured, its absorption lying mainly in the UV range. This is due to the high energy of its next lowest energy canonical form **16a** (Scheme 1.2).

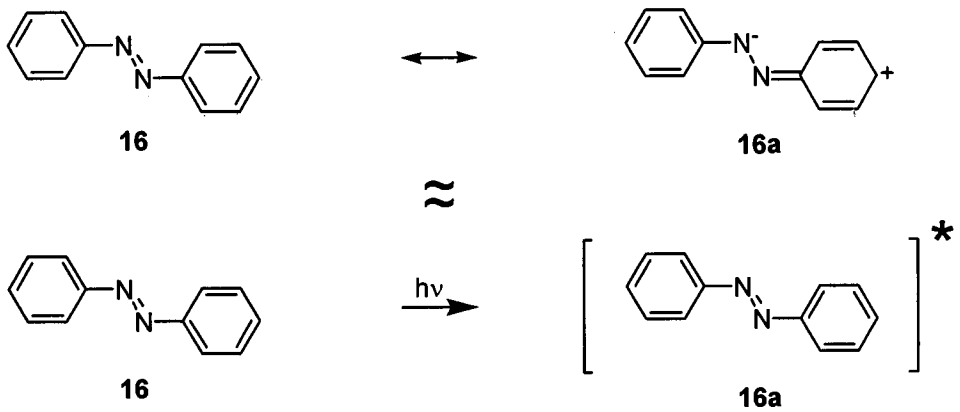

Scheme 1.2

The negative charge resides on nitrogen and is relatively stable, however the presence of the carbocation destabilises this resonance form and thus the large energy gap gives a short λ_{max}.

The addition of a nitro group (**17**) stabilises the excited state by providing an extra resonance form **17a** and delocalising the negative charge onto oxygen **17b**, giving a bathochromic shift (*i.e.* a lowering in energy of the transition, Scheme 1.3).

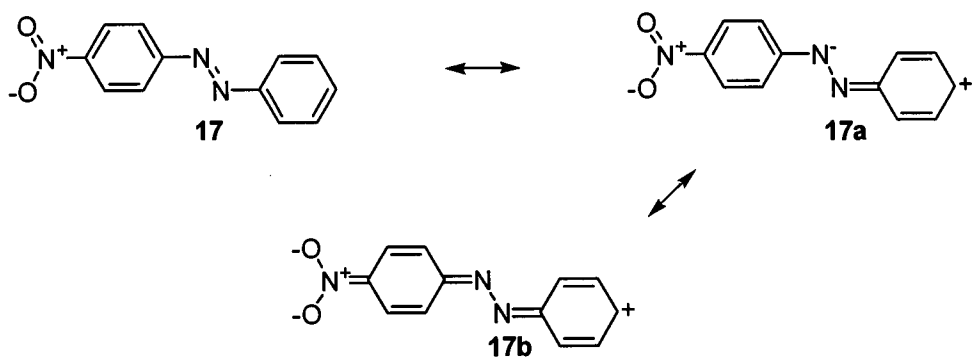

Scheme 1.3

When an electron donating group is added (**20**) a large bathochromic shift is observed. This is due to the removal of the carbocationic centre, with the positive charge residing on nitrogen **20a** (Scheme 1.4)

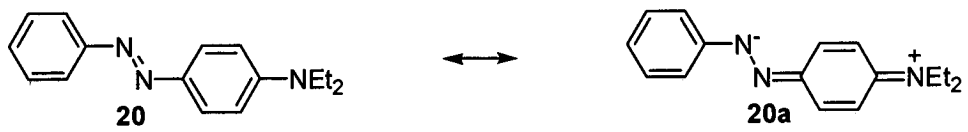

Scheme 1.4

When these effects are combined (**21**), the increase in charge stabilisation, resonance forms and conjugation produces a significant bathochromic shift (Scheme 1.5).

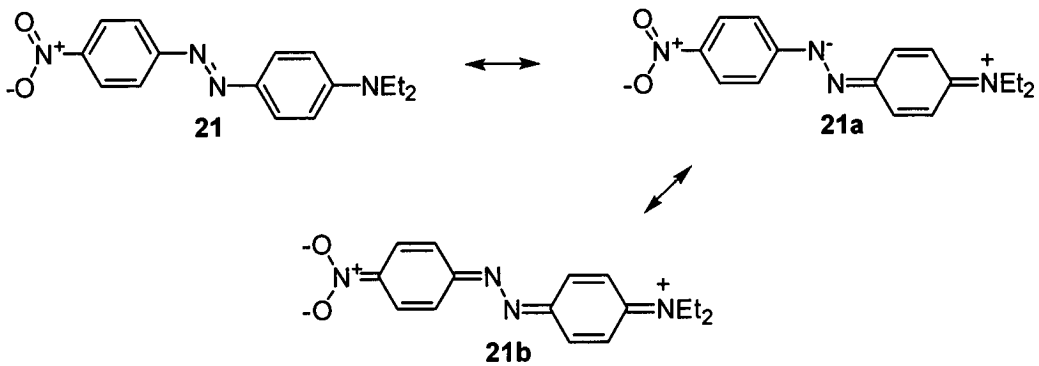

Scheme 1.5

Valence bond theory is generally successful in predicting relative λ_{max} values, although there are some cases where it fails to predict correctly the observed shift. This is particularly true where steric interactions are involved. For instance the λ_{max} of **21**, where the electron-withdrawing nitro group is in the *para*-position, is 486 nm. If the nitro-group is in the *ortho*-position (**22**), however, the λ_{max} is 462 nm. Based on electronic arguments alone, the two isomers would be expected to have similar absorption characteristics. If the structure of **22** is considered, however, it can be seen that the *o*-nitro group has a destabilising steric interaction with one of the azo nitrogen atoms (Scheme 1.6).

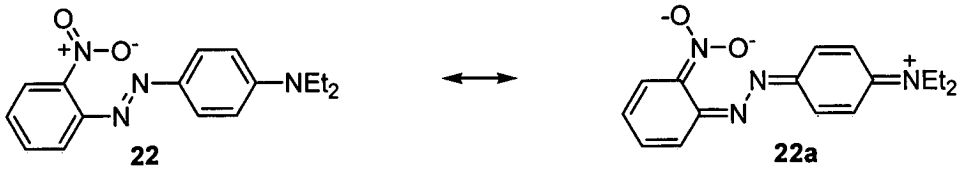

22 **22a**

Scheme 1.6

This forces the molecule to adopt a non-planar conformation by rotation about the C-N bond of the nitro or azo group. However, in the first excited state this bond has a higher bond order than in the ground state and it is energetically disfavourable to rotate about it. This raises the energy of the first excited state, resulting in a hypsochromic shift relative to the planar **21b**. If electron-withdrawing substituents in the *ortho*-position are required it is common to employ the cyano group, since its linear shape minimises steric interactions.

Large bathochromic shifts may be observed by replacing the acceptor phenyl ring with an aromatic heterocycle. This, combined with the other principles, is demonstrated in **23** (Figure 1.12), the first azo dye to have a λ_{max} in the near-infrared region of the spectrum (806 nm in DMSO).[27] The donor / acceptor rings are extremely electron rich/deficient respectively and there is extensive conjugation throughout the system.

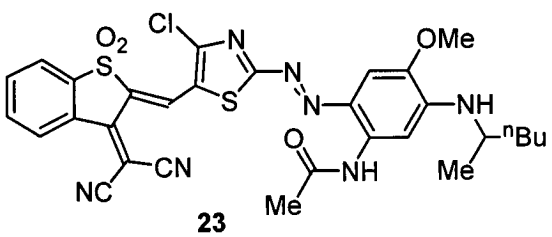

23

Figure 1.12[27]

Valence bond theory can be used to explain qualitatively the relative λ_{max} of many dyes. It is poor at describing quantitatively the colour of a hypothetical dye, however. This limitation is being overcome by rigorous molecular-orbital (MO) theory calculations, with some success. It is now possible to predict the λ_{max}, as well as the position of the azo / hydrazone equilibrium, of some dyes using computational methods.[28-30]

1.6.4 The Theory of Colour

In basic colour theory there are three additive primary colours (red, green and blue) and three subtractive primary colours (yellow, magenta and cyan). The additive and subtractive primaries are called complementary colours because of the paired relationship in which each subtractive colour absorbs its complementary one-third of the white light spectrum (Figure 1.13) *i.e.* on white paper, cyan is the complementary colour of red as it will absorb red light, allowing green and blue light to be reflected and the colour cyan observed. To create blue, both cyan and magenta dyes must be used, which will absorb red and green light respectively, allowing only the reflected blue light to be observed.

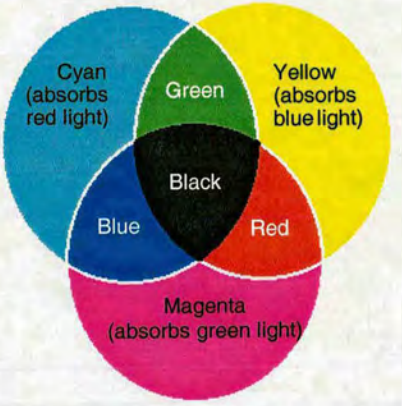

Figure 1.13 Complementary colours

Theoretically, every colour can be made by a combination of the three subtractive primary colours. In practice this is not possible, however, as a dye will always absorb some colours it should reflect and *vice versa*. In order to produce a full colour gamut (range), the three subtractive primary colours are required, cyan, magenta and yellow along with black.

1.6.5 Colour properties of aqueous dyes

The apparent colour of a dye to an observer is not merely a matter of the λ_{max} value, but encompasses other factors. These include the λ_{max} (which affects the absolute

colour), but also the shape of the absorption curve.[31] Secondary absorptions also affect the colour of the dye. Bright dyes should have sharp, narrow curves, as shown in Figure 1.14.[9] These are required to produce a comprehensive colour gamut.

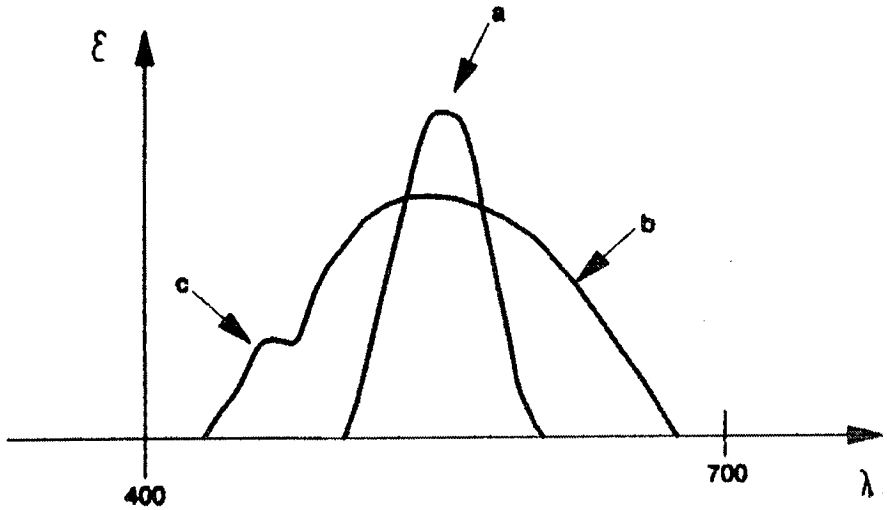

Figure 1.14 **Absorption curves of (a) a bright, ideal magenta dye and (b) a duller, non-ideal magenta dye having unwanted secondary absorptions (c)**

Bright dyes can be made duller by adding a secondary colour such as black, but dull dyes cannot be made brighter. Any functionalisation of a dye *e.g.* in order to improve fastness, must take this into account. The inherent tinctorial strength (the area under the absorption curve, a measure of intensity) of the dye should be as high as possible, for several reasons. The first is so that prints have high optical density, an obviously attractive feature; the second is that if the dye has high tinctorial strength, it can be used in lower concentrations in the final ink formulation. The advantages of this are two-fold. The first is the obvious economic benefit, and the second is that a lower dye concentration means that there is less chance of the dye precipitating and more potential for additives, giving more flexibility to the ink formulation.

1.6.6 Colour Description

The perception of colour by individuals is highly subjective, and as such it is necessary to define an objective framework around which colours can be judged.

This is known as a colour space, and there are now several colour space standards in use. The artist Albert H. Munsell developed one of the first in 1905. It was based on human perception, where the colour was compared visually to charts in the Munsell Colour Book. This was developed into a series of international standards by the CIE (Commission Internationale de l'Eclairage) following extensive research into human colour vision and the generation of a "standard observer". The CIE standards provided a repeatable, device-independent system by which colour could be measured.[32]

The first of these was the CIEYxy (Figure 1.15), a colour space that represented the ability of the standard observer to see different amounts of the three additive primaries (red, green and blue). The colour space appears skewed due to the ability of the eye to observe changes from red to blue more than yellow to green.[33]

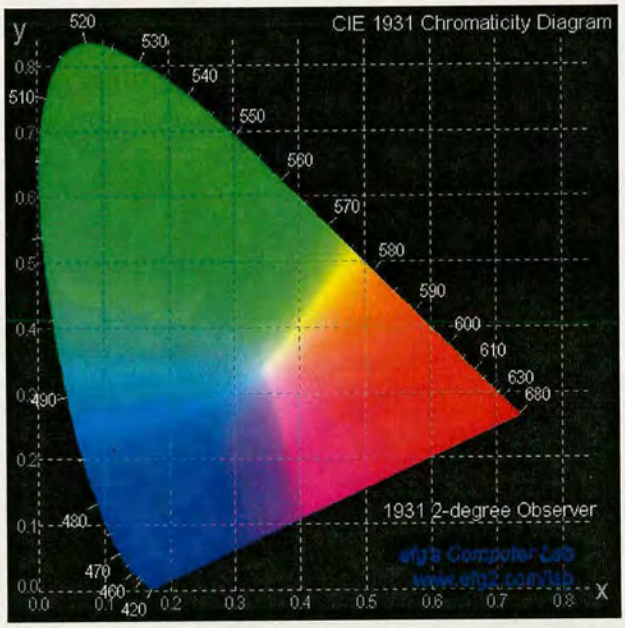

Figure 1.15 CIEYxy colour space[32]

The CIEYxy was developed into the CIELab colour space (Figure 1.16). This was based on the fact that a colour can be neither yellow and blue, nor red and green at the same time, and allowed a colour to be described in terms of three angular coordinates:

L – a measure of lightness (0 black to 100 white)

a – a measure of redness (positive a) or greenness (negative a)

b – a measure of yellowness (positive b) or blueness (negative b)

For neutral colours (white, grey and black) the a and b values approach zero, the higher the a or b value, the more saturated the colour is.[32]

An alternative description of colour space employs polar coordinates, known as CIELch (Figure 1.16).

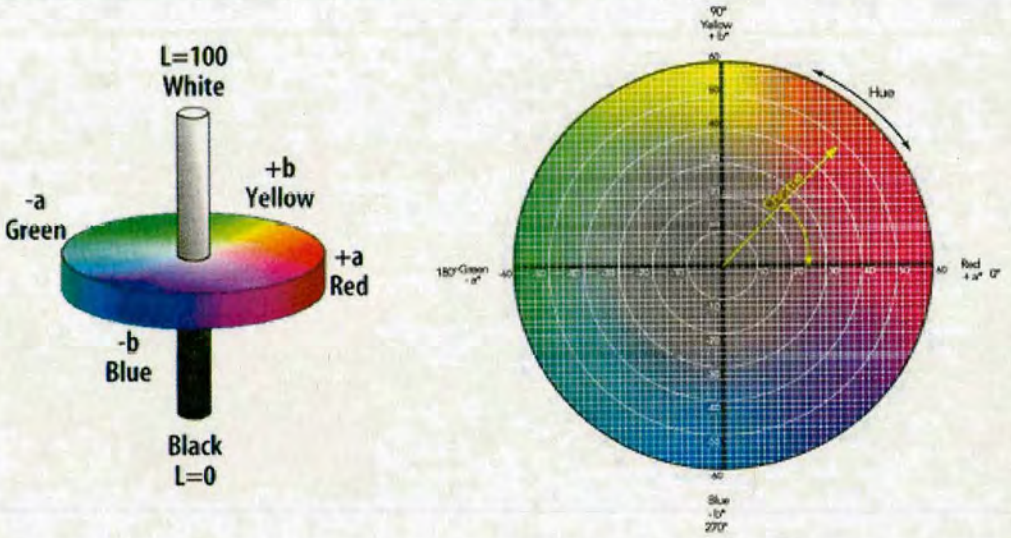

Figure 1.16 CIELab and Lch colour space[32]

CIELch measures colour in terms of lightness (L), chroma (c) and hue (h). The hue can be considered as the absolute colour (*i.e.* red, orange etc.), measured in polar coordinates with the origin being pure red (as seen by the standard observer). Chroma is the distance from the neutral colour and is a measure of saturation or intensity, *i.e.* red and pink would have a similar hue value but a different chroma. L is again on a scale of 0 – 100 from black to white as in Lab colour space.[32]

1.6.7 Colour Measurement

There are three main colour measurement devices available: densitometers; colourimeters; and spectrophotometers. These photoelectric devices measure how

much of a known amount of incident light is reflected from a substrate. Densitometers simply measure the amount of light reflected from a substrate to give a colour density. A colourimeter breaks down the light into its RGB components, similar to the human eye. These components can then be translated into a colour measurement using colour space, *e.g.* CIELab etc. A spectrophotometer is the most sophisticated and accurate measuring device, as it measures full spectral data. This can be converted into density or colour space coordinates with simple calculations.[34]

1.7 Fastness Properties of Dyes

Dye fastness refers to the ability of a dye to resist some detrimental process, be it smearing if a print becomes wet or fading due to degradation of the chromophore through exposure to light or pollutants.[21]

Dyes fade to varying degrees when in contact with the atmosphere, the media and components within the ink. A dye that fades quickly is obviously unsatisfactory, and the colour images which are produced through ink jet printing are required to have excellent stability.[35]

The understanding of the controlling mechanisms of fading is somewhat limited, although certain trends and guidelines have been useful in developing correlations with dye structure.[35]

1.7.1 Water Fastness

One of the first developments required of dyes used in ink jet printing was water fastness. This refers generally to the ability of the dye not to smudge if the paper becomes wet, or is handled by a person with wet hands. Water fastness can be enhanced either individually or by a combination of two ways: the smelling salts (ammonium carbonate) principle and differential solubility.[3] Ammonium carbonate is unstable and decomposes to give its gaseous components, ammonia, carbon dioxide and water vapour. It is possible to utilise this phenomenon to confer a degree of water fastness to a dye by changing the counterion from a metal salt to an ammonium salt. By changing the sulfonic acid groups of the dye (which enhance water solubility) to carboxylic acid groups, the ammonium carboxylate salt is formed. This is soluble in water (*i.e.* the ink formulation). When printing, however,

the salt decomposes to liberate ammonia and the free acid, which should be water insoluble (Scheme 4).

$$Dye{-}CO_2^-NH_4^+ \longrightarrow Dye{-}CO_2H + \uparrow NH_3$$

Scheme 1.7

This is not an ideal solution, as the decomposition is not instant (and can take several hours for completion), and the process produces ammonia, which has obvious consequences in a confined environment such as an office.

Another approach to water fastness is the concept of differential solubility.[14] This is where a dye is used which has high solubility in the ink, which is usually slightly alkaline, and low solubility on the paper, which is usually slightly acidic. By funtionalising a dye with groups which have a pK_a of around 7, it is possible to make the dye highly soluble in the alkaline ink, where the group will be in its ionised form (conferring water solubility). On the paper, however, the dye will exist in the nonionised form, making the dye less water-soluble. Two substituents used for this purpose are carboxy (CO_2H) and hydroxy (OH) moieties. A group at Avecia replaced two of the sulfonic acid groups in CI Food Black II **24** with carboxylic acid groups to produce a dye with enhanced water fastness properties **25** (Figure 1.17).[11]

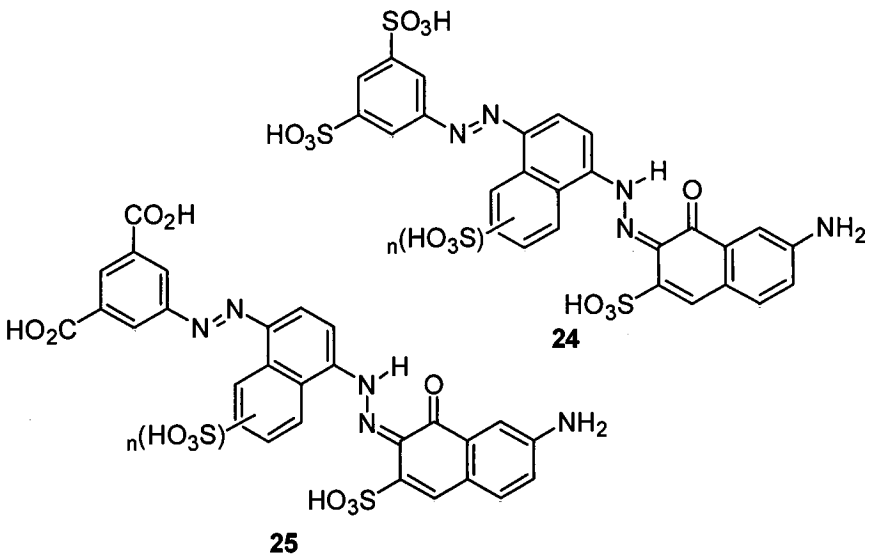

Figure 1.17 **CI Food Black II before 24 and after modification 25 (n=0 or 1)**

The ideal system for conferring water fastness would obviously be instantaneous, 100% fast, with no loss of colour properties. A promising approach is the use of a combination of zwitterion formation and stereochemistry (Scheme 1.8).[3]

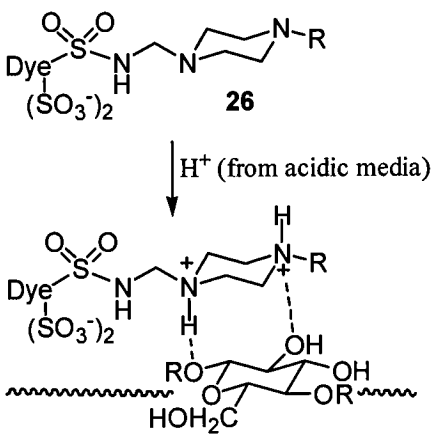

Scheme 1.8

Sulfonamide linkers are used to attach piperazino groups to a dye to give **26**. In the (alkaline) ink, the dye is soluble due to the sulfonate and free amino groups. On the acidic paper, the dye is waterfast because of zwitterion formation between the protonated amino groups and the sulfonate groups. This renders the dye insoluble,

and the strong hydrogen bond interactions between the dye and the cellulose of the paper are further enhanced by the stereochemical fit

1.7.2 Light Fastness

Light fastness is perhaps one of the main priorities of dye chemists, and it is one of the principal factors that influence the longevity of a printed image. It is generally accepted that it is the chromophore that is most susceptible to light ageing, but it has long been known that the nature and position of substituents significantly affects the light ageing properties of a dye. [36, 37]

In general, electron-withdrawing groups in the aryl ring improve light fastness of arylazonaphthol dyes; electron-donating groups decrease light fastness.[38] For instance, addition of hydroxy and amino groups (*i.e.* electron-donating groups) to the diazo component reduces the light fastness of azo dyes. Methylation of the hydroxy group reduces light fastness further, whereas acetylation or benzoylation reduces the effect.[39] Too many electron-withdrawing groups may dramatically reduce the light fastness of a dye, however.[40] It has also been observed in disazo systems that addition of sulfonic acid groups to the coupling component decreases light stability, the opposite effect being observed when they are added to the diazo component.[41]

When a dye absorbs a photon, it is excited to a higher energy singlet state (S_1). It can then either return to the ground state (S_0) directly, resulting in fluorescence, or *via* inter system crossing (ISC) to the triplet state (T_1), resulting in phosphorescence (Figure 1.18).

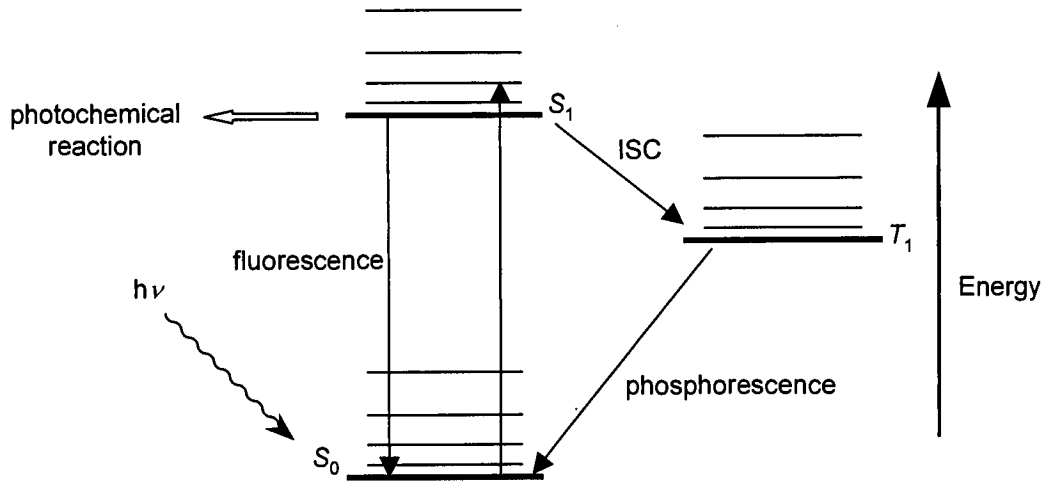

Figure 1.18 **Processes by which an excited molecule can return to the ground state**

The energy can also be lost *via* photochemical reaction with, for example, another dye molecule. Oxidative fading mechanisms can be caused by direct photoreaction of the dye *i.e.* from the excited state, or indirect, caused by another photoexcited molecule *e.g.* singlet oxygen.[35, 42]

In azo dyes, the hydrazone tautomer is thought to be responsible for the fading characteristics of the dye, since dyes that are predominantly in the hydrazone form show poorer light fastness than those that are predominantly in the azo form.[42] The postulated mechanism involves an initial attack by singlet oxygen on the hydrazone form **9b** (Scheme 1.9). This is supported by plots of (log) fading rate versus the Hammett σ constants for a variety of aromatic azo compounds, which show a straight line with a negative slope, indicating an oxidative mechanism.[35]

Singlet oxygen can arise from sensitisation of ground state triplet oxygen by a dye in an excited state, although other molecules can also lead to sensitisation. The reactive singlet oxygen then participates in a thermally allowed 6π Ene reaction to give peroxide **27**, which then decomposes to give 1,4-naphthoquinone **8** and benzenediazonium salt **5**.[35]

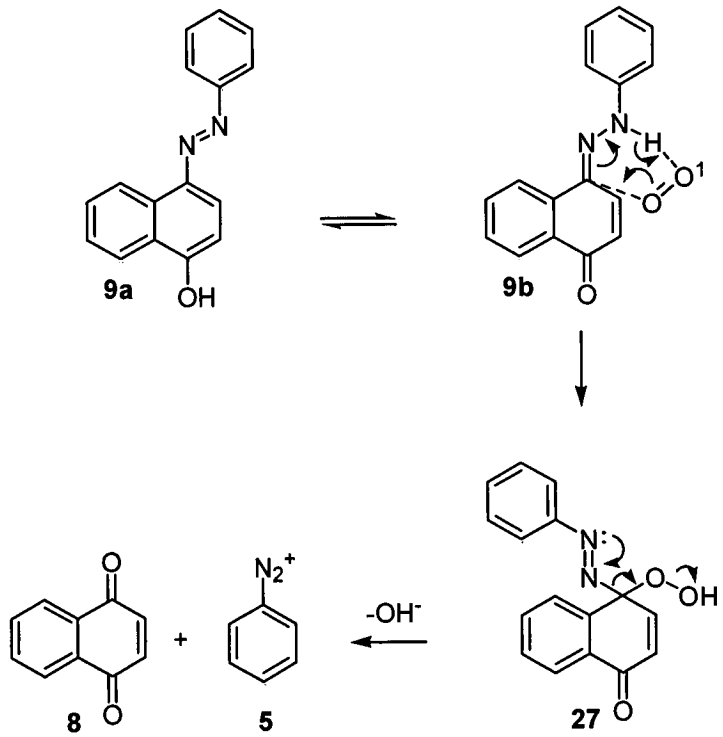

Scheme 1.9

1,4-Naphthoquinone has been observed experimentally following photodegradation, as has the coupling product of the diazonium salt **5** and the starting 4-phenylazo-1-naphthol **9**. Further observations that support this mechanism are: singlet oxygen produced non-photolytically produces similar results; singlet oxygen sensitisers promote fading / quenchers suppress fading and *O*-methylation of the phenylazonaphthol, thereby preventing formation of the hydrazone tautomer, reduces fading.[35]

Recent work has shown that it is possible to incorporate into a dye molecule substrates that act either to scavenge reactive oxygen species or absorb the UV light, without affecting the chromophore.[43] The compounds that were tested were generally naphthalene based aromatic esters, acting as both UV and singlet oxygen quenchers. Each showed improved fastness properties over the parent dye.

Dyes can also fade *via* a reductive mechanism, either in the absence of oxygen or in the presence of oxygen and a reductive species capable of promoting reduction of the azo dye. This mechanism is less well understood, although there has been some experimental evidence that the mechanism proceeds *via* radical formation.[35]

1.7.3 Pollutant Fastness

The fading of dyes and pigments by gaseous pollutants has been recognised for some time. It was thought until the 1950s that oxides of nitrogen caused the observed fading. In one study, textiles coloured with a blue anthroquinone dye known to be resistant to NO_x fading were examined, in ambient conditions and in the absence of light. Some of the textiles still showed fading, and so it was postulated that some hitherto unknown agent was causing the degradation. Three studies in the early 1970s showed conclusively that ozone was responsible for the fading of the anthroquinone dye.[44-46]

Ozone is present throughout the lower atmosphere, with a large peak in concentration in the stratosphere, known as the ozone layer. Ozone is also found in small quantities in the troposphere (ground-level atmosphere). It is present naturally, and in an unpolluted atmosphere self-governing photolytic reactions between NO, NO_2 and O_3 govern the level of ozone present (Scheme 1.10).

$$NO + O_3 \longrightarrow NO_2 + O_2 \quad (1)$$

$$NO_2 + h\nu \longrightarrow NO + O \quad (2)$$

$$O + O_2 \longrightarrow O_3 (+ M) \quad (3)$$

Scheme 1.10

Under normal atmospheric conditions the background level of ozone is only a few ppb and there is no net loss or gain of any of the components. When other reactions occur which supplement the available NO_2 for reaction (2), ozone levels can increase. These processes are complex, involving other NO_x gases, organic compounds and radicals, mainly produced by industrial processes.[47] It is estimated that northern hemisphere background ozone concentration level is 30 ppb, although the level frequently approaches 100 ppb in susceptible areas.[48]

Workers at Avecia (Blackley) have recently observed that the results of laboratory tests on the photostability of their azo dyes do not correlate with results observed "in the field".[49] Ozone was thought to be a prime candidate for this failure in reciprocity, as areas where images were seen to be less stable correlated with high

levels of tropospheric ozone. Relatively little work has been done examining the ozone stability of dyes used in printing systems, or the prints themselves. However, ozone is commonly used at dye works to decolourise wastewaters. This means that most investigations of the reaction of azo dyes with ozone tend to examine kinetics, modifications in reactor design or the addition of catalysts to improve the decolourisation process.[50] Work on mechanistic aspects suggests that, in the case of azo dyes, it is the hydrazone tautomer which is involved in the degradation, similar to the photooxidation reaction (Scheme 1.11).[51] It was found that the model system studied was broken down into simple aryl structures and compounds derived from the ozonolysis of 1,4-naphthoquinone. The nitrogen of the azo group is lost as molecular nitrogen, probably *via* decomposition of a diazonium salt intermediate **5**.

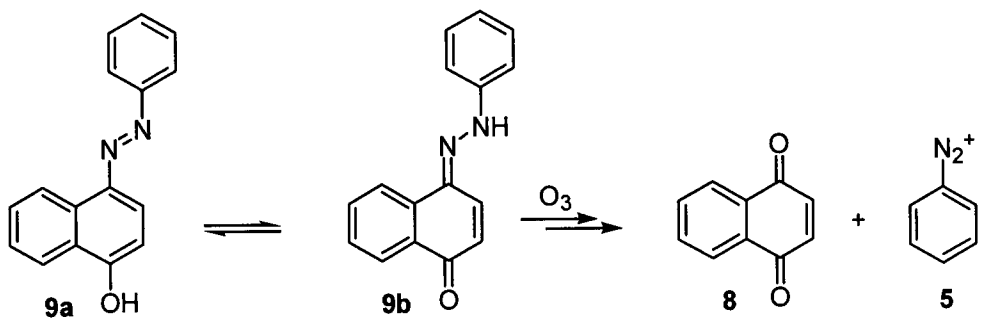

Scheme 1.11

A more in-depth analysis of the mechanisms and substituent effects proposed for the reaction of ozone with azo dye systems will be presented in Chapter 5.2.

Investigations into dye fastness by workers at Avecia (Blackley) showed that dyes functionalised with a hydrazide moiety appeared to have improved fading properties. The mechanism by which this protection was afforded was not understood, however, and so a study was required into the nature of the effect of the hydrazide. This report details the synthesis, characterisation, light and ozone fastness properties of hydrazide substituted dyes. Investigations have also be carried out into the reaction of ozone with simple phenylazonaphthol dyes, in order to better understand the mechanism of ozonolysis and possible means of improving fastness properties.

2 Hydrazides

Hydrazides, also known as acyl hydrazines or aza peptides, are an old class of compound, first mentioned in 1850.[52]

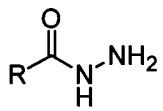

28

Figure 2.1 General structure of hydrazides

They have the general structure **28**, the two possible nitrogen substitution positions making them interesting targets for regioselective synthesis. This potential for multiple and diverse substitution has lead to much interest in the synthesis of both substituted and unsubstituted hydrazides

Hydrazides find utility as precursors and intermediates in many fields, such as pharmaceuticals, heterocyclic synthesis, polymers, dyestuffs and photographic products.[53] Cyclic and acyclic hydrazides are known to exhibit chemiluminescence upon oxidation.[54] Hydrazides can also be used as peptidomimetics, where a nitrogen atom replaces the α-carbon atom, as they do not significantly affect the conformation of the peptide, and are less susceptible to enzymatic cleavage (Figure 2.2).[55]

Peptide Azapeptide

Figure 2.2 Comparison of classical peptides and azapeptides

Recent uses of substituted hydrazides have been in applications such as: traceless linkers for solid-phase synthesis;[56] the synthesis of fluorobutenoic acid hydrazide pesticides;[57] the synthesis of new androstane steroid derivatives;[58] and as intermediates in the synthesis of antimycobacterials.[59] The synthesis and applications of di- and tri-substituted hydrazides have been reviewed.[60]

We believe that hydrazides can also be useful in improving the degradation fastness of azo dyes.[49] This chapter details the synthesis of *N*-symmetrically and *N*-

unsymetrically substituted hydrazides, which were coupled to an azo dye in order to investigate their effect on the light and ozone fastness properties of the dye. The hydrazides were coupled to a typical azo dye *via* a triazine linker, afforded by sequential condensations onto cyanuric chloride. The series of hydrazides chosen allowed analysis of electronic effects *via* Hammett relationships, and also the investigation of potential mechanistic pathways by the selective substitution of the hydrazide nitrogen atoms.

Since regioselective preparation of a range of hydrazides is required, a brief review of hydrazide syntheses is presented in the following sections.

2.1 Classic Synthesis

2.1.1 Reaction of a hydrazine with an ester

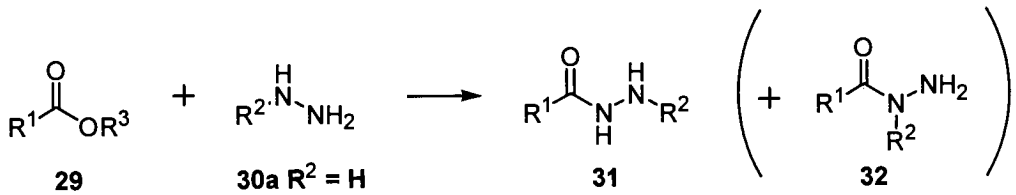

29 **30a** R^2 = H, **b** R^2 = Me, **c** R^2 = Ph **31** **32**

Scheme 2.1

Reactions of esters **29** with hydrazine **30a** (R^2 = H) readily give the corresponding hydrazide **31** (R^2 = H, Scheme 2.1).[61] The reaction is facile in ethanol or DMF, or in the absence of solvent,[62, 63] although some unreactive esters may require more forcing conditions.[64] In the case of substituted hydrazines **30** ($R^2 \neq$ H) there are two potential regioisomers, *N'*-substituted hydrazides **31** or *N*-substituted hydrazides **32**. With methylhydrazine **30b** (R^2 = Me), esters react regioselectively to give **31**. The ratio of **31** : **32** increases with increasing bulk of R^1, such that with very large R^1 substituents the reaction is highly regioselective and the amount of **32** is negligible.[53] The regiochemistry was proven by chemical analysis of the reaction product of methylhydrazine and methyl benzoate.[65] The product was isolated as the hydrochloride salt, and the regiochemistry demonstrated by the failure of the product to produce hydrazones with various aromatic aldehydes, and its cleavage to benzamide on refluxing with Raney nickel in ethanol. The reaction of

phenylhydrazine **30c** (R^2 = Ph) with esters of any size is highly regioselective for **31**. This is due to both steric effects and the electron withdrawing nature of the phenyl substituent, decreasing the nucleophilicity of the lone pair on the substituted nitrogen atom.[66]

1,1-Dimethylhydrazine **30d** is generally unreactive towards esters under standard conditions.[65] Addition of sodium methoxide yields the desired hydrazide in variable yield for a number of substituted aromatic esters.[67] 1,2-Dimethylhydrazine **30e** is essentially unreactive towards even activated esters.[68]

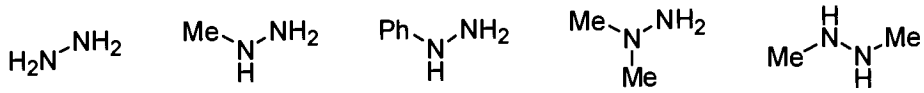

30a **30b** **30c** **30d** **30e**

Figure 2.3 Substituted hydrazines

2.1.2 Reaction of a hydrazine with acid chlorides or anhydrides

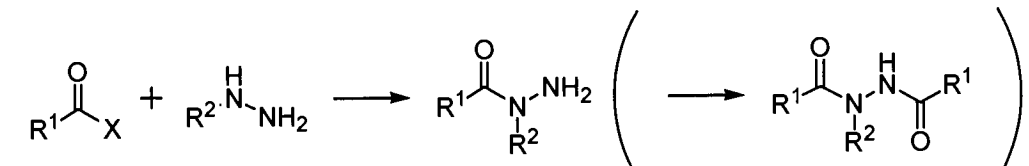

33a X = Cl **b X = OC(O)R** **30** **32** **34**

Scheme 2.2

The reaction of hydrazine **30a** with acid chlorides **33a** or anhydrides **33b** is generally extremely vigorous, with further reaction of the mono-acylhydrazide to yield the 1,2-diacyl product **34**.[61] This can be suppressed by diluting the reaction mixture or lowering the reaction temperature.[53] Hydrazides of unreactive hydrazines, such as 1,2-diphenylhydrazine, can be formed by reaction in pyridine[69] or in organic solvents in the presence of potassium carbonate.[70]

The reaction of unsymmetrically substituted hydrazines again presents regioselectivity issues. In the case of acylation using acid chlorides or anhydrides and alkyl substituted hydrazines, reaction takes place preferentially at the substituted nitrogen atom due to the electron-donating nature of the substituent.[65, 71] For example, methylhydrazine **30b** (R^2 = Me) reacts with benzoic anhydride **33b** (R = R^1 = Ph) to give benzoic acid *N*-methylhydrazide **32a** (R^1 = Ph; R^2 = Me).[65] The regiochemistry was again demonstrated by chemical means, based on the ability of

the product to form hydrazones with aromatic aldehydes.[65] As in the case of esters, phenylhydrazine **30c** (R^2 = Ph) reacts with the unsubstituted nitrogen atom due to the decreased nucleophilicity of the substituted nitrogen atom's lone-pair.[69]

2.1.3 Regioselectivity

The regioselectivity of the reaction of a hydrazine with either an ester or an acid chloride or anhydride has been rationalised in terms of the stability of the reactive intermediates.[72] The reaction of methylhydrazine **30b** (R^2 = Me) with acetic anhydride **33b** (R = R^1 = Me) and ethyl acetate **29a** (R^1 = Me; R^3 = Et) is taken as an example (Scheme 2.3 and 2.4).

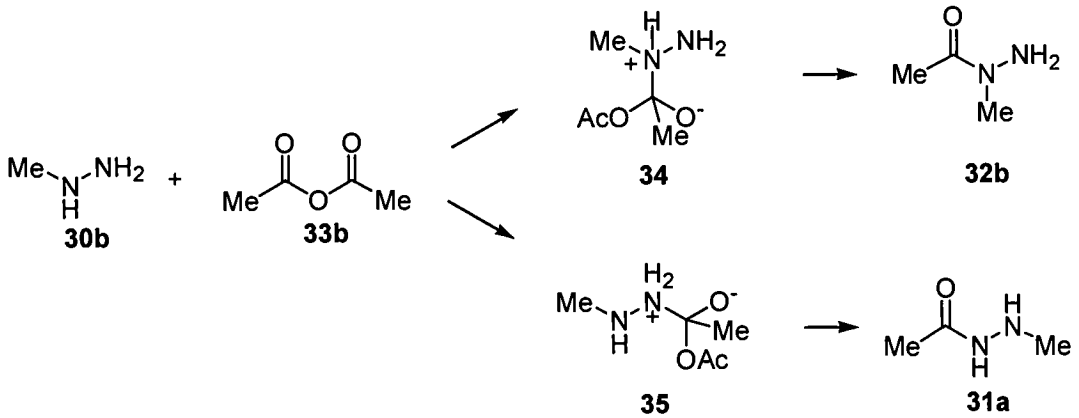

Scheme 2.3

In the reaction with acetic anhydride (Scheme 2.3), the positive charge on the nitrogen atom of **34** is stabilised by the inductive effect of the methyl group. No such stabilisation is afforded in intermediate **35**, increasing the activation energy and therefore the reaction proceeds rapidly to form **32b**.

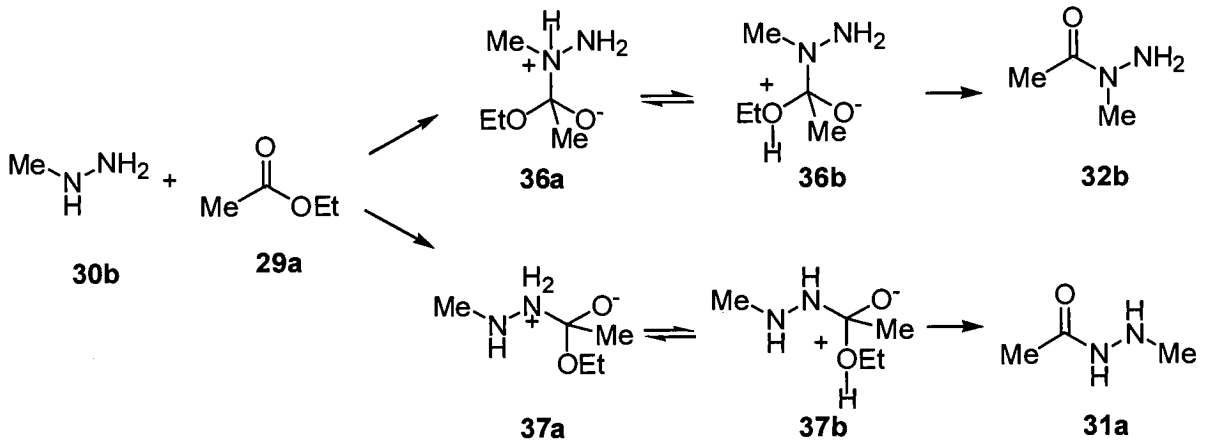

Scheme 2.4

In the case of the reaction with ethyl acetate (Scheme 2.4), it is more favourable for intermediates **36a** and **37a** to lose the weaker base, methylhydrazine, than ethoxide anion. They can rearrange by tautomerism to form **36b** and **37b**, which can then easily lose ethanol to form the products. Product **31a** is lower in energy than **32b** (since there is no unfavourable steric interaction between the methyl and acyl groups), and so it tends to be **31a** that is formed in greater yield (although a distribution of products is commonly observed).

2.2 Other Hydrazide Syntheses

The synthesis of hydrazides by other methods has principally been driven by a need for specific substitution patterns or to overcome the limitations of the previously described reactions, such as regioselectivity or the unreactivity of highly substituted hydrazines towards acyl electrophiles. A brief overview is given in the following sections.

2.2.1 Chloramination of amides

Chloramine has been shown to be a successful aminating agent for nucleophilic groups and its use has been applied to the synthesis of hydrazines, aminophosphine derivatives and, latterly, *N*-substituted hydrazides.[73] Addition of chloramine to the sodium salts of *N*-phenylbenzamide, *N*-phenylacetamide **38**, *N*-methylacetamide and *N*-ethylurethane afforded the respective *N*-substituted hydrazides in moderate to good yield (50 – 80%, Scheme 2.5).

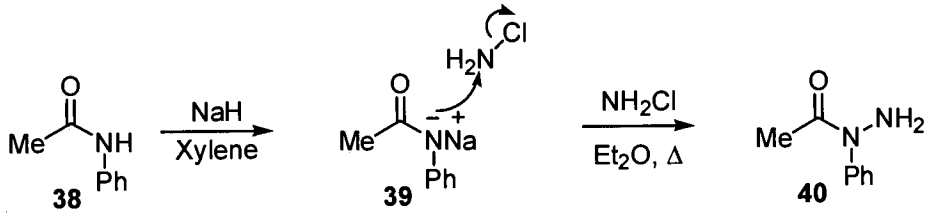

Scheme 2.5

This reaction is advantageous as it is regiospecific for *N*-substituted hydrazides, and allows ready access to otherwise troublesome *N*-phenylhydrazides.

2.2.2 Reduction and acylation of hydrazones

A "one-pot" procedure for the synthesis of tetra-substituted hydrazides using a two-step reduction / acylation strategy has been described. This is illustrated for the reaction of of 1,1-dimethylhydrazine **30d** and acetic acid **45** in Scheme 2.6.[74]

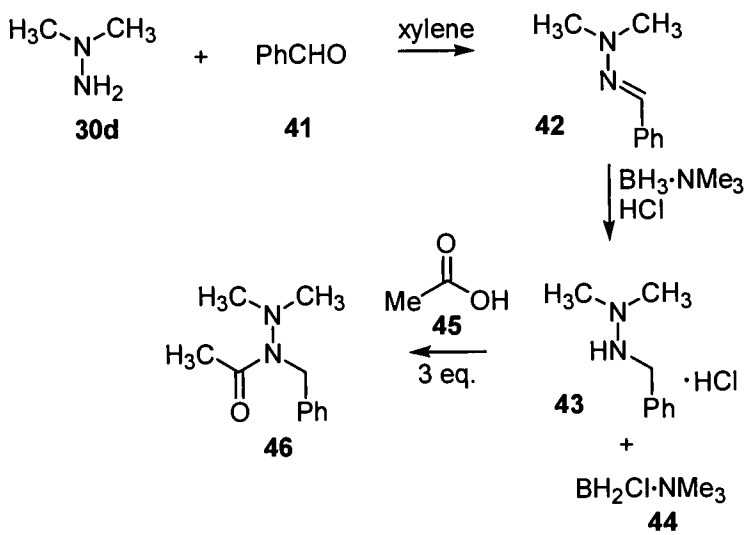

Scheme 2.6

The reaction mechanism is given in Scheme 2.7. The iminium ion **47** generated from condensation of an amine and an aldehyde is reduced by borane – trimethylamine complex. Chloroborane **45** generated in the reduction step then reacts the carboxylic acid **48** to generate the acyloxyborane species **49**, which then acylates the hydrazine hydrochloride intermediate **50** to give the hydrazide **51** (Scheme 2.7).

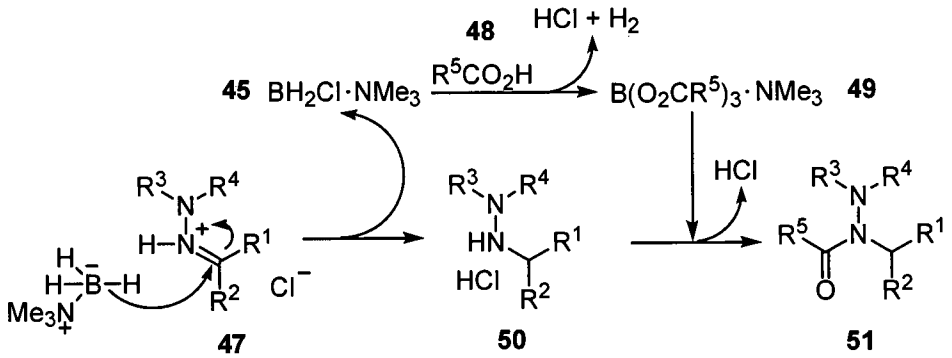

Scheme 2.7

A number of hydrazides were synthesised in moderate to excellent yield from a range of aryl, alkyl and heterocyclic aldehydes and alkyl and aryl carboxylic acids. The reaction conditions were generally tolerant of the nature of the substrate, although *ortho* substitution in aryl acid components showed a reduction in yield, presumably due to steric effects. The procedure was shown to be amenable to large-scale preparation, without isolation of intermediates, by synthesising hydrazide **46** on a multigram scale in 92% overall yield.

2.2.3 Microwave assisted carbonylation

N,N'-Diacylhydrazines can be synthesised *via* a microwave promoted palladium catalysed carbonylation reaction, utilising molybdenum hexacarbonyl as a source of CO (Scheme 2.8).[75]

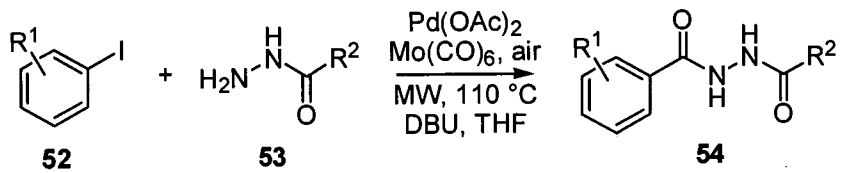

Scheme 2.8

The use of Boc-hydrazine **53** (R^2 = O^{t}Bu) allows the reaction to be used in the synthesis of Boc-protected arylhydrazides **54** (R^2 = O^{t}Bu). A variety of aryl iodides and hydrazides was coupled in variable yield (36 – 78%). Analysis by LC-MS indicated that the major side-products were benzamide and benzonitrile. The

absence of dehalogenated starting material suggested that the reactions went to completion but the products were unstable under the reaction conditions.

Use of Fu's phosphonium salt, $[(^tBu)_3PH]BF_4$,[76] and Herrmann's palladacycle as precatalyst[77] extended the scope of the reaction to include aryl bromides, although the attempted coupling of aryl chlorides was unsuccessful.

2.2.4 Reaction of esters with dimethylaluminium hydrazines

The previously reported difficulties in reacting hindered hydrazines with esters[65] can be overcome by converting the hydrazine **55** into the corresponding organoaluminium reagent **56** (Scheme 2.9),[66] in a synthesis based on the amide preparation of Weinreb *et al.*[78-80]

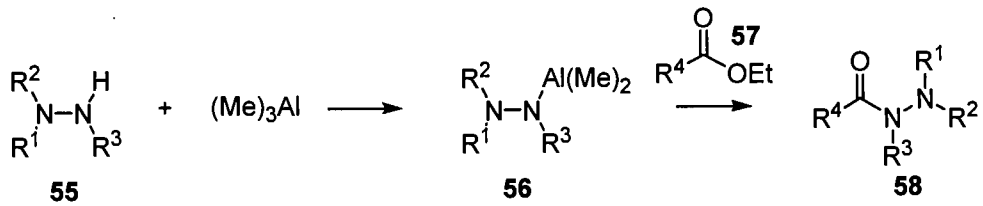

55 **56** **58**

Scheme 2.9

A variety of hydrazides are produced from 1,1-dimethylhydrazine, 1,2-dimethylhydrazine, phenylhydrazine and 2-hydrazinopyridine in good to excellent yield (71 – 92%) from alkyl, aryl and heteroaryl ethyl esters **57** to give hydrazides **58**. In the case of the unsymmetrical aryl hydrazines, reaction was at the unsubstituted nitrogen, presumably for the steric and electronic reasons discussed previously.

2.2.5 EDC coupling of activated carboxylic acids with hydrazines

Hydrazides make obvious and attractive targets for peptide coupling reactions, however they often provide low yields and difficult work-up.{Patterson, 1996 #94;Miyasaka, 1986 #95} These problems have recently been overcome by a new procedure{Zhang, 2002 #96} for the coupling of hydrazines with carboxylic acids using HOBt and EDC Scheme 2.10.

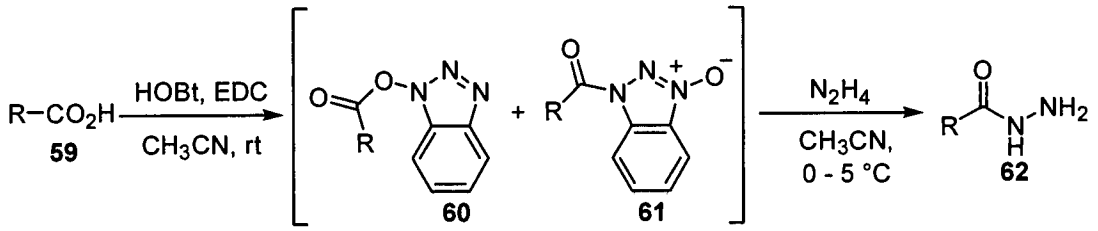

Scheme 2.10

The order in which the reactants were added was found to be of crucial importance. Addition of the hydrazine component before the coupling reagent led to a reduction in yield of around 30% and the formation of a number of side products. A range of saturated and unsaturated aliphatic hydrazides **62** was produced in excellent yield (> 90%) under mild conditions. Acids **59** with an α-chiral centre were successfully coupled without racemisation.

2.3 Synthesis of hydrazides

In order to study the effect of hydrazides on the fastness properties of azo dyes, aryl hydrazides with alkyl substituents in the *N*- and *N'*-positions (**63** and **65**), as well as *N,N'*-disubstituted hydrazides **64** will be synthesised. Each substitution series will be further functionalised with a series of electron-donating and -withdrawing substituents in the *para* position of the aryl ring (X = OMe **a**; Me **b**; H **c**; Cl **d**; NO_2 **e**) in order to carry out studies into the electronic nature of the reaction *via* Hammett correlations. Efficient synthetic routes to the following hydrazides will be demonstrated:

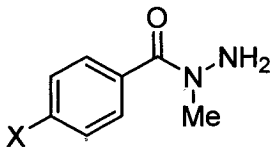
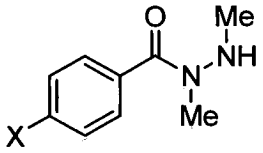
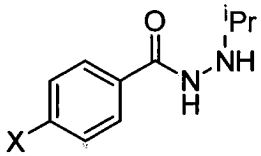

X = OMe	**63a**	**64a**	**65a**
X = Me	**63b**	**64b**	**65b**
X = H	**63c**	**64c**	**65c**
X = Cl	**63d**	**64d**	**65d**
X = NO_2	**63e**	**64e**	**65e**

2.3.1 *N*-methylhydrazides 63

Synthesis of *N*-methyl hydrazides **63** using the method described by Smith[67] produced the desired hydrazides in reasonable yield but low purity. The crude products were almost invariably oils (with the exception of *N*-methyl 4-nitrobenzoic acid hydrazide **63e**, which precipitated from the reaction mixture as a pale yellow powder). Standard distillation proved troublesome, as the pure product tended to crystallise in the condenser. The products were not amenable to column chromatography. The best purification procedure was by bulb-to-bulb distillation, requiring low pressures (< 0.1 mmHg) and modest temperatures (~50 – 100 °C) to obtain pure material, though in generally moderate yield (61 – 69%). Following distillation the pure compounds were obtained as oils, which crystallised after several hours or days standing. The impracticalities, and at best only reasonable yields, of this method necessitated its modification. In order to overcome the observation of some workers that addition of the hydrazine to a solution of the acid chloride resulted in the formation of the diacyl hydrazide[61] the acid chloride was added to methylhydrazine, keeping the concentration of free acid chloride low, minimising the possibility of di-addition. The acid chloride was diluted in DCM and added slowly *via* syringe pump (~ 0.5 mM, ~ 0.2 $cm^3\ min^{-1}$) to a cooled excess of methylhydrazine (0 – 5 °C, 20 eq.). This addition protocol, in conjunction with a basic work-up to remove any hydrolysed acid chloride, produced the desired hydrazides in excellent purity and yield (Scheme 2.11, Table 2.1)

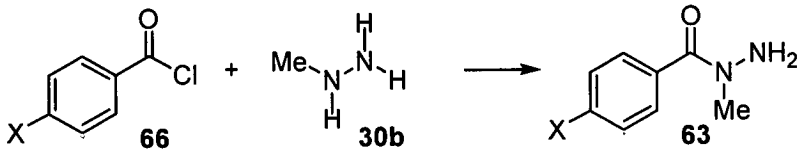

Scheme 2.11

X	Compound	Method A	Method B
OMe	**63a**	66	93
Me	**63b**	68	92
H	**63c**	69	90
Cl	**63d**	65	92
NO_2	**63e**	61	79

Table 2.1 Method A: RT, rapid addition;[67] method B: 0°C, slow addition, basic work-up

Since it was imperative that the regiochemistry of the reaction was established beyond doubt, a series of NMR experiments was carried out to determine the position of the methyl group. The 1D ^{1}H NMR spectrum of **63a** showed the presence of a single NH resonance at 4.51 ppm integrating to two protons. 2D NOESY NMR confirmed the product as the *N*-substituted hydrazide, Figure 2.4 shows the key [^{1}H, ^{1}H] NOESY correlation H2 → H3.

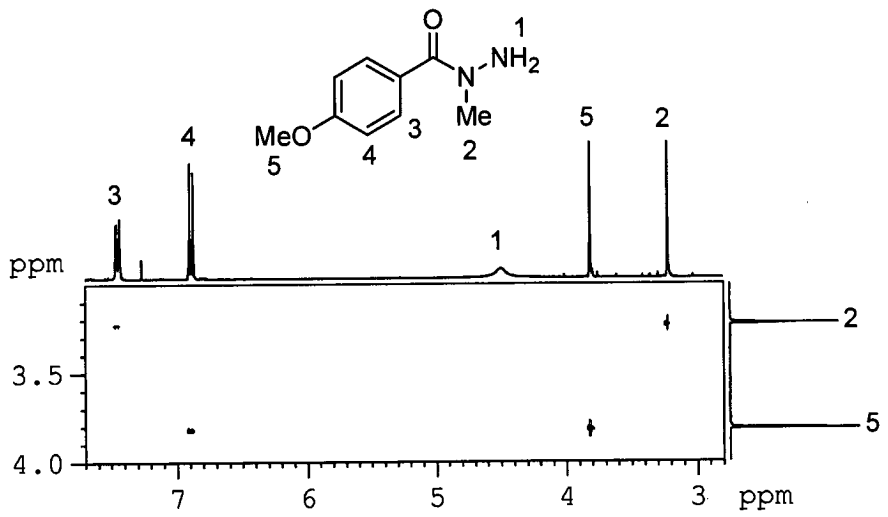

Figure 2.4 Selected view of the [^{1}H, ^{1}H] NOESY spectrum of 63a

2.3.2 *N,N'*-dimethylhydrazides 64

Previous syntheses of *N,N'*-dialkylhydrazides have generally utilised the reaction of a dialkyl hydrazine with an acid chloride or anhydride. This method is effective, however it suffers from the same drawbacks as synthesis of monoalkyl hydrazides, such as diaddition and problems with reactivity of bulky or electron-deficient hydrazines. The carcinogenicity of 1,2-dimethylhydrazine **30e** also makes synthesis of *N,N'*-dimethylhydrazides **64** by this method unattractive on a large scale. Because of these limitations, a more reliable synthesis, without the use of 1,2-dimethylhydrazine **30e**, was sought.

It was hoped that the series of *N,N'*-dimethylhydrazides **64** could be accessed *via* a reductive amination strategy (Scheme 2.12). Reductive amination is a commonly used method of introducing alkyl substituents to amines, providing ready access to a wide range of substitutions under relatively mild conditions. It is a two-step procedure involving the condensation of an amine with an aldehyde or ketone to form an imine intermediate, which can then be reduced *via* a hydride reducing agent or catalytic hydrogenation.

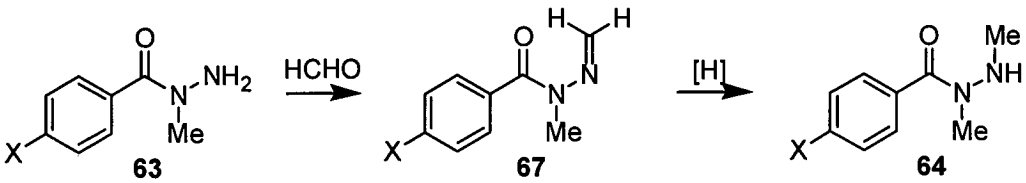

Scheme 2.12

N-Substituted methylidene arylhydrazones of the type **67** are unreported in the literature. There are only two references to similar systems, derived from alkyl hydrazides[81] or carbamates.[82]

Examples of methylidine hydrazones of alkyl hydrazides,[54, 83] aryl hydrazides,[84] hydrazines,[85] hydrazine phosphonate esters,[86] semicarbazides,[87] amino guanidines,[88-90] oxamic hydrazides[91] and thiocarbohydrazides[92] in which there is no *N*-substituent have been reported. Some workers have reported the trimerisation of various hydrazones of this type.[85, 100]

It was anticipated that *N,N'*-dimethylhydrazides **64** could be synthesised by reduction of the methylidene hydrazone **67**, generated from the reaction of available *N*-methylhydrazides **63** with formaldehyde.

Early studies using aqueous formaldehyde solution proved troublesome, as addition of an excess of formaldehyde resulted in the presence of an unknown formaldehyde derivative in the product, even after aqueous workup. This was visible in the ^{1}H NMR spectrum of the crude product as a multiplet at ~5.5 ppm. Failure to remove this product by column chromatography resulted in dialkylation of the hydrazide during the reduction step. In order to allow accurate addition of formaldehyde, the aqueous solution was standardised using Brady's reagent.[84] To an excess of Brady's reagent was added a known volume of 36% aqueous formaldehyde solution. The precipitate of *N*-(2,4-dinitrophenyl)-*N'*-methylidenehydrazone was filtered, dried and weighed, and an exact value for the concentration of the formaldehyde solution determined. This method proved satisfactory, however a preferred solution was the use of paraformaldehyde as the formaldehyde source, allowing one equivalent to be easily and accurately added to the reaction mixture. Paraformaldehyde requires thermal cracking to release the formaldehyde monomer and so the reaction was performed in refluxing toluene under Dean-Stark conditions. This allowed the hydrazone to be formed in excellent yield and purity, allowing it to be used in the reduction step without further purification (Scheme 2.13 and Table 2.2)

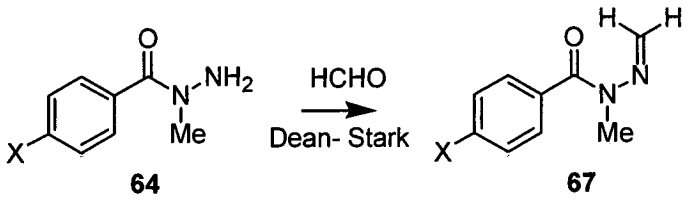

Scheme 2.13

X	Compound	Yield / %
OMe	**67a**	95
Me	**67b**	96
H	**67c**	96
Cl	**67d**	93
NO_2	**67e**	89

Table 2.2 Synthesis of *N*-methyl, *N'*-methylidenehydrazones 67. *N*-methylhydrazide 64 (10 mmol); paraformaldehyde (10 mmol); Dean-Stark; 18 h.

The hydrazone was readily identified using NMR spectroscopy by the anti-phase CH_2 resonance in the ^{13}C DEPT135 spectrum at ~130 ppm, along with two doublets in the ^1H NMR spectrum at ~ 6.6 and 6.4 ppm (^2J ~ 10 Hz). An X-ray crystal structure of hydrazone **67d** was obtained, confirming the assigned structure (Figure 2.5). Full crystallographic data are presented in Appendix 7.1

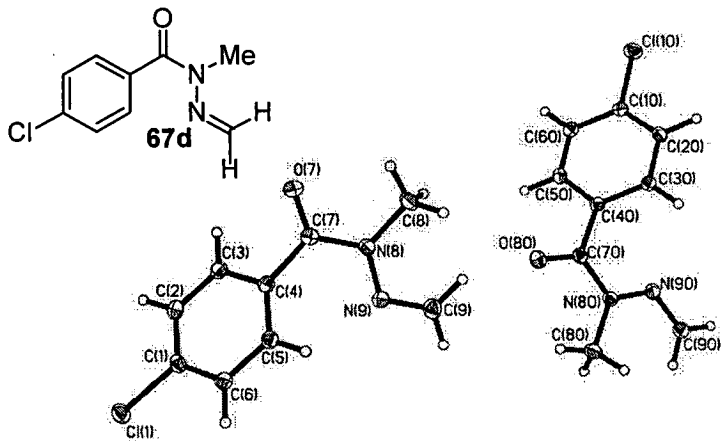

Figure 2.5 X-ray crystal structure of the two crystallographically independent molecules of 67d

This is the first example of a crystal structure of an *N'*-methylidene substituted hydrazide lacking substituents on the methylene group. The key C=N bond length is 1.272(3) Å, similar to known systems with substituted methylene groups. Examples are known with phenyl substituents[93] and where the imine carbon is tertiary and present in an otherwise saturated six-membered ring.[94]

Reduction of hydrazone **67b** by catalytic hydrogenation, using Pd/C in ethanol, proved ineffective. When the catalyst was changed to $Pd(OH)_2/C$, reduction could be achieved at modest pressures (~6 bar). The reaction did not proceed cleanly, and the desired dimethylhydrazide could not be isolated from the crude reaction mixture (although its presence was shown by NMR and ESI-MS). It was thought that the protic solvent may be interfering with the reaction, and so the reduction of the hydrazone was attempted in aprotic solvents: ethyl acetate; toluene; DCM at 10 bar. The reaction was significantly improved in each case (*cf.* ethanol as solvent), and ethyl acetate was chosen as the solvent owing to its relatively low boiling point, allowing it to be easily removed in the workup, and the good yield of the reaction. Results are shown in Table 2.3.

Solvent	Catalyst	Pressure / bar	Temperature	% remaining s.m.[a]
Toluene	Pd/C	10	RT	75
EtOAc	Pd/C	10	RT	56
DCM	Pd/C	10	RT	52
Toluene	$Pd(OH)_2/C$	10	RT	6
EtOAc	$Pd(OH)_2/C$	10	RT	7
DCM	$Pd(OH)_2/C$	10	RT	3

Table 2.3 Optimisation of catalytic hydrogenation reaction conditions using hydrazone 67b.
[a] Based on NMR integrals in isolated product

The reaction did not proceed at all with H_2 pressures of less than ~5 bar. Reaction times were around 24 – 72 h, and so the H_2 pressure was increased and the reaction heated in attempt lower reaction times and improve yield. Optimum conditions were determined to be ethyl acetate; $Pd(OH)_2/C$; 20 bar H_2; 50 °C for 5 h. Although this

system was not suitable for the synthesis of the *p*-nitro substituted hydrazone **66e** (owing to anticipated reduction of the nitro substituent), it was effective for the remaining substrates. The *p*-chlorohydrazone **67d** gave poor yields, halogenated substrates being known to be problematic in catalytic hydrogenation reactions, due to concomitant reduction of the carbon – halogen bond.[95] Pure material could be obtained following bulb-to-bulb distillation, however.

Chemical hydride reducing agents were also investigated. Many reducing agents, such as sodium borohydride, sodium cyanoborohydride, lithium aluminium hydride and others have been shown to be effective in the reduction of C=N double bonds.[96] Sodium cyanoborohydride is selective for imine reduction, *via* the iminium ion,[97] and was tested for reduction of hydrazone **67b** to hydrazide **64b**, although it was anticipated that sodium borohydride would also be suitable as this should not cause the reduction of amides, avoiding reduction of the hydrazide.

Addition of acetic acid was necessary to catalyse the formation of the reducible iminium ion species before reduction could occur. No reaction was observed in the absence of acid. Optimum reaction conditions were determined to be sodium cyanoborohydride (1.1 eq.), acetic acid (1.1 eq) in methanol, 18 h at room temperature, giving the hydrazide in good yield and > 95 % purity (Table 2.4).

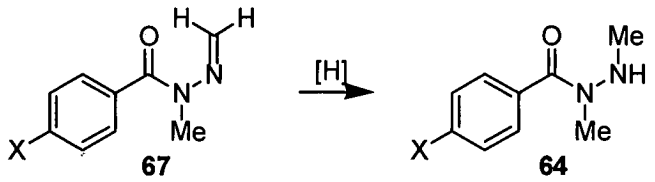

Scheme 2.14

X	Compound	Method A yield / %	Method B yield / %
OMe	**64a**	56	97
Me	**64b**	58	92
H	**64c**	61	95
Cl	**64d**	48	97
NO_2	**64e**	N/A	83

Table 2.4 **Synthesis of *N,N′*-dimethylhydrazides 64. Method A: hydrazone 67 (5.5 mmol); H_2 (20 bar); 50 °C; 5 h. Method B: hydrazone 67 (5.5 mmol); $NaCNBH_3$ (6.0 mmol, 1.1 eq.); AcOH (6.0 mmol, 1.1 eq.) in MeOH (25 cm^3); 18 h**

2.3.3 Attempted synthesis of *N′*-methylhydrazides 69

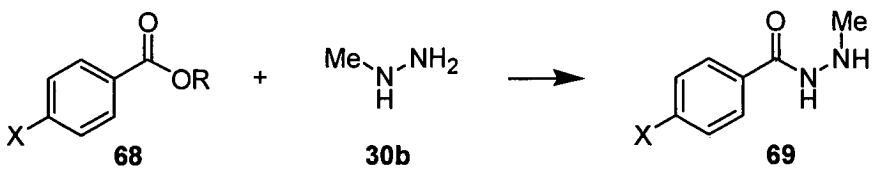

Scheme 2.15 **Attempted synthesis *N′*-methylhydrazides 69**

It was anticipated that the synthesis of a series of *N′*-methylhydrazides **69** would be a facile process *via* the coupling of an aroyl ester **68** with methylhydrazine **30b**(Scheme 2.15), based on literature precedent (see Section 2.1.1).

Initial studies showed that the reaction of *N*-methylhydrazine **30b** (0.98 eq.) with ethyl acetate **29a** in refluxing ethanol for 72 h formed what appeared by ^1H NMR spectroscopy to be a mixture of *N*- and *N′*-methylacetic acid hydrazides. The products were unstable and were unable to be separated by distillation or other techniques.

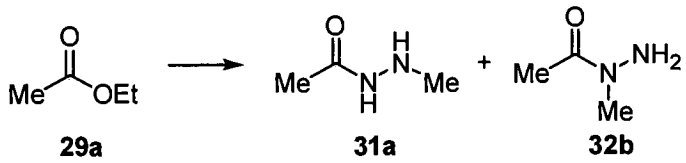

Scheme 2.16

When the reaction was attempted with aroyl esters **68**, no reaction was observed, with full recovery of starting material. Further investigation with methyl 4-methylbenzoate **68b** (X = Me), involving reaction time, acid or base catalysis and the addition of catalytic amounts of water or methoxide anion, gave none of the desired hydrazide, with the starting material generally being recovered in high yield (Scheme 2.17 and Table 2.5).

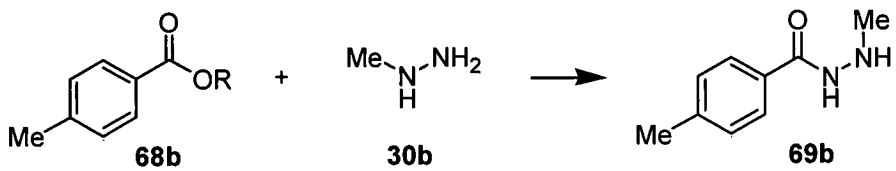

Scheme 2.17

R	Time	Solvent	Additive	% rec'd sm
Me	72 h	MeOH	N/A	Quant.
Me	72 h	MeOH	H_2O	Quant.
Me	72 h	MeOH	NaOMe	Quant.
Et	72 h	EtOH	N/A	Quant.
Me	300 h	MeOH	*p*-TSA	58[a]
Me	300 h	MeOH	N/A	76[a]
Me	300 h	MeOH	Et_3N	51[a]
Me	96 h	Neat[b]	N/A	[c]

Table 2.5 Attempted syntheses of *N'*-methylhydrazides. Aroyl ester 68b (0.7 mmol); methylhydrazine 30b (0.68 mmol, 0.98 eq.); reflux. [a]Recovered following column chromatography; [b] heated to 100 °C; [c]no evidence of reaction by TLC

Since the reaction was expected to proceed under thermodynamic control,[81] necessitating long reaction times and high temperatures it was thought that the reaction would be amenable to microwave synthesis. Microwave synthesis has been shown to be an effective way of promoting reactions at high temperatures with drastically reduced reaction times.[98] Synthesis of *N'*-methyl-4-methylbenzoic acid hydrazide **69b** was attempted under microwave conditions. *N*-methylhydrazine **30b** (0.15 g, 0.30 mmol, 0.98 eq.) and methyl 4-methylbenzoate **68b** (0.05 g, 0.33 mmol) in the appropriate solvent were irradiated under the given conditions (Scheme 2.17 and Table 2.6).

Solvent	Power / mW	Temperature / °C	Pressure / psi	Time / min	Yield
DMF	300	120	250	5	N/A
DMF	300	120	250	10	N/A
MeCN	250	100	250	10	N/A

Table 2.6 Attempted syntheses of *N'*-methylhydrazides under microwave conditions.

None of the desired hydrazide was recovered from the reaction and none could be detected in the crude mixture (NMR or ESI-MS). It was therefore decided to investigate alternative routes to *N'*-substituted hydrazides **69**. Following the successful condensation / reduction in the synthesis of *N,N'*-dimethylhydrazides **65**, it was hoped that this strategy could be applied to the synthesis of *N'*-methylhydrazides, using commercially available hydrazides **67** as starting materials (Scheme 2.18).

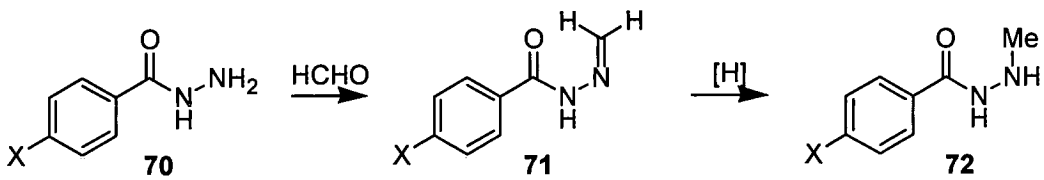

70 **71** **72**

Scheme 2.18

Unfortunately, the product obtained from the condensation of 4-methylbenzoic acid hydrazide **70b** (X = Me) and paraformaldehyde was not the desired hydrazone **71**, but the trimeric product **73**.

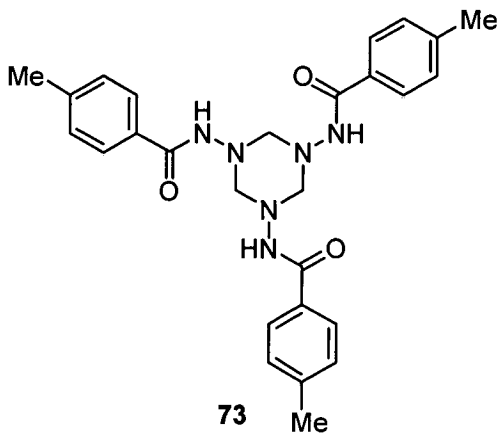

73

Figure 2.6

This type of cyclisation has been previously reported in a related system (from the condensation of benzoic acid hydrazide and formaldehyde),[99] and the trimer has latterly been shown to undergo allylation, Mannich-type, and cyanide addition reactions,[100] indicating that the product shows similar reactivity to the expected hydrazone. Evidence reported for the structure[99] was based on an elaborate series of chemical analyses, the authors discarding possible straight chain polymeric, structures and a dimeric structure featuring a diazetidine ring. Unfortunately, the report of Kobayashi *et al.*[100] provided no further evidence for the structure. We have shown that the product of the reaction between 4-methylbenzoic acid hydrazide **70b** and formaldehyde is the symmetrical triazetidine product **73**, based on NMR and HRMS analyses. ^{13}C DEPT135 experiments show a methylene signal at 142.0 ppm, 2D [^{1}H, ^{1}H] COSY and [^{1}H, ^{13}C] HSQC experiments were further used to confirm the structure, with cross-peaks between the two methylene protons demonstrating their geminal non-equivalence (Figure 2.7).

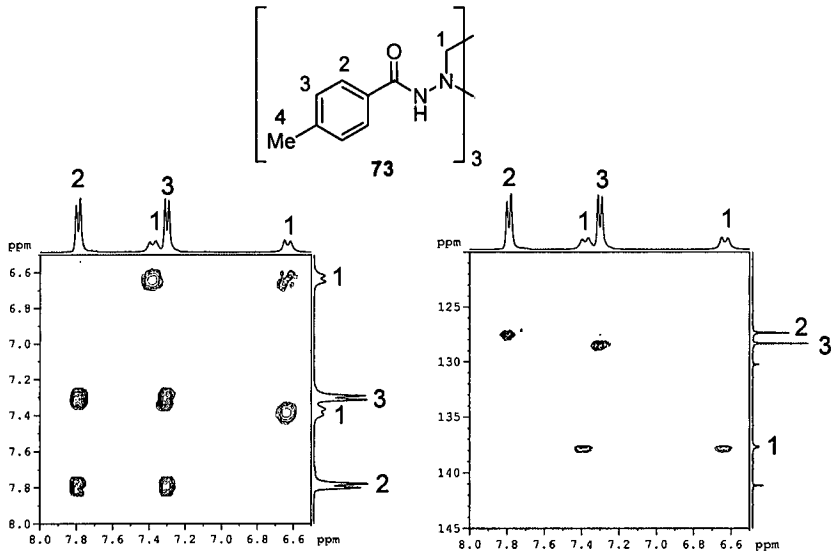

Figure 2.7 **Selected views of the [^{1}H, ^{1}H] COSY and [^{1}H, ^{13}C] HSQC spectra of 73**

EI-MS showed a mass of 487, with no evidence of the presence of higher oligomers. HRMS agreed with the assigned chemical formula $C_{27}H_{31}N_6O_3^+$ (requires 487.2458, found 487.2458). Unfortunately a crystal structure could not be obtained due to the poor solubility of **73** in common recrystallisation solvents. Attempts were made to "trap" the hydrazone at low temperatures (-78 °C), with sodium borohydride added and the reaction mixture allowed to warm slowly to room temperature. In this way it was hoped that reduction would occur before cyclisation. The cyclic product **73** was still formed, however. Reduction of **73** to **72b** with sodium borohydride, sodium cyanoborohydride or catalytic hydrogenation in a manner analogous to that of the *N,N′*-methylhydrazide preparation was also unsuccessful. Following the difficulties that were encountered with the synthesis of *N′*-methylhydrazide **72b,** it was decided to investigate other possible substitutions of the *N′*-position. It was hoped that *N′*-isopropyl substituted hydrazides would be available *via* reduction of the propylidine hydrazone, as the steric bulk of the methyl groups would disfavour trimer formation.

2.3.4 *N'*-^{i}propylhydrazides 74

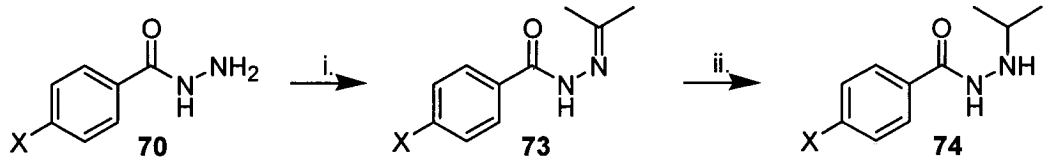

Scheme 2.19 i. Me_2CO (1.1 eq.), Na_2SO_4; ii. $NaCNBH_3$, (1.1 eq.) AcOH (1.1 eq.), MeOH

The condensation of propanone and hydrazide **70** (X= OMe **70a**; Me **70b**; H **70c**; Cl **70d**; NO_2 **70e**) was successfully carried out in anhydrous methanol, with sodium sulfate as a dehydrating agent, to yield the desired hydrazone **73** in quantitative yield (Scheme 2.19).

This preparation has the benefit that the excess ketone can be removed easily following the reaction, unlike excess formaldehyde, of which exactly 1 equivalent must be added in order to avoid purification problems. The hydrazone can then be reduced to hydrazide **74** using one of the methods previously described, sodium cyanoborohydride again being preferable, and showing improvement in yield over catalytic hydrogenation (Table 2.7). Again, a benefit of hydride reduction is that there is no complication with the carbon – halogen bond in hydrazone **70d**, or reduction of the *p*-nitro substituent of hydrazone **70e**.

X	Compound	Method A	Method B
OMe	**74a**	68	89
Me	**74b**	61	92
H	**74c**	63	93
Cl	**74d**	52	91
NO_2	**74e**	N/A	79

Table 2.7 Synthesis of *N'*-^{i} propylhydrazides 70. Method A: hydrazone 71 (5.5 mmol); H_2 (20 bar); 50 °C; EtOAc; 5 h. Method B: hydrazone 70 (5.5 mmol); $NaCNBH_3$ (6.0 mmol, 1.1 eq.); AcOH (6.0 mmol, 1.1 eq.) in MeOH (25 cm^3); 18 h

The reductive amination strategy employed allowed the synthesis of *N'*-substituted hydrazides in good yield and > 95 % purity.

2.4 Conclusions

Synthetic methodologies to a range of hydrazides have been developed, allowing access to all of the desired *N*-substitution patterns. The hydrazides were obtained in excellent yield and purity, enabling them to be used in dye coupling reactions without the need for purification. The series of hydrazides constructed also allowed the investigation of certain physical characteristics of the hydrazide moiety, specifically the hindered rotation about the C-N amide bond. This was achieved by variable temperature NMR spectroscopic methods and is detailed in the following section.

The hydrazides synthesised, once coupled to a suitable dye, should allow for investigation into their effects on the ozone and light fastness of azo dye systems, specifically *N*-substitution and electronic effects.

We have also confirmed the proposed trimeric structure of the product isolated by previous workers[99, 100] from the reaction of benzoic acid hydrazides with formaldehyde by means of HRMS and NMR spectroscopic methods.

3 Hydrazide rotamers

An interesting phenomenon observed in substituted amides is restricted rotation about the C-N amide bond. σ-Bonds normally rotate freely at ambient temperatures. In substituted amides, such as hydrazides, delocalization of the lone-pair of the nitrogen atom into the carbonyl π-system gives the C-N bond some double bond character, raising the energy barrier to rotation and allowing observation of two distinct rotameric species in NMR experiments, with two separate methyl signals observed for the σ-*Z* **63a** and the σ-*E* **63a** rotamers (Scheme 3.1). There has been a recent review of NMR exchange processes such as this.[101]

***Z*-63a** ***E*-63a**

Scheme 3.1

The maximum separation of these two signals (observed at low temperature) and the temperature at which they coalesce can be used to determine the rate of exchange and the free energy barrier to rotation about the bond.

At low temperatures, the two rotamers do not interconvert significantly, and two sharp, individual signals can be seen. As the temperature is increased, the two signals broaden and then coalesce. As the temperature is increased further, a single signal is seen as the two rotamers interconvert too rapidly to be distinguished on an NMR timescale. Figure 3.1 shows the NMR spectra recorded for the *N*-Me region of 4-chlorobenzoic acid hydrazide **64d** from + 233 K to + 313 K.

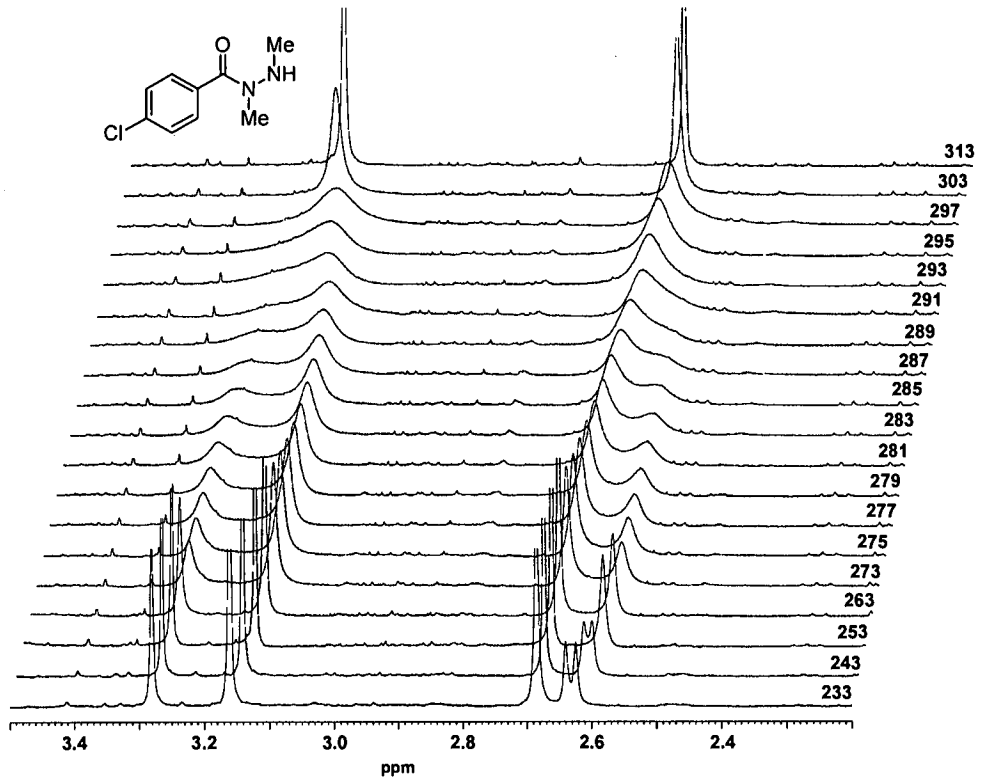

Figure 3.1 ^{1}**H NMR spectra of the *N*-Me region of 64d from +233 K to +313 K**

In systems with equal population of both rotamers, it is straightforward to obtain the rate of exchange at the coalescence temperature and the free energy barrier to rotation using Equation 3.1 and Equation 3.2.[102]

$$k_c = \frac{\pi.\Delta\nu}{\sqrt{2}}$$

Equation 3.1

$$\Delta G_c^{\ddagger} = 2.3RT_c[10.32 + \log(T_c/k_c)]$$

Equation 3.2

Where k_c = rate at point of maximum peak broadening

$\Delta\nu$ = distance between peaks at slow exchange (Hz)

$\Delta G_c^{\ddagger}$ = free energy of activation (kJ mol^{-1})

T_c = coalescence temperature (K)

When dealing with systems in which the two rotamers are of unequal population, a more rigorous approach must be used.[102] This usually takes the form of a line-shape analysis, where experimental data are fitted to a theoretical model using a computer program. The model is then improved iteratively until a good match is obtained. A less accurate, but simpler, method of determining the free energy uses the difference in populations and maximum separation of the two rotamers at low temperature and the coalescence temperature, and allows values to be obtained from empirically determined graphs.[103] This method is only applicable to the calculation of free energy. Figure 3.2 shows the energy diagram for interconversion of the two possible rotamers (A and B).*

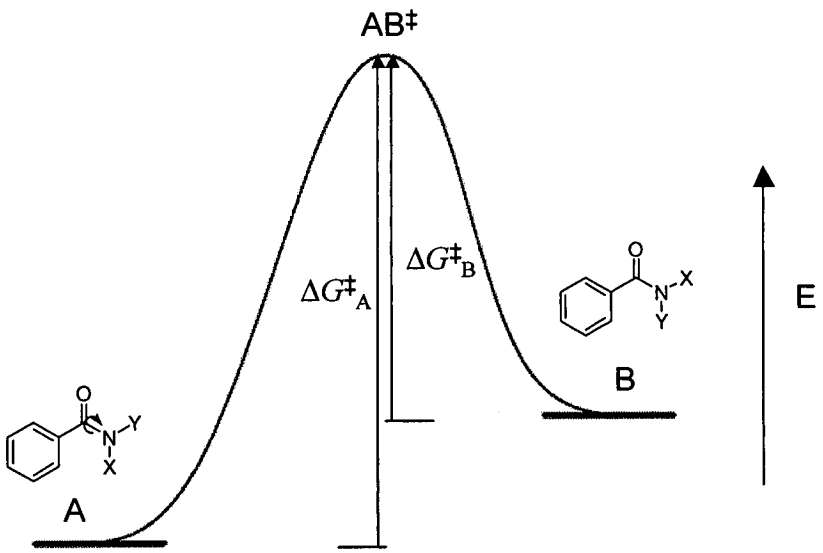

Figure 3.2

The value of $\Delta G^{\ddagger}$ can be calculated using the value of {log[X/2π(1±ΔP)]} obtained from the graph shown in Figure 3.3. $\Delta G^{\ddagger}_{A}$ is calculated from the function of (1 – ΔP) (Equation 3.3); $\Delta G^{\ddagger}_{B}$ is calculated from the function of (1 + ΔP) (Equation 3.4), where ΔP is the difference in population of the two isomers.

* Unfortunately, despite attempts using both [^{1}H, ^{1}H] NOESY and nOe difference NMR spectra it was not possible to identify the *E* and *Z* isomers in these experiments.

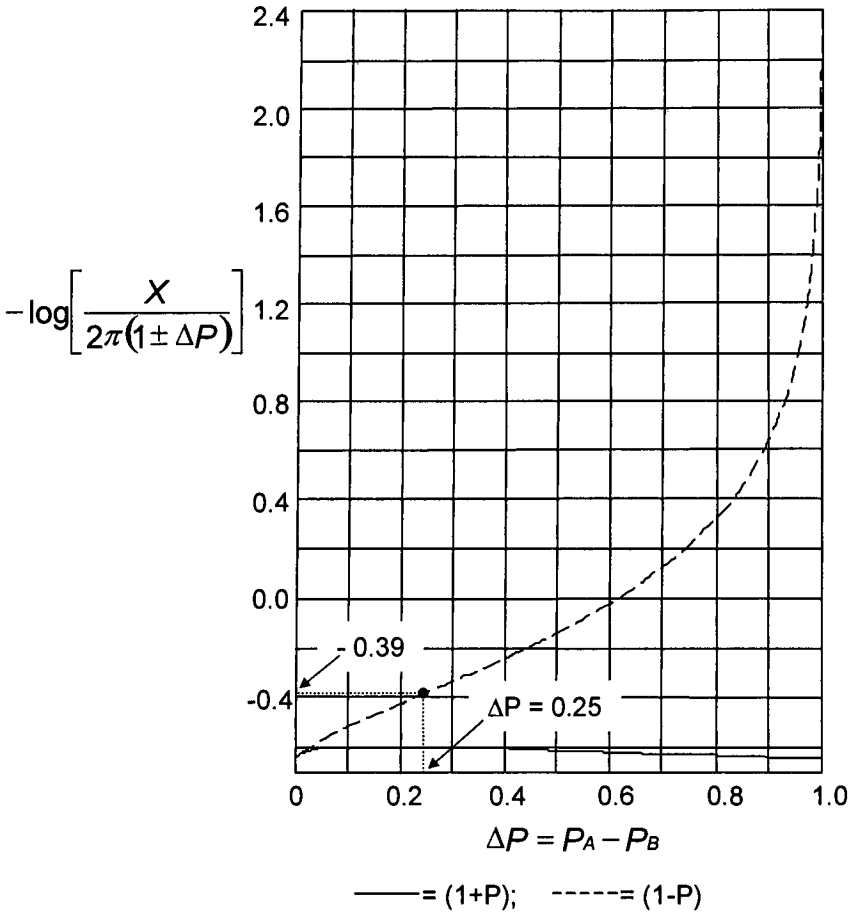

Figure 3.3

$$\Delta G_A^{\ddagger} = 19.2T_c\left[10.62 + \log\left(\frac{X}{2\pi - \Delta P}\right)\right] \text{ kJ mol}^{-1}$$

Equation 3.3

$$\Delta G_B^{\ddagger} = 19.2T_c\left[10.62 + \log\left(\frac{X}{2\pi + \Delta P}\right)\right] \text{ kJ mol}^{-1}$$

Equation 3.4

The data for **64d** are marked in Figure 3.3. The coalescence temperature was determined to be 297 K (Figure 3.1), giving $\Delta G^{\ddagger}_{A}$ = 65 kJ mol^{-1}. For comparison, the $\Delta G^{\ddagger}$ calculated for *N*,*N*-dimethylbenzamide in $CDCl_3$ by lineshape analysis is 67 kJ mol^{-1}.[104]

NMR samples of hydrazides **63** and **64** were prepared in $CDCl_3$ and their ^1H NMR spectra recorded over the temperature range + 213 K to + 333 K. The two rotamers were of unequal population for all species, and so values of $\Delta G^{\ddagger}$ were calculated for all compounds using Figure 3.3 and the coalescence data obtained. Table 3.1 shows the data obtained for the *N*-methyl series of hydrazides **63**.

Hydrazide	T_c / K	$\Delta\nu$ / Hz	ΔP	$\Delta G^{\ddagger}_A$ / kJmol^{-1}	$\Delta G^{\ddagger}_B$ / kJmol^{-1}
63a	263	22.7	0.63	61	55
63b	279	34.7	0.65	64	58
63c	291	42.0	0.65	66	60
63d	293	51.2	0.55	65	60
63e	309	70.1	0.16	66	63

Table 3.1

Free energies of activation for hindered rotation around C-N bonds in aryl amides have been previously shown to exhibit a linear correlation with Hammett σ constants.[104, 105] $\Delta G^{\ddagger}_A$ obtained for *N*-substituted hydrazides **63** was plotted against Hammett's σ constants; the best fit was obtained against σ^+ (Figure 3.4). The graph shows a reasonable linear correlation with a small positive slope.

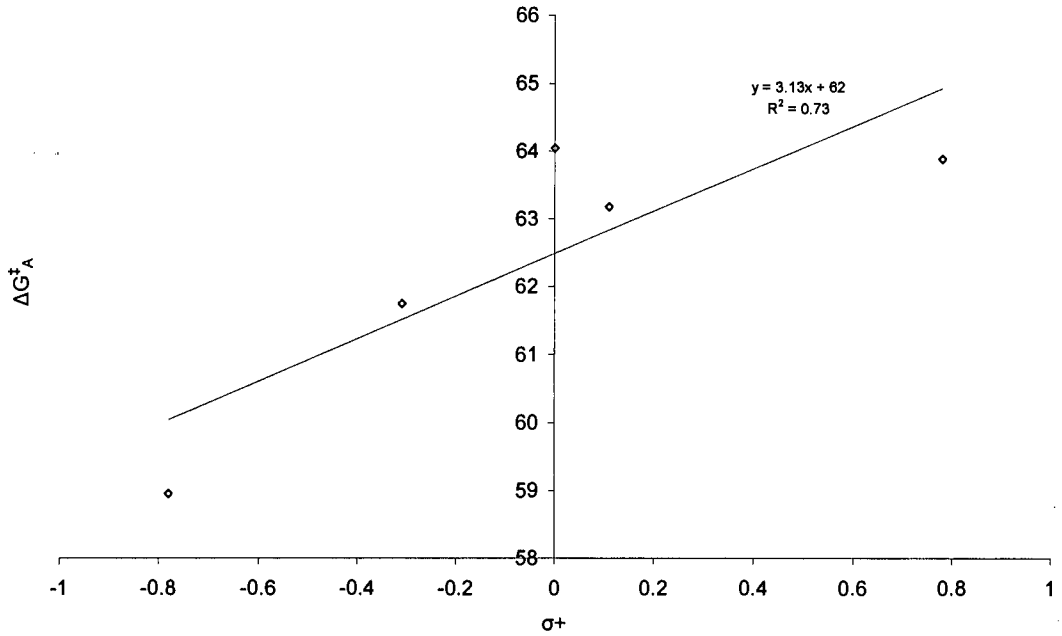

Figure 3.4 Plot of σ^+ versus $\Delta G^{\ddagger}_A$ for hydrazides 63

Table 3.2 shows the data obtained for the *N,N'*-disubstituted series of hydrazides **64**. A plot of $\Delta G^{\ddagger}_A$ versus Hammett σ^+ constants is given in Figure 3.5. The graph shows a good linear correlation with a small positive slope.

Hydrazide	T_c / K	$\Delta\nu$ / Hz	ΔP	$\Delta G^{\ddagger}_A$ / kJmol^{-1}	$\Delta G^{\ddagger}_B$ / kJmol^{-1}
64a	281	42.7	0.74	60	58
64b	281	34.4	0.73	63	58
64c	291	38.2	0.60	64	61
64d	297	42.9	0.62	65	62
64e	315	60.7	0.36	68	64

Table 3.2

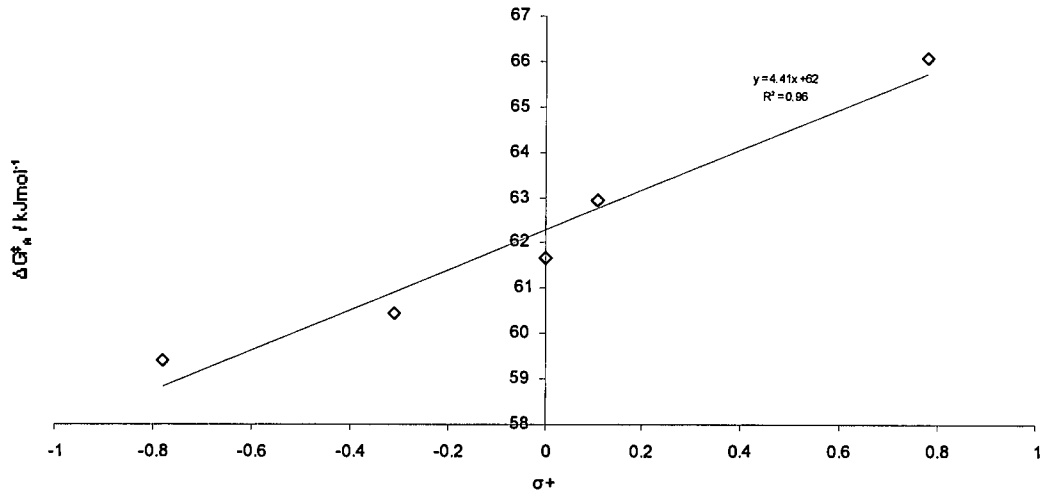

Figure 3.5 Plot of σ^+ versus $\Delta G^{\ddagger}_{A}$ for hydrazides **64**

The positive slope of both plots shows that electron withdrawing groups in the aryl ring increase the barrier to rotation. This can be explained by consideration of the resonance forms shown in Scheme 3.2.

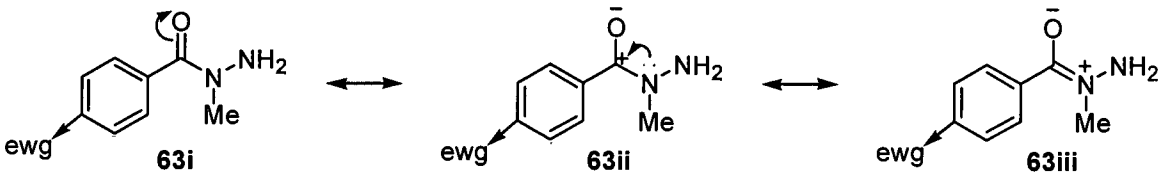

Scheme 3.2

The presence of an electron-withdrawing group forces **63ii** to draw more electron density from the nitrogen atom lone-pair to compensate for the positive charge on the carbon atom. This gives the C-N amide bond more double-bond character, increasing the barrier to rotation.

An interesting observation is that the rate of proton exchange is slow enough at low temperatures that coupling between the proton of the *N'*-nitrogen atom and the *N'*-methyl protons is seen. In hydrazides **64a**, **64b**, **64d** and **64e**, the methyl signal is split into a doublet at temperatures below *ca.* 250 K; $^3J \sim 8$ Hz. This can be seen for **64d** at 233 K in Scheme 3.1.

4 Dye Coupling

In order to functionalise a dye a linker is commonly used, which can be easily attached to both dye and, in this instance, hydrazide (Figure 4.1).

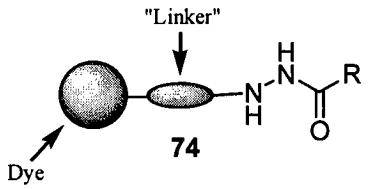

Figure 4.1

The advantages of this are twofold: 1) it allows ready synthesis of substituted dyes based on existing dyestuffs 2) the linker can be used to provide electronic isolation of the dye from the hydrazide, meaning the addition of the hydrazide should not affect the colour properties of the dye.

One of the most common types of linker is the triazine group, developed from the reactive series of textile dyes.

4.1 Reactive dyes

Reactive dyes were developed by ICI in the early 1950s as a way to improve the wash fastness of cotton dyes, and were marketed as the Procion dye series[106-108] *e.g.* reactive red 2 **75** (Procion Red MX-5B).

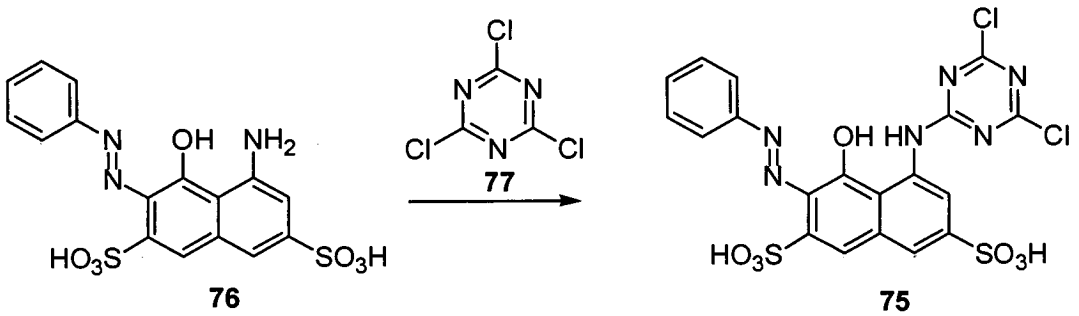

Scheme 4.1

75 is formed from the reaction of 5-amino-4-hydroxy-3-phenylazo-naphthalene-2,7-disulfonic acid **76** with cyanuric chloride **77** (Scheme 4.1). During the dying process, mild alkaline conditions allow nucleophilic substitution of chloride by hydroxyl groups on the cellulosic cotton fibres. This forms a covalent bond between the dye and the fibre, significantly enhancing wash fastness (Scheme 4.2).

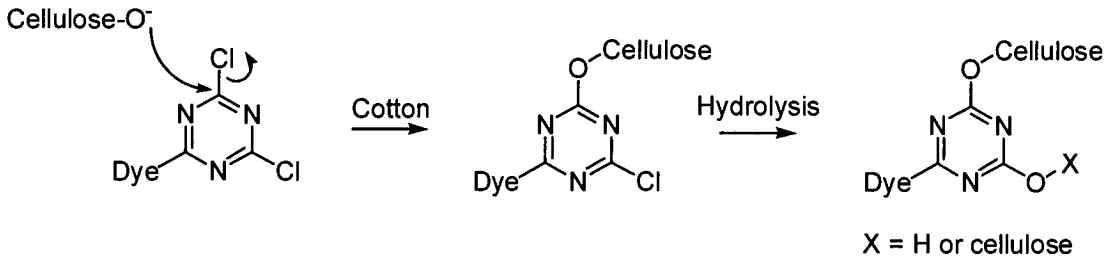

Scheme 4.2

The reactive dyes proved a commercial success and many other types of heterocyclic reactive group were developed, such as the trichloropyrimidines 78, the dichloropyridizines **79**, the dichloroquinoxalines **80** and the chlorobenzothiazolyl dyes **81**.

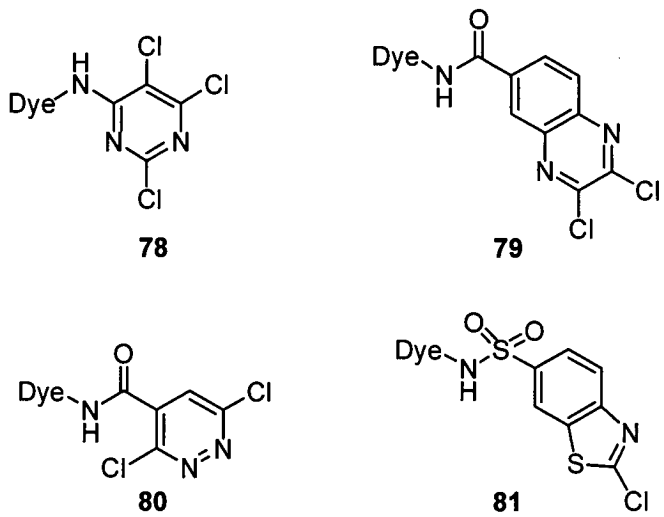

Figure 4.2 **Heterocyclic reactive dyes**

Other examples of reactive groups not based around heterocyclic systems are vinylsulfone **82** and α-bromoacrylamide **83** (for cotton and wool respectively).

These react with the fibre *via* a nucleophillic addition process. The nomenclature refers to the reactive intermediates which are generated on hydrolysis, facilitating reaction with the fibre.

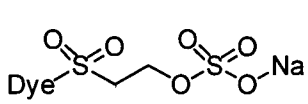

82

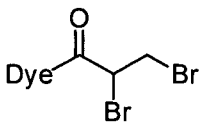

83

Figure 4.3 Non-heterocyclic reactive dyes

The heterocyclic linker can also be used to couple the dye with another component in order to influence the physical properties of the dye, *e.g.* colour. An example is the use of a triazine linker to couple two coloured components to give direct green 26 (**84**). There is no interaction between the two coloured components as the triazine ring provides electronic isolation between the two chromophores.

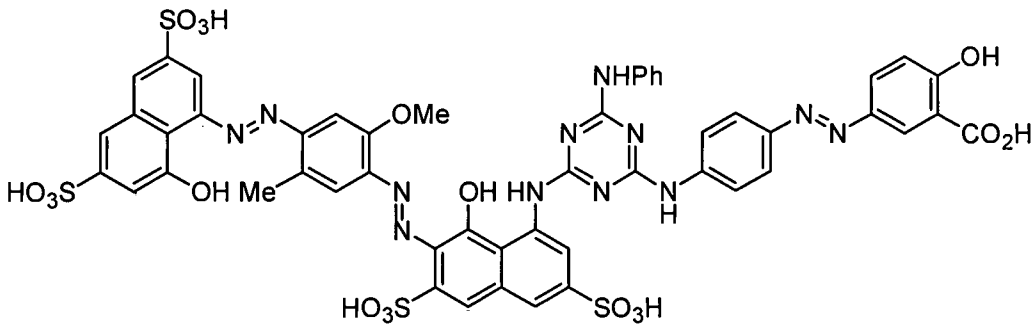

84

Figure 4.4 Direct Green 26 (84)

Triazine linkers can also be used to functionalise a dye to provide an enhancement in some other property, such as fastness. It is this ability that was utilised in order to attach the hydrazide series to a typical azo dye.

4.2 Cyanuric chloride / dye coupling

Cyanuric chloride **77** is well suited to reactions where unsymmetrical substitution is required, due to the progressive difficulty with which the chloride leaving groups are substituted (Scheme 4.3). The reasons behind this are thought to lie with the increase

in electron density in the triazine ring following each nucleophilic substitution, meaning that subsequent nucleophilic attack is disfavoured.

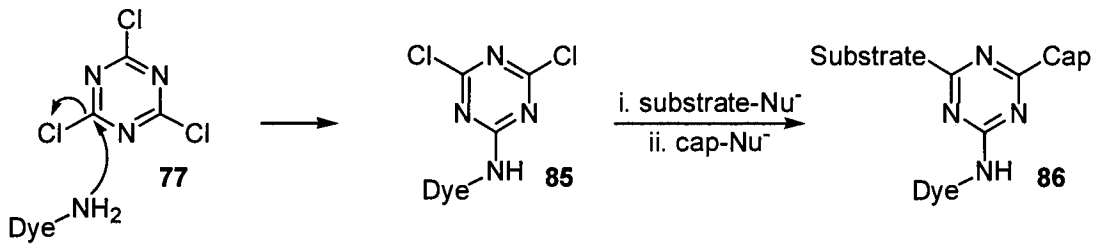

Scheme 4.3 **Dye functionalisation using a triazine linker**

Monosubstitution of the triazine ring by the dye to give **85** will occur if the temperature is kept below ~5 °C. In order to avoid base hydrolysis of the cyanuric chloride a pH < 7 must be maintained. Once this step is complete, the substrate can be added to the reaction mixture and the temperature increased to 45 °C. Again, careful control of pH and temperature allows highly selective monosubstitution. By increasing the temperature to 75 °C the final chloride can be substituted with a capping component to give **86**. This is commonly a simple base hydrolysis, performed by adjusting the pH to 12 - 14, although other substituents, such as phenol or aniline, can be used.

Since the reaction produces HCl at each stage, the pH must be maintained by addition of base. If the pH of the reaction is allowed to fall too low then the reaction will be slow, as the protonated form of the dye / substrate will predominate. Acidic dyes may also precipitate from the reaction mixture. If the pH is too high, however, then base hydrolysis of the cyanuric chloride will occur. During the coupling of the dye and substrate, pH is maintained at 6.6 – 6.8 as a compromise between these two positions.

A standard protocol for the coupling of azo dyes with cyanuric chloride **77** was obtained from Avecia (Grangemouth).[109] As this method was based on a large scale preparation (*ca.* 1 kg), the reaction was modified to make it more amenable to lab-scale synthesis (*ca.* 5 g.; 300 cm^3 of solvent). The reaction was performed in an open beaker, allowing easy monitoring of pH and addition of reagents. Temperature was controlled by external cooling / heating, although the reaction could also be cooled

by direct addition of ice to the reaction mixture. Stirring was by means of an overhead mechanical stirrer. Cyanuric chloride **77** is extremely hydrophobic, and as such is difficult to disperse in aqueous solutions. Calsolene oil (*ca.* 2 – 3 drops) was added to the reaction mixture in order to lower surface tension, allowing efficient suspension of the cyanuric chloride **77**.

Reaction monitoring by thin layer chromatography on standard silica plates is possible, even with these highly polar substrates, using a suitable eluent system (propan-1-ol : MEK : 35% $NH_{3(aq)}$; 4 : 4 : 2).[109] This method has the benefit of being rapid and simple to perform, however it does not allow quantitative analysis of the reaction mixture. Attempts were made to follow the reaction by ESI-MS. This was unsuccessful, probably due to the high salt content of the reaction mixture and the possibility of several charge states of the dye. An HPLC system obtained from Avecia (Grangemouth)[110] allowed the reaction to be followed by reversed-phase HPLC at 254 nm (simultaneous detection in the visible range was unfortunately not possible). This method is quantitative, with extremely low levels of detection. An analysis method obtained from Avecia (Grangemouth)[111] was initially used, although this was later modified to provide faster analysis times (see experimental section).

The dye initially chosen for the coupling was a commercially available azo dye, acid red 37 **87**. This was chosen as it was readily available and had been indicated as being particularly susceptible to ozonolysis.[112] With a synthesis method and analysis system in hand, a test reaction coupling **87** and oxamic hydrazide **88** using a triazine linker was attempted.

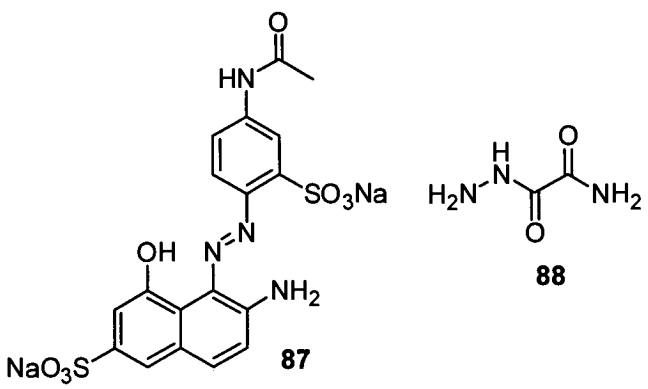

Figure 4.5 **Acid red 37 and oxamic hydrazide 88**

Unexpectedly, the coupling of **87** with cyanuric chloride **77** proceeded in only around 10% conversion. This low reactivity may be due to the presence of a sulfonyl group *ortho-* to the azo group. This gives an extended network of hydrogen bonding, in favourable intra-molecular, six-membered rings, meaning the amine group is relatively sterically hindered (Figure 4.6). The 3D structure was calculated using energy minimisation MM2 parameters, the lengths of the hydrogen bonds are calculated as 2.2 ′ (N-H) and 2.1 ′ (O-H).

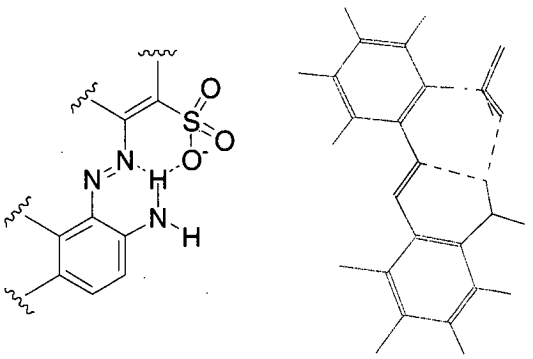

Figure 4.6 H-bonding in acid red 37

Azo / hydrazone tautomerism could also be responsible for the low reactivity of **87**, as it would be expected that the hydrazone would be less nucleophilic (Scheme 4.4). This is probably a minor contributing factor, however, since as a general rule *o*-azo amine systems exist as the azo tautomer.[113]

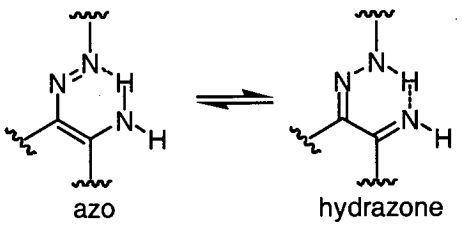

Scheme 4.4 Acid red 37 azo / hydrazone forms

Following this setback **89,** known to be appropriate for coupling with cyanuric chloride, was used, supplied by Avecia (Blackley)[114] (Scheme 4.5).

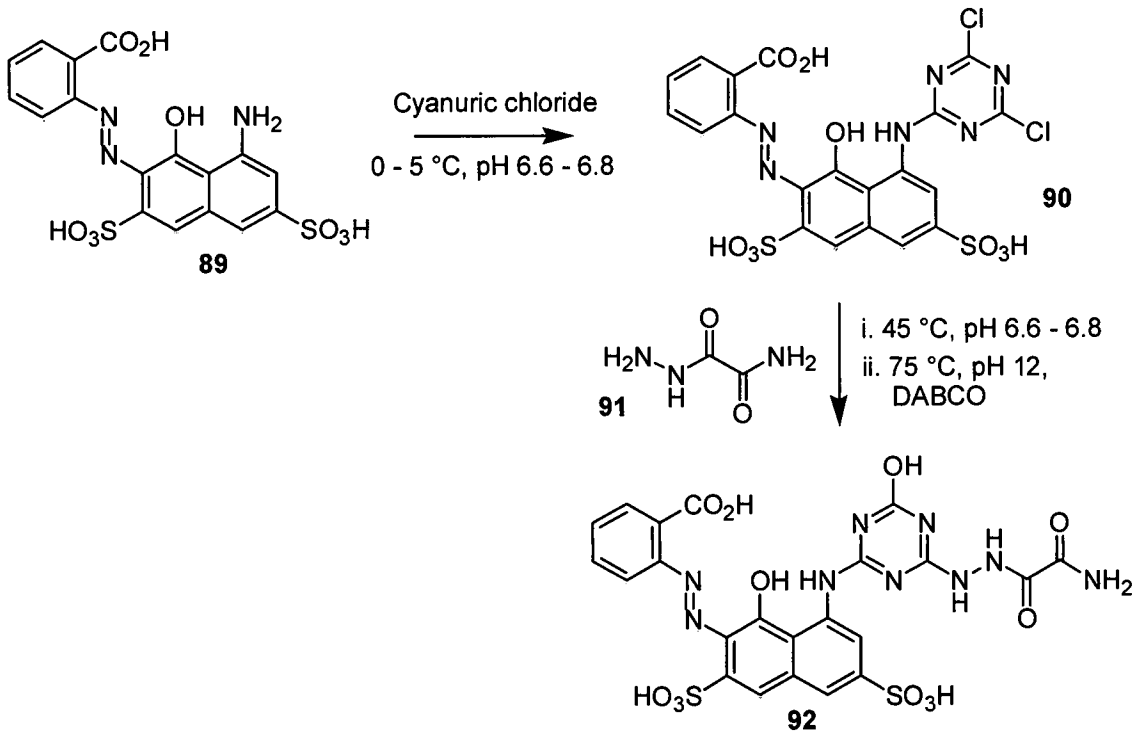

Scheme 4.5 **Coupling of 89 with oxamic hydrazide 90 using a triazine linker**

Coupling of **89** with cyanuric chloride **77** proceeded cleanly, affording the dichloro intermediate **90**. Oxamic hydrazide was then added, the reaction heated to 45 °C. NaOH (0.1 M) was added to maintain the pH at 6.6 – 6.8. Hydrolysis of the final chloride was carried out at 75 °C, pH 12 to give **92**. 1,4-diazabicyclo[2.2.2]octane (DABCO) **93** is added as a catalyst to facilitate the final hydrolysis. It is a strong nucleophile and is most commonly used as a catalyst in the Bayliss-Hillman reaction,[115, 116] however in this case it acts in a similar fashion to dimethylaminopyridine (DMAP), displacing the chloride and activating the triazine ring to nucleophilic attack (Scheme 4.6).

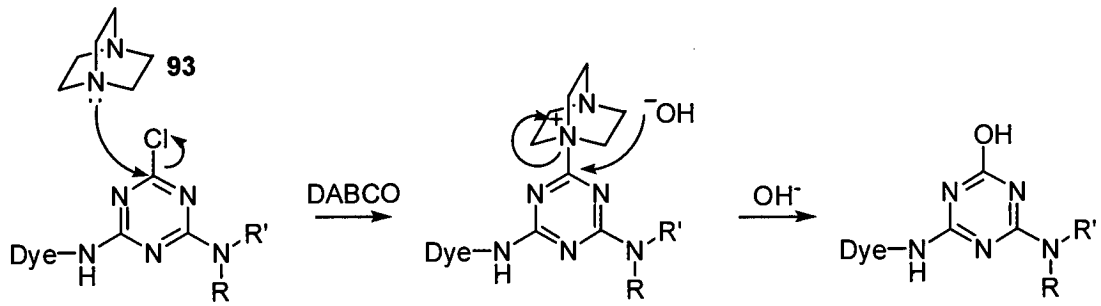

Scheme 4.6

The final product is recovered from the aqueous reaction mixture by a "salting-out" procedure. Sodium chloride (*ca.* 15% w/v) is dissolved in the hot solution and the pH adjusted to 3 – 4 with 1 M $HCl_{(aq.)}$. The reaction mixture is allowed to cool and the precipitate is collected by suction filtration. Inorganic impurities mean that the dye is typically around 50% pure at this point. The salts can be removed by dialysis, using a semi-permeable membrane with a molecular weight cut-off (MWCO) of around 3,500 Da. Although this is significantly above the molecular weight of the dye, the difference in permeation rate between the salts and the dye mean that the dye can be recovered in around 80 –90% purity following dialysis. Purity can be calculated using either the Beer-Lambert law (if the extinction coefficient is known), or by using Equation 4.1 in conjunction with the results of elemental analysis.

$$P = \frac{MW \times a}{N \times AW}\%$$

Equation 4.1

Where: P = purity

MW = molecular weight

a = atom % in elemental analysis

N = number of atoms of type a

AW = atomic weight of atoms of type a

With this synthesis in hand, the previously synthesised *N*-methyl-; *N,N'*-dimethyl- and *N'*-isopropylhydrazides (**63**, **64** and **65**) were successfully coupled with **89**.

Coupling of the commercially available unsubstituted hydrazides **70** proved difficult, however. Despite the success of the reaction with oxamic hydrazide, results from the attempted coupling of other hydrazides were less reliable. Although benzoic acid hydrazide **70c** and 4-chlorobenzoic acid hydrazide **70d** were both successfully coupled, the other hydrazides did not hydrolyse cleanly, and a major side product was observed, illustrated for the reaction of **70b** in Figure 4.7.

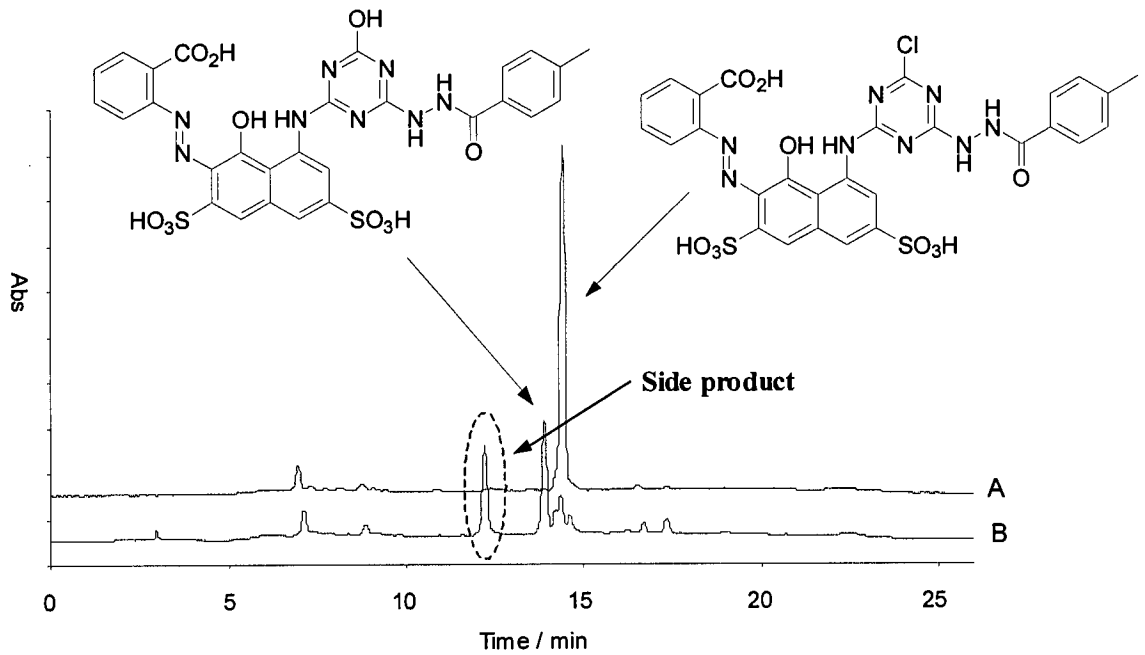

Figure 4.7 Hydrolysis step in the reaction of 70b. Trace A: before hydrolysis (pH 6.8, 45 °C); trace B: after hydrolysis (pH 12 – 14, 75 °C)

Unfortunately the product could not be identified by HPLC-MS, nor could it be separated by preparative scale HPLC. Attempts were made to prevent or limit its formation by performing the hydrolysis at lower temperatures or by adding 1 mole equivalent of base. These reactions proved unsuccessful, however. Why some of the hydrazides couple cleanly whilst others do not is unknown.

The series of dyes synthesised is shown in Table 4.1.

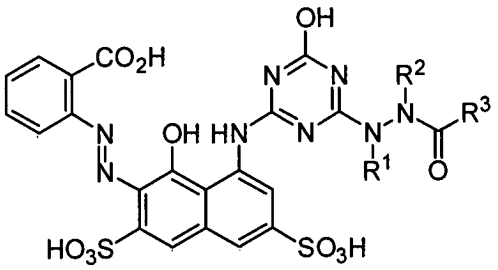

	R^1	R^2	R^3
94c	H	H	Ph
94d	H	H	4-Cl-Ph
94f	H	H	$C(O)NH_2$
95a	H	Me	4-OMe-Ph
95b	H	Me	4-Me-Ph
95c	H	Me	Ph
95d	H	Me	4-Cl -Ph
95e	H	Me	4- NO_2-Ph
96a	^{i}Pr	H	4-OMe-Ph
96b	^{i}Pr	H	4-Me-Ph
96c	^{i}Pr	H	Ph
96d	^{i}Pr	H	4-Cl-Ph
97a	Me	Me	4-OMe-Ph
97b	Me	Me	4-Me-Ph
97c	Me	Me	Ph

Table 4.1

No yields are reported for the synthesis of the dyes. This is because a variable proportion of the dye is lost in the isolation procedure, and so yield can vary accordingly. Each step of the reaction proceeds in > 95 % yield based on HPLC area% data. Following salting-out and dialysis, the dyes are typically > 95 % pure with respect to organic impurities (*i.e.* side products, remaining starting material *etc.*). Inorganic impurities, such as sodium chloride, are generally around 10 – 20 %. Final mass recovery of dye is typically around 60 % (including inorganic impurities).

4.3 Dye Testing

The series of hydrazide-modified dyes **94 - 97** was subjected to standard testing protocols in order to determine their relative light and ozone fastness. These tests simulate typical environments where prints might be stored or displayed, using standard classes of paper (media). It was hoped that the relative differences in fading between the substitution patterns may reveal aspects of the mechanism by which protection is afforded from light and ozone degradation.

The dyes were loaded into a standard ink vehicle and printed using a standard printer and print-head. A test pattern was printed and subjected to the tests. Fading can then be measured from any changes in colour or optical density.

4.3.1 Ink and Printing

Dyes **94** – **97** were tested for ozone and light fastness at Avecia (Blackley). A generic ink vehicle was chosen, the dye making up 3.5% w/v of the ink. Also added to the ink were glycerol (7.5%), diethylene glycol (7.5%), urea (7.5%) and Surfynol 465 (1%). The remainder of the ink was made up of deionised water. Glycerol and diethylene glycol are humectants, high boiling, water-miscible co-solvents that prevent the evaporation of water from the ink when the printer is not in use. Urea is used to suppress the freezing point of the ink, without affecting viscosity. Surfynol 465 is a surfactant that lowers surface tension, allowing the ink to diffuse rapidly into the medium (see Chapter 1.4). The inks were adjusted to pH 8.5 – 9.5 before being sonicated, filtered and loaded into the ink cartridge. The inks were then printed, using a Canon printer, onto six different types of media: HP printing paper (plain paper); HP Premium Plus MkII (swellable polymer); Ilford Printasia Photo (swellable polymer); Canon Pr101 (microporous alumina); SEC Premium Photo (microporous silica); Ilford Instant Dry (nanoporous metal oxide). These papers were chosen as they represent the spectrum of available media today, covering plain printing paper, swellable polymer media and porous media (see Chapter 1.4). Only a limited number of dyes were tested on swellable polymer media for ozone fastness, as it is known that dyes printed on such media are extremely resistant to ozone fading.[117] This was corroborated by the results obtained for dyes **95**, and so no further tests for ozone fastness were carried out on swellable polymer media.

4.3.2 On-media Colour Measurement

Once printed, the colour properties of a dye may vary significantly from those of the dye in solution. This can be influenced by factors such as pH, paper properties, lighting source *etc.* On-media colour properties are generally measured using a colorimeter (see Chapter 1.6), which simply measures and computes how much of a known amount of light is reflected from an object under a specified light source

(known as the reflectance). From this measurement, reflectance optical density (ROD) can be calculated (Equation 4.2).

$ROD = \log_{10}R^{-1}$, where R = reflectance

Equation 4.2

The ROD is essentially a measure of colour strength across all wavelengths. It is desirable to have a large ROD value, as the dye will give a denser colour on the medium. Table 4.2 shows ROD values for the benzoic acid hydrazide substituted series of dyes on HP Printing Paper.

Dye	ROD
94c	1.06
95c	0.99
96c	1.03
97c	1.02

Table 4.2 ROD values for each dye type on HP Printing Paper

A ROD of > 1 is considered acceptable. The L, a, b, C and h values (see Chapter 1.6) can also be measured using a colorimeter.

As an indication of variation of ROD across paper type, values for **94f** are given in Table 4.3.

Paper	ROD
HP Printing Paper	1.11
HP Premium Plus MkII	1.68
Ilford Printasia Photo	1.66
Canon PR101	1.65
Ilford Instant Dry	1.62
SEC Premium Photo	1.43

Table 4.3 Representative ROD values for each medium

ROD values for all of the dyes studied ranged from ~ 1.0 – 1.7 across all media types. This was not unexpected, as the parent dye is a strong magenta, however it does show that functionalisation of the dye has not adversely affected its optical properties. Higher ROD values are observed for the coated papers compared with plain paper, as on plain paper there are a greater number of voids for the ink to flow into and therefore prints exhibit greater lateral spread and depth of penetration, giving less concentrated surface coverage.

4.3.3 Fastness Tests

Dyes were tested for light and ozone fastness according to Avecia standard protocols. The ozone test is an accelerated test in which the printed ink is exposed to a constant ozone concentration of 1 ppm for 24 h. This test is designed to simulate 100 days in an office environment. The standard light fastness test lasts 100 h at 40% relative humidity. This test represents approximately four years exposure. A reference ink was also tested as an internal standard (Canon reference ink). This acts as a check to ensure that the equipment is functioning correctly, and also allows the comparison of data collected in different experiments. It can also be used to give an estimation of the margin of error present in the tests.

Dye fading is best determined from the ROD percentage loss, a lower value representing less fading. Changes in L, a, b, C and h values can also be useful indicators of fading.

4.3.4 Dye fading results

In general, the dyes tested all performed similarly, with % ROD losses of around 30 – 50% for light fastness. The ozone fastness tests performed on swellable polymer media all gave negligible % ROD losses, as was expected. On the remaining media types the losses observed were around 20 – 40%. All of the results were broadly in line with the results observed for the Canon reference ink (CRI). The results are tabulated in full in Appendix 7.2. As the results were obtained over the course of two separate experiments, the % ROD loss values for both ozone and light fastness were scaled for CRI = 1.00 in order to allow comparison between data sets.

Table 4.4 shows the average ROD loss for each dye across all media (not including the swellable polymer papers for ozone fastness).

	Average ROD Loss[a]	
Dye	Light fastness	Ozone fastness
94f	0.73	1.61
95d	0.88	1.44
95a	0.90	1.28
95c	0.90	1.50
95b	0.94	1.50
95e	1.00	1.56
94c	0.79	1.25
97c	0.91	1.07
96c	0.79	1.14
96b	0.96	1.43
97a	0.89	1.21
96a	0.87	1.32

Table 4.4 Average light and ozone fastness; [a] relative ROD loss *cf.* CRI

Figure 4.8 shows the colour of **94f** (oxamic hydrazide) before and after fading, interpreted from the obtained Lab values. It is intended only as an indication of the changes that occur on fading, as exact reproduction of the data is impossible and the values only have relevance when viewed under the correct lighting source etc.

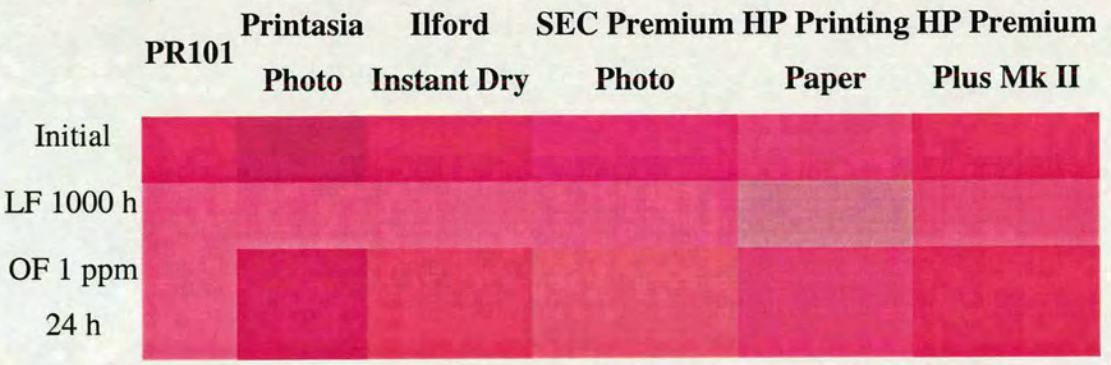

Figure 4.8 Colour change observed following light (LF) and ozone (OF) fastness testing of 94f

The average light and ozone fastness % ROD loss values for each hydrazide substitution pattern across all media types are shown in Table 4.5

	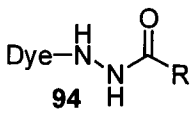 **94**	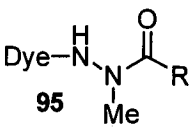 **95**	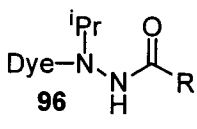 **96**	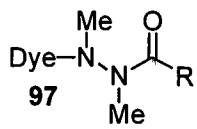 **97**
Light Fastness	0.78	0.96	0.87	0.90
Ozone Fastness	1.47	1.45	1.32	1.15

Table 4.5 Average relative light and ozone fastness test results for each hydrazide substitution pattern

Since the structure of the CRI is not related to the test dyes, no conclusions about the apparently superior light fastness and inferior ozone fastness of the hydrazide-substituted dyes can be drawn. Conclusions can only be made about the relative fastness properties displayed by each of the dyes within the group.

The unsubstituted hydrazide series of dyes **94** appears to show improved light fastness relative to the substituted dyes **95 - 97**. Dye aggregation is known to play a major role in the light fastness of dyes,[118] and it may be that the potential increase in hydrogen bonding in the unsubstituted-hydrazide dyes increases aggregation. It is thought that in dyes that show high aggregation, light fastness is enhanced since there is less surface area per unit mass of the dye available for reaction. Another factor is that the lifetime of the photo-excited state of the dye is possibly shorter in the aggregated dyes, allowing less time for the dye to react.

The reaction of hydrazides with ozone is not well reported in the literature. It has recently been shown, however, that trisubstituted-hydrazides **98** (*e.g.* $R^1 \rightarrow R^5$ = alkyl) undergo oxidative cleavage in the presence of peroxides such as *m*-CPBA **99** *via* electrophilic attack on the more nucleophilic nitrogen atom to generate *N*-oxide **100**. This undergoes a pericyclic rearrangement to give an amine **101** and an *N*-oxide **102** (Scheme 4.7).[119]

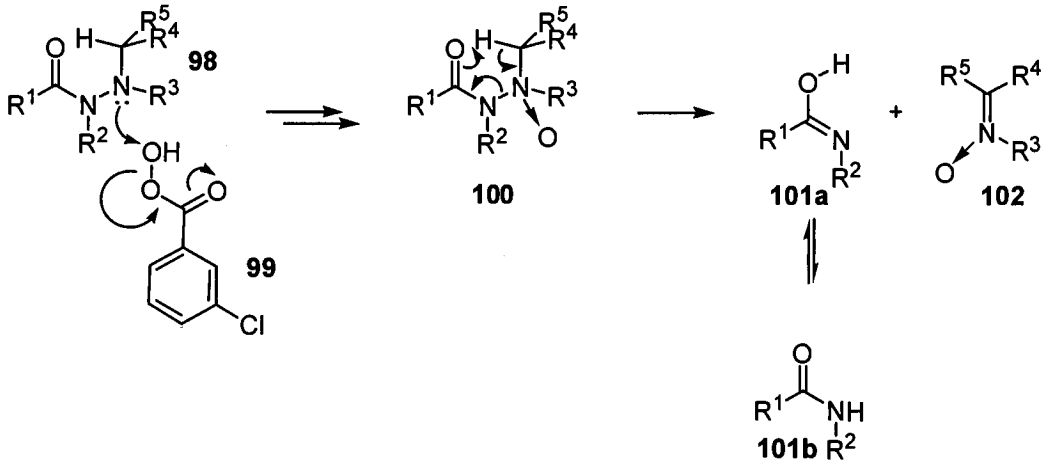

Scheme 4.7

Although this type of reaction was previously unreported in hydrazides, the oxidation of tertiary amines to amine oxides with ozone is well understood.[120] Amides are known to be resistant to ozonolysis, and so the *N*-substituent should not affect the rate of ozonolysis. Since it is thought the *N*-oxide is generated *via* electrophilic attack of ozone then electron-donating groups on the *N'*-nitrogen atom should increase the rate of reaction with ozone. This, then, may represent a pathway by which the *N,N'*-dimethyl-substituted hydrazide dyes could undergo sacrificial oxidation, protecting the chromophore from ozone degradation.

Figure 4.9 shows plots of Hammett's σ and σ^+ constants *versus* corrected % ROD loss for the *N*-methylhydrazide series **95**.

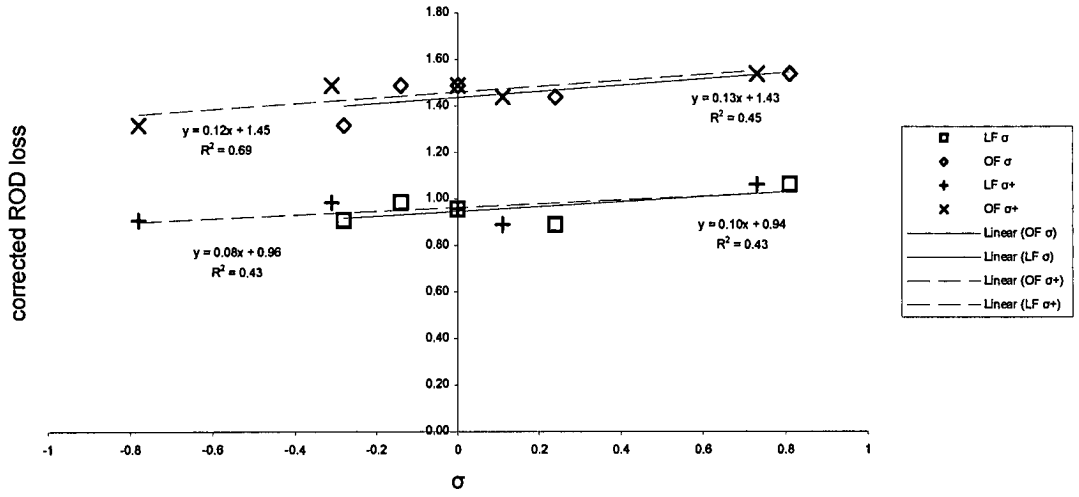

Figure 4.9 Plot of relative light and ozone fastness of 95 versus Hammett σ and σ^+ constants: □ = light fastness *v.* σ; ◊ = ozone fastness *v.* σ; + = light fastness *v.* σ^+; × = ozone fastness *v.* σ^+

Although the differences in reactivity between each substitution pattern are relatively small, if it is assumed that they are significant then some conclusions can be drawn. The slope of the Hammett plot for both light fastness and ozone fastness is < 0.2 in both cases, suggesting that whatever the nature of the protection afforded by the hydrazide, it is independent of the electronic nature of the amide bond. That the *p*-substituent has an appreciable effect on the nature of the hydrazide can be seen in the Hammett relationship obtained from the variable temperature NMR experiments (see Section 3). It can therefore be concluded that either: the site of ozonolysis is too distant from the amide and is not subject to changes in the electronic nature of the amide bond; there is no significant electronic change between the reactants and the transition state; or that there is no appreciable fading resistance afforded by the hydrazide.

All of the dyes tested are comparable with respect to ozone fastness. As has been stated, no appreciable electronic effects on the rate of ozonolyis are apparent. If it is thought that ozone would react with the hydrazide *via* electrophilic attack of a nitrogen atom, it is likely that reaction would occur at the non-amide nitrogen atom, since amides have been shown to be unreactive toward ozone.[120] This would mean the reactive site may be too distant from the aryl ring to be influenced by its electronic effects. If we assume that ozone attack is at the non-amide nitrogen atom

then alkylation of that position would increase the nucleophilicity of the nitrogen atom lone pair, increasing reactivity of the hydrazide moiety with respect to electrophilic attack of ozone. This would allow the hydrazide to act as sacrificial protection for the azo chromophore, increasing the ozone fastness of the dye as a whole. This is borne out by the superior ozone fastness results observed for dyes **96** and **97** *cf.* **94** and **95**. If, on the other hand, the reaction with ozone was one of hydrogen abstraction (*i.e.* a reductive process), the opposite fastness results would be expected to be observed. Since this is not the case, this probably rules out this method of reaction with ozone.

With respect to light fastness, all dyes show similar results. The best individual dye is **94f** (oxamic hydrazide), suggesting that it may the oxamate moiety which offers protection from photolytic degradation. This may be a consequence of the aforementioned tendency of aggregating dyes to resist light fading, as the oxamic hydrazide would be expected to show the most potential for H-bonding.

Analysis of the CIELCh (lightness, L; chroma, C; hue, h; see Chapter 1.6) values reveals that over the timescale of these tests it would appear that the chromophore is being destroyed outright, and no other coloured species are being generated *via* the degradation pathway. This is evidenced by the fact that the hue angle (h) remains roughly the same following degradation. If the dye were reacting at a point distant from the chromophore, without affecting the chromogen, h would be expected to change, reflecting a change in λ_{max} due to the new substituents. The lightness (L) value increases (*i.e.* indicates more whiteness) suggesting that the dye coverage is diminished and that more of the paper is showing through. A decrease in the chroma (C) value also indicates a diminishing in the brightness of the colour, as would be expected if the dye were degrading to colourless components.

4.4 Conclusions

Superior synthetic routes to a series of mono- and di-substituted hydrazides have been developed, showing improvements over literature preparations in terms of both yield and ease of isolation. We have also confirmed the postulated trimeric structure of the product obtained from reaction of benzoic acid hydrazides with formaldehyde, and obtained X-ray crystallographic data on a previously unknown class of hydrazone featuring an unsubstituted methylidene group.

The synthesised hydrazides were then coupled to a dye in order that their effect on the light and ozone fastness of the dye could be assessed. Our studies indicate that hydrazides with no *N*-substituent show slightly improved light fastness compared with substituted hydrazides. Alkylation of both nitrogen atoms appears to enhance ozone fastness, possibly supporting an oxidative mechanism for the reaction of ozone and dye, with the hydrazide providing sacrificial protection of the chromophore.

In order to understand the degradation of the azo chromophore in azonaphthol dyes such as **86**, investigations were made into the reaction in solution of simple azo systems and ozone. From these solution ozonolyses it was hoped that a better understanding of the reaction mechanism could be obtained by examining the initial products of the reaction. These studies are presented in the following chapter.

5 Solution Ozonolysis

Ozone is an extremely powerful oxidising agent ($E° = + 2.07$ V).[121] It is capable of reacting with most unsaturated species (e.g. C=C, C=N, N=N etc.), although it is generally unreactive towards saturated species (C-C, C-O, O-H). Oxidisable ions such as S^{2-} are also highly reactive, forming oxyanions such as SO_3^{2-} and SO_4^{2-}.[122] Ozone can react as an electrophile, nucleophile or *via* 1,3-dipolar cycloaddition.[121] In order, therefore, to understand the process by which the azo chromophore is destroyed by ozone an investigation into the mechanism of the reaction is required. As has already been reported, it is thought that ozone is more reactive towards the hydrazone tautomer than the azo tautomer in azo dye systems. This theory is supported by studies of ozone reactivity towards various functional groups, which have shown the following structure / reactivity relationship:[121]

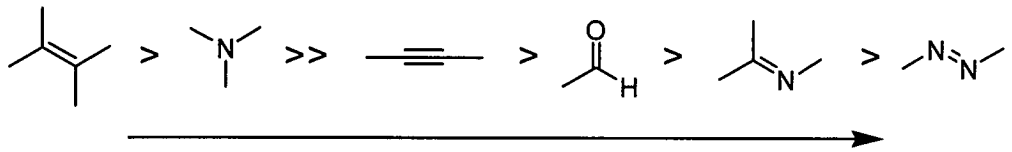

Figure 5.1

5.1 Reaction of ozone with commercial azo dyes†

There have been a number of studies investigating the effects of ozone on the decolourisation of wastewater from dye works. These have been mainly concerned with the rate of decolourisation as related to reactor design and efficiency; there has been a recent review.[50] Broad ranging studies are rare and generally focus on rates of reaction and provide little mechanistic insight. One of the problems with the volume of work published is that it is very difficult to compare the results from different studies. Many studies cover only one or two dyes, and are of little use in determining overall trends. There are many factors that influence the ability to compare results between studies. Differing solvent leads to problems with differences in ozone solubility and the position of the azo / hydrazone equilibrium, as

† The terms azo dye and azonaphthol are used throughout this section. This is for convenience, and is not intended to denote the predominant tautomeric form of the compound under discussion.

well as the possibility of generating other reactive species *e.g.* OH· in aqueous alkaline solutions.[123] Commercially available dyes are often of relatively low purity, hence dye concentration is variable and there may be possible competing side reactions if the dyes are not purified prior to use. The concentration of ozone in solution is frequently not determined, and therefore only pseudo-first order rate constants can be quoted *i.e.* $k_{obs} = k[O_3]$. Meaningful comparison can therefore only be drawn if ozone concentration is identical in each study (which is unlikely). Perhaps the largest problem is that many authors are only concerned with decolourisation; therefore the reaction is monitored by UV/vis spectroscopy at the absorption maximum of the dye. This potentially leads to the results being skewed by the generation of species that absorb in the same region as the parent dye. A better and more accurate method is analysis by HPLC or GC. This allows precise monitoring of the dye during ozonolysis without interference from degradation products (assuming optimised conditions are used).

Since these factors are often either uncontrolled or vary significantly, it is only really possible to compare results within a single study. Unfortunately, there have been few studies covering a large range of dyes. Of those that do cover a range of substrates, such as work published by Shu and Huang on eight different dyes,[124] the structures of the dyes studied tend not to lend themselves to the formation of structure / activity relationships. This particular work also highlights potential problems of dye purity. Acid red 14 and acid red 18 (**103** and **104,** Figure 5.2) are two monoazo dyes included in the study, it is stated that all dyes are used as obtained from the Aldrich Chemical Company, without further purification.

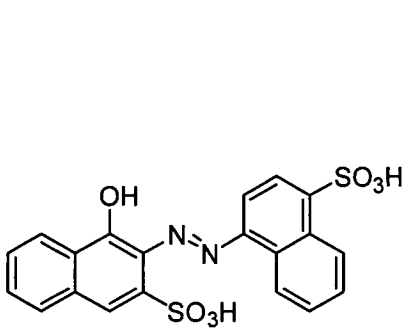

103

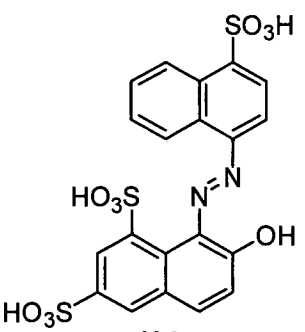

104

Figure 5.2

Observed pseudo first order reaction rate constants for decolourisation are reported to be 0.937 min^{-1} (**103**) and 0.726 min^{-1} (**104**). If these are corrected for purity the rates are essentially the same, as the compounds are obtained from Aldrich with 50% and 75% dye content respectively.

It has been reported that the more azo and other functional groups a dye contains, the slower the reaction with ozone. This would seem reasonable, since complex dyes have more possible reaction pathways for ozonolysis before degradation of the chromophore occurs. Differences in the rate of decolourisation tend to be small, suggesting that in most cases reaction with ozone is rapid regardless of dye complexity *e.g.* the following reactivity order has been observed (Table 5.1):[125]

Dye	$k[O_3]$ / s^{-1}	k^a / M^{-1} s^{-1}
Reactive Black **105**	3.8×10^{-4}	1.9
Direct Red 80 **106**	2.4×10^{-4}	1.2
Direct Green 26 **107**	1.6×10^{-4}	0.8

Table 5.1 Rates of reaction of 105, 106 and 107; $^a[O_3]$ = 0.2 mM

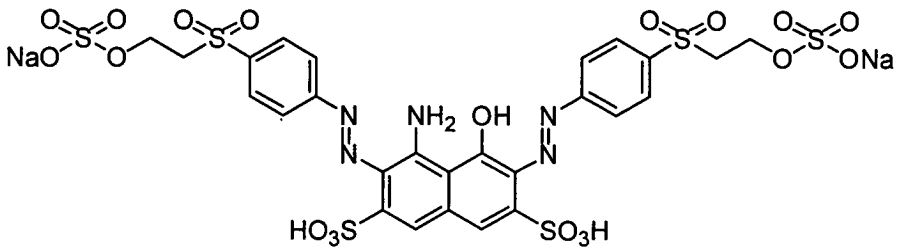

105

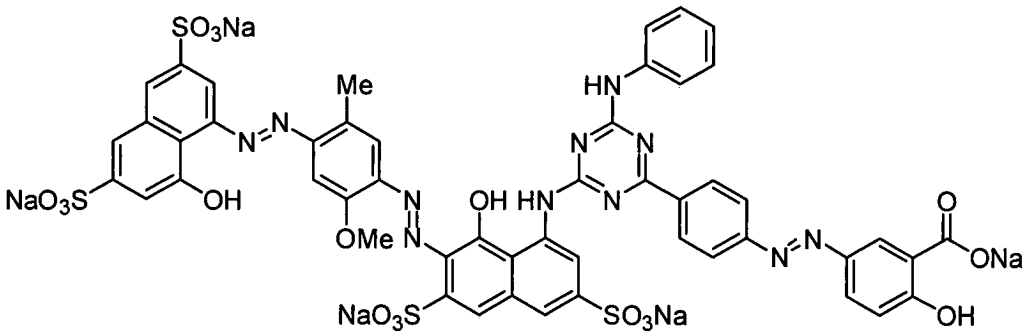

106

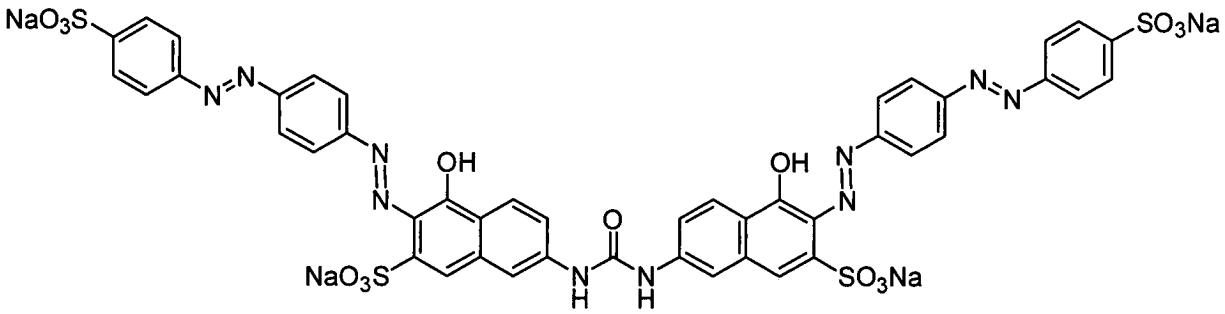

107

Figure 5.3

In this and most other studies reaction monitoring was by carried out by UV/vis spectroscopy. It is therefore probable that the reason for the lower rates observed for more complex dyes is that there is more scope for degradation before colour loss. Rate constants being claimed for the reaction of dye + O_3 are probably incorrect, as it is rates of decolourisation that are observed and no conclusions about the mechanism of ozonolysis or substituent effects can be drawn from these studies.

The conclusion that increasing dye complexity reduces the rate of ozonation is also occasionally misapplied. It has been observed that acid black 1 **4** and direct yellow 4 **108** decolourised slower in the presence of ozone than a range of monoazo dyes (Figure 5.4). [124]

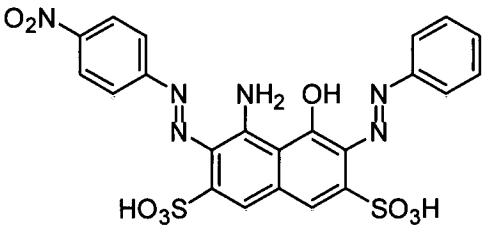

4

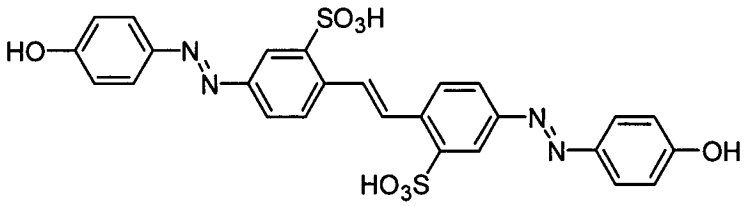

108

Figure 5.4

The authors cite this as evidence that more azo groups decrease the reaction with ozone. In this instance, however, there are probably other factors affecting the observed rate of reaction. In the case of **4**, the dye contains essentially two chromophore units and will therefore still appear coloured after one unit has been destroyed. Since analysis was by λ_{max} measurements only, it is again therefore rates of decolourisation that are being reported, not rates of ozonolysis. The probable reason for the slow apparent rate of degradation of **108** is the ethylene link between the two azophenol components. It has been shown that this undergoes rapid cleavage by ozone in a similar system, direct yellow 12 (**109**), to the azophenol derivative **110** (Scheme 5.1).[126]

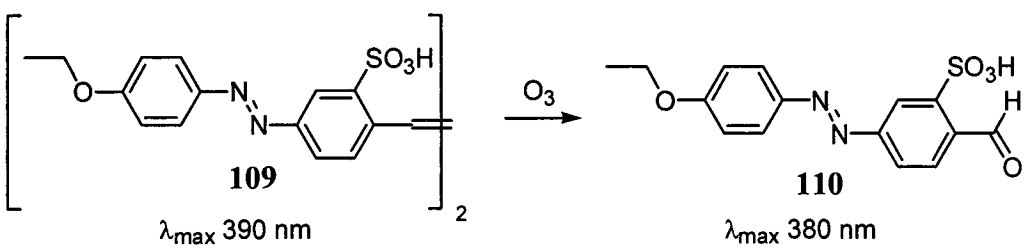

109 λ_{max} 390 nm

110 λ_{max} 380 nm

Scheme 5.1

The small difference in λ_{max} between **109** and **110** means that analysis by UV/vis spectroscopy would not give accurate results for the rate of reaction. Also azophenols, such as those which would be expected to be generated following ozonolysis of **108**, are thought to exist predominantly as the azo tautomer.[127-129] This means that the initial products generated would be expected to be less reactive to ozone than, say, a similar azonaphthol, and so **108** might show a slower rate of reaction than might be anticipated.

5.2 Mechanistic aspects of the reaction of ozone with arylazonaphthols

It is possible to draw some conclusions about the effects of dye substitution on ozonolysis rates from studies that have been performed on simpler azo dye systems, where it is easier to isolate individual effects.

5.2.1 Azo / hydrazone tautomerism, electronic and steric effects

Azo / hydrazone tautomerism, electronic and steric effects are intrinsically linked, since changes in one will affect the others. It is difficult therefore to isolate the cause of changes in ozonolysis rate when, for example, changing dye substitution patterns. Changes in reactivity due to functionalisation of simple arylazonaphthol dyes tend to be relatively small (a 2-fold difference between the fastest and slowest rates is commonly observed), making it difficult to draw definitive conclusions about the effects of functionalisation. A brief summary of the main studies present in the literature is given below.

As has already been mentioned, it is thought that the hydrazone tautomer is more reactive than the azo tautomer in ozonolysis reactions e.g. azobenzene **111** is relatively unreactive towards ozone when compared with *N*-phenyl-*N'*-(1-phenyl-ethylidene)-hydrazine **113** (Scheme 5.2).[130-132]

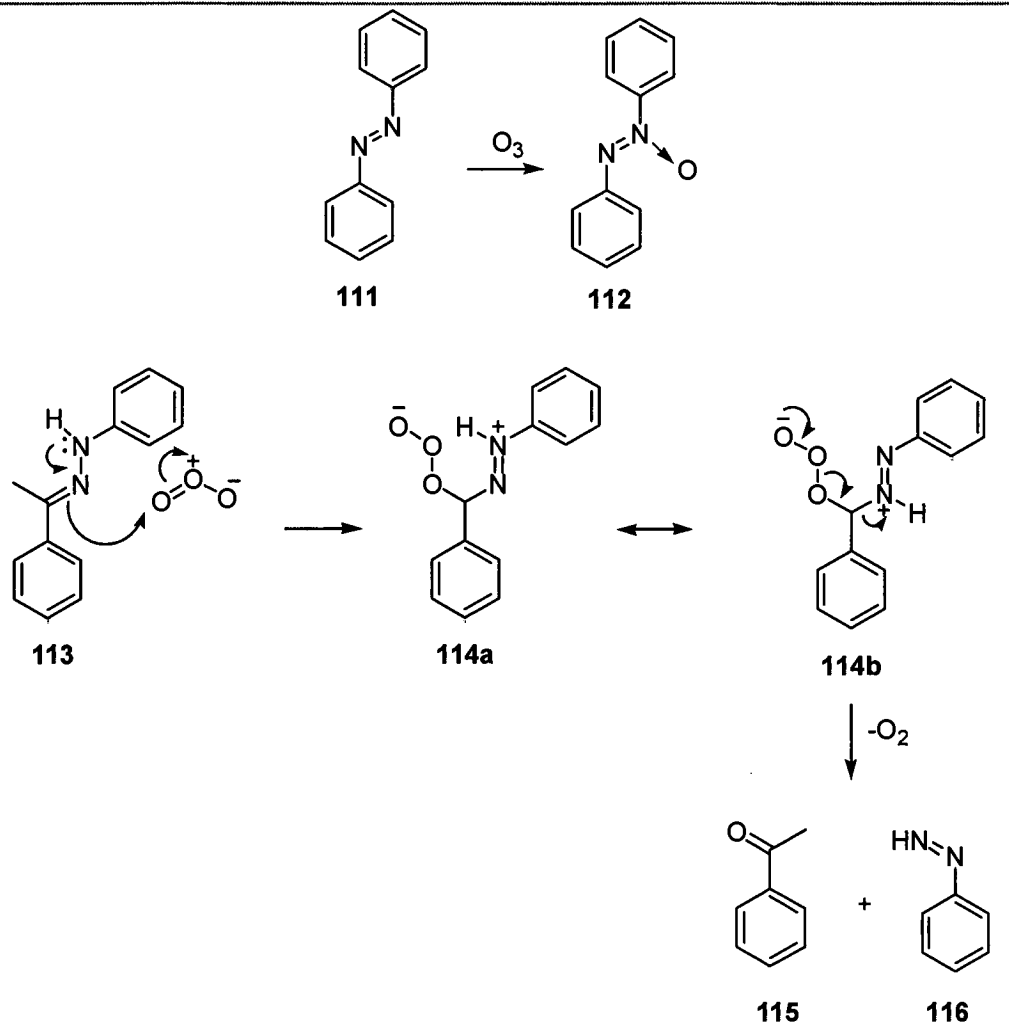

Scheme 5.2

The azo bond of **111** reacts relatively slowly with ozone to form the azoxybenzene **112**, whilst reaction of **113** with ozone rapidly forms acetophenone **115**, and is explained by the electrophilic attack of ozone on the imine carbon atom.

Other evidence for preferential reaction of the hydrazone tautomer is that systems where the hydrazone form is predominant react faster than those where it is not *e.g.* 4-phenylazophenol **117** reacts 3.5 times slower than 2-phenylazophenol **118**,[133] where the intramolecular hydrogen bond stabilises the hydrazone tautomer (Scheme 5.3).[127]

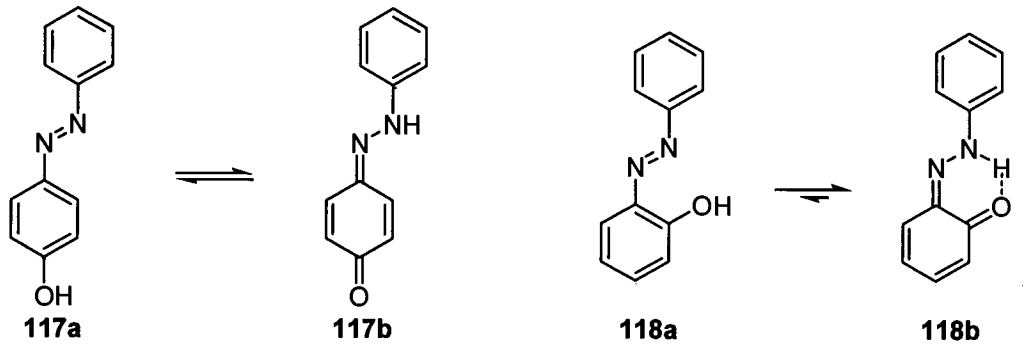

117a **117b** **118a** **118b**

Scheme 5.3

Studies performed in a range of solvents favouring different tautomers of 1-phenylazo-2-naphthol **10** have also shown that reaction is faster in solvents where the hydrazone form is predominant.[51]

It is generally believed that ozone attack on azo dyes is electrophilic, based on observations that increasing the number / strength of electron donating groups in the phenyl ring increases dye reactivity towards ozone whilst electron withdrawing groups decrease reactivity.[51, 134-138] An example is the observed difference in rate: acid red 138 **119** > acid red 1 **120**.[136]

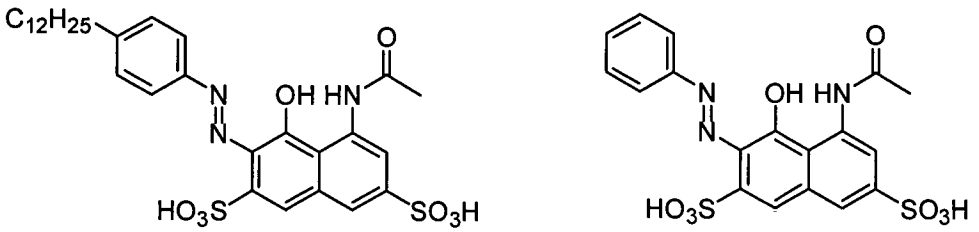

119 **120**

Figure 5.5

The effect of substituents on the rate of ozonolysis of 1-phenylazo-2-naphthol derivatives **121** also supports this theory.[51] Analysis of the reaction was carried out by gas chromatography, and so the results are an accurate determination of the rate of ozonolysis.

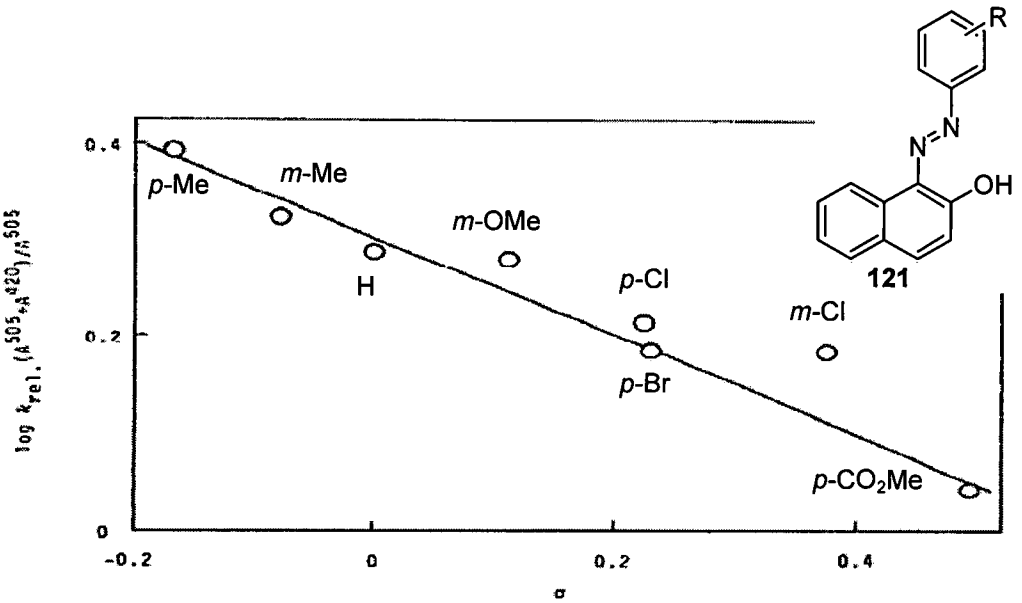

Figure 5.6 **Hammett plot for the ozonolysis of 1-(substituted phenylazo)-2-naphthols 121.**

The reaction exhibits a linear relationship with Hammett's σ constants: ρ = – 0.5 (Figure 5.6), which is consistent with an electrophilic attack of ozone. The authors correct the observed rate constants to reflect the amount of hydrazone tautomer present for each dye, however they do not present the data for the azo / hydrazone ratio and so it is not clear what effect this has on the results.

The authors[51] also present data that provide evidence for the attack of ozone on the hydrazone tautomer. These are based on ozonolysis rates of **121** (R = H) in different solvents, with correspondingly different azo / hydrazone ratios. These ratios are calculated from the intensities of the UV/vis absorbance bands at 505 nm and 420 nm, corresponding to the hydrazone and azo tatuomers respectively (Table 5.2).[139]

Entry	Solvent	A^{505} / A^{420} [a]	η (cp)	Dissolved O_3 mmol l^{-1}	$k \times 10^3$ (s^{-1})
1	*n*-C_6H_{14}	0.65	0.397	2.5	1.39
2	CH_2Cl_2	1.23	0.537	3.7	7.92
3	*n*-C_8H_{18}	0.67	0.703	2.2	0.76
4	$CHCl_3$	1.45	0.701	3.6	8.3
5	CCl_4	1.13	0.734	4.7	3.97
6	C_2H_5OH	1.07	1.78	6.5	0.24
7	*n*-C_3H_7OH	1.13	3.85	4.8	0.18

Table 5.2 **Ozonolysis of 121 (R = H) in various solvents. η = viscosity; [a]ratio of UV/vis absorbance of Hydrazone (505 nm) : Azo (420 nm)[139]**

The data show that the rate of ozonolysis is dependent on both the position of the azo / hydrazone tautomeric equilibrium, and also on the viscosity of the solvent. Entries 3, 4 & 5 show the dependence on the amount of hydrazone tautomer present, with the rate constants increasing with increasing proportion of hydrazone (*n*-C_8H_{18} < CCl_4 < $CHCl_3$). Entries 1 & 3, and 5 & 7 demonstrate the increased rate of ozonolysis for solvents of lower viscosity, compared to those of higher viscosity with a similar azo / hydrazone ratio, suggesting that diffusion of ozone plays a role in the rate of reaction.

A study of 2-arylazo-1-naphthol-3,6-disulfonates **122**[135] with ozone indicates that addition of electron-withdrawing groups decreases the rate of ozonolysis, although the series of dyes chosen makes it difficult to draw definite conclusions from the data (Table 5.3). The intramolecular hydrogen bond in 2-phenylazo-1-naphthols renders the position of the azo / hydrazone tautomeric equilibrium less susceptible to external effects, with the hydrazone form favoured. In this study, however, the presence of substituents in the 2-position of the phenyl ring generally destabilise the hydrazone form due to steric interactions with the hydrazone proton, so it is not clear where the position of the equilibrium is likely to lie, and may be highly substituent dependent

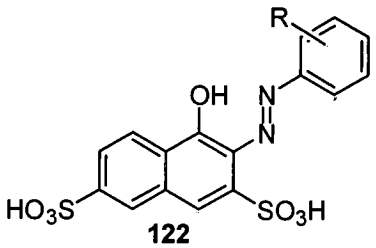

122

Entry	R	$k_{(obs)} \times 10^3$ (s^{-1})
1	H	5.3 ± 0.4
2	2-CF_3	4.3 ± 0.1
3	3-CF_3	5.7 ± 0.5
4	4-CF_3	3.6 ± 0.1
5	3,5-diCF_3	4.5 ± 0.5
6	2-C_4F_9	2.9 ± 0.3
7	2-CH_3	5.4 ± 0.6
8	2-NO_2	2.7 ± 0.3
9	2-Br	4.6 ± 0.1

Table 5.3 Rates of ozonolysis for substituted dyes 122

The observed rates do not differ widely, suggesting that the ozonolysis is generally tolerant of the electronic nature of the dye. The small changes that are observed allow some general conclusions on the influence of substituents in the phenyl ring to be drawn. Addition of electron withdrawing groups at the 2-position inhibits reactivity slightly (entry 1 *cf.* 2, 6-9), supporting the theory that ozone attack is electrophilic, however the differences in rate could also be attributed to steric effects. The importance of steric factors is demonstrated in the difference by reactivity between entries 2 and 6, with the nonafluorobutyl moiety (entry 6) retarding ozonolysis compared with the smaller trifluoromethyl group, which possesses similar electron-withdrawing strength (entry 2).[140] This is attributed to the greater steric bulk of the nonafluorobutyl group preventing access of ozone to the hydrazone reactive centre.

The previously mentioned studies have shown Hammett correlations indicating electrophilic attack of ozone *i.e.* electron-donating groups in the phenyl ring increase

the rate of ozonolysis. It has also been shown that the rate of reaction is dependent on the amount of hydrazone tautomer present in the reaction. However, UV/vis spectroscopic studies have shown that electron-donating substituents favour the less reactive azo form *e.g.* the azo tautomer has been shown in both 1-arylazo-2-naphthols to increase in the order of substituents in the order 4-OMe > 4-Me > 4-H ≈ 4-Cl,[139] and in 4-arylazo-1-naphthols 4-OMe > 4-Me > 4-H ≈ 4-Cl > NO_2.[24, 141] This has been subsequently confirmed by NMR spectroscopic analysis.[142] The ^{13}C NMR shifts of 4-methoxy-; 4-cyano- and 4-nitrophenylazo-2-naphthol were recorded and compared with 2-naphthol **123** and 1,2-naphthoquinone **124** as reference materials (Figure 5.7 and Table 5.4).

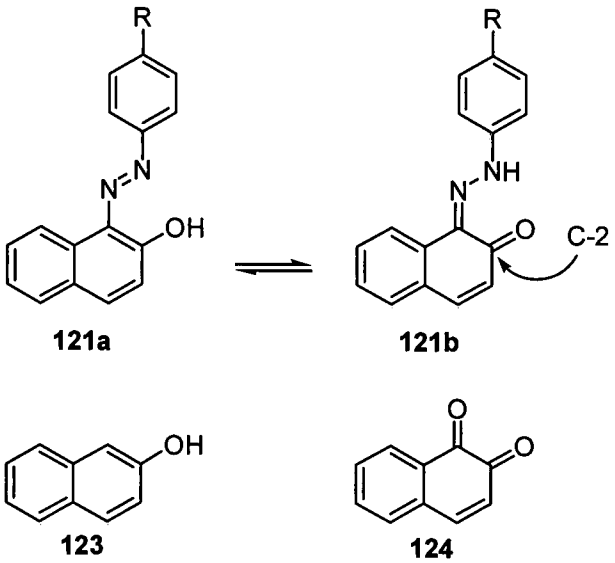

Figure 5.7

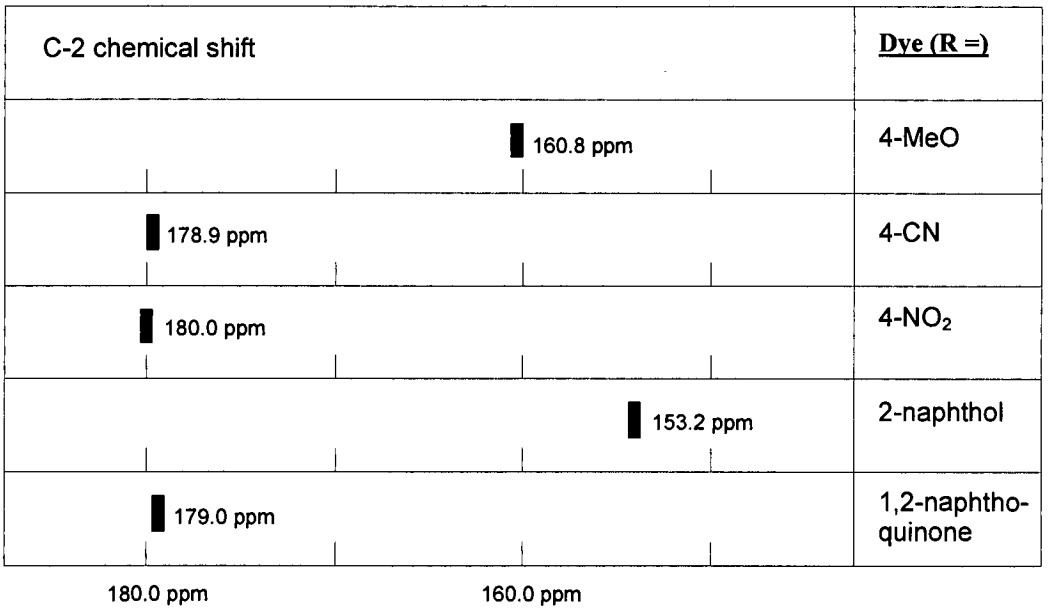

Table 5.4 ^{13}**C NMR shifts of azo dyes 121 and reference compounds 123 and 124**[142]

This indicates that 4-cyano- and 4-nitro-phenylazo-2-naphthol exist as predominantly the hydrazone tautomer **121b**, whereas 4-methoxyphenylazo-2-naphthol is predominantly in the azo form **121a** in $CDCl_3$ solution. This conclusion has also been supported by theoretical studies,[143, 144] and a quantitative analysis of UV/vis data in a series of reports.[145-147]

This trend can be explained in terms of the differing electronic natures of the azo and hydrazone groups. The azo group is an electron acceptor and the hydrazone group is an electron donor, so that the azo group is stabilised by the more electron-donating 4'-substituent, while an electron-accepting group stabilizes the hydrazone form.[24]

5.2.2 Conclusions

The increased rate of ozonolysis observed when electron-donating groups are present in the phenyl ring can be rationalised according to the increase in electron density at the imine carbon (Scheme 5.4), making it more susceptible to electrophilic attack.

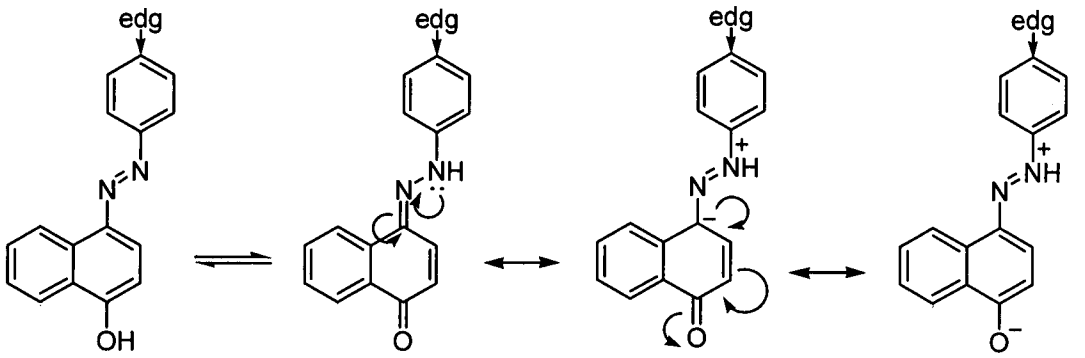

9a **9b** **9c** **9d**

Scheme 5.4

For instance, it has been shown that electron-donating groups in the 4-position of the phenyl ring in arylazonaphthols **9** enhance the rate of ozonolysis. It has also been shown, however, that these same groups favour the azo form of the dye **9a**, which has been shown to be less reactive. Essentially, addition of electron-donating groups enhances the reactivity of the hydrazone tautomer **9b**, but shifts the azo / hydrazone equilibrium position towards the more unreactive azo form **9a**. These opposing effects potentially cancel out, as can be seen by the relatively small Hammett ρ values and reactivity changes observed in studies of 4-arylazo-1-naphthols **9**.[51] In 1-phenylazo-2-naphthol systems **10**, a similar effect could be expected. This is complicated by the fact that substituents in the 2-position of the phenyl ring favour the azo tautomer for steric reasons.[127] This effect is less predictable and so conclusions drawn from dyes of this type should be treated cautiously. For instance, fluoromethyl and (the more bulky) n-fluorobutyl groups have similar electron-withdrawing strengths, but the rate of reaction is slower for 1-(2-C_4F_9)-phenylazo-2-naphthol *cf.* 1-(2-CF_3)-phenylazo-2-naphthol. It is not clear, however, whether the reduction in rate is due to steric crowding of the reactive site or the preference of dyes featuring bulky 2-substituents to form the less reactive azo tautomer. Both probably contribute to the observed results. This is not always apparent, however, since 4-CF_3 and 2-CF_3 substituted dyes exhibit similar reactivities toward ozone. This suggests that the position of the azo / hydrazone equilibrium does not greatly affect rate, yet ozonolysis in different solvents shows markedly increased rates in solvents that favour the hydrazone form.

When looking at commercial dyes, the complexity of the dye is probably not the reason for smaller rates of reaction seen for larger dyes *per se*. If the additional functionality has any effect it is likely to be for the steric or electronic reasons discussed above. Probably the main reason for slower observed degradation of larger dye molecules is that it is the rate of decolourisation that is being measured, rather than the rate of the reaction between dye and ozone.

In order to understand fully the effect that electronic and tautomeric phenomena play in the reaction of azo dyes with ozone, systems must be found where the effects are isolated. This has been done in the case of the azo / hydrazone equilibrium by using different solvents, and has shown that the amount of hydrazone tautomer has a reasonably large effect on rate. Isolating the electronic effects is harder. Ideally a set of substituted arylazonaphthol dyes locked in the hydrazone form would be investigated. This would allow direct analysis of the effect of electron-donating and electron-withdrawing substituents without the complication of a dynamic azo / hydrazone equilibrium. It would also allow the steric effects of substitution in the 2-position of the aryl ring to be investigated.

5.2.3 Reaction mechanism and products

Very little work has been carried out on mechanistic aspects of ozone / dye interaction examining the reaction pathway. Many studies report a significant decrease in pH of the reaction mixture following extended ozonolysis, indicating that the final products of the reaction are organic or inorganic acids. Formate, sulfate, nitrate, oxalate and benzenesulfonate have all been observed following ozonolysis of azo dyes.[148-150] Little has been done to isolate or identify the products formed immediately after ozone attack. All of the useful work that has been done focuses on simple arylazonaphthol systems. The basis of the mechanism is that there is an electrophilic attack of ozone on the hydrazone tautomer.

The dipolar form **9c** has been suggested as the reactive species in ozonolysis reactions,[133, 151] however other authors have questioned the existence of this form.[127] Both of these views are essentially invalid, as **9c** is not a distinct entity, but a canonical form of **9b**.

A proposed mechanism for the reaction of ozone with 4-phenylazo-1-naphthol, *via* the dipolar resonance structure **9c**, is given in Scheme 5.5.[133]

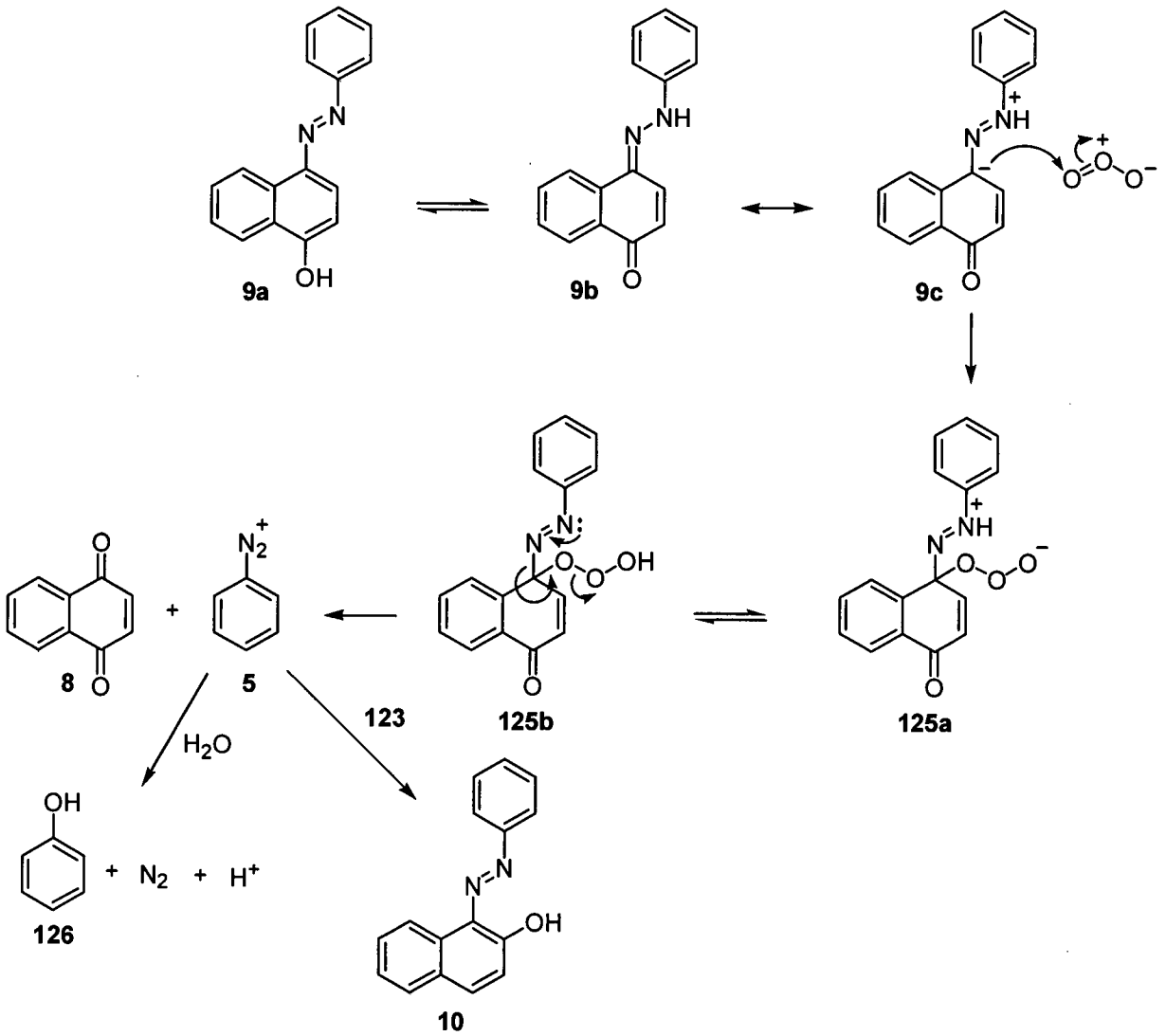

Scheme 5.5 **Proposed mechanism for the ozonolysis of 4-phenylazo-1-naphthol 10**

The two main organic reaction products, 1,4-naphthoquinone **8** and phenol **126**, are detected early in the reaction. The presence of the phenyldiazonium ion **5** was confirmed by trapping with 2-naphthol **123** to form 1-phenylazo-2-naphthol **10**. Nitrogen gas was detected only after extensive ozonation. The scheme presented explains the formation of the observed products, however there are two issues with the arguments in this paper. One is that molecular nitrogen is not observed until long after phenol is first detected, yet they are formed from the same intermediate; the other is that ozone attack could equally be nucleophilic, and the same products would be observed. Both types of reaction (electrophilic and nucleophilic) have been proposed for the reaction of ozone with hydrazones, although it is generally believed

that the reaction is electrophilic with respect to the attack of ozone.[131, 152] The same authors later investigated the reaction of ozone with 1-phenylazo-2-naphthol **10** (Scheme 5.6).[51]

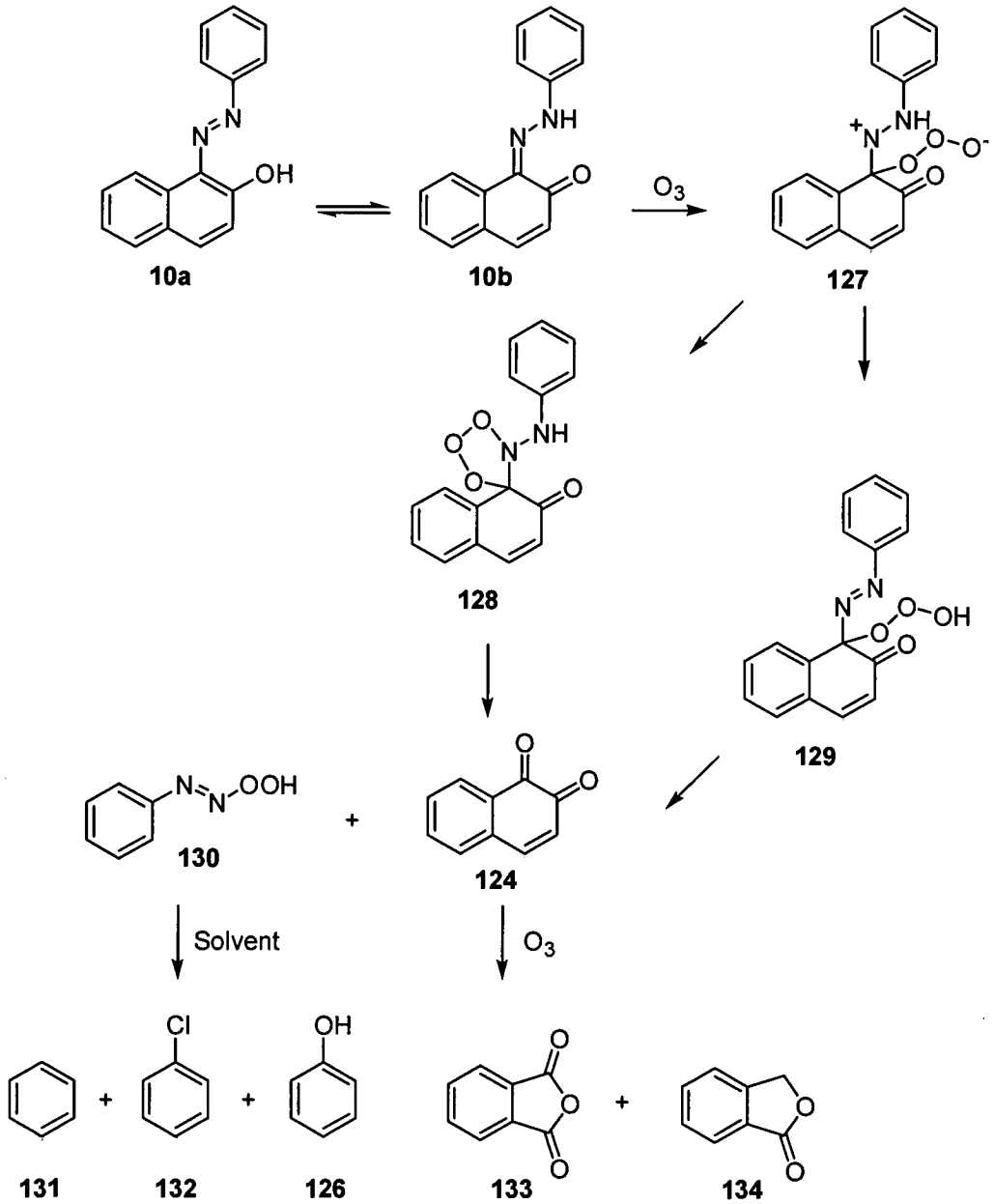

Scheme 5.6 Proposed mechanism for the ozonolysis of 1-phenylazo-2-naphthol 10

In this instance they do not discuss a dipolar resonance structure as a possible contributing canonical form, merely showing that the reaction proceeds *via* electrophilic attack of ozone on the C=N carbon atom of the hydrazone form **10b**. Nor do they suggest that the phenyldiazonium ion **5** is formed, although it is not

stated whether attempts were made to trap it with 2-naphthol **123** as in the previous study.

It seems likely that the malozonide **128** is formed *via* a concerted 1,3-dipolar cycloaddition, rather than the stepwise process proposed by the authors. Chlorobenzene **132** is formed when the ozonolysis is performed in DCM solution, and suggests a radical mechanism is involved somewhere in the reaction. This is also seen in work by the same authors in a study of the ozonolysis of phenylazopyrazolones,[138] where a similar reaction mechanism is proposed and chlorophenol and biphenyl are observed.

Although the reaction mechanisms proposed for the reaction of ozone with simple azonaphthol systems account for the observed reaction products, there is no experimental evidence to support the existence of the reactive intermediates, such as the peroxides **129** and **130**, which have been postulated.

Given the uncertainty over the exact roles played by azo / hydrazone tautomerism and electronic effects in the reaction of ozone with arylazonaphthol systems it was hoped that a series of arylazonaphthol derivatives could be synthesised. Ideally these would allow separate investigation into both effects. It was hoped that the effect of the position of the azo-hydrazone equilibrium could be analysed by ozonolysis of *o*-phenylazonaphthols **10** and **11**, and 4-phenylazo-1-naphthol **9**, since the former is though to exist predominantly in the hydrazone form, the latter in the azo.[127]

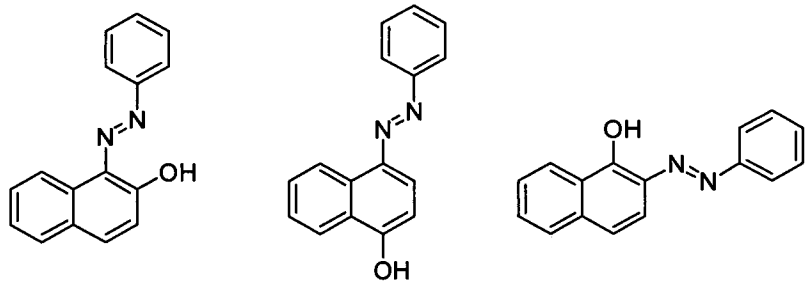

10 **9** **11**

Figure 5.8

Although there have been studies on the rate of ozonolysis of 1-phenylazo-2-naphthol **10** and 4-phenylazo-1-naphthol **9** previously,[51, 133] they have never been reported in the same study and so direct comparison of the rates of ozonolysis is

difficult. To the best of our knowledge, no work has been published on the ozonolysis of 2-phenylazo-1-naphthol **11**.

In a further attempt to determine the effect of the azo / hydrazone equilibrium, ozonolysis of derivatives which are "locked" in the azo and hydrazone forms by methylation of the appropriate functional group will be examined. In this way it is also hoped to synthesise a series of dyes locked in the hydrazone form with a variety of *p*-substituents in the phenyl ring. This should allow investigation of the electronic effects of ring functionalisation with respect to the reactivity of the hydrazone form of the dye, without interference from tautomerism.

5.3 Synthesis of phenylazonaphthols

The most common method of generating azo dyes commercially is *via* a diazo coupling reaction.[9] In the synthesis of naphthol based dyes used in ink jet printing applications this method has the advantage that the regioselectivity of the reaction can be controlled by pH or directing effects (see Chapter 1.5), and the reaction can be performed in aqueous solution.

The coupling reaction of diazonium salts **5** and phenols **126** has been known since the 1860s.[153] At the time, it was postulated that the products were hydroxyazo compounds **117** and **118** (Figure 5.9).

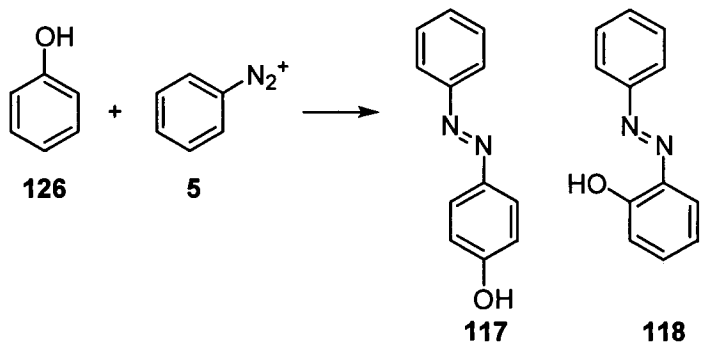

Figure 5.9 **Diazo coupling of phenol 126 and benzenediazonium salt 5**

It was later thought that the hydroxyl proton of 1-phenylazo-2-phenol **118** was labile, and could be capable of bonding to the nitrogen atom of the azo group.[154]

This theory was supported by the work of Zincke and Bindewald (Scheme 5.7).[22]

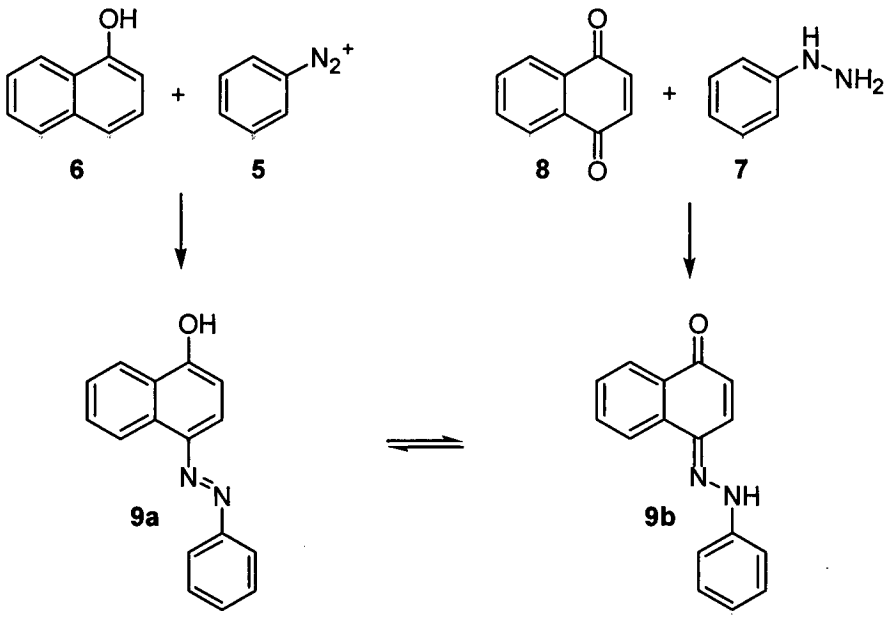

Scheme 5.7 **Diazo coupling of 1-naphthol 6 and benzenediazonium salt and condensation of 1,4-naphthoquinone 8 and phenylhydrazine 7 to give 9**

Condensation of 1,4-naphthoquinone **8** with phenylhydrazine **7**, and the diazo-coupling of the benzenediazonium salt **5** and 1-naphthol **6**, were expected to generate 4-(phenylhydrazono)-4*H*-naphthalen-1-one **9b** and 4-phenylazo-1-naphthol **9a** respectively

It was observed, however, that the two products were indistinguishable. There was much debate on the exact nature of the product, since there was clear chemical evidence for both hydroxyl and carbonyl functionality.[155] This was resolved when the products were shown to exist as a rapidly equilibrating mixture of the azo **9a** and hydrazone **9b** tautomeric forms (Scheme 5.7).[23]

For the investigation into the ozone reactivity of azo dyes, it was hoped to examine three phenylazonaphthol isomers: 1-phenylazo-2-naphthol **10**; 2-phenylazo-1-naphthol **11** and 4-phenylazo-1-naphthol **9** (Figure 5.10); **10** is commercially available, however **11** and **9** must be synthesised.

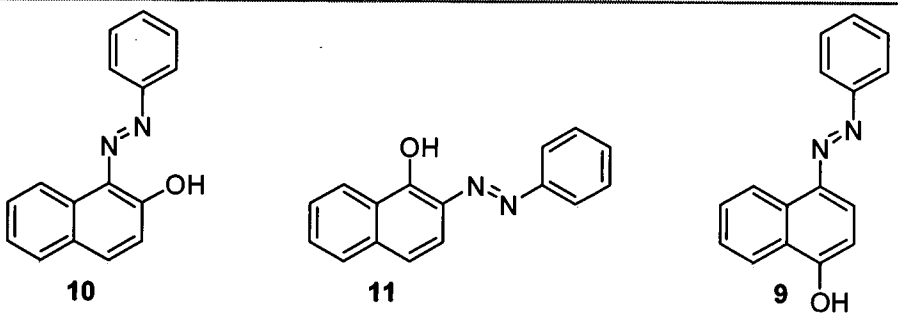

Figure 5.10 **Isomeric phenylazonaphthols**

The synthesis of **9** and **10** was carried out *via* the diazo coupling of diazotised aniline and 2-naphthol. Since the hydroxyl group is *o*- / *p*-directing, this has the advantage that both of the desired isomers are formed in the reaction (Scheme 5.8).

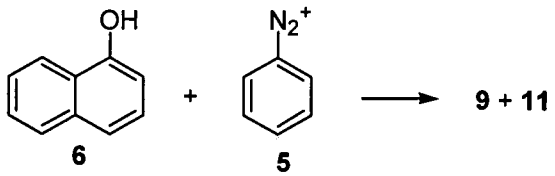

Scheme 5.8 **Diazo coupling of 1-naphthol 6 and benzenediazonium salt 5**

It has been reported that reaction conditions can affect the ratio of the two isomers.[156] In our hands the reaction was performed under standard diazo coupling conditions,[157] as both isomers were required. Aniline (5.0 g, 0.05 mol) in c. H_2SO_4 (16 cm^3) and water (16 cm^3) was cooled to 0 – 5 °C and diazotised by addition of sodium nitrite (4.0 g, 0.06 mmol, 1.2 eq.) in water (20 cm^3). The cooled diazonium **5** salt was added slowly to 1-naphthol **6** (7.2 g, 0.05 mmol, 1.0 eq.) in 10% NaOH (45 cm^3) at 0 – 5 °C. The azo products rapidly formed as a red precipitate. The reaction mixture was allowed to stand in an ice bath for 30 min, before being filtered, washed with water and purified by dry-flash chromatography to give a pure sample of each isomer. The structure of **9** and **11** was confirmed by NMR spectroscopy, using 1D ^1H and ^{13}C spectra, 2D [^1H, ^{13}C] HSQC, [^1H, ^1H] COSY spectra.

5.3.1 Identification of 9

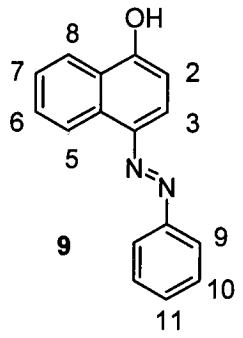

Figure 5.11 4-phenylazo-1-naphthol 9

The lack of coupling between H-2 or H-3 and the other naphthalene ring protons (H-5 / H-8) in the [^{1}H, ^{1}H] COSY spectrum is the key feature identifying 4-phenylazo-1-naphthol **9** (Figure 5.12).

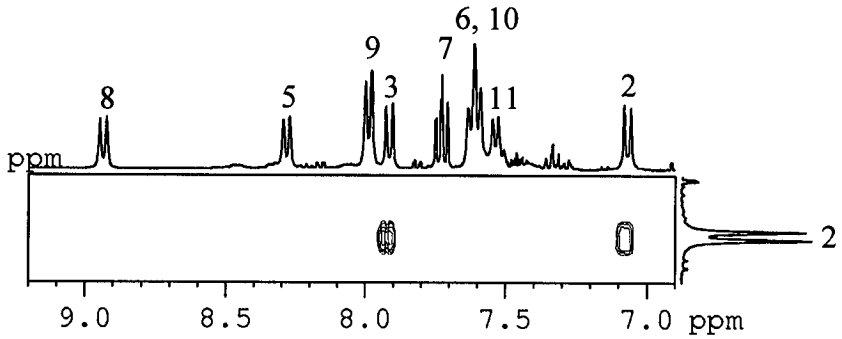

Figure 5.12 Selected view of the [^{1}H, ^{1}H] COSY spectrum of 9

As illustrated in Section 5.2.1, ^{13}C chemical shifts can be used as a guide to the position of the tautomeric equilibrium.[142, 158] The chemical shift of the carbon attached to the hydroxyl group in the azo tautomer is approximated to be *ca.* 151 ppm (using 1-naphthol as a reference) and 184 ppm in the hydrazone tautomer (using 1,4-naphthoquinone as a reference). Since tautomerism is fast on an NMR timescale, an average signal between these two limits is seen. The percentage of hydrazone tautomer present may be calculated using Equation 5.1, where δ_C is the chemical shift of the carbon in question.[158]

$$\%\,\text{hydrazone} = \left(\frac{\delta c - 151}{184 - 151}\right) \times 100\%$$

Equation 5.1

The approximations used in this method do not take into account the potential electronic effects of the hydrazone or azo moieties on the ^{13}C shift. Synthetic routes to 4-phenylazo-1-naphthol derivatives locked in the azo and hydrazone forms will be described later in this chapter. This allows a potentially more accurate determination of the azo / hydrazone tautomeric equilibrium by modification of Equation 5.1 to reflect the ^{13}C chemical shifts observed in these compounds. The locked hydrazone tautomer shows a quaternary signal at 184.6 ppm, the locked azo tautomer shows a signal at 157.4 ppm. Using these values in Equation 5.1 gives the ratio of azo : hydrazone tautomers as 74 : 26 (δ_C = 159 ppm). This validates the assumptions made by the previous authors, as the ratio when using 1-naphthol and 1,4-naphthoquinone as reference compounds is 76 : 24.

5.3.2 Identification of 11

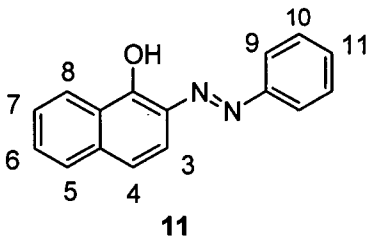

11

Figure 5.13 2-phenylazo-1-naphthol **11**

The key information for identification of 2-phenylazo-1-naphthol **11** is found in the [^1H, ^1H] COSY NMR spectrum. Figure 5.14 shows the cross-peak from H-4 → H-8, due to the long range W-coupling through the naphthalene ring. There is also a small coupling from H-4 → H-5, although this is not visible in the figure shown.

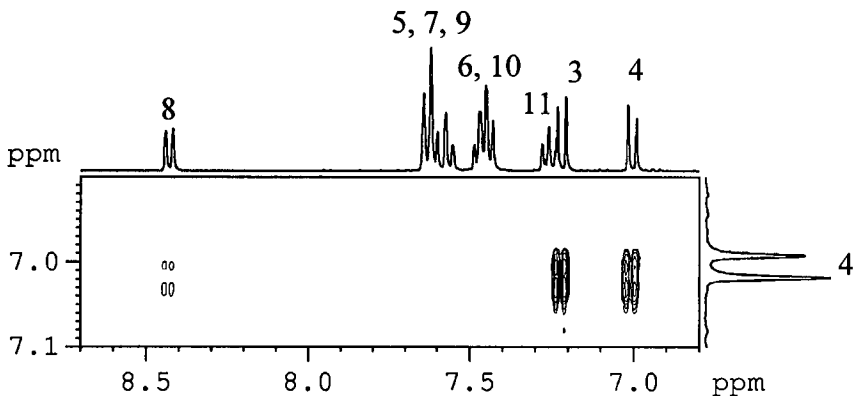

Figure 5.14 **Selected view of the [^{1}H, ^{1}H] COSY spectrum of 11**

The azo / hydrazone ratio can be calculated in a similar manner to **9**. Unfortunately the locked hydrazone tautomer of **11** could not be synthesised, and so 2-naphthol and 1,2-naphthoquinone were used as reference compounds for the approximation of the azo and hydrazone tautomers respectively (Equation 5.2).

$$\%\ \text{hydrazone} = \left(\frac{\delta c - 154}{180 - 154}\right) \times 100\ \%$$

Equation 5.2

Compound **11** has a quaternary resonance in the ^{13}C NMR spectrum at 174 ppm, giving an azo : hydrazone ratio of 24 : 76. Compared with **9**, the hydrazone form is stabilised by the presence of the intramolecular hydrogen bond between the amine and the carbonyl groups, and so the azo / hydrazone tautomeric equilibrium position lies towards the hydrazone tautomer.

5.4 Synthesis of phenylazonaphthol derivatives

In order to study the effects of azo / hydrazone tautomerism on the rate of ozonolysis of phenylazonaphthols, syntheses of *O*- and *N*-methyl derivatives of **9** – **11** were required. These derivatives are "locked" in the azo and hydrazone forms respectively, and should give an insight into the relative rates of ozonation of the azo and hydrazone tautomers of the parent phenylazonaphthols.

5.4.1 1,2 compounds

This section will deal with attempted synthetic routes to the following compounds:

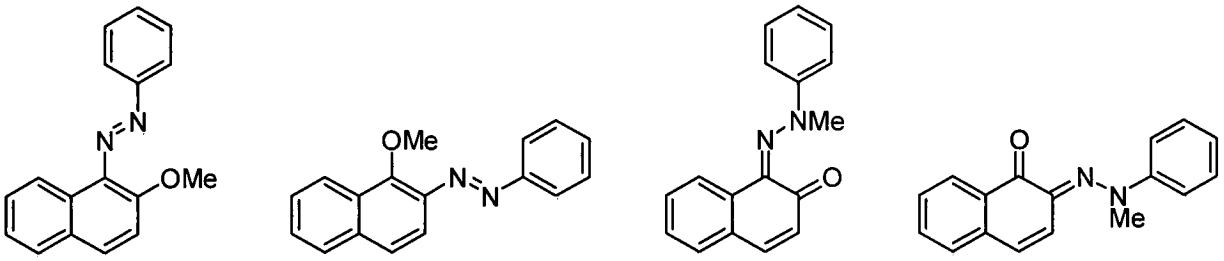

135 **136** **137** **138**

Figure 5.15 **Locked tautomers of 1-phenylazo-2-naphthol 10 and 2-phenylazo-1-naphthol 11**

5.4.2 *O*-methyl derivatives 135 and 136

There have been a number of syntheses of the *O*-methyl derivatives of the type **135** and **136**. All are based on methylation of the OH group of the parent azonaphthol, using diazomethane,[23, 159] dimethyl sulphate,[156] or methyl iodide.[160-162] Since the arylazonaphthols are known to show the chemical behaviour of both azo and hydrazone forms,[163, 164] it was hoped that HSAB theory could be applied in order to influence the site of methylation.[165] HSAB theory predicts that using a hard base / methylating agent should favour methylation of the hard oxygen anion, whereas the reverse would favour methylation of the softer nitrogen anion. There has been a recent review of the concept.[166]

The most recent reference to methylation of **10** uses methyl iodide in toluene at 70 °C, with potassium hydride as base.[161] The authors report a 62% yield of **135** for the reaction, following column chromatography. The formation of **137** is not reported. In our hands, the reaction of **10** with methyl iodide under these conditions produced a complex mixuture of products, from which **135** was isolated in *ca.* 30% yield following dry-flash chromatography. Another major product was isolated from the crude reaction mixture, in *ca.* 20% yield. This has been identified as methyl-naphtho[1,2-*d*]oxazol-1-yl-phenylamine **139**. The structure was confirmed by MS and NMR spectral analyses, as described in the following section.

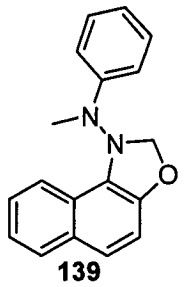

139

Figure 5.16 **Major side product in the methylation of 1-phenylazo-2-naphthol 10**

5.4.3 Identification of 139

ESI-MS analysis of compound **139** gave a molecular weight of 276. [^{1}H, ^{1}H] and [^{1}H, ^{13}C] 2D NMR spectroscopic data showed that the naphthalene and phenyl rings were unchanged. A methyl signal is observed at δ_H = 3.36 ppm and δ_C = 45.6 ppm in the ^{1}H and ^{13}C NMR spectra respectively. This shift is consistent with a H_3C-N shift. For comparison, the H_3C-O shift in **135** is observed at δ_H = 4.00 ppm and δ_C = 57.3 ppm. 1D ^{13}C NMR DEPT experiments show the presence of an additional signal corresponding to a CH_2 carbon. The CH_2 resonance is observed at 71.6 ppm, indicating that it must be adjacent to at least two inductive electron withdrawing groups. The 1D ^{1}H nmr spectrum shows two doublets at 5.42 ppm and 5.85 ppm, ^2J = 10.2 Hz. A geminal coupling between these two protons is observed in the 2D [^{1}H, ^{1}H] COSY spectrum. The 2D [^{1}H, ^{13}C] HSQC spectrum confirms they are located on the same carbon atom (Figure 5.17).

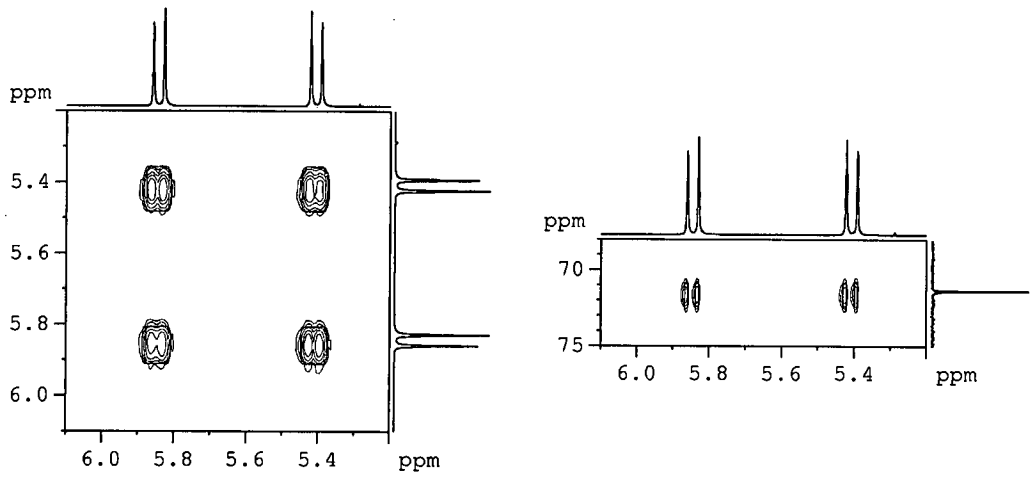

Figure 5.17 **Selected views of the [^{1}H, ^{1}H] COSY and [^{1}H, ^{13}C] HSQC spectra of 139**

The 2D [^{1}H, ^{1}H] NOESY spectrum allows complete characterisation of the product. The key features (shown in Figure 5.18) are: H3 → H10a (s) and H10b (w) (phenyl ring to methylene); H11 → H10b (s) and H10a (w) (methylene to methyl); H11 → H9 (methyl to naphthyl ring) and H9 → H3 (naphthyl ring to phenyl ring).

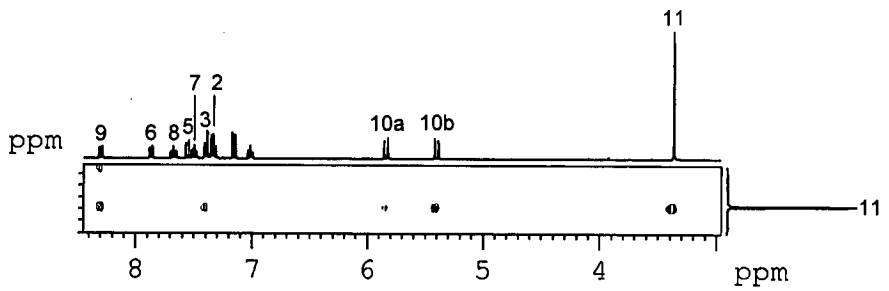

Figure 5.18 **Selected view of the [^{1}H, ^{1}H] NOESY spectrum of 139**

Figure 5.19 demonstrates how these interactions support the proposed tricyclic ring structure for **139**. The structure shown is an energy-minimised structure obtained using MM2 molecular modelling parameters.

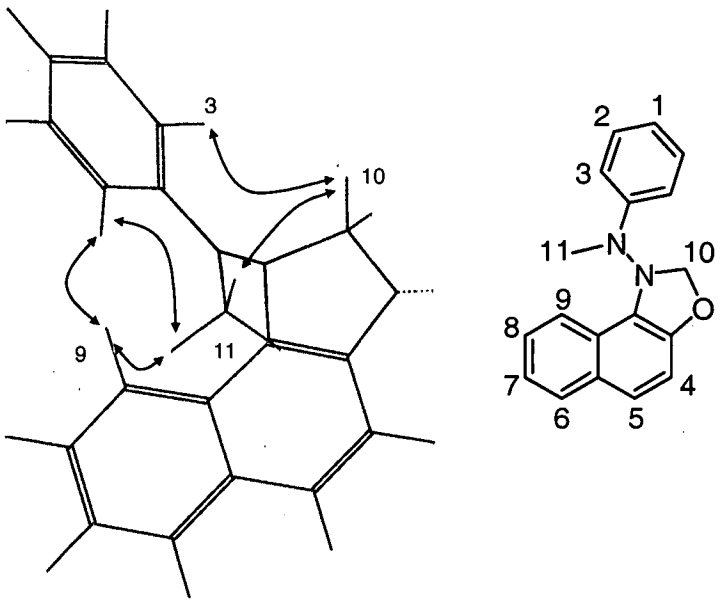

Figure 5.19 Key NOESY interactions of 139

The full NMR spectroscopic data used to characterise **139** is given in Appendix 7.2

A reaction mechanism accounting for the formation of **139** is proposed in Scheme 5.9.

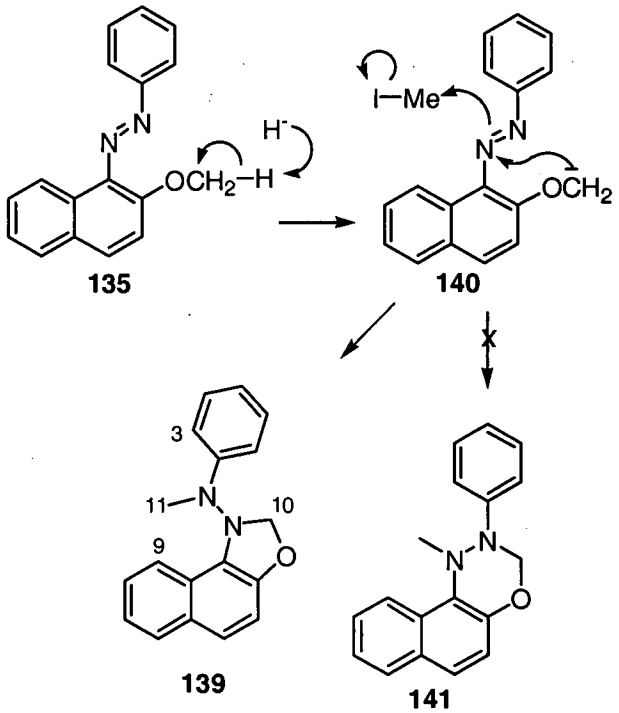

Scheme 5.9 Proposed mechanism for the formation of 139

Although the anion **140** is an unusual species, it would appear to be the most rational explanation for the observed product. The cyclisation step is 5-*exo-trig*, which is favoured by Baldwin's rules.[167] The alternative cyclisation, to form the six-membered ring **141,** would be 6-*endo-trig*, which is also favoured, but less so than 5-*exo-trig*. If **141** were the structure of the product, however, it seems unlikely that there would be the observed NOESY correlation between H10 and H11. Free rotation around the N-N bond of **139** means that both the H3 and H11 protons would be expected to see H10a+b and the naphthalene *peri*-proton H9.

5.4.4 Methylation optimisation

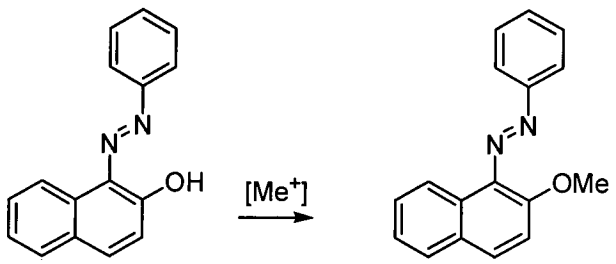

10 **135**

Figure 5.20 Methylation of 1-phenylazo-2-naphthol 10

Since the previous synthesis of *O*-methyl derivatives had proved unreliable in our hands, an improved synthetic route was sought. 1-Phenylazo-2-naphthol **10** is commercially available, and so it was chosen as a test compound for the investigation. HSAB theory predicts that K_2CO_3 / Me_2SO_4 would favour *O*-methylation, whilst Cs_2CO_3 / MeI would favour *N*-methylation. Attempted syntheses using Me_2SO_4 were unsuccessful, even after extended reaction times and heating, with starting material recovered fully. Microwave irradiation also failed to yield any of the desired product.

It can be reasoned that use of K_2CO_3, MeI and DMF (a hard base, a soft alkylating agent and a hard solvent) may produce a mixture of *N*- and *O*-alkylation, giving access to both desired compounds. Table 5.5 outlines the reaction conditions used in optimisation of the method on a 0.5 g scale.

Run	MeI / eq.	Base /eq.	Time	T / °C	% yield[a]
1	1.5	1.1[b]	18 h	RT	< 5
2	5.0	1.5[b]	18 h	RT	< 5
3[c]	5.0	1.5[b]	18 h	RT	< 5
4	5.0	1.1[b]	18 h	50	< 5
5	5.0	1.1[b]	10 min	ω[d]	< 5
6	5.0	1.1[e]	18 h	RT	< 5
7	10	2.2[e]	72 h	RT	~ 50
8	40	5.0[b]	120 h	RT	94[f]

Table 5.5 [a]**135, based on HPLC area %;** [b]**K_2CO_3;** [c]**Ag_2O, 5 eq. added[168];** [d]**ω: 300mW; 250 psi; 120 °C;** [e]**Cs_2CO_3; 0.05 g scale;** [f]**isolated yield, recovered as a mixture of *cis* and *trans* isomers**

Use of Purdie methylating conditions[168] or microwave irradiation (entries 3 and 5 respectively) did not yield any methylated product. Changing the base from K_2CO_3 to Cs_2CO_3 and extending reaction times gave the *O*-methyl product **135**, but did not yield any of the desired *N*-methyl product **137**, as might be expected using a softer base (entry 7). Using a hard base (K_2CO_3), extended reaction times (120 h) and a large excess of methyl iodide (~ 40 eq.) the desired *O*-methyl product was obtained in 94% yield. HPLC analysis showed the presence of two products, with retention times of 11.4 and 13.4 min. It was initially hoped that these would represent the *N*- and *O*-methylated derivatives **135** and **137**, however following workup the product was obtained as a red oil and shown to be a mixture of two *O*-methyl derivatives, identified by two resonances in the 1D ^{13}C NMR spectrum at 55.5 ppm and 57.3 ppm. Further spectroscopic observations suggested that the product was a mixture of *E* and *Z* stereoisomers of **135**. The mixture crystallised on prolonged standing to give a single product, HPLC RT 13.4 min. This product was characterised as the *E*-stereoisomer **135** by 1D and 2D NMR experiments. Formation of the previously observed cyclisation product **139** did not occur, presumably due to the weaker base (K_2CO_3 *cf.* KH) and generally milder conditions employed in the optimisation reactions.

5.4.5 Identification of *E*-135

The key features identifying the methylation product as the ***E*-135** isomer are as follows. The position of the CH_3 signal in the 1D ^1H and ^{13}C spectra (δ_H = 4.00 ppm; δ_C = 57.3 ppm) unambiguously confirms the presence of a O-Me group. This is confirmed by the [^1H, ^1H] NOESY correlation between the OCH_3 and the naphthalene proton in the 3-position (Figure 5.21).

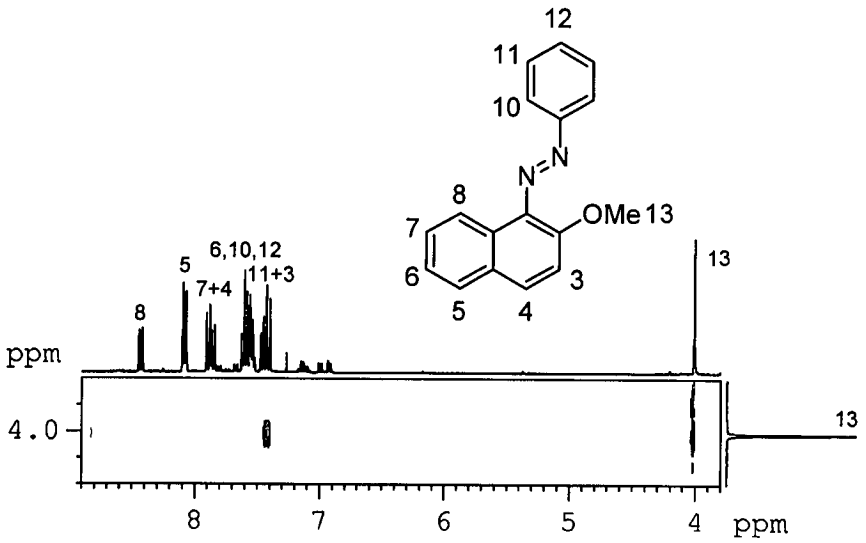

Figure 5.21 **Selected view of the [^1H, ^1H] NOESY spectrum of 135**

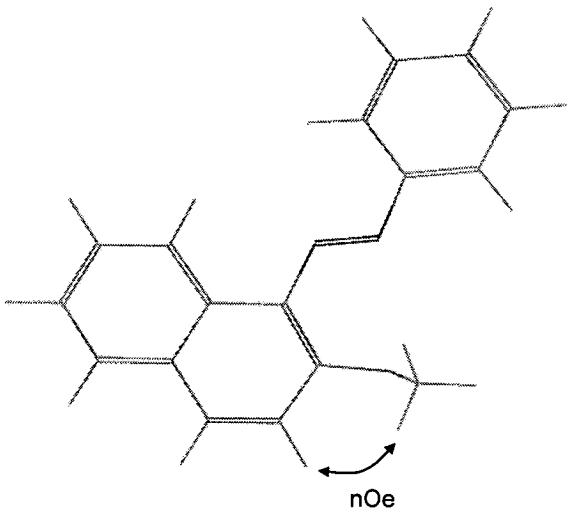

Figure 5.22 **Energy minimised structure of 135, obtained using MOPAC parameters**

There are no NOESY correlations visible between the two aromatic rings, indicating the *E*-isomer. Our findings support the theoretical calculations that the *E* form of 1-phenylazo-2-naphthol **10** is the preferred stereoisomer (Figure 5.22).[169]

It was possible to induce re-isomerisation using UV light at 340 nm. After 1.5 h the mixture was an approximately 1 : 1 ratio of *E* and *Z* stereoisomers, showing identical spectroscopic data to the crude reaction mixture.

5.4.6 Synthesis of 2-phenylazo-1-methoxynaphthalene 136

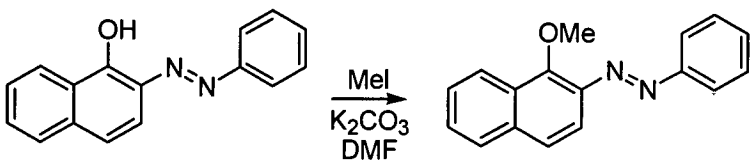

11 **136**

Figure 5.23 **Methylation of 2-phenylazo-1-naphthol 11**

Interestingly, the reaction of 2-phenylazo-1-naphthol **11** with methyl iodide was much more facile, with complete reaction observed in around 30 min, with only 5 eq. of methyl iodide and 2 eq. of K_2CO_3 to give 94% yield of **136**, present as the *E* isomer. The reaction proceeds in high yield and purity, the structure was confirmed by similar methods to that of **135**. The ^1H and ^{13}C chemical shifts observed for the methyl signal are at 4.42 and 65.0 ppm respectively, characterising **136** as the O-CH_3 product. **135** is thought to be present as the *E* stereoisomer as there are no visible [^1H, ^1H] NOESY correlations between the phenyl and naphthyl rings. It is acknowledged that the absence of nOe data cannot be considered definitive in structural assignments, however. It is not clear why the methylation reaction proceeds faster for **136** *cf.* **135**. It might be expected that the reaction would be less favourable, due to adverse interactions with the *peri* proton of the naphthalene ring. This is clearly not the case, although no obvious explanations are apparent. The isolation of **136** as a single stereoisomer is also unexpected; however it may be that the methylation of 1-phenylazo-2-naphthol **10** also yields a single stereoisomer **135**, which then isomerises over the extended course of the reaction.

5.4.7 Synthesis of *N*-methyl derivatives

As none of the desired hydrazone products **137** or **138** were recovered from the methylation reactions, attention was turned to other methods for their synthesis. The condensation of a *N*-phenyl-*N*-benzylhydrazine **142** and 1,2-naphthoquinone **124** has been reported to give **143** (Scheme 5.10).[170]

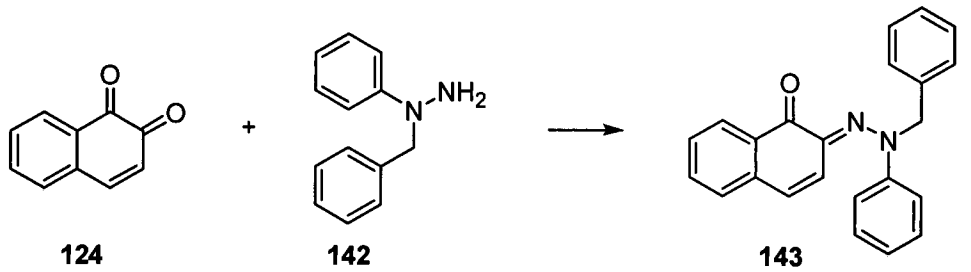

124 **142** **143**

Scheme 5.10

In Bergmann's preparation, solutions of 1,2-naphthoquinone **121** in glacial acetic acid and *N*-benzyl-*N*-phenylhydrazine **142** in conc. hydrochloric acid were mixed and left at 0 °C for twenty-four hours.[170] The dark violet precipitate of **143** was then filtered and recrystallised from ethanol. Identification was by means of elemental analysis ($C_{23}H_{18}N_2O$ requires 81.6% C, 5.4% H; found 81.3% C, 6.1% H). The authors state that condensation is at the 2-position, although offer no evidence for this regioselectivity.

It was hoped that this methodology might be adapted to the synthesis of **137** and **138** (Scheme 5.11). As has been noted, it is thought that the reaction favours condensation at the 2-position **138**.[170, 171] This may be due to *peri*-interactions, disfavouring condensation at the 1-position **137**.[172]

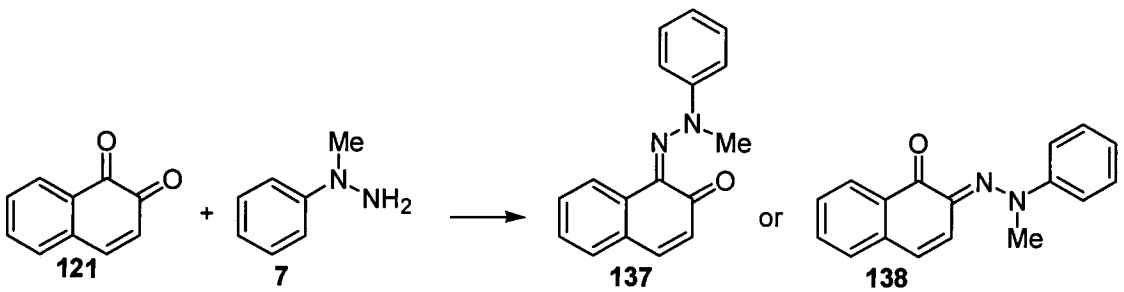

121 **7** **137** **138**

Scheme 5.11

A solution of *N*-methyl-*N*-phenylhydrazine **7** (0.05 g, 0.4 mmol) in aqueous acetic acid (20%, 5 cm^3) was added slowly to a stirred suspension of 1,2-naphthoquinone **124** (0.06 g, 0.4 mmol, 1.0 eq.) in aqueous acetic acid (20%, 10 cm^3). A red precipitate rapidly formed and the solution was stirred for 1 h. The precipitate was recovered by suction filtration, washed with acetic acid (20%, 20 cm^3) and water (20 cm^3) and dried in a dessiccator. ESI-MS analysis of the product showed a MW of 278, indicating that the product was not the expected hydrazone but the 1,4-addition product **144**. Detailed discussions on the structure of the product are given in the next section.

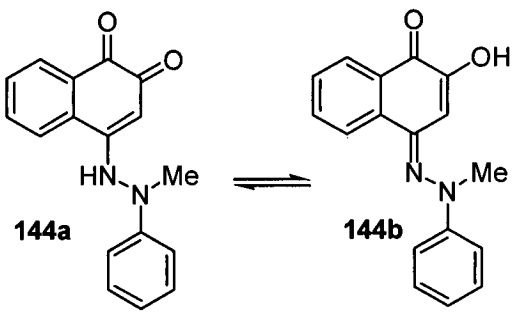

Scheme 5.12 Michael addition product of 124 and 7

5.4.8 Identification of 144

^1H NMR, ^{13}C NMR and MS data confirmed the identity of the product from the reaction shown in Scheme 5.11 as **144**, present in $CDCl_3$ solution as the eniminol tautomer **144b**.

The ESI-MS shows a MW of 279 $[M+H]^+$, corresponding to structure **144**. The main features in the NMR spectra indicating the addition product **144** (as opposed to the condensation products **137** or **138**) are the singlet in the ^1H NMR spectrum at 7.03 ppm, and the 8 CH resonances visible in the ^{13}C DEPT135 NMR spectrum (*cf.* 9 CH peaks in the expected hydrazone). The ^{13}C 1D NMR spectrum shows six quaternary signals (*cf.* 5 in the hydrazone) and a single peak in the carbonyl region, at 179.2 ppm, indicating that eniminol **144b** is the major tautomeric form. The structure is further confirmed by the NOESY correlations between the *N*-methyl signal H13 and H3 / H10 (Figure 5.24)

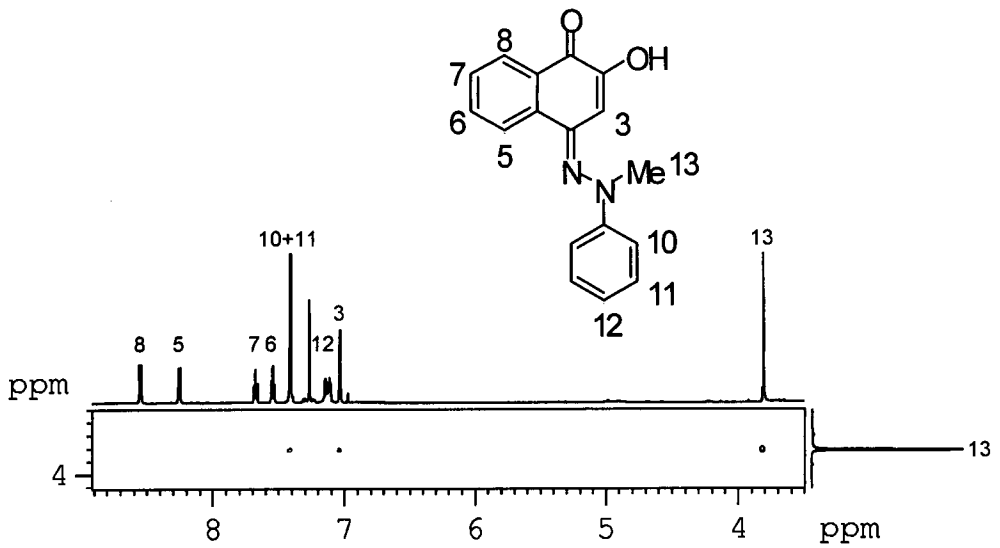

Figure 5.24 **Selected view of the NOESY spectrum of 144b**

This structural assignment is further supported by EI-MS fragment data. The main breakdown peak is 261 $[M\text{-}OH]^+$. Fragments corresponding to phenyl (77), Ph-N (91), Ph-N-Me (106) are also observed.

An interesting difference between **144** and products isolated from similar reactions with amines[173] is the preferred tautomeric form of the two structures. We have unambiguously identified **144** as the eniminol **144b**, whereas the product of the reaction of 1,2-naphthoquinone with aryl amines **145** exists as the enaminone tautomer (Figure 5.25)

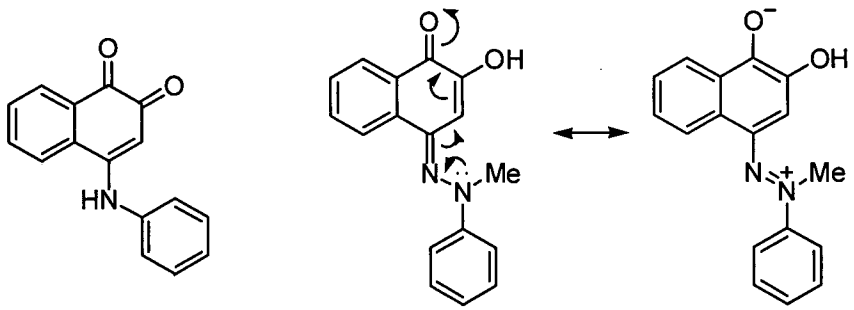

145 **144b** **144c**

Figure 5.25

It is thought the reason for this difference lies with the ability of the lone-pair of the second nitrogen atom in **144b** to delocalise into the ring system (**144c**). This push-pull system stabilises the eniminol form **144b** and is not available to compounds derived from amines, such as **145**.

5.4.9 Michael-Addition reaction

The reaction was repeated under a variety of conditions, using the same method as previously (Table 5.6). In each case the product was that of the Michael addition of the hydrazine to the naphthoquinone ring (Scheme 5.13).

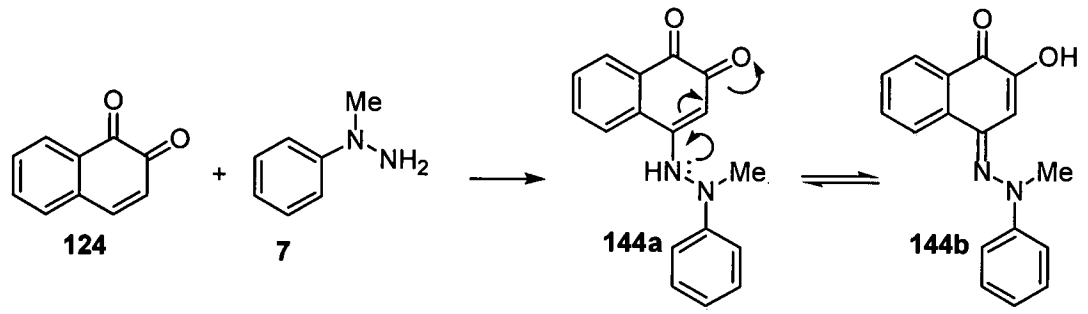

Scheme 5.13

Run	Solvent	Temperature	Yield of **144**
1	Aq. AcOH (20 %)	RT	48
2	MeOH	RT	59
3	DCM	RT	62
4	H_2O (pH 3)	RT	51
5	H_2O (pH 7)	RT	38
6	H_2O (pH 11)	RT	49

Table 5.6 Attempted syntheses of 144

Michael reactions of 1,2-naphthoquinones are known to occur with aromatic and aliphatic amines,[173, 174] and there have been some reports of the addition of hydrazines in this manner.[175]

The results of our investigation differ from those of Bergmann *et al.* (Scheme 5.10) *i.e.* condensation versus Michael addition. The experimental procedure and

characterisation data presented are brief, and no yield is reported. It is therefore unclear whether this is the major product of the reaction or a minor isolated side product. The elemental analysis data given shows some discrepancy with the assigned structural formula, however it is entirely incompatible with the Michael addition product **146** ($C_{23}H_{18}N_2O$ **143** requires 81.6% C, 5.4% H; $C_{23}H_{18}N_2O_2$ **146** requires 78.0% C, 5.12% H; found 81.3% C, 6.1% H)

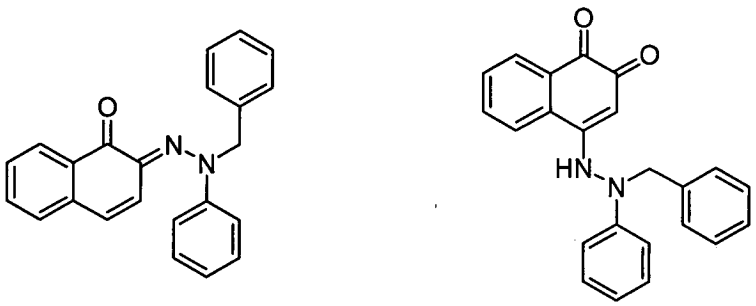

143 **146**

Figure 5.26 **Possible products from the reaction shown in Scheme 5.10**

Variable amounts of 2-phenylazo-1-naphthol **11** are also recovered from the reaction in acidic solution (0 – 5% yield).

When the reaction is performed in glacial acetic acid, the main reaction product is 2-phenylazo-1-naphthol **11**, obtained in around 50% yield. A small amount of the addition product **144** is observed but there is no evidence of hydrazone **137** or **138**. By what mechanism this reaction occurs is not at all clear. The product is definitely 2-phenylazo-1-naphthol, as MS and NMR data were identical to the sample prepared *via* the diazo coupling of 1-naphthol and benzenediazonium salt. The suggestion is that the condensation reaction does occur at the 2-position, as predicted, but is then followed by demethylation in acidic solution. This step would be highly unusual, and there is no obvious mechanism by which it could occur.

When 4-sulfonic acid-1,2-naphthoquinone is used in the reaction in aqueous acetic acid (20%), the yield of the addition product increases to 81%. This is potentially due to the increased solubility of the naphthoquinone, but is most probably a consequence of the leaving group in the 4-position. In the case where there is no leaving group (*i.e.* 1,2-naphthoquinone **124**), the initial product formed must be oxidised to **144** (Scheme 5.14)

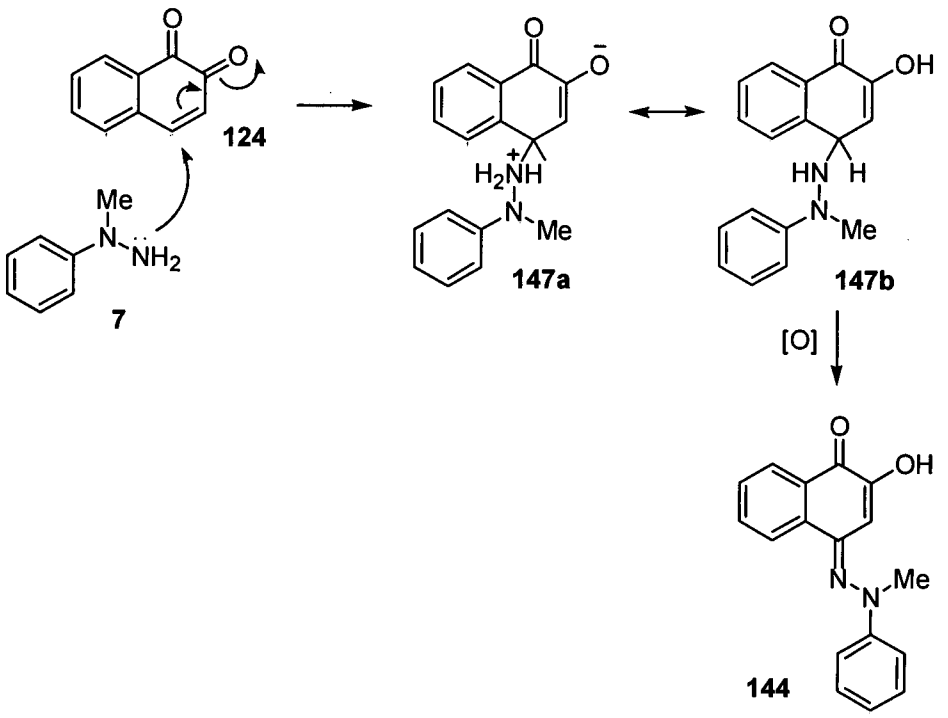

Scheme 5.14

It has been shown in related systems (derived from amines) that compounds such as **147** can undergo air oxidation to **144**.[174] It must also be considered, however, that naphthoquinone is an oxidant, and so could participate in the reaction. This would have a detrimental effect on yield in situations where there is one equivalent or less of naphthoquinone, since it would be reduced to naphthalenediol.

If there is a leaving group in the 4-position, **144** can form directly, without the need for oxidation, as shown in Scheme 5.15.

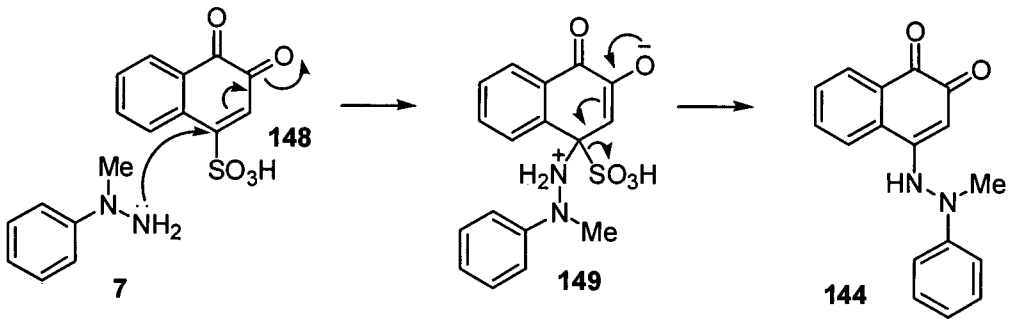

Scheme 5.15

5.4.10 Alternative routes to 137 and 138

The reaction of 1-nitroso-2-naphthol derivative **150** and *N*-methyl-*N*-phenylhydrazine sulfate **151** has been reported to give the hydrazone product **152** (Scheme 5.16), although it proceeds in poor yield (31%).[176] The method should regiospecifically give the 1-hydrazono isomer, whereas the condensation reaction was expected to yield the 2-isomer.

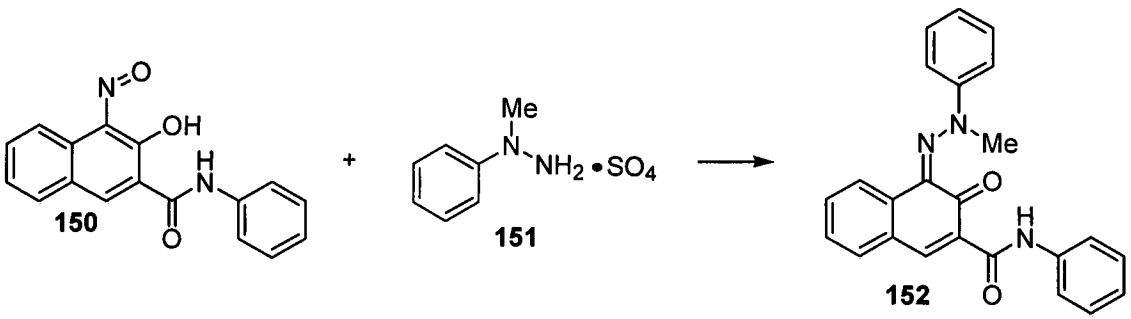

Scheme 5.16

Attempts to repeat this synthesis using 1-nitroso-2-naphthol **153** and *N*-methyl-*N*-phenylhydrazine **7** gave a complex mixture of over ten products (t.l.c.), from which none of the desired hydrazone **137** could be recovered by column chromatography or preparative scale HPLC.

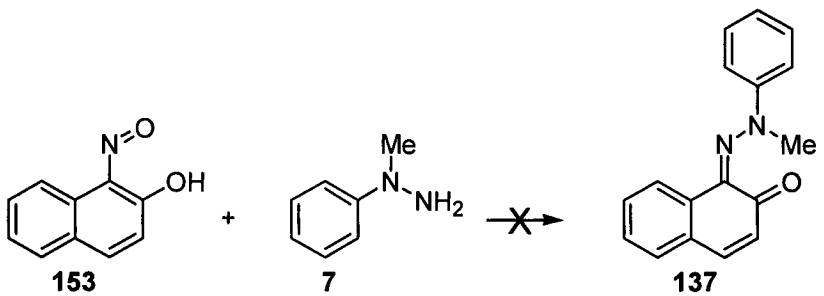

Scheme 5.17

It has been shown that azo compounds **154** are available *via* condensation of primary aromatic amines **155** and nitrosobenzenes **156** under acidic conditions (Scheme 5.18).[177, 178]

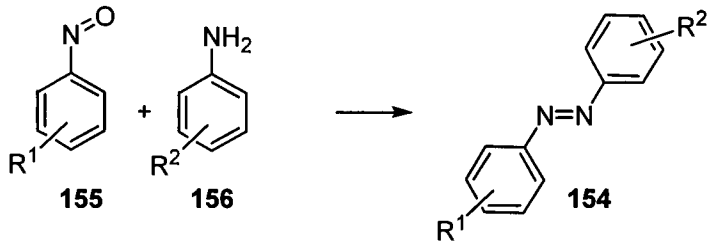

Scheme 5.18

It was not thought that this route would be applicable to **137** or **138**, however, as when this method is applied to nitrosonaphthols **153** the product is the 2-(alkylamino)-1-nitrosonaphthalene **157** (Scheme 5.19).[179]

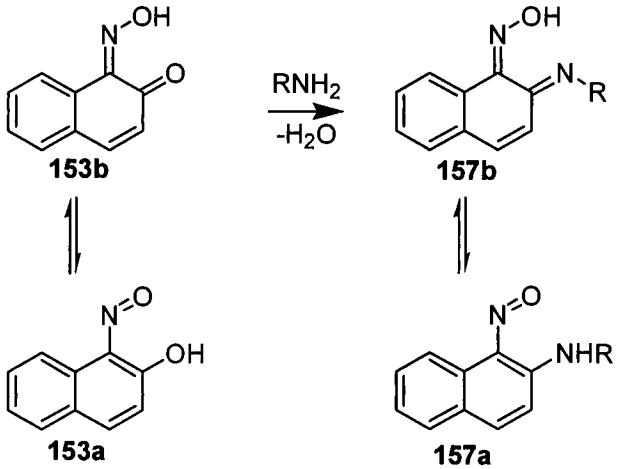

Scheme 5.19

The difference in reactivity is due to the fact that **153** would be expected to be present as the oxime **153b**, thereby favouring condensation at the 2-position (Scheme 5.19).

Clearly the current methodology for the synthesis of *N*-substituted derivatives **137** and **138** requires further development. It is not clear what might be done to obtain the hydrazone products as they were not observed in any of the reactions shown. Protection of the double bond to prevent Michael addition may allow access to the desired condensation products.

5.5 4-phenylazo-1-naphthol derivatives

This section will deal with synthetic routes to the following compounds:

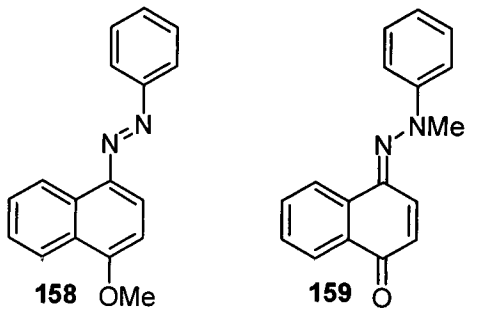

158 159

Figure 5.27

5.5.1 *O*-methyl derivative 158

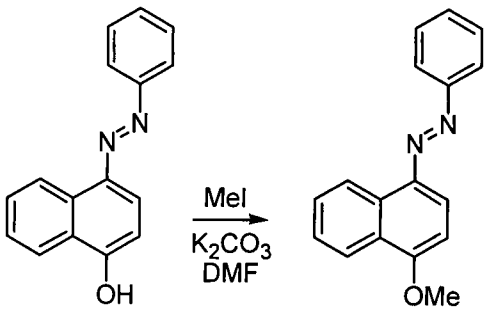

9 158

Scheme 5.20 **Methylation of 4-phenylazo-1-naphthol 9**

Following the reaction optimisation carried out for the *O*-methylation in the previous section, synthesis of **158** was straightforward. The conditions employed were: MeI (5 eq.); K_2CO_3 (2 eq.); DMF. The reaction was complete after 2 h, and **158** was obtained in 91% yield and good purity. **158** was isolated solely as the *E* isomer, as with **135**. Again, it is thought that the initial product of the methylation is the *E* isomer, and the short reaction time does not allow isomerisation. Methylation of the oxygen atom was confirmed by 1D ^{1}H and ^{13}C NMR spectroscopy, the methyl signal being observed at $\delta_H = 4.12$ ppm and $\delta_C = 56.1$ ppm.

5.5.2 *N*-methyl derivative 159

The sole method by which **159** has previously been synthesised is *via* hydrazine condensation with 1,4-naphthoquinone (Scheme 5.21).

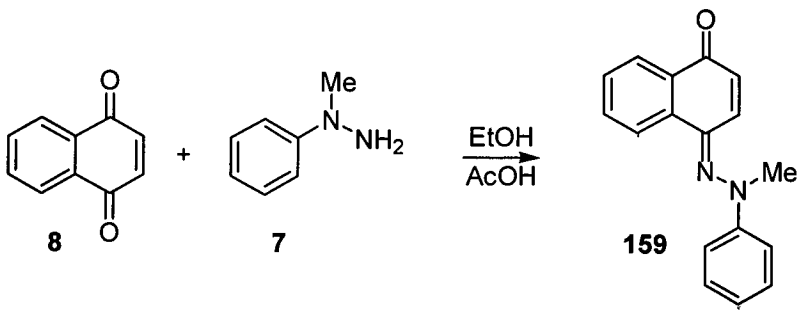

Scheme 5.21

There have been some reports of **159** synthesised by this method,[24, 180-182] although they cite the early work of McPherson[183] for their experimental procedure. *N*-Methyl-*N*-phenylhydrazine **7** is added to a solution of 1,4-naphthoquinone **8** in ethanolic acetic acid (20%) at 0 °C. When the reaction is complete, the reaction mixture is diluted with water and the precipitate is collected by filtration or extracted with chloroform. The product is then purified by recrystallisation, McPherson reports a 2% yield for the hydrazone **159**, although it is not recorded if any side products were isolated. Identification of the product was by elemental analysis. A modification of this procedure has been presented,[184] in which the addition order is reversed, with 1,4-naphthoquinone added to 1.5 eq. of *N*-methyl-*N*-phenylhydrazine hydrochloride in absolute ethanol. The product from the reaction is recovered following recrystallisation in 50% yield.

Characterisation of the product from the reaction is often poor. Both methods are reported to give products with a m.p. of ~120 °C, a λ_{max} of ~460 nm and satisfactory elemental analysis (although only on the basis of one or two elements). Unfortunately no definitive structural characterisation, in the form of NMR, MS or X-ray crystallographic analysis, appears to have been performed. The carbonyl frequency in the IR spectrum of **159** has been reported as 1624 cm^{-1}.[181] The authors do not ascribe a band to the –C=N– vibration.

As with 1,2-naphthoquinone, a possible alternative reaction pathway has also been observed, proceeding *via* a Michael type addition at the 4-position to yield the arylazaquinone **161** (Scheme 5.22).[185]

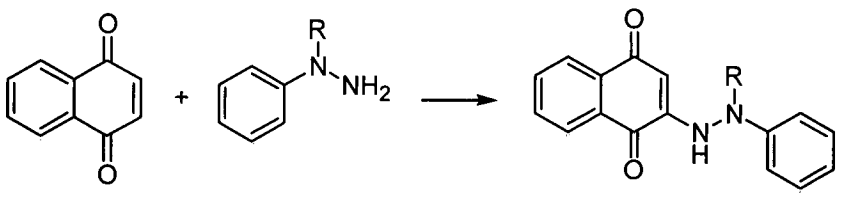

8 **160** **161**

Scheme 5.22[185]

In general, reactions that are thought to proceed to give the hydrazone tend to use the hydrochloride or sulfate salt of the phenylhydrazine. Use of the free base and elevated temperature (60 °C) appears to give the Michael addition product in around 30% yield.[185] This observation is not universal, however, and so it is not clear if use of the salts influences the reaction outcome.

In our hands, attempts to synthesise the hydrazones by these methods proved relatively unsuccessful (Table 5.7).

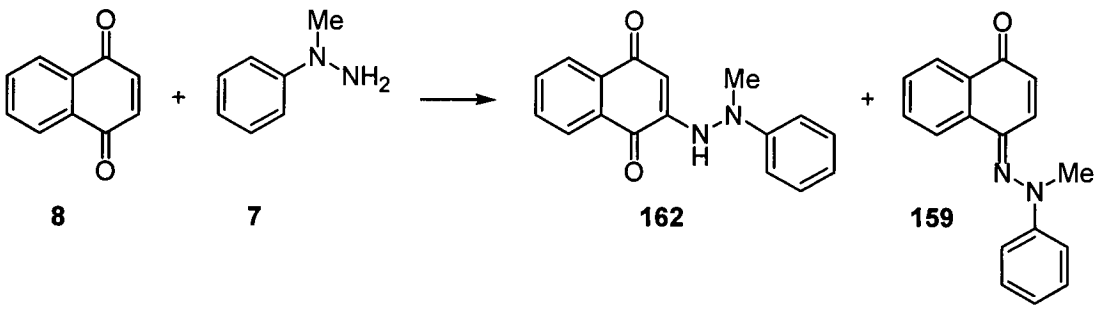

8 **7** **162** **159**

Scheme 5.23

Run	Solvent	Temperature	Yield of **162** / %	Yield of **159** / %
1	MeOH	RT	58	0
2	MeOH	0 °C	51	0
3	MeOH[a]	RT	46	0
4	DCM	RT	64	0
5	Aq. AcOH (20 %)	RT	38	5

Table 5.7 Attmepted syntheses of 159. [a]*N*-methyl-*N*-phenylhydrazine hydrochloride used.

For each reaction the main product was that of the Michael addition of the hydrazine (**162**). Only once was it possible to isolate any of the desired hydrazone **159** (run 5), and then in only very low (~5%) isolated yield following dry-flash chromatography. Comparison with the small amount of literature data available suggests that the previous structural assignments of **159** were correct. The λ_{max} values reported for **159** are 457 nm[184] and 460 nm[182] in ethanol; the product isolated from run 5 (Table 5.7) shows a λ_{max} of 464 nm in methanol and a carbonyl stretching frequency in the IR spectrum at 1631 cm^{-1}. The carbonyl frequency of **159** is reported as 1624 cm^{-1}.[182] The λ_{max} of the Michael addition product **162** is 467 nm and there are two visible carbonyl frequencies observed at 1674 and 1612 cm^{-1}. This suggests that the product isolated by previous workers is hydrazone **159**, but the main (and unreported) product is probably **162**. We confirmed the structure of hydrazone **159** by means of MS and NMR analysis. ESI-MS showed a single peak of m/z 263 $[M+H]^+$; the methyl signal is observed in the ^1H NMR spectrum at δ_H = 3.90 ppm and in the ^{13}C NMR spectrum at δ_C = 45.7 ppm, indicating that it is attached to a nitrogen atom. There are also the 9 anticipated CH resonances observed in the ^{13}C DEPT135 spectrum. There were no useful correlations observed in 2D NMR experiments.

5.5.3 Identification of 162

MS, ^1H and ^{13}C NMR data confirmed the identity of the major product **142** from the reaction shown in Scheme 5.23. The ESI-MS shows a single peak at *m/z* 279 $[M+H]^+$. The indicative features of the NMR spectra are the singlet at 6.12 ppm in the ^1H NMR spectrum and the additional quaternary and one less CH signal in the ^{13}C spectrum *cf.* the expected hydrazone. Two quaternary signals at 183.4 and 181.9 suggest that **162** adopts the enaminone structure, as opposed to the eniminol, in solution.

HRMS data confirmed the molecular weight - found 278.1055, $C_{17}H_{14}N_2O_2$.requires 278.1055. The EI-MS break down shows signals for 173 $[M\text{-}MeNPh+H]^+$, 77 $[Ph]^+$ and 92 $[PhNH]^+$.

5.6 Ozonolysis of phenylazonaphthols

As has already been mentioned, the majority of literature reports on the solution ozonolysis of dyes have concentrated on the development of industrial processes for decolourising aqueous dye-house wastewaters. The main concern with the use of ozone in effluent treatment is the cost of generating the ozone, meaning that efficient transfer of ozone from the gas phase into the aqueous phase is essential. The simplest reactors use column bubble chambers. Ozone transfer efficiency can be maximised by increasing the effective interfacial area of contact, achieved by reducing bubble size through the use of porous glass diffusers[186] or ceramic membranes[187, 188] and / or increasing the contact time between the gas and the effluent by increasing the length of the reaction column. This type of reactor is most suitable for laboratory use, and some small-scale examples are commercially available e.g. Figure 5.1.[189]

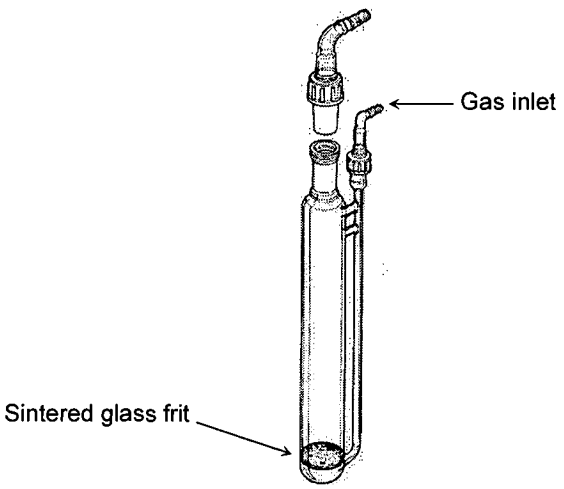

Figure 5.28 [189]

Commercially available gas reactors do have some drawbacks, however. Simple models, such as that shown in Figure 5.28, do not have a convenient means of sampling the reaction, those that do are more costly. The range of volumes, frit porosity etc. available is also limited. It was therefore decided to construct a custom piece of glassware suitable for our requirements.

5.6.1 Experimental Design

An experimental procedure for solution ozonolysis was required. The method had to be reproducible and controlled, with a suitable system for reaction monitoring.

The key piece of apparatus was the reaction vessel in which the ozonolysis was performed. One of the main considerations in this design is the mass transfer of ozone into the reaction mixture. In the case of very fast ozonolysis reactions this can be the rate-limiting step, and therefore the reactor design must allow rapid dissolution of the gaseous ozone. The details of the design of the reaction vessel are given in appendix 7.4. The final design was based on those commercially available, although it has been modified slightly (Figure 5.29).

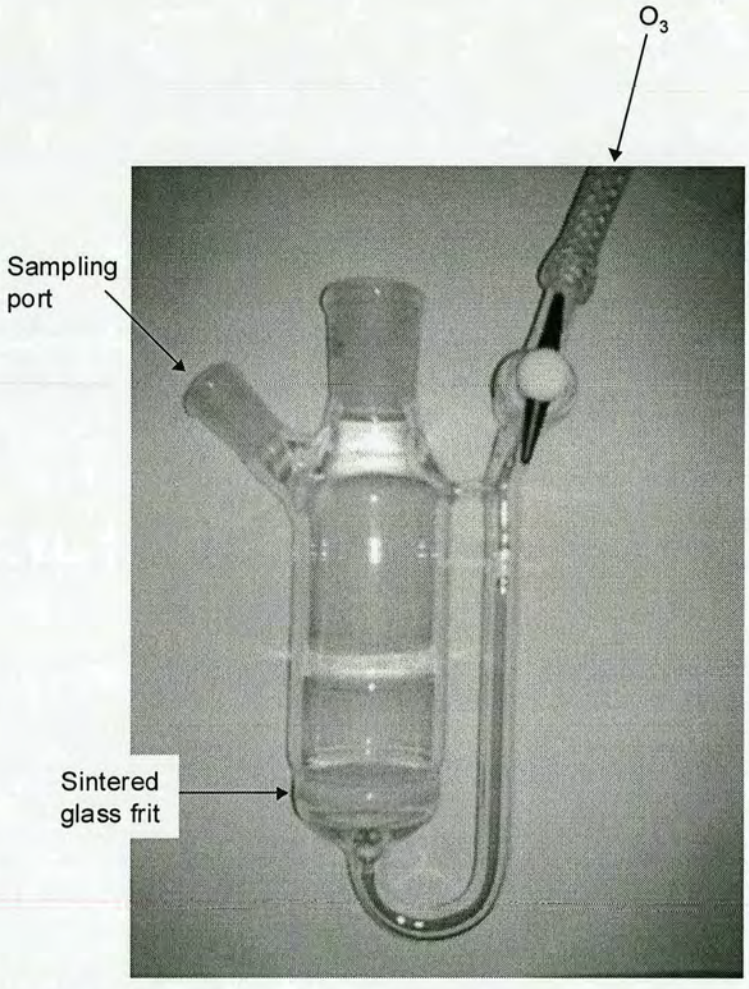

Figure 5.29 Ozonolysis apparatus

The main features of the design are the porosity 3 glass frit, giving a fine, even distribution of bubbles; the side arm, allowing easy sampling; and the stop-cock in

the gas inlet line, which can be closed to prevent the sample solution passing back through the frit when there is no gas flow.

Ozone was generated using an electric spark apparatus from a stream of pure oxygen. Ozone is generated by a high voltage electric discharge, which splits the oxygen molecule into two oxygen atoms. These can then combine with a further molecule of oxygen to form ozone.[157] An O_2 flow rate of 240 cm^3 min^{-1} and a generating voltage of 135 V, 0.22 A gave satisfactory conditions for decolourisation of the studied dyestuffs. Saturation of the reaction solvent took around 20 min.

Ozone has been shown to have a reasonable lifespan in aqueous solution under acidic or neutral conditions. Under basic conditions it undergoes hydroxyl ion initiated decomposition to form singlet oxygen and other reactive species. The rate of decomposition is ~10 – 100 times greater than that of acidic or neutral solutions. [123, 190] It is thought that the rate of dye oxidation by ozone is several orders of magnitude faster than the rate of singlet oxygen formation and so it is not considered a significant species in the reaction.[186] Our reactions were performed in neutral solution, and the pH was expected to decrease as the reaction progressed. Ozone stability in solution was therefore not deemed to be a problem.

Ozone concentration can be measured in a number of ways, the most common being either titration of liberated I_2 with sodium thiosulfate (Scheme 5.24), or by UV spectroscopy of an aqueous solution of ozone.[191]

$$O_3 + 2KI + H_2O \longrightarrow I_2 + KOH + O_2$$

$$I_2 + 2Na_2S_2O_3 \longrightarrow 2NaI + Na_2S_4O_6$$

Scheme 5.24

The extinction coefficient of an aqueous solution of ozone has been shown to be between 2900 - 3300 mol dm^3 cm^{-1} at 260 nm by a number of researchers.[122, 190-192] The UV method was used to determine the ozone concentration in our experiments, as it is the most convenient technique. Absorbance was measured at 260 nm, using an extinction coefficient of 3292 mol dm^{-3} cm^{-1}.[191] This is the most recently reported value for neutral aqueous solutions, obtained from original data. The ozone solution was sampled using a gas-tight syringe, as reproducibility was poor when a ground glass syringe or pipette was used. We have shown that a neutral aqueous solution of

ozone, in a stoppered cuvette, loses less than 5% of its UV absorbance at 260 nm over a period of at least 5 min. This allows sufficient time for sampling and UV measurement in order to determine ozone concentration (Figure 5.30). The linear fit to the data shows the reaction is zero-order and gives a $t_{½}$ of ~54 min and a rate constant for the depletion of ozone of 3.1×10^{-7} mol dm^{-3} s^{-1}.

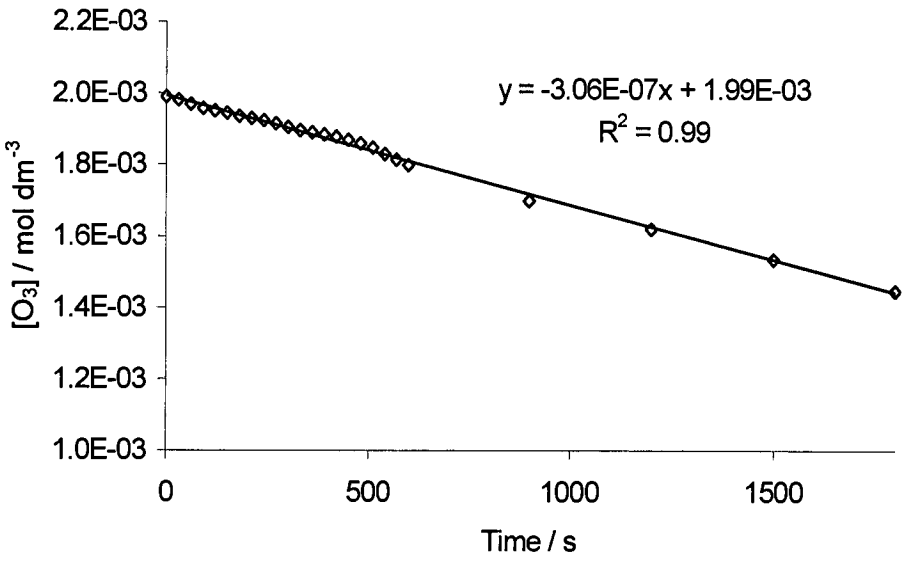

Figure 5.30 **Rate of ozone loss in a neutral aqueous solution.**

Where ozonolysis was carried out in non-aqueous solvents an aliquot of solvent was taken and diluted with distilled water before measuring the UV absorbance.

5.6.2 Ozonolysis of "simple" dyes

This section will discuss the solution ozonolysis of the following dyes:

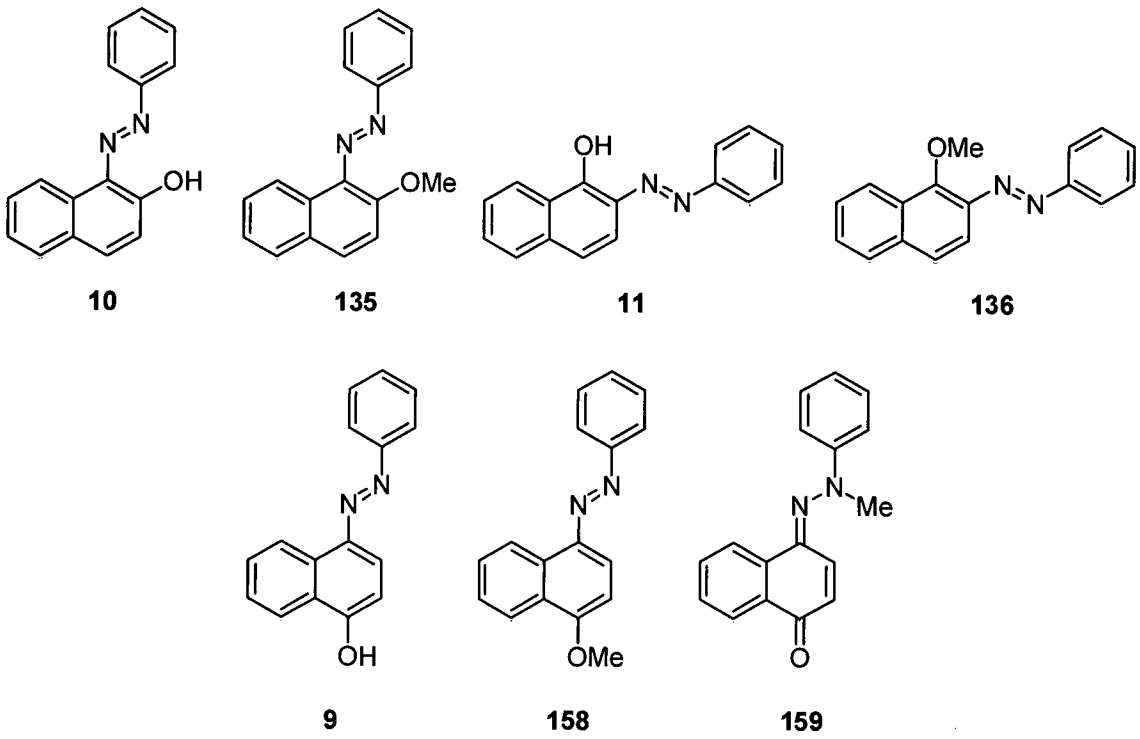

10 135 11 136

9 158 159

Figure 5.31

The ozonolysis of dyes **9-11, 136, 136, 158** and **159** was performed in IPA solution, at a dye concentration of ~ 0.4 mM. These conditions were chosen for maximum dye solubility, to allow for direct sampling and analysis without the need for sample manipulation or dilution, and to minimise dye aggregation, which is known to affect dye degradation in oxidation reactions and can occur at high dye concentrations.[9, 118] The reaction mixture was sampled at timed intervals, 100 μl aliquots were taken using an automatic pipette in order to minimize the change in reaction volume. Analysis was carried out by reversed-phase HPLC and the concentration of the remaining dye component was determined from the peak area. Typical ozone concentrations, for a saturated IPA solution, are 2 – 3 mM. This 5 – 8 fold excess of ozone, along with the continual replenishment of ozone in the solution, means that the reaction conditions can be considered pseudo first-order. This is confirmed by the plots of ln[Dye] vs time, which give a straight line for each dye studied.

The pseudo first-order rate constants for the degradation of each dye are given in Table 5.8.

Dye	k_{obs} / s^{-1}
159	1.2×10^{-2}
10	5.4×10^{-3}
9	3.3×10^{-3}
11	3.2×10^{-3}
159	6.4×10^{-4}
135	5.6×10^{-4}
126	4.5×10^{-4}

Table 5.8 **Rates of ozonolysis for dyes 9-11, 136, 136, 158 and 159**

Figure 5.32 shows the data obtained for the 4-phenylazo-1-naphthol series of dyes **9, 158** and **159**.

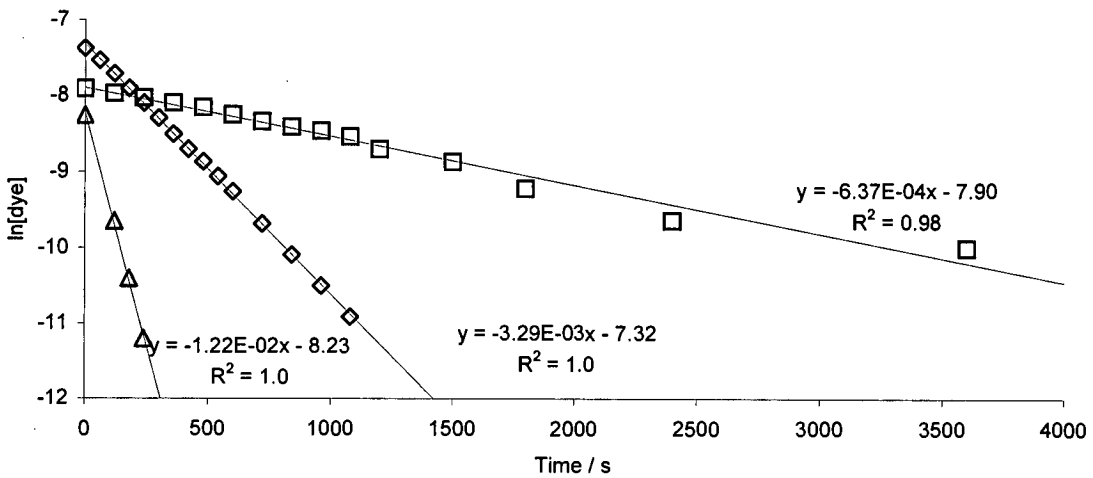

Figure 5.32 **Ozonolysis data for □ 158; ◊ 9; Δ 159.**

The rate of ozonolysis of **159** *cf.* **158** supports the theory that it is the hydrazone tautomer that reacts preferentially with ozone, with the reaction rate for the locked hydrazone form **159** approximately twenty times faster than the locked azo form **158**.

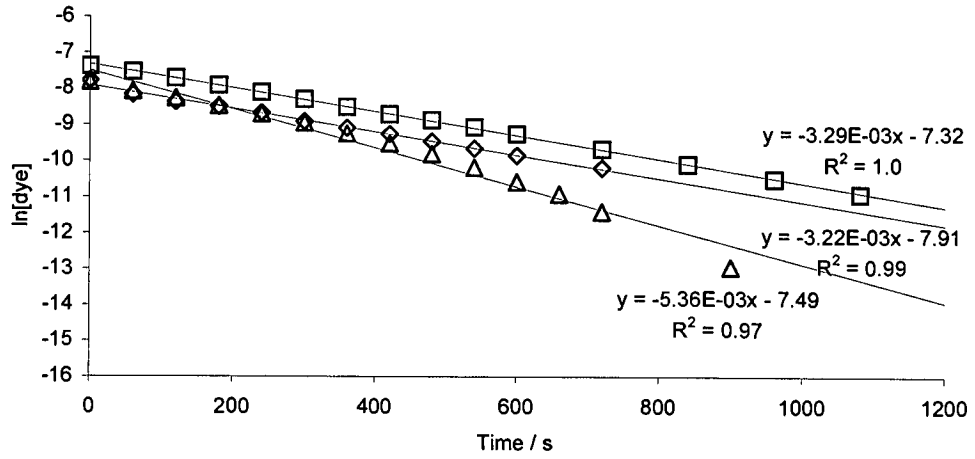

Figure 5.33 Ozonolysis data for □ 9; ◊ 11; Δ 10.

As can be seen, the rates for the unlocked dyes are similar, however the data for **10** do not give as good a linear fit as **9** and **11**. If we examine the initial rates (first 300 s of the reaction), it can be seen that the data gives a better linear fit and the rates are essentially identical (Figure 5.34).

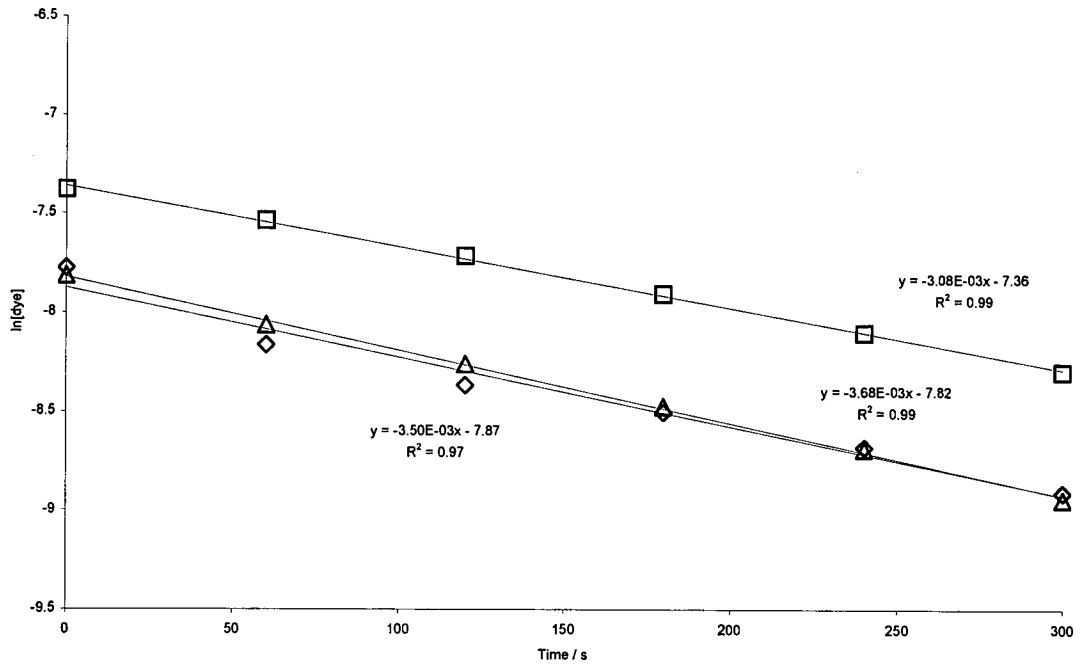

Figure 5.34 Initial rates of ozonolysis for □ 9; ◊ 11; Δ 10.

This suggests that the position of the azo / hydrazone tautomeric equilibrium does not influence the rate of ozonolysis. Although this disagrees with previously published reports, it could be argued that provided some hydrazone tautomer is present then it is probable that the rate of intramolecular proton transfer to re-establish the equilibrium position is faster than the rate of ozonolysis. Therefore, even if the hydrazone tautomer is present in relatively small amounts the re-equilibration of the azo / hydrazone tautomeric position will be faster than the ozonolysis itself.

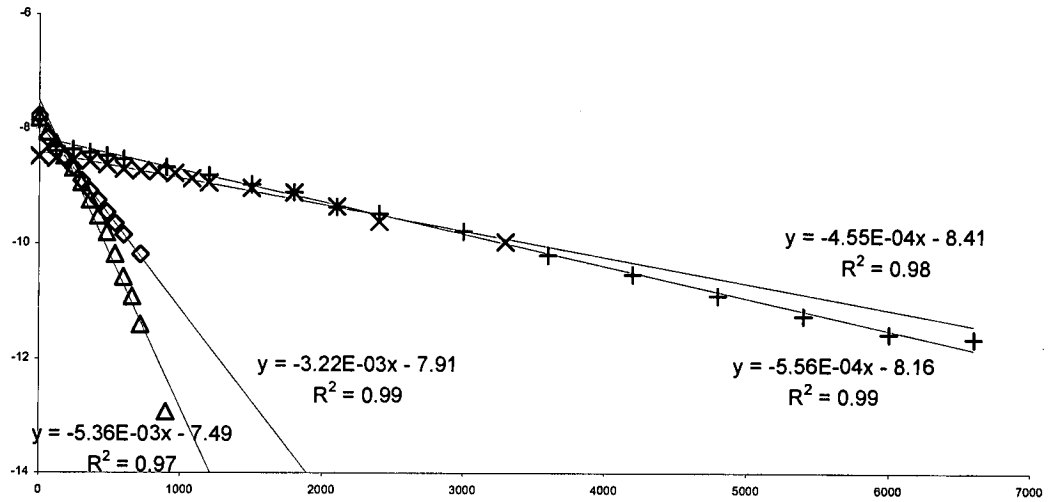

Figure 5.35 **Ozonolysis data for ◊ 11; Δ 10; × 136; +135.**

Figure 5.35 shows the ozonolysis data obtained for **11**, **10**, **136** and **135**. The rates for the azo locked compounds are ~ 10-fold less than for the respective unlocked compounds. This confirms that the azo form is relatively unreactive, although it suggests that there is still an available pathway for degradation *via* this tautomer.

In an effort to understand the reaction mechanism of ozonolysis, the products of the solution ozonolyses were analysed by HPLC and LC-MS. In the reaction of dyes **9** – **11** and **159**, the main degradation product was naphthoquinone, confirming the results obtained by previous authors.[133, 135, 151] Ozonolysis of 2-phenylazo-1-naphthol appears to follow a similar pathway to 1-phenylazo-2-naphthol *i.e.* it proceeds *via* 1,2-naphthoquinone. We could find no experimental evidence to

support the existence of peroxides or other postulated intermediates in this study. This is not surprising; as such products would be expected to be short-lived.

In an attempt to identify the initial products formed following the attack of ozone, the reaction mixture was analysed by direct injection into an electrospray mass spectrometer. This was achieved by the mixing of a solution of dye and a solution of ozone in two syringes being injected simultaneously *via* syringe pump into a mixing chamber. The reaction mixture then passes into the ESI-MS source, allowing data to be collected a short time after the initial reaction (Figure 5.36).

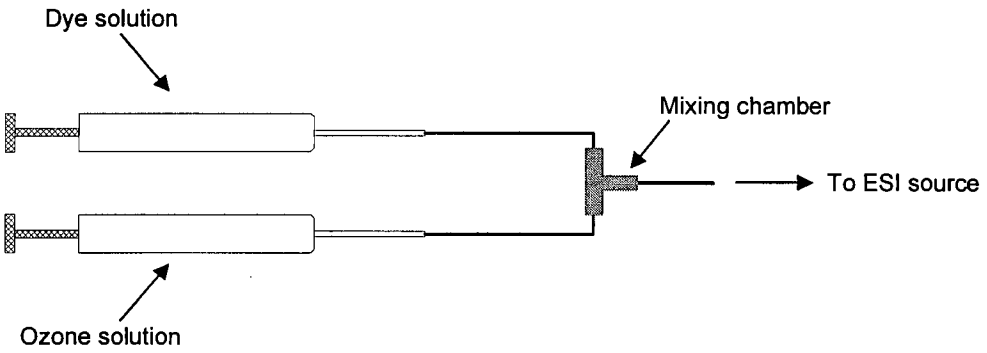

Figure 5.36

PEEK HPLC tubing (0.17 mm i.d.) was used, as it is easier to handle than stainless steel and was not thought to be incompatible with ozone. The mixing chamber was a PEEK T-piece adaptor. The syringe pump injected the two reagents at a rate of 50 μl min^{-1}.

The dye concentration (1-phenylazo-2-naphthol **10**) varied from 0.1 → 0.001 mM in methanol. A saturated solution of ozone in methanol was used.

When the 0.1 mM dye solution and ozone solution were injected into the ESI-source, no degradation was observed, and so the dye concentration was reduced 100-fold. No degradation was observed, however.

The contact time between the dye and ozone solutions can be adjusted by varying the length of tubing between the mixing chamber and the ESI source inlet. This should allow the ozonolysis to be monitored at different time points in the reaction. In the initial reactions the tubing length was ~ 5 cm between the mixing chamber and the ESI source inlet. When no degradation was observed, this was increased to ~ 30 cm

in an effort to extend the mixing time between the ozone and dye solutions. Unfortunately this did not result in the observation of any degradation products.

It had been hoped that if even the initial products of the ozonolysis could not be detected it would be possible to observe some 1,2-naphthoquinone as a validation of the system. No naphthoquinone was seen, however, and so it is not clear if any reaction occurred at all. This may have been due to the reaction of ozone with the PEEK tubing; insufficient time allowed for the reaction (the mixing time for the two solutions using 30 cm of tubing and a flow rate of 50 μl min^{-1} is ~ 40 s) or ozone was not present in sufficient excess. The procedure was similar to that of a stopped flow experiment, where it is known that the mixing chamber plays an important role in the system. Since the mixing chamber in the above set-up was relatively crude, it may be that enhancements in the design would allow the ozonolysis reaction to be observed.

5.6.3 Ozonolysis of "real" dyes

Since the diisopropylhydrazide- and dimethylhydrazide-substituted series of dyes **95** and **96** gave the best ozone ozone fastness results on-media, it was decided to examine the solution ozonolysis of this substitution pattern against the parent dye **89**. Ozonolysis was performed at Avecia (Blackley), however the conditions were essentially the same as those employed at the University of Edinburgh in the previous section. The dyes were dissolved in deionised water before being added to a saturated aqueous solution of ozone (final conc. ~ 1.0 mM). Samples were taken at timed intervals over 30 min, after which complete decolourisation was observed (Figure 5.37). Analysis was performed by reversed phase HPLC.

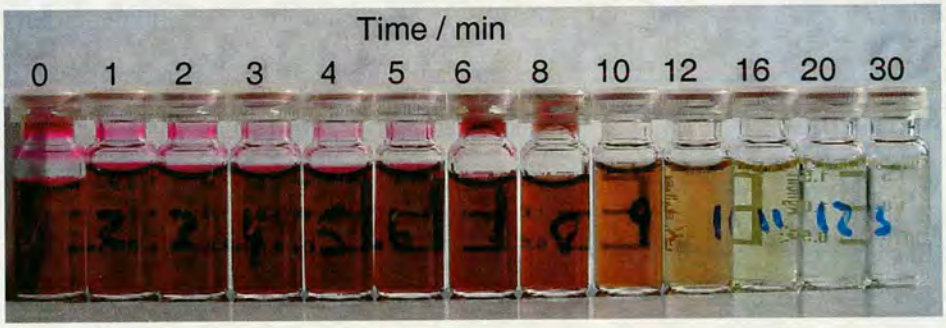

Figure 5.37 **Illustration of the changes in colour which occur on ozonolysis**

Rate data was calculated for each dye, based on the HPLC area of the peak. Since ozone was continually being replenished in the system it was assumed that reaction occurred under pseudo first-order. Rate constants were calculated using a linear fit to the data log[dye] versus time (s) (Figure 5.38).

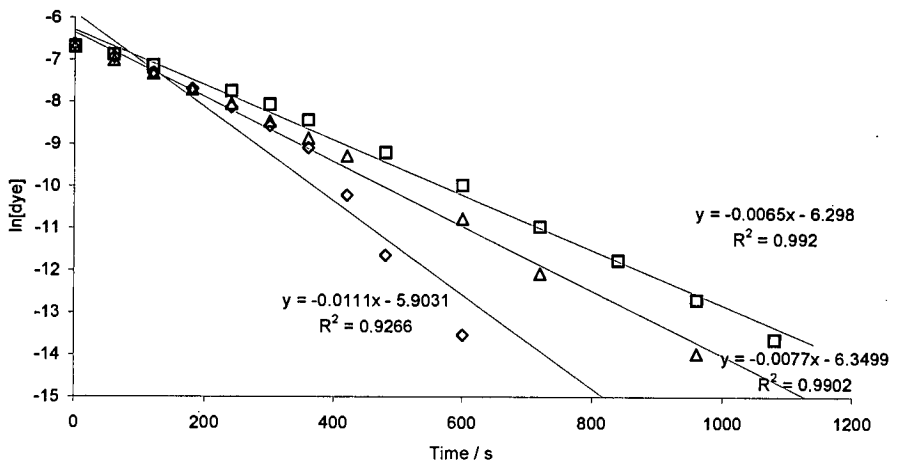

Figure 5.38 **Rates of ozonolysis for □ 95c; ◊ 89; Δ 96c**

The hydrazide substituted dyes show the same trend in solution as they do on-media (*i.e.* **96c** > **95c**). Both show better fastness than **89**, although only by a factor of ~2. The parent shows a relatively poor linear correlation, suggesting that the reaction does not occur under pseudo first-order conditions. An examination of the initial rates (the first 300 s of the reaction) shows good linear correlation, and in this instance the rates are essentially equal.

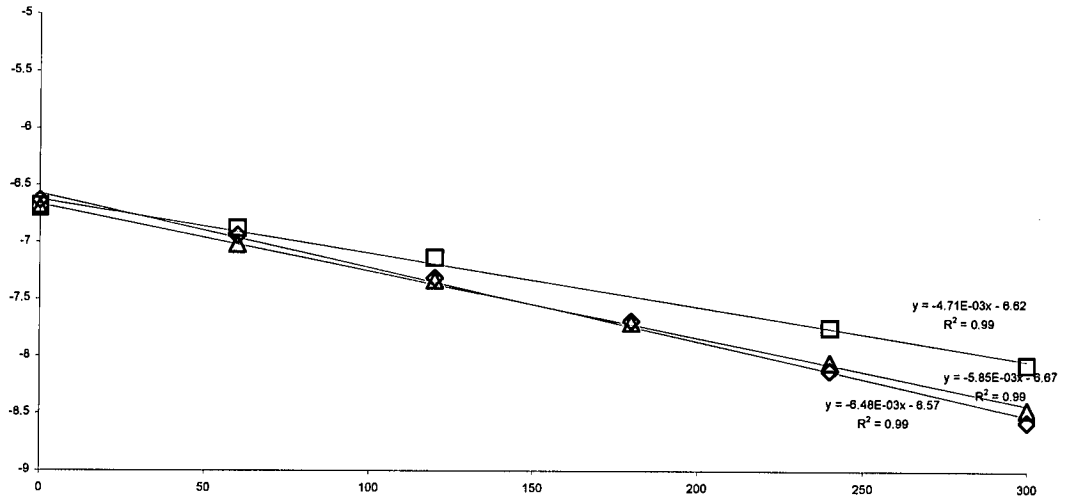

Figure 5.39 **Rates of ozonolysis for □ 95c; ◊ 89; Δ 96c**

This indicates, in the solution phase at least, that ozonolysis is fast and indiscriminate with respect to the site of ozone attack. This may be different on-media, where the concentration of both reactants is low and ozone is unlikely to be in great excess. It would be difficult to assess the rate under these conditions, however.

If we examine the progress of the ozonolysis of **89**, **95c** and **96c** we can draw some conclusions about the manner in which the dyes are degraded. Figure 5.40 shows the HPLC trace at 254 nm and 530 nm of the reaction mixture for each dye at t = 60 s. Peaks denoted with ↓ are present in the t = 0 s trace and decrease in concentration as the reaction progresses. Peaks denoted with ↑ increase in concentration initially, but start to decrease as the reaction progresses.

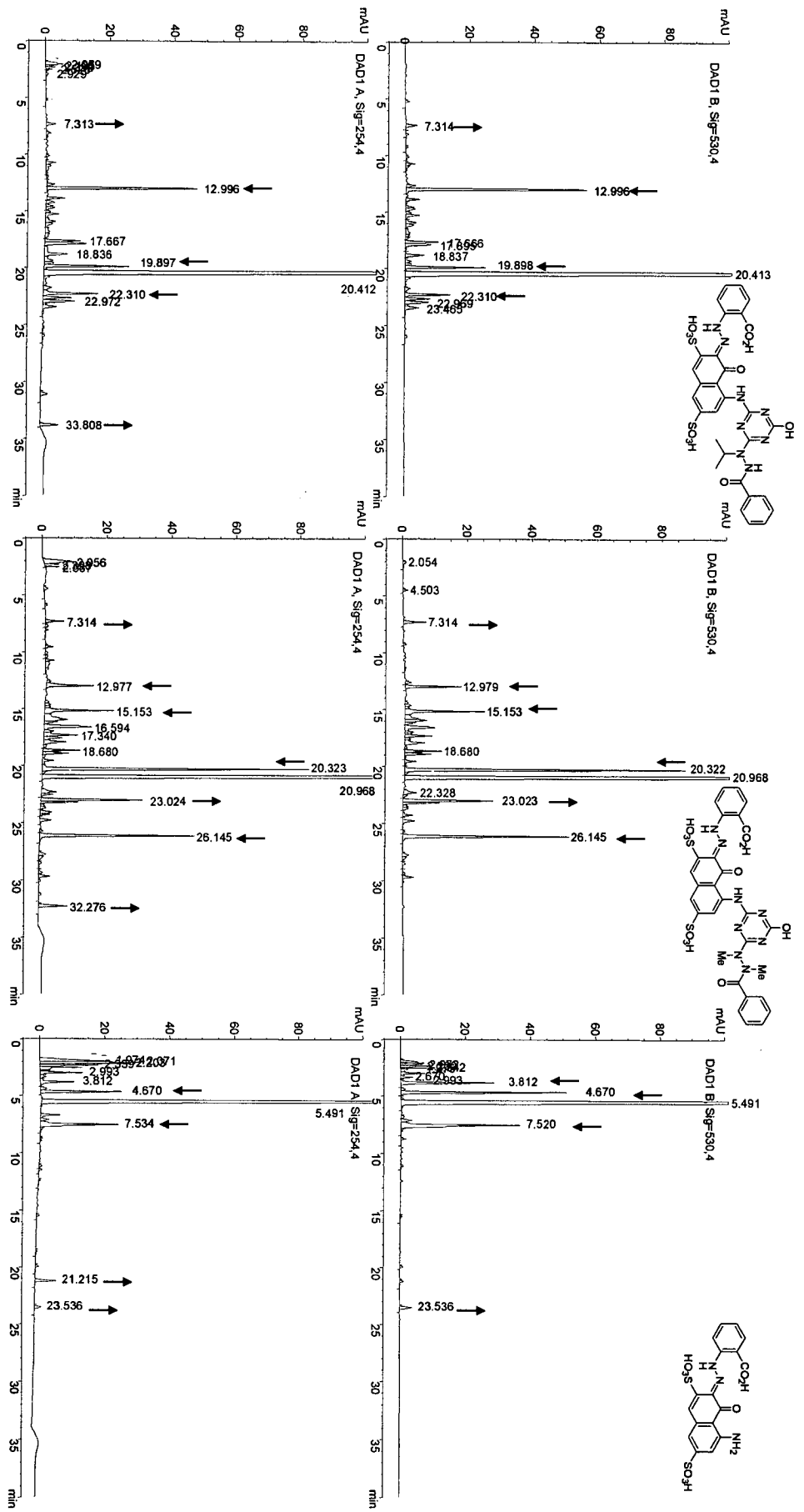

Figure 5.40 HPLC traces at t = 60 s, showing the degradation of dyes 96c, 95c and 89. Trace DAD1A = 254 nm, DAD1B = 530 nm. ↑ indicates increase in concentration; ↓ indicates decrease in concentration.

The most interesting feature of the traces is the common intermediate generated in the ozonolysis of the hydrazide-substituted **95c** and **96c** dyes at R_t = 7.1 min. This product appears coloured and is likely to arise from ozonolytic cleavage of either the hydrazide or the triazine moiety, showing that the hydrazide reacts with ozone in the first stages of the reaction. It is not observed in the ozonolysis of the parent compound.

There is also evidence of the rapid formation of colourless compounds in each of the dyes (**96c**, R_t = 33.8 min; **95c**, R_t = 32.3 min; **89**, R_t = 23.5 min). This suggests that the azo linkage reacts quickly with ozone; these peaks are therefore likely to be naphthoquinone derivatives, given the conclusions in the previous section.

These products are formed rapidly, and there is no evidence of other degradation products formed during the reaction. They are presumably then broken down into simple polar molecules with very short retention times, and cannot be distinguished. This theory is supported by previous work, which observed that the products of extended ozonolysis are organic and inorganic acids.[148-150]

5.7 Conclusions

An efficient synthetic route for the *O*-methylation of phenylazonaphthols has been demonstrated, offering improvements over some current literature procedures. Access to the complementary *N*-methylated series of phenylazonaphthols was somewhat less facile. It was possible to repeat the poor yielding synthesis of *N*-methylhydrazone **159**, allowing definitive confirmation of the structure of the previously reported product. Synthesis of the isomeric *N*-methylhydrazones **137** and **138** was unfortunately not successful. During the course of these investigations we have synthesised novel compounds from the Michael addition reactions of 1,2- and 1,4-naphthoquinone and *N*-methyl-*N*-phenylhydrazine, complementing literature reports on similar systems. We have also characterised an unexpected by-product from the reaction of 1-phenylazo-2-naphthol **9,** methyliodide and potassium hydride.

The dyes synthesised, along with 1-phenylazo-2-naphthol, 2-phenylazo-1-naphthol and 4-phenylazo-1-naphthol, were then used in ozonolysis experiments in order to determine the rates of reaction of each dye and its respective locked tautomers with

ozone. It was shown that a dye locked in the hydrazone form reacted with ozone approximately twenty times faster than a dye locked in the azo form. Attempts to determine the initial products formed in the reaction unfortunately failed, however previous reports on the ozonolysis of simple azo dyes were confirmed, and were extended to include 2-phenylazo-1-naphthol. Ozonolysis of commercially useful dyes showed that both coloured and colourless products are formed early in the reaction with ozone, suggesting that ozone attack is indiscriminate in the systems studied.

6 Experimental

6.1 General Techniques

^{1}H nuclear magnetic resonance (NMR) spectra were recorded on Varian Gemini-200 (200.0 MHz); Bruker AC250 (250.1 MHz); Bruker DPX360 (360.1 MHz) (UoE) or Bruker DPX300 (300.1 MHz) [Avecia (Blackley)] Fourier transform instruments. Chemical shifts are reported on the δ scale (relative to $\delta_{TMS} = 0$) in parts per million (ppm) and coupling constants in Hertz (Hz). The following abbreviations are used: br., broad; s, singlet; d, doublet; t, triplet; q, quartet; spt, septet; m, multiplet; *J*, coupling constant. The data are presented as follows: chemical shift, integration, multiplicity, coupling constant and interpretation. Residual protic solvent was used as the internal standard in ^{1}H spectra. ^{13}C NMR spectra were recorded on Bruker AC250 (62.9 MHz); Bruker DPX300 (75.5 MHz) or Bruker DPX360 (90.6 MHz) Fourier transform instruments and were referenced to the solvent carbon peak with broadband decoupling. The data are presented as follows: chemical shift, relative signal intensity, and interpretation (quat., quaternary centre), and were generally confirmed by DEPT90 and DEPT135 experiments.

Analytical high performance liquid chromatography (HPLC) was performed using either a Gilson or Agilent 1100 instrument fitted with a variable wavelength UV detector monitoring at 254 nm, using either a Jones Chromatography Genesis column (25 cm × 4.6 mm internal diameter, 4 μ) or a Waters Spherisorb column (15 cm × 4.6 mm internal diameter, 5 μ), fitted with an in-line filter. Preparative HPLC was performed using a Gilson instrument fitted with a variable wavelength UV detector monitoring at 254 nm, using a Phenomenex Luna column (6 cm × 21.2 mm internal diameter, 10 μ), fitted with an in-line filter. Eluent was HPLC grade supplied by Fisher Scientific and was vacuum degassed before use.

Electrospray ionisation (ESI) mass spectra were recorded on Finnigan LCQ (UoE) or Micromass Platform instruments [UoE or Avecia (Blackley)]. The sample was introduced either from an HPLC outlet (Finnigan or Waters Alliance instruments respectively) or *via* direct injection.

Infra-red spectra were recorded on a Biorad FTS-7, a Perkin-Elmer Paragon 100 FT-IR, or a Jasco FT/IR-410 instrument using 5 mm sodium chloride plates or potassium bromide discs. The wavenumbers of maximum absorbance (ν_{max}) are quoted in cm^{-1}.

UV spectra were recorded on a Perkin-Elmer Lambda 900 instrument in the stated solvent. The wavelengths of maximum absorbance (λ_{max}) are quoted in nm.

pH was measured using a Hanna Instruments "Checker", two point calibrated using pH 4.0 (phthalate) and pH 7.0 (phosphate) buffers at 20 °C.

Ozone was generated *in situ* by an Argentox GLX ozone generator from a stream of compressed pure oxygen supplied by BOC Gases.

Melting points were obtained on a Gallenkamp Electrothermal melting point apparatus and are uncorrected.

Elemental analysis was carried out on a Perkin-Elmer 2400 CHN Elemental Analyser.

T.l.c. was performed on Merck $60F_{254}$ aluminium backed silica plates and visualised by ultraviolet (UV) light at 254 nm if necessary. Flash chromatography was carried out on Merck Silicagel 60. Dry flash chromatography was carried out on either Merck Silicagel G or Merck Aluminiumoxide G. All solvent ratios quoted are v/v.

Light fastness testing was performed using an Atlas Ci 5000 Xenon Weatherometer at Avecia (Blackley), using a water cooled xenon argon lamp as a light source, over 100 h, 40% relative humidity.

Ozone fastness testing was performed using a 903 Hampden Ozone Test Chamber at Avecia (Blackley) over 24 h, 50% relative humidity, 1 ppm ozone on a rotating carousel.

Colour measurement was performed using a Spectrolino Gretag Macbeth instrument at Avecia (Blackley), illumination source D50, observer angle 2° using density standard ANSI A.

Dyes were purified by dialysis using Spectra/Por 3 membrane tubing [molecular weight cut-off (MWCO) 3,500 Da]. Conductivity was measured using a Primo 5 conductivity meter.

Solvents were standard laboratory grade and used without further purification unless otherwise stated. Starting materials were purchased from Aldrich or Acros, or were

kindly donated by Avecia. All starting materials were used as received unless otherwise stated.

Experimental Procedures and Data

Hydrazide nomenclature

Hydrazides have been named based on the carboxylic acid parent. The two possible nitrogen substitution positions are named as C(O)*N* and C(O)N*N'*.

***N*-Methylhydrazides**

The general procedure for the preparation of the *N*-methylhydrazide series was as follows: A solution of acid chloride (30 mmol) in DCM (20 cm^3) was added to an ice-bath cooled (0-5 °C) solution of methyl hydrazine (12 g, 0.30 mol, 10 eq.) in DCM (20 cm^3) *via* syringe pump over a period of 1 h. The reaction mixture was stirred for 1 h at 0-5 °C before being allowed to warm to room temperature and stirred for a further 1 h. The reaction mixture was then washed with sat. aqueous Na_2CO_3 (3 × 50 cm^3) and the organics dried over Na_2SO_4 and concentrated under reduced pressure to yield the desired product, which was used in subsequent steps without further purification. The following compounds were prepared using this procedure.

4-Methoxybenzoic acid *N*-methylhydrazide

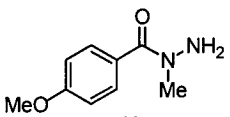

63a

4-Methoxybenzoic acid *N*-methylhydrazide was prepared from 4-methoxybenzoyl chloride (5.01 g, 30.0 mmol) and was obtained as a colourless solid (4.90 g, 93% yield); mp 73 – 74 °C (from toluene) (lit.,[67] 72 – 73.5 °C); ^{1}H NMR (250 MHz, $CDCl_3$) 7.51 (2H, d, ^3J 8.7, Ar*H*), 6.95 (2H, d, ^3J 8.7, Ar*H*), 4.46 (2H, br s, NH_2), 3.87 (3H, s, OCH_3) and 3.29 (3H, s, NCH_3); ^{13}C NMR (63 MHz, $CDCl_3$) 170.2 (quat.), 161.0 (quat.), 129.6 (2C, CH), 127.1 (quat.), 113.1 (2C, CH), 55.4 (CH_3) and 40.8 (CH_3); ν_{max} (thin film) 3312, 3212, 1609, 1251, 1173, 841; *m/z* (ESI+) 203 $[M+Na]^+$.

4-Methylbenzoic acid *N*-methylhydrazide

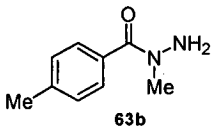

63b

4-Methylbenzoic acid *N*-methylhydrazide was prepared from 4-methylbenzoyl chloride (5.00 g, 30.0 mmol) and was obtained as a colourless solid (5.20 g, 98% yield); mp 55 °C (from toluene) (lit.,[200] 55 - 56 °C); ^{1}H NMR (250 MHz, $CDCl_3$) 7.42 (2H, d, Ar*H*, ^{3}J 8.2), 7.13 (2H, d, Ar*H*, ^{3}J 8.2), 4.54 (2H, br s, NH_2), 3.16 (3H, s, NCH_3) and 2.31 (3H, s, ArCH_3); ^{13}C NMR (63 MHz, $CDCl_3$) 169.8 (quat.), 139.5 (quat.), 131.4 (quat.), 128.2 (2C, CH), 126.8 (2C, CH), 39.8 (CH_3) and 20.7 (CH_3); ν_{max} (thin film) 3310, 3211, 1612, 1259, 1079, 828; *m/z* (ESI+) 165 $[M+H]^+$.

Benzoic acid *N*-methylhydrazide

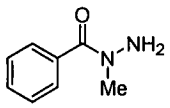

63c

Benzoic acid *N*-methylhydrazide was prepared from benzoyl chloride (4.26 g, 30.3 mmol) and was obtained as a clear, pale yellow oil (4.11 g, 90% yield); b.p. 70 °C at 0.3 mm Hg (lit.,[193] 45 °C at 0.1 mm Hg) ^{1}H NMR (250 MHz, $CDCl_3$) 7.21 (5H, m, Ar*H*), 4.47 (2H, br s, NH_2) and 3.02 (3H, s, NCH_3); ^{13}C NMR (63 MHz, $CDCl_3$) 170.2 (quat.), 135.1 (quat.), 130.1 (CH), 128.4 (2C, CH), 127.4 (2C, CH) and 40.5 (CH_3); ν_{max} (thin film) 3312, 3212, 1625, 1574, 1084, 713; *m/z* (ESI+) 151 $[M+H]^+$.

4-Chlorobenzoic acid *N*-methylhydrazide

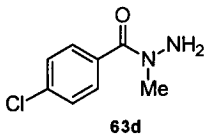

63d

4-Chlorobenzoic acid *N*-methylhydrazide was prepared from 4-chlorobenzoyl chloride (4.63 g, 30.0 mmol) and was obtained as a colourless solid (4.53 g, 92% yield) mp 102 - 103 °C (from toluene); ^{1}H NMR (360 MHz, 50 °C, $CDCl_3$) 7.44 (2H, d, Ar*H*, ^{3}J 8.2), 7.38 (2H, d, Ar*H*, ^{3}J 8.2), 4.48 (2H, br s, NH_2) and 3.22 (3H, s, NCH_3); ^{13}C NMR (91 MHz, 50 °C, $CDCl_3$) 169.4 (quat.), 136.1 (quat.), 133.5

(quat.), 129.0 (2C, CH), 128.4 (2C, CH), and 40.2 (CH_3); ν_{max} (thin film) 3328, 3217, 1652, 1601, 1089, 844; *m/z* (ESI+) 185 $[^{35}M+H]^+$, 187 $[^{37}M+H]^+$.

4-Nitrobenzoic acid *N*-methylhydrazide

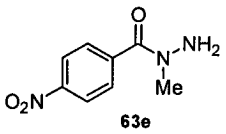

63e

4-Nitrobenzoic acid *N*-methylhydrazide was prepared from 4-nitrobenzoyl chloride (5.00 g, 30.0 mmol) and was obtained as a yellow solid (3.81 g, 72% yield) mp 133.5-134.0 °C (from toluene) (lit.,[67] 132-134 °C); ^{1}H NMR (250 MHz, $(CD_3)_2CO$) 8.43 (2H, d, Ar*H*, ^3J 8.8), 7.93 (2H, d, Ar*H*, ^3J 8.8), 5.07 (2H, br s, NH_2) and 3.40 (3H, s, NCH_3); ^{13}C NMR (63 MHz, $(CD_3)_2CO$) 168.7 (quat.), 145.0 (quat.), 143.4 (quat), 129.2 (2C, CH), 122.3 (2C, CH), and 37.9 (CH_3); ν_{max} (thin film) 3328, 3229, 1625, 1598, 1518, 1353, 851, 719; *m/z* (ESI+) 196 $[M+H]^+$.

N-Methyl N′-methylidenehydrazones

The general procedure for the preparation of the *N*-methyl *N′*-methylidenehydrazone series was as follows: To a stirred solution of *N*-methylhydrazide (2.0 g, *ca.* 10 mmol) in toluene (25 cm^3) was added paraformaldehyde (1.0 eq.). The reaction mixture was heated to reflux under Dean-Stark conditions for 18 h. The toluene was removed under reduced pressure to yield the desired *N*-methyl *N′*-methylidenehydrazone. The following compounds were prepared using this procedure.

4-Methoxybenzoic acid *N*-methyl *N′*-methylidenehydrazone

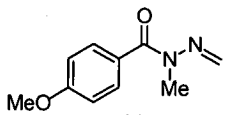

67a

4-Methoxybenzoic acid N-methyl N′-methylidenehydrazone was prepared from **x** (2.00 g, 11.1 mmol) and was obtained as a colourless oil (2.02 g, 95% yield); ^{1}H NMR (250 MHz, $CDCl_3$) 7.63, (2H, d, Ar*H*, *J* 9.1), 7.00 (2H, d, Ar*H*, *J* 9.1), 6.89, (1H, d, N′=CH_aH$_b$, *J* 10.2), 6.54 (1H, d, N′=CH$_a$$H_b$, *J* 10.2), 3.85 (3H, s, ArOCH_3) and 3.38 (3H, s, NCH_3); ^{13}C NMR (63 MHz, $CDCl_3$) 170.0 (quat.), 161.1 (quat.), 131.8 (2C, CH), 131.4 (CH_2.), 127.4 (quat.), 113.1 (2C, CH), 55.5 (CH_3) and 28.0 (CH_3); ν_{max} (KBr disc) 2838, 1652, 1603, 1371, 1254, 840; *m/z* (EI) 192 $[M]^+$ (74), 165 (40), 77 (88), 135 (100 %); HRMS (EI) $[M]^+$ found 192.0899, $C_9H_{10}N_2O$ requires 192.0899

4-Methylbenzoic acid *N*-methyl *N′*-methylidenehydrazone

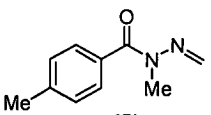

67b

4-Methylbenzoic acid N-methyl N′-methylidenehydrazone was prepared from **x** (2.01 g, 12.2 mmol) and was obtained as a colourless solid (2.07 g, 96% yield); ^{1}H NMR (250 MHz, $CDCl_3$) 7.54, (2H, d, Ar*H*, *J* 8.0), 7.20 (2H, d, Ar*H*, *J* 8.0), 6.71, (1H, d, N′=CH_aH$_b$, *J* 10.6), 6.44 (1H, d, N′=CH$_a$$H_b$, *J* 10.6), 3.38 (3H, s, NCH_3) and 2.39 (3H, s, ArCH_3); ^{13}C NMR (63 MHz, $CDCl_3$) 171.3 (quat.), 140.4 (quat.), 131.8

(quat.), 129.3 (2C, CH), 128.9 (CH_2), 128.1 (2C, CH), 28.0 (CH_3) and 21.3 (CH_3); ν_{max} (KBr disc) 2920, 1661, 1600, 1404, 1372, 1044, ; *m/z* (EI) 162 $[M]^+$ (82), 176 $[M]^+$ (73), 149 (6), 91 (85), 119 (100 %); HRMS (EI) found 176.0949 $[M]^+$, $C_{10}H_{12}N_2O$ requires 176.0950.

Benzoic acid *N*-methyl *N'*-methylidenehydrazone

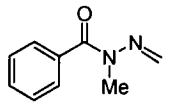

67c

Benzoic acid N-methyl N'-methylidenehydrazone was prepared from **x** (2.01 g, 13.4 mmol) and was obtained as a clear, pale yellow oil (2.08 g, 99% yield); ^{1}H NMR (250 MHz, $(CD_3)_2CO$) 7.28 (5H, m, Ar*H*), 6.62, (1H, d, N'=CH_aH$_b$, *J* 10.3), 6.37 (1H, d, N'=CH$_a$$H_b$, *J* 10.3), 3.38 (3H, s, NCH_3); ^{13}C NMR (63 MHz, $CDCl_3$) 170.1 (quat.), 135.1 (quat.), 130.5 (CH), 128.8 (CH_2.), 128.2 (2C, CH), 127.1 (2C, CH), and 40.5 (CH_3); ν_{max} 2920, 1663, 1598, 1374, 1045, 1024 (thin film); *m/z* (EI) 162 $[M]^+$ (82), 135 (20), 77 (88), 105 (100 %); HRMS (EI) $[M]^+$ found 162.0793, $C_9H_{10}N_2O$ requires 162.0793.

4-Chlorobenzoic acid *N'*-methyl *N'*-methylidenehydrazone

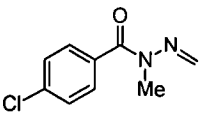

67d

4-Chlorobenzoic acid N-methyl N'-methylidenehydrazone was prepared from **x** (2.04 g, 11.0 mmol) and was obtained as a colourless solid (2.02 g, 93% yield); ^{1}H NMR (250 MHz, $CDCl_3$) 7.58, (2H, d, Ar*H*, *J* 8.5), 7.36 (2H, d, Ar*H*, *J* 8.5), 6.72, (1H, d, N'=CH_aH$_b$, *J* 10.5), 6.44 (1H, d, N'=CH$_a$$H_b$, *J* 10.5), and 3.38 (3H, s, NCH_3); ^{13}C NMR (63 MHz, $CDCl_3$) 170.1 (quat.), 136.2 (quat.), 133.1 (quat.), 129.5 (2C, CH), 128.7 (CH_2), 127.6 (2C, CH), and 27.5 (CH_3); ν_{max} (KBr disc) 2918, 1653, 1602, 1413, 1383, 1051; *m/z* (EI) 196 $[M]^+$ (18), 169 (8), 111 (42), 75 (20), 139 (100 %); HRMS (EI) found 196.0403 $[M]^+$, $C_{10}H_{12}N_2O$ requires 196.0403.

4-Nitrobenzoic acid *N*-methyl *N'*-methylidenehydrazone

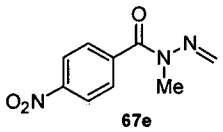

67e

4-Nitrobenzoic acid N-methyl N'-methylidenehydrazone was prepared from **x** (1.99 g, 10.2 mmol) and was obtained as a yellow solid (1.89 g, 89% yield); ^{1}H NMR (250 MHz, $CDCl_3$) 8.24 (2H, d, Ar*H*, *J* 9.0), 7.73 (2H, d, Ar*H*, *J* 9.0), 6.78, (1H, d, N'=CH_aH$_b$, *J* 10.3), 6.46 (1H, d, N'=CH$_a$$H_b$, *J* 10.3), and 3.42 (3H, s, NCH_3); ^{13}C NMR (63 MHz, $CDCl_3$) 169.4 (quat.), 148.3 (quat.), 141.2 (quat.), 130.4 (CH_2), 129.9 (2C, CH), 122.7 (2C, CH), and 27.4 (CH_3); ν_{max} (KBr disc) 2964, 1673, 1598, 1508, 1351, 1044; *m/z* (EI) 207 $[M]^+$ (23), 179 (12), 104 (48), 76 (34), 150 (100 %); HRMS (EI) found 207.0644 $[M]^+$, $C_{10}H_{12}N_2O$ requires 207.0644.

N,N'-Dimethylhydrazides

The general procedure for the preparation of the *N,N'*-dimethylhydrazide series was as follows: To a solution of *N'*-methylidene hydrazone (*ca.* 5.5 mmol) in MeOH (25 cm^3) was added $NaCNBH_3$ (0.31 g, 6.0 mmol, 1.1 eq.) and AcOH (0.36 g, 6.0 mmol, 1.1 eq.). The reaction mixture was stirred at room temperature for 18 h before being poured cautiously onto sat. Na_2CO_3 (100 cm^3) and extracted with CH_2Cl_2 (3 × 100 cm^3). The combined organics were dried (Na_2SO_4) and concentrated under reduced pressure to give the pure *N,N'*-disubstituted hydrazide. The following compounds were prepared using this procedure.

4-Methoxybenzoic acid *N,N'*-dimethylhydrazide

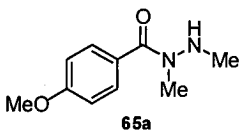

65a

4-Methoxybenzoic acid *N,N'*-dimethylhydrazide was prepared from **x** (1.01 g, 5.25 mmol) and was obtained as a colourless solid (0.990 g, 97% yield); mp 113-115 °C (from toluene) (lit.,[66] 112-113 °C); ^{1}H NMR (250 MHz, $CDCl_3$) 7.46, (2H, d, Ar*H*, *J* 8.5), 6.88 (2H, d, Ar*H*, *J* 8.5), 3.81 (3H, s, ArOCH_3), 3.17 (3H, s, NCH_3) and 2.65 (3H, s, N'CH_3); ^{13}C NMR (63 MHz, $CDCl_3$) ~170.2 (br. quat.), 160.7 (quat.), 129.3 (2C, CH), 127.1 (quat.), 113.2 (2C, CH), 55.2 (CH_3), 45.0 (CH_3) and 35.9 (CH_3); ν_{max} (KBr disc) 3284, 2955, 1633, 1505, 1253, 1173; *m/z* (ESI+) 195 $[M+H]^+$.

4-Methylbenzoic acid *N,N'*-dimethylhydrazide

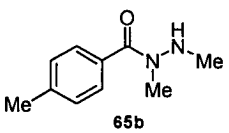

65b

4-Methylbenzoic acid *N,N'*-dimethylhydrazide was prepared from **x** (1.04 g, 5.90 mmol) and was obtained as a colourless solid (0.970 g, 92% yield); ^{1}H NMR (250 MHz, $CDCl_3$) 7.54 (2H, d, Ar*H*, ^3J 7.3), 7.35 (2H, d, Ar*H*, ^3J 7.3), 3.33 (3H, s, NCH_3), 2.54 (3H, s, N'CH_3) and 2.31 (3H, s, ArCH_3); ^{13}C NMR (63 MHz, $CDCl_3$) 69.3 (quat.), 139.8 (quat.), 128.6 (2C, CH), 127.8 (quat.), 127.1 (2C, CH), 42.7 (CH_3), 35.7 (CH_3) and 21.1 (CH_3); ν_{max} (KBr disc) 3285, 2922, 1634, 1376, 1263,

828; *m/z* (ESI+) 179 $[M+H]^+$. Spectroscopic data is in good agreement with the literature.[194]

Benzoic acid *N,N'*-dimethylhydrazide

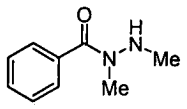

65c

Benzoic acid *N,N'*-dimethylhydrazide was prepared from **x** (1.02 g, 6.29 mmol) and was obtained as a clear oil (0.980 g, 95% yield); ^{1}H NMR (250 MHz, $CDCl_3$) 7.29 (5H, m, Ar*H*), 3.26 (3H, s, NCH_3) and 2.72 (3H, s, N'CH_3); ^{13}C NMR (63 MHz, $CDCl_3$) 170.1 (quat.), 135.1 (quat.), 130.5 (CH), 128.2 (2C, CH), 127.1 (2C, CH), 55.8 (CH_3) and 36.3 (CH_3); ν_{max} (KBr disc) 3235, 1654, 1532, 1487, 1306, 693; *m/z* (ESI+) 165 $[M+H]^+$.

4-Chlorobenzoic acid *N,N'*-dimethylhydrazide

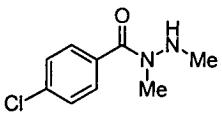

65d

4-Chlorobenzoic acid *N,N'*-dimethylhydrazide was prepared from **x** (0.98 g, 4.98 mmol) and was obtained as a pale yellow solid (0.960 g, 97% yield); ^{1}H NMR (360 MHz, 50 °C, $CDCl_3$) 7.46 (2H, d, Ar*H*, ^3J 8.3), 7.38 (2H, d, Ar*H*, ^3J 8.3), 3.12 (3H, s, NCH_3) and 2.62 (3H, s, N'CH_3); ^{13}C NMR (91 MHz, 50 °C, $CDCl_3$) 169.4 (quat.), 136.1 (quat.), 133.5 (quat.), 129.0 (2C, CH), 128.4 (2C, CH), 40.2 (CH_3) and 34.2 (CH_3); ν_{max} (KBr disc) 3286, 2958, 1633, 1379, 1090, 836; *m/z* (ESI+) 199 $[^{35}M+H]^+$, 201 $[^{37}M+H]^+$.

4-Nitrobenzoic acid *N,N'*-dimethylhydrazide

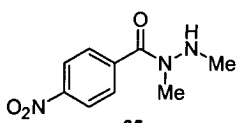

65e

4-Nitrobenzoic acid *N,N'*-dimethylhydrazide was prepared from **x** (1.03 g, 4.97 mmol) and was obtained as a yellow solid (0.870 g, 83% yield); ^{1}H NMR (250 MHz, $(CD_3)_2CO$) 8.46 (2H, d, Ar*H*, ^3J 8.5), 7.89 (2H, d, Ar*H*, ^3J 8.5), 3.23 (3H, s, NCH_3)

and 2.66 (3H, s, N′CH_3); ^{13}C NMR (63 MHz, $(CD_3)_2CO$) 168.7 (quat.), 145.0 (quat.), 143.4 (quat), 129.2 (2C, CH), 122.3 (2C, CH), 42.3 (CH_3) and 37.9 (CH_3); *m/z* (ESI+) 209 $[M+H]^+$.

N'-Isopropylidenehydrazones

The general procedure for the preparation of the *N'*-isopropylidenehydrazone series was as follows: To a stirred solution of unsubstituted hydrazide (ca. 30 mmol) in acetone (25 cm^3) was added Na_2SO_4 (~100 eq.). The reaction mixture was stirred at room temperature for 18 h, then filtered and concentrated under reduced pressure to yield the *N'*-isopropylidene hydrazone as a crystalline solid. The following compounds were prepared using this procedure.

4-Methoxybenzoic acid *N'*-isopropylidenehydrazone

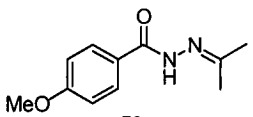

73a

4-Methoxybenzoic acid *N'*-isopropylidenehydrazone was prepared from 4-methoxybenzoic acid hydrazide (5.00 g, 30.1 mmol) and was obtained as a colourless solid (6.06 g, 98% yield); mp 133 – 134 °C (from cyclohexane/toluene, lit.[195] 128 – 129 °C from ethanol); ^{1}H NMR (250 MHz, $CDCl_3$) 8.89 (1H, br. s, C(O)N*H*) 7.70 (2H, br. d, *J* 7.5, Ar*H*), 6.80 (2H, d, *J* 7.5, Ar*H*), 3.73 (3H, s, ArOCH_3), 2.00 (3H, s, CCH_3) and 1.89 (3H, s, CCH_3); ^{13}C NMR (63 MHz, $CDCl_3$) 163.4 (quat.), 161.9 (quat.), 155.5 (quat.), 128.8 (2C, CH), 125.4 (quat.), 113.3 (2C, CH), 55.0 (CH_3), 25.2 (CH_3), 16.4 (CH_3); ν_{max} (KBr disc) 3251, 2841, 1637, 1606, 1504, 1254; *m/z* (ESI+) 207 $[M+H]^+$.

4-Methylbenzoic acid *N'*-isopropylidenehydrazone

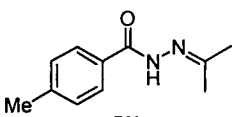

73b

4-Methylbenzoic acid *N'*-isopropylidenehydrazone was prepared from from 4-methyl benzoic acid hydrazide (5.01 g, 33.4 mmol) and was obtained as a colourless solid (6.03 g, 95% yield); mp 143 – 145 °C (from cyclohexane/toluene); ^{1}H NMR (250 MHz, $CDCl_3$) 8.79 (1H, br. s, C(O)N*H*), 7.65 (2H, d, *J* = 8.1 Hz, Ar*H*), 7.25 (2H, d, *J* = 8.1 Hz, Ar*H*), 2.35 (3H, s, ArCH_3), 2.12 (3H, s, CCH_3), 1.93 (3H, s, CCH_3); ^{13}C NMR (63 MHz, $CDCl_3$) 163.6 (quat.), 155.6 (quat.), 142.0 (quat.), 130.5 (quat.),

129.0 (2C, CH), 127.0 (2C, CH), 25.3 (CH_3), 21.3 (CH_3), 16.4 (CH_3); ν_{max} (KBr disc) 3287, 2911, 1664, 1612, 1527, 1286; m/z (ESI+) 191 $[M+H]^+$.

Benzoic acid *N'*-isopropylidenehydrazone

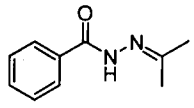

73c

Benzoic acid *N'*-isopropylidenehydrazone was prepared from benzoic acid hydrazide (5.04 g, 38.1 mmol) and was obtained as a colourless solid (6.36 g, 97% yield); mp 145 – 149 °C (from cyclohexane/toluene, lit.[196], 141 – 143 °C); ^{1}H NMR (250 MHz, $CDCl_3$) 8.93 (1H, br s, C(O)N*H*), 7.53 (5H, m, Ar*H*), 2.05 (3H, s, CCH_3), and 1.92 (3H, s, CCH_3); ^{13}C NMR (63 MHz, $CDCl_3$) 163.8 (quat.), 156.2 (quat.), 133.4 (quat.), 131.4 (CH), 128.3 (2C, CH), 126.9 (2C, CH), 25.2 (CH_3), and 16.5 (CH_3); ν_{max} (KBr disc) 3281, 2913, 1653, 1536, 1294, 1142; *m/z* (ESI+) 177 $[M+H]^+$.

4-Chlorobenzoic acid *N'*-isopropylidenehydrazone

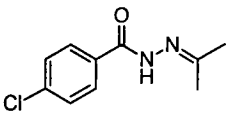

73d

4-Chlorobenzoic acid *N'*-isopropylidenehydrazone was prepared from from 4-chloro benzoic acid hydrazide (0.500 g, 2.91 mmol) and was obtained as a colourless solid (0.58 g, 95% yield); mp 184 – 186 °C (from cyclohexane/toluene, lit.[197] 188 – 189 °C); ^{1}H NMR (250 MHz, $CDCl_3$) 8.82 (1H, br. s, C(O)N*H*) 8.10 (2H, br. d, *J* 7.5, Ar*H*), 7.43 (2H, d, *J* 7.5, Ar*H*), 2.16 (3H, s, CCH_3) and 2.01 (3H, s, CCH_3); ^{13}C NMR (63 MHz, $CDCl_3$) 164.9 (quat.), 161.9 (quat.), 139.5 (quat.), 131.1 (quat.), 129.0 (2C, CH), 128.4 (2C, CH), 25.9 (CH_3), 16.8 (CH_3); ν_{max} (KBr disc) 3302, 2992, 1657, 1636, 1369, 1264; *m/z* (ESI+) 213 $[^{37}M+H]^+$, 211 $[^{35}M+H]^+$.

4-Nitrobenzoic acid *N'*-isopropylidenehydrazone

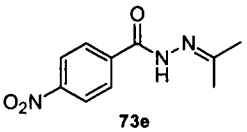

73e

4-Nitrobenzoic acid *N'*-isopropylidenehydrazone was prepared from 4-nitro benzoic acid (4.98 g, 27.5 mmol) and was obtained as a yellow solid (5.64 g, 91% yield); mp 162 – 165 °C (from cyclohexane/toluene, lit.[195] 158 – 159 °C from ethanol); ^{1}H NMR (250 MHz, $(CD_3)_2SO$) 10.93 (1H, br. s, C(O)N*H*), 8.34 (2H, d, *J* = 8.5 Hz, Ar*H*), 8.08 (2H, d, *J* = 8.5 Hz, Ar*H*), 2.05 (3H, s, CCH_3), 1.99 (3H, s, CCH_3); ^{13}C NMR (63 MHz, $CDCl_3$) 161.7 (quat.), 161.5 (quat.), 148.7 (quat.), 139.7 (quat.), 129.0 (2C, CH), 123.2 (2C, CH), 24.8 (CH_3), 18.0 (CH_3); ν_{max} (KBr disc) 3334, 1661, 1601, 1519, 1348, 1107; *m/z* (ESI+) 221 $[M+H]^+$.

N'-Isopropylhydrazides

The general procedure for the preparation of the *N'*-isopropyl hydrazide series was as follows: To a solution of *N'*-isopropylidene hydrazone (11 mmol) in MeOH (25 cm^3) was added $NaCNBH_3$ (0.73 g, 12 mmol, 1.1 eq.) and AcOH (0.69 g, 12 mmol, 1.1 eq.). The reaction mixture was stirred at room temperature for 18 h before being poured cautiously onto sat. Na_2CO_3 (100 cm^3), and extracted with CH_2Cl_2 (3 × 100 cm^3). The combined organics were dried (Na_2SO_4) and concentrated under reduced pressure to give the pure *N'*-substituted hydrazide. The following compounds were prepared using this procedure.

Benzoic acid *N'*-isopropylhydrazide

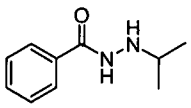

73c

Benzoic acid *N'*-isopropylhydrazide was prepared from **x** (1.851 g, 10.8 mmol) and was obtained as a colourless solid (1.69 g, 90% yield); mp 118 – 119 °C (from cyclohexane, lit.[198] 115 – 117 °C); ^{1}H NMR (250 MHz, $CDCl_3$) 7.54 (5H, m, Ar*H*), 3.26 [1H, spt, C*H*$(CH_3)_2$, *J* 6.3 Hz], 1.13 [6H, d, CH(C*H*$_3)_2$, *J* 6.3 Hz]; ^{13}C NMR (63 MHz, $CDCl_3$) 167.3 (quat.), 132.8 (quat.), 131.7 (CH), 128.6 (2C, CH), 126.7 (2C, CH), 51.2 (CH), 20.7 (2C, CH_3); ν_{max} (KBr disc) 3292, 3236, 2917, 1640, 1539, 1131; *m/z* (ESI+) 179 $[M+H]^+$.

4-Methoxybenzoic acid *N'*-isopropylhydrazide

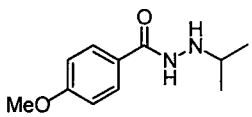

73a

4-Methoxybenzoic acid *N'*-isopropylhydrazide was prepared from **x** (2.17 g, 10.5 mmol) and was obtained as a colourless solid (2.05 g, 94% yield); mp 109 – 110 °C (from cyclohexane, lit.[197] 107 – 108 °C from diisopropyl ether); ^{1}H NMR (250 MHz, $CDCl_3$) 7.74 (2H, d, *J* = 8.8 Hz, Ar*H*), 6.93 (2H, d, *J* = 8.8 Hz, Ar*H*), 3.85 (3H, s, ArOC*H*$_3$), 3.20 [1H, spt, C*H*$(CH_3)_2$, *J* = 6.3 Hz], 1.11 [6H, d, CH(C*H*$_3)_2$, *J* = 6.3 Hz]; ^{13}C NMR (63 MHz, $CDCl_3$) 166.9 (quat.), 162.3 (quat.), 128.5 (2C, CH), 125.0

(quat.), 113.7 (2C, CH), 55.3 (CH_3), 51.2 (CH), 20.7 (2C, CH_3); ν_{max} (KBr disc) 3302, 3247, 2967, 1634, 1609, 1484; *m/z* (ESI+) 231 $[M+Na]^+$.

4-Methylbenzoic acid *N'*-isopropylhydrazide

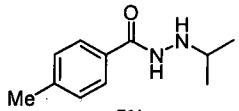

73b

4-Methylbenzoic acid *N'*-isopropylhydrazide was prepared from **x** (2.01 g, 10.6 mmol) and was obtained as a colourless solid (2.01 g, 99 % yield); mp 107 – 110 °C (from cyclohexane); ^{1}H NMR (250 MHz, $CDCl_3$) 7.68 (2H, d, Ar*H*, *J* 8.3), 7.27 (2H, d, Ar*H*, *J* 8.3), 3.26 (1H, spt, C*H*$(CH_3)_2$), *J* 6.3), 2.42 (3H, s, C*H*$_3$Ar), 1.14 (6H, d, CH(C*H*$_3)_2$, *J* 6.3); ^{13}C NMR (63 MHz, $CDCl_3$) 167.3 (quat.), 142.2 (quat.), 129.9 (quat.), 129.2 (2C, CH), 126.7 (2C, CH), 51.2 (CH), 21.4 (CH_3), 20.7 (2C, CH_3); ν_{max} (KBr disc) 3309, 3244, 2965, 1638, 1539, 1485; *m/z* (ESI+) 193 $[M+H]^+$.

4-Chlorobenzoic acid *N'*-isopropylhydrazide

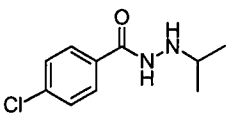

73d

4-Chlorobenzoic acid *N'*-isopropylhydrazide was prepared from **x** (0.12 g, 0.56 mmol) and was obtained as a colourless solid (0.12 g, 91% yield); mp 133 – 134 °C (from cyclohexane, lit.[197] 135 °C); ^{1}H NMR ($CDCl_3$, 250 MHz) 7.64 (2H, d, *J* = 8.6 Hz, Ar*H*), 7.36 (2H, d, *J* = 8.6 Hz, Ar*H*), 3.17 [1H, spt, C*H*$(CH_3)_2$, *J* = 6.3 Hz], 1.05 [6H, d, CH(C*H*$_3)_2$, *J* = 6.3 Hz]; ^{13}C NMR (63 MHz, $CDCl_3$) 166.3 (quat.), 137.9 (quat.), 131.1 (quat.), 128.8 (2C, CH), 128.2 (2C, CH), 51.2 (CH), 20.7 (2C, CH_3); ν_{max} (KBr disc) 3305, 3268, 2965, 1638, 1541, 1092; m/z (ESI+) 215 $[^{37}M+H]^+$, 213 $[^{35}M+H]^+$.

4-Nitrobenzoic acid *N'*-isopropylhydrazide

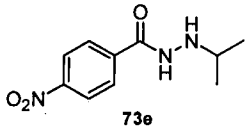

73e

4-Nitrobenzoic acid *N'*-isopropylhydrazide was prepared from **x** (2.32 g, 10.5 mmol) and was obtained as a yellow solid (1.86 g, 79% yield); mp 142 – 144 °C (from cyclohexane/toluene, lit.[199] 140 – 141 °C); ^{1}H NMR (360 MHz, $CDCl_3$) 8.29 (2H, d, J = 8.9 Hz, Ar*H*), 7.95 (2H, d, J = 8.9 Hz, Ar*H*), 3.25 [1H, spt, C*H*$(CH_3)_2$, J = 6.3 Hz], 1.11 [6H, d, CH(C*H*$_3)_2$, J = 6.3 Hz]; ^{13}C NMR (90 MHz, $CDCl_3$) 165.2 (quat.), 149.6 (quat.), 138.3 (quat.), 128.0 (2C, CH), 123.8 (2C, CH), 51.4 (CH), 20.7 (2C, CH_3); ν_{max} (KBr disc) 3303, 3234, 1644, 1596, 1515, 1348; *m/z* (ESI+) 224 $[M+H]^+$.

Substituted dyes

The general procedure for the synthesis of the series of hydrazide-substituted dyes is given below. The reaction was monitored by HPLC using the following conditions:

Column: Waters Spherisorb (15 cm × 4.6 mm internal diameter, 5 μ)

Eluent A: H_2O (1 % Ammonium Acetate)

Eluent B: 9:1 MeCN:H_2O (1 % Ammonium Acetate)

Monitoring Wavelength: 254 nm

Gradient Table:

Time / min	% B	Flow / $cm^3 min^{-1}$
0	5	1.0
3	5	1.0
10	60	1.0
13	60	1.0
15	5	1.0
20	5	1.0

To a suspension of cyanuric chloride (10 mmol, 1.0 eq.) and calsolene oil (0.1 cm^3) in ice/water (100 cm^3) was added a solution of S178095 monoazo (10 mmol, corrected for strength) in water (200 cm^3, adjusted to *ca.* pH 8 by addition of 0.1 M $NaOH_{(aq.)}$). The reaction was cooled in an ice bath and maintained at 0-5 °C by direct addition of ice. The pH was maintained at 6.6-6.8 by addition of 0.1 M $NaOH_{(aq.)}$. When the reaction was adjudged complete by HPLC,[†] the temperature was raised to 35 °C and a suspension of hydrazide (10 mmol, 1.0 eq) in water (50 cm^3) was added dropwise. The pH was maintained at 6.6-6.8 by addition of 0.1 M $NaOH_{(aq.)}$. Following complete reaction of the hydrazide the reaction mixture was adjusted to pH 12 by addition of 1 M $NaOH_{(aq.)}$, and the temperature raised to 70 °C. Once hydrolysis was complete the reaction mixture was adjusted to pH 4 and sodium

[†] Reaction is adjudged complete when < 2 % by area of the starting material remains.

chloride added (15 % w/v, *ca.* 45 g). The reaction mixture was allowed to cool to room temperature and the product collected as a red precipitate by suction filtration. The product was purified by dialysis.[‡] In NMR analysis of compounds of this type, some quaternary signals are often not apparent. The compounds synthesised have been fully or partially characterised by NMR spectroscopy. Because products are usually contaminated with variable amounts of sodium chloride, elemental analysis generally does not provide satisfactory characterisation data. In this field, satisfactory MS and HPLC analyses are generally considered sufficient for characterisation, but in one case, FAB mass spectrometry (supported by accurate mass measurement) was used to confirm the constitution of the product. The following compounds were prepared by this method.

2-(N′-{8-[4-(*N*′-Aminooxalylhydrazino)-6-oxo-1,6-dihydro-[1,3,5]triazin-2-ylamino]-1-oxo-3,6-disulfo-1*H*-naphthalen-2-ylidene}-hydrazino)-benzoic acid

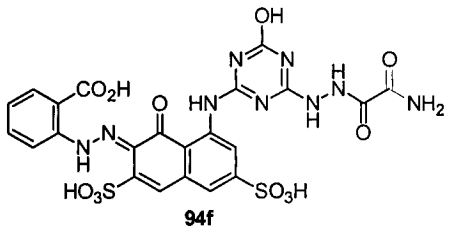

94f

2-(N′-{8-[4-(*N*′-Aminooxalylhydrazino)-6-oxo-1,6-dihydro-[1,3,5]triazin-2-ylamino]-1-oxo-3,6-disulfo-1*H*-naphthalen-2-ylidene}-hydrazino)-benzoic acid was prepared from S178095 monoazo (4.87 g, 6.00 mmol), cyanuric chloride (1.11 g, 6.00 mmol) and oxamic hydrazide (0.61 g, 5.99 mmol) ^{1}H NMR [360 MHz, 80 °C, $(CD_3)_2SO$] 9.34 (1H, s, Ar*H*), 8.45 (1H, d, ^3J = 8.2 Hz, Ar*H*), 8.18 (1H, d, ^3J = 7.5 Hz, Ar*H*), 7.62 – 7.34 (3H, m, Ar*H*) and 7.21 (1H, t, ^3J = 7.5 Hz, Ar*H*); ^{13}C NMR [91 MHz, 80 °C, $(CD_3)_2SO$] 180.4 (quat.), 171.7 (quat.), 159.0 (quat.), 158.5 (quat.), 153.9 (quat.), 145.6 (quat.), 145.4 (quat.), 138.3 (quat.), 132.8 (quat.), 132.7 (quat), 132.6 (CH), 130.5 (quat.), 125.7 (CH), 125.1 (quat.), 122.7 (CH), 122.6 (quat.), 118.8 (CH), 118.7 (quat.), 117.9 (quat.), 117.0 (CH) and 97.4 (quat.); *m/z* (ESI-) 662 $[M-H]^-$ (15 %), 331 $[M-2H]^{2-}$ (100); HPLC RT, 9.2 min; λ_{max} (H_2O) 542 nm. A single quaternary resonance is not apparent in the ^{13}C NMR spectrum.

[‡]An aqueous solution of dye (*ca.* 0.5 M) was dialysed until the conductivity of the dialysis medium was consistently < 50 μS cm^{-1} after 30 min.

2-[*N'*-(8-{4-[*N'*-(4-Methylbenzoyl)-hydrazino]-6-oxo-1,6-dihydro-[1,3,5]triazin-2-ylamino}-1-oxo-3,6-disulfo-1*H*-naphthalen-2-ylidene)-hydrazino]-benzoic acid

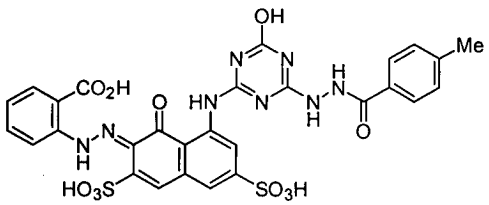

2-[*N'*-(8-{4-[*N'*-(4-Methylbenzoyl)-*N*,*N'*-dimethylhydrazino]-6-oxo-1,6-dihydro-[1,3,5]triazin-2-ylamino}-1-oxo-3,6-disulfo-1*H*-naphthalen-2-ylidene)-hydrazino]-benzoic acid was prepared from S178095 monoazo (4.87 g, 6.00 mmol), cyanuric chloride (1.11 g, 6.00 mmol) and 4-methylbenzoic acid hydrazide (0.89 g, 6.00 mmol) ^{1}H NMR [360 MHz, 80 °C, $(CD_3)_2SO$] 9.08 (1H, s, Ar*H*) 8.38 (1H, s, Ar*H*), 8.09 (2H, t, ^{3}J = 7.1 Hz, Ar*H*), 7.65 – 7.37 (5H, m, Ar*H*), 7.18 (1H, t, ^{3}J = 7.5 Hz, Ar*H*) and 2.31 (3H, s, ArCH_3); ^{13}C NMR [91 MHz, 80 °C, $(CD_3)_2SO$] 178.2 (quat.), 169.6 (quat.), 163.3 (quat.), 152.2 (quat.), 143.9 (quat.), 143.7 (quat.), 143.3 (quat.), 136.7 (quat.), 131.2 (quat.), 131.1 (CH), 130.3 (2C, CH), 128.8 (quat.), 128.6 (CH), 128.0 (CH), 127.1 (CH), 126.9 (2C, CH), 125.9 (CH), 124.0 (CH), 120.7 (CH), 118.1 (CH),, 116.6 (CH), 116.1 (quat.), 114.3 (CH) and 21.6 (CH_3); *m/z* (ESI-); HPLC RT, 10.1 min; λ_{max} (H_2O) 542 nm. Two quaternary resonances are not apparent in the ^{13}C NMR spectrum.

2-[*N'*-(8-{4-[*N'*-(4-Chlorobenzoyl)-hydrazino]-6-oxo-1,6-dihydro-[1,3,5]triazin-2-ylamino}-1-oxo-3,6-disulfo-1*H*-naphthalen-2-ylidene)-hydrazino]-benzoic acid

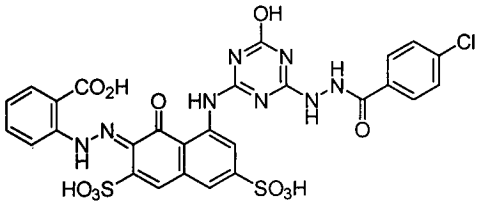

94d

2-[*N'*-(8-{4-[*N'*-(4-Chlorobenzoyl)-hydrazino]-6-oxo-1,6-dihydro-[1,3,5]triazin-2-ylamino}-1-oxo-3,6-disulfo-1*H*-naphthalen-2-ylidene)-hydrazino]-benzoic acid was prepared from S178095 monoazo (12.92 g, 10.0 mmol), cyanuric chloride (1.82 g, 10.0 mmol) and 4-chlorobenzoic acid hydrazide (1.67 g, 9.80 mmol) ^{1}H NMR [360 MHz, 80 °C, $(CD_3)_2SO$] 9.02 (1H, s, Ar*H*), 8.32 - 8.15 (2H, m, Ar*H*), 7.82 – 7.24 (8H, m, Ar*H*) and 7.17 (1H, t, ^3J = 7.5 Hz, Ar*H*); ^{13}C NMR [91 MHz, 80 °C, $(CD_3)_2SO$] 180.1 (quat.), 174.2 (quat.), 167.4 (quat.), 167.1 (quat.), 163.1 (quat.), 155.8 (quat.), 144.2 (quat.), 141.2 (quat.), 139.0 (quat.), 135.4 (quat.), 133.2 (quat.), 132.4 (CH), 132.2 (quat.), 131.8 (2C, CH), 130.1 (2C, CH), 129.8 (quat.), 129.4 (CH), 129.2 (CH), 125.8 (CH), 122.1 (quat.), 118.6 (CH), 117.1 (CH) and 116.0 (CH); *m/z* (ESI-) 729 $[M-H]^-$ (100 %), 751 $[M+Na-2H]^-$ (65); HPLC RT, 10.4 min; λ_{max} (H_2O) 542 nm. Two quaternary resonances are not apparent in the ^{13}C NMR spectrum.

2-(*N'*-{8-[4-(*N'*-Benzoylhydrazino)-6-oxo-1,6-dihydro-[1,3,5]triazin-2-ylamino]-1-oxo-3,6-disulfo-1*H*-naphthalen-2-ylidene}-hydrazino)-benzoic acid

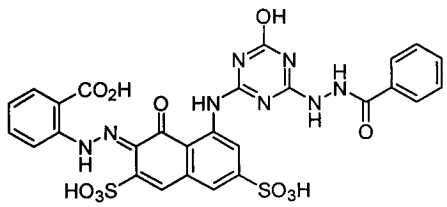

94c

2-(*N'*-{8-[4-(*N'*-Benzoylhydrazino)-6-oxo-1,6-dihydro-[1,3,5]triazin-2-ylamino]-1-oxo-3,6-disulfo-1*H*-naphthalen-2-ylidene}-hydrazino)-benzoic acid was prepared from S178095 monoazo (5.64 g, 12.0 mmol), cyanuric chloride (2.21 g, 12.0 mmol) and benzoic acid hydrazide (1.62 g, 12.0 mmol) ^{1}H NMR [360 MHz, 80 °C, $(CD_3)_2SO$] 8.56 (1H, s, Ar*H*), 8.22 (1H, d, ^3J = 7.1 Hz, Ar*H*), 7.98 (1H, d, ^3J = 7.1

Hz, Ar*H*), 7.73 – 7.41 (8H, m, Ar*H*), 7.11 (1H, t, ^3J = 7.5 Hz, Ar*H*); ^{13}C NMR [91 MHz, 80 °C, $(CD_3)_2SO$] 179.3 (quat.), 170.1 (quat.), 167.2 (quat.), 164.8 (quat.), 158.2 (quat.), 156.1 (quat.), 151.4 (quat.), 144.7 (quat.), 143.9 (quat.), 138.2 (quat.), 132.2 (CH), 131.8 (CH), 131.5 (quat.), 130.9 (CH), 130.4 (quat.), 128.9 (2C, CH), 127.6 (2C, CH), 124.3 (CH), 121.2 (CH), 119.8 (CH), 118.7 (CH) and 117.3 (CH); *m/z* (ESI-) 695 $[M-H]^-$ (28 %), 347 $[M-2H]^{2-}$ (100); HPLC RT, 9.9 min; λ_{max} (H_2O) 542 nm. Three quaternary resonances are not apparent in the ^{13}C NMR spectrum.

2-[*N'*-(8-{4-[*N'*-(4-Methoxybenzoyl)-*N'*-methylhydrazino]-6-oxo-1,6-dihydro-[1,3,5]triazin-2-ylamino}-1-oxo-3,6-disulfo-1*H*-naphthalen-2-ylidene)-hydrazino]-benzoic acid

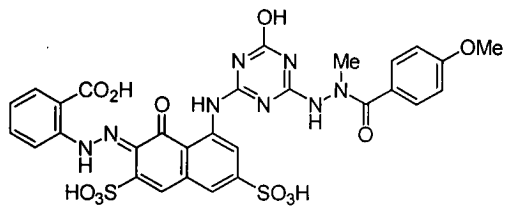

95a

2-[*N'*-(8-{4-[*N'*-(4-Methoxybenzoyl)-*N'*-methylhydrazino]-6-oxo-1,6-dihydro-[1,3,5]triazin-2-ylamino}-1-oxo-3,6-disulfo-1*H*-naphthalen-2-ylidene)-hydrazino]-benzoic acid was prepared from S178095 monoazo (12.92 g, 10.0 mmol), cyanuric chloride (1.84 g, 10.0 mmol) and 4-methoxybenzoic acid *N*-methylhydrazide (1.73 g, 9.80 mmol) ^{1}H NMR [360 MHz, 80 °C, $(CD_3)_2SO$] 8.97 (1H, s, Ar*H*), 8.44 (1H, d, ^3J = 8.3 Hz, Ar*H*), 8.07 (2H, d, ^3J = 7.6 Hz, Ar*H*), 7.63 (2H, d, ^3J = 7.6 Hz, Ar*H*), 7.55 (1H, s, Ar*H*), 7.50 (1H, s, Ar*H*), 7.47 (1H, t, ^3J = 7.2 Hz, Ar*H*), 7.19 (1H, t, ^3J = 7.5 Hz, Ar*H*), 6.89 (1H, d, ^3J = 7.6 Hz, Ar*H*), 3.75 (s, 3H, ArOCH_3), and 3.33 (br. s, 3H, (CO)NCH_3); ^{13}C NMR [91 MHz, 80 °C, $(CD_3)_2SO$] 178.3 (quat.), 171.2 (quat.), 160.4 (quat.), 158.1 (quat.), 152.3 (quat.), 144.2 (quat.), 143.7 (quat.), 142.1 (quat.), 136.7 (quat.), 130.9 (quat.), 130.6 (CH), 129.3 (2C, CH), 128.8 (quat.), 126.8 (CH), 124.9 (quat.), 123.9 (CH), 120.5 (CH), 119.5 (CH), 117.1 (CH), 116.9 (quat.), 115.6 (CH), 112.9 (2C, CH), 55.0 (CH_3), and 44.4 (CH_3); *m/z* (ESI-) 739 $[M-H]^-$ (100 %), 761 $[M+Na-2H]^-$ (20); HPLC RT, 10.5 min; λ_{max} (H_2O) 542 nm. Three quaternary resonances are not apparent in the ^{13}C NMR spectrum.

2-[*N'*-(8-{4-[*N'*-(4-Methylbenzoyl)-*N'*-methylhydrazino]-6-oxo-1,6-dihydro-[1,3,5]triazin-2-ylamino}-1-oxo-3,6-disulfo-1*H*-naphthalen-2-ylidene)-hydrazino]-benzoic acid

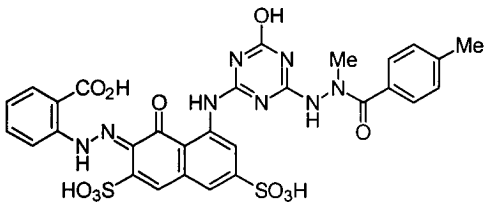

95b

2-[*N'*-(8-{4-[*N'*-(4-Methylbenzoyl)-*N'*-methylhydrazino]-6-oxo-1,6-dihydro-[1,3,5]triazin-2-ylamino}-1-oxo-3,6-disulfo-1*H*-naphthalen-2-ylidene)-hydrazino]-benzoic acid was prepared from S178095 monoazo (12.92 g, 10.0 mmol), cyanuric chloride (1.84 g, 10.0 mmol) and 4-methylbenzoic acid *N*-methylhydrazide (1.57 g, 9.80 mmol) ^{1}H NMR [360 MHz, 80 °C, $(CD_3)_2SO$] 8.97 (1H, s, Ar*H*), 8.44 (1H, d, ^3J = 8.3 Hz, Ar*H*), 8.07 (1H, d, ^3J = 7.6 Hz, Ar*H*), 7.64 – 7.52 (3H, m, Ar*H*), 7.49 (1H, s, Ar*H*), 7.46 (1H, t, ^3J = 6.9 Hz, Ar*H*), 7.19 (1H, t, ^3J = 7.1 Hz, Ar*H*), 7.14 (2H, d, ^3J = 7.3 Hz, Ar*H*), 3.32 (br. s, 3H, (CO)NCH_3) and 2.32 (s, 3H, ArCH_3); ^{13}C NMR [91 MHz, 80 °C, $(CD_3)_2SO$] 180.0 (quat.), 173.4 (quat.), 160.2 (quat.), 154.0 (quat.), 146.0 (quat.), 145.4 (quat.), 143.9 (quat.), 141.0 (quat.), 133.8 (quat.), 132.7 (CH), 132.2 (CH), 130.5 (quat.), 129.7 (2C, CH), 129.1 (2C, CH), 127.0 (quat.), 125.7 (CH), 122.2 (CH), 121.2 (CH), 118.9 (CH), 118.7 (quat.), 117.4 (CH), 105.7 (quat.), 96.1 (quat.), 42.3 (CH_3), and 22.3 (CH_3); *m/z* (ESI-) 723 $[M-H]^-$ (100 %), 745 $[M+Na-2H]^-$ (45); HPLC RT, 10.2 min; λ_{max} (H_2O) 542 nm. Two quaternary resonances are not apparent in the ^{13}C NMR spectrum.

2-(*N'*-{8-[4-(*N'*-Benzoyl-*N'*-methylhydrazino)-6-oxo-1,6-dihydro-[1,3,5]triazin-2-ylamino]-1-oxo-3,6-disulfo-1*H*-naphthalen-2-ylidene}-hydrazino)-benzoic acid

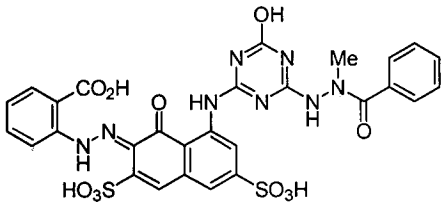

95c

2-(*N'*-{8-[4-(*N'*-Benzoyl-*N'*-methylhydrazino)-6-oxo-1,6-dihydro-[1,3,5]triazin-2-ylamino]-1-oxo-3,6-disulfo-1*H*-naphthalen-2-ylidene}-hydrazino)-benzoic acid was prepared from S178095 monoazo (12.92 g, 10.0 mmol), cyanuric chloride (1.84 g, 10.0 mmol) and benzoic acid *N*-methylhydrazide (1.47 g, 9.80 mmol) ^{1}H NMR [360 MHz, 80 °C, $(CD_3)_2SO$] 8.97 (1H, s, Ar*H*), 8.45 (1H, d, ^{3}J = 8.2 Hz, Ar*H*), 8.08 (1H, d, ^{3}J = 7.5 Hz, Ar*H*), 7.62 – 7.34 (8H, m, Ar*H*), 7.19 (1H, t, ^{3}J = 7.5 Hz, Ar*H*), 3.34 (br. s, 3H, (CO)NCH_3); ^{13}C NMR [91 MHz, 80 °C, $(CD_3)_2SO$] 180.0 (quat.), 173.4 (quat.), 160.2 (quat.), 154.0 (quat.), 146.0 (quat.), 145.4 (quat.), 143.9 (quat.), 138.4 (quat.), 136.8 (quat.), 132.7 (CH), 132.3 (CH), 131.2 (CH), 130.5 (quat.), 129.1 (2C, CH), 128.9 (2C, CH), 126.9 (quat.), 125.7 (CH), 125.1 (quat.), 122.2 (CH), 121.2 (CH), 118.9 (CH), 118.7 (quat.), 117.4 (CH), 105.7 (quat.), 96.1 (quat.), and 41.4 (CH_3); *m/z* (ESI-) 709 $[M-H]^-$ (100 %), 731 $[M+Na-2H]^-$ (75), 753 $[M+2Na-3H]^-$ (20); HPLC RT, 10.9 min; λ_{max} (H_2O) 542 nm.

2-[*N'*-(8-{4-[*N'*-(4-Chlorobenzoyl)-*N'*-methylhydrazino]-6-oxo-1,6-dihydro-[1,3,5]triazin-2-ylamino}-1-oxo-3,6-disulfo-1*H*-naphthalen-2-ylidene)-hydrazino]-benzoic acid

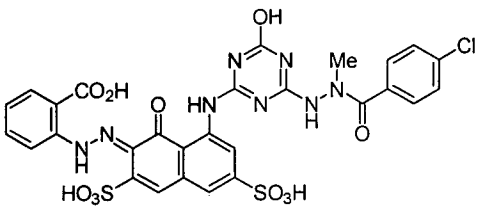

95d

2-[*N'*-(8-{4-[*N'*-(4-Chlorobenzoyl)-*N'*-methylhydrazino]-6-oxo-1,6-dihydro-[1,3,5]triazin-2-ylamino}-1-oxo-3,6-disulfo-1*H*-naphthalen-2-ylidene)-hydrazino]-benzoic acid was prepared from S178095 monoazo (12.92 g, 10.0 mmol), cyanuric chloride (1.81 g, 10.0 mmol) and 4-chlorobenzoic acid *N*-methylhydrazide (1.81 g, 9.80 mmol) ^{1}H NMR [360 MHz, 80 °C, $(CD_3)_2SO$] 9.18 (1H, s, Ar*H*), 8.42 (1H, d, ^{3}J = 8.0 Hz, Ar*H*), 8.09 (1H, d, ^{3}J = 7.7 Hz, Ar*H*), 7.82 – 7.24 (7H, m, Ar*H*), 7.17 (1H,

t, ^3J = 7.5 Hz, Ar*H*), 3.36 (br. s, 3H, (CO)NCH_3); ^{13}C NMR [91 MHz, 80 °C, $(CD_3)_2SO$] 180.3 (quat.), 173.0 (quat.), 166.6 (quat.), 166.1 (quat.), 162.8 (quat.), 153.3 (quat.), 146.3 (quat.), 145.3 (quat.), 138.3 (quat.), 136.6 (quat.), 135.5 (quat.), 132.8 (CH), 132.6 (quat.), 131.2 (2C, CH), 130.7 (2C, CH), 130.5 (quat.), 130.0 (CH), 129.2 (2C, CH), 125.5 (CH), 122.6 (quat.), 118.5 (CH), 117.6 (quat.), 116.4 (CH) and 42.4 (CH_3); *m/z* (ESI-) 743 $[M-H]^-$ (100 %), 765 $[M+Na-2H]^-$ (82); HPLC RT, 10.8 min; λ_{max} (H_2O) 542 nm. A single quaternary resonance is not apparent in the ^{13}C NMR spectrum.

2-[*N'*-(8-{4-[*N'*-(4-Nitrobenzoyl)-*N'*-methylhydrazino]-6-oxo-1,6-dihydro-[1,3,5]triazin-2-ylamino}-1-oxo-3,6-disulfo-1*H*-naphthalen-2-ylidene)-hydrazino]-benzoic acid

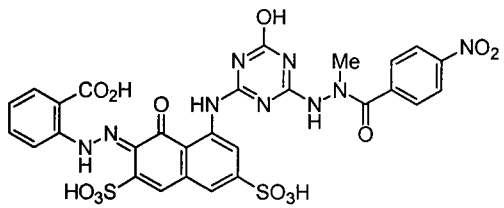

95e

2-[*N'*-(8-{4-[*N'*-(4-Nitrobenzoyl)-*N'*-methylhydrazino]-6-oxo-1,6-dihydro-[1,3,5]triazin-2-ylamino}-1-oxo-3,6-disulfo-1*H*-naphthalen-2-ylidene)-hydrazino]-benzoic acid was prepared from S178095 monoazo (12.92 g, 10.0 mmol), cyanuric chloride (1.84 g, 10.0 mmol) and 4-nitrobenzoic acid *N*-methylhydrazide (1.91 g, 9.80 mmol) ^{1}H NMR [360 MHz, 80 °C, $(CD_3)_2SO$] 8.99 (1H, s, Ar*H*), 8.44 (1H, d, ^3J = 7.8 Hz, Ar*H*), 8.15 (2H, d, ^3J = 6.5 Hz, Ar*H*), 8.08 (1H, d, ^3J = 7.8 Hz, Ar*H*), 7.87 (2H, d, ^3J = 6.5 Hz, Ar*H*), 7.61 (1H, s, Ar*H*), 7.55 (1H, s, Ar*H*), 7.48 (1H, t, ^3J = 7.8 Hz, Ar*H*), 7.21 (1H, t, ^3J = 7.3 Hz, Ar*H*), and 3.37 (3H, br. s, (CO)NCH_3); ^{13}C NMR [91 MHz, 80 °C, $(CD_3)_2SO$] 178.3 (quat.), 169.8 (quat.), 158.6 (quat.), 152.5 (quat.), 152.0 (quat.), 148.0 (quat.), 144.0 (quat.), 143.6 (quat.), 142.0 (quat.), 141.7 (quat.), 136.8 (quat.), 131.1 (CH), 130.9 (CH), 128.8 (CH), 128.5 (quat.), 125.0 (quat.), 124.4 (CH), 122.7 (2C, CH), 120.7 (CH), 119.8 (2C, CH), 117.2 (CH), 115.8 (CH), 104.1 (quat.), 94.4 (quat.), and 44.1 (CH_3); *m/z* (ESI-) 754 $[M-H]^-$ (75 %), 776 $[M+Na-2H]^-$ (100), 898 $[M+2Na-3H]^-$ (35); HPLC RT, 9.2 min; λ_{max} (H_2O) 542 nm. A single quaternary resonance is not apparent in the ^{13}C NMR spectrum.

2-[*N'*-(8-{4-[*N'*-(4-Methoxybenzoyl)-*N*-isopropylhydrazino]-6-oxo-1,6-dihydro-[1,3,5]triazin-2-ylamino}-1-oxo-3,6-disulfo-1*H*-naphthalen-2-ylidene)-hydrazino]-benzoic acid

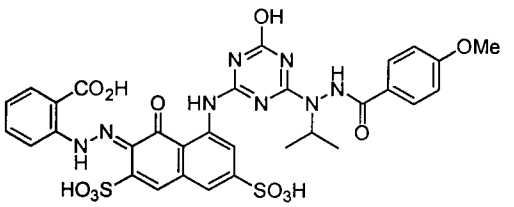

96a

2-[*N'*-(8-{4-[*N'*-(4-Methoxybenzoyl)-*N*-isopropylhydrazino]-6-oxo-1,6-dihydro-[1,3,5]triazin-2-ylamino}-1-oxo-3,6-disulfo-1*H*-naphthalen-2-ylidene)-hydrazino]-benzoic acid was prepared from S178095 monoazo (4.86 g, 6.00 mmol), cyanuric chloride (1.09 g, 6.00 mmol) and 4-methoxybenzoic acid isopropylhydrazide (1.20 g, 6.00 mmol) ^{1}H NMR [360 MHz, 80 °C, $(CD_3)_2SO$] ^{1}H NMR [360 MHz, 80 °C, $(CD_3)_2SO$] 8.91 (1H, s, Ar*H*), 8.46 (1H, d, ^3J = 8.0 Hz, Ar*H*), 8.01 (2H, d, ^3J = 7.5 Hz, Ar*H*), 7.61 (2H, d, ^3J = 7.5 Hz, Ar*H*), 7.57 (1H, s, Ar*H*), 7.54 (1H, s, Ar*H*), 7.42 (1H, t, ^3J = 6.8 Hz, Ar*H*), 7.18 (1H, t, ^3J = 7.2 Hz, Ar*H*), 6.91 (1H, d, ^3J = 7.6 Hz, Ar*H*) 5.27 (1H, sept., ^3J = 6.2 Hz, C*H*$(CH_3)_2$) and 1.26 (6H, d, ^3J = 6.2 Hz, $(CH_3)_2$CH); ^{13}C NMR [75 MHz, 80 °C, $(CD_3)_2SO$] 178.2 (quat.), 169.2 (quat.), 166.2 (quat.), 164.0 (quat.), 162.7 (quat.), 161.6 (quat.), 152.4 (quat.), 144.1 (quat.), 143.5 (quat.), 143.3 (quat.), 136.5 (quat.), 130.7 (CH), 129.8 (CH), 129.4 (2C, CH), 128.7 (quat.), 126.2 (quat.), 125.4 (quat.), 123.5 (CH), 120.3 (CH), 118.0 (CH), 116.8 (quat.), 116.2 (CH), 115.2 (CH), 113.2 (2C, CH), 55.1 (CH_3), 50.9 (CH), and 21.1 (2C, CH_3); *m/z* (ESI-) 767 $[M-H]^-$ (75 %), 383 $[M-2H]^{2-}$ (100); HPLC RT, 10.1 min; λ_{max} (H_2O) 542 nm. A single quaternary resonance is not apparent in the ^{13}C NMR spectrum.

2-[*N'*-(8-{4-[*N'*-(4-Methylbenzoyl)-*N*-isopropylhydrazino]-6-oxo-1,6-dihydro-[1,3,5]triazin-2-ylamino}-1-oxo-3,6-disulfo-1*H*-naphthalen-2-ylidene)-hydrazino]-benzoic acid

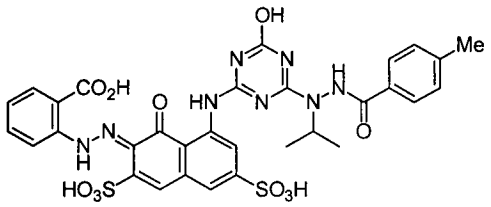

96b

2-[*N'*-(8-{4-[*N'*-(4-Methylbenzoyl)-*N*-isopropylhydrazino]-6-oxo-1,6-dihydro-[1,3,5]triazin-2-ylamino}-1-oxo-3,6-disulfo-1*H*-naphthalen-2-ylidene)-hydrazino]-benzoic acid was prepared from S178095 monoazo (4.87 g, 6.00 mmol), cyanuric chloride (1.09 g, 6.00 mmol) and 4-methylbenzoic acid isopropylhydrazide (1.15 g, 6.00 mmol) ^{1}H NMR [360 MHz, 80 °C, $(CD_3)_2SO$ + D_2O] 9.19 (1H, s, Ar*H*), 8.34 (1H, d, ^3J = 8.3 Hz, Ar*H*), 7.99 (2H, d, ^3J = 7.7 Hz, Ar*H*), 7.81 (2H, d, ^3J = 7.7 Hz, Ar*H*), 7.64 (1H, s, Ar*H*), 7.56 – 7.49 (2H, m, Ar*H*), 7.30 (1H, d, ^3J = 7.8 Hz, Ar*H*), 7.24 (1H, t, ^3J = 7.5 Hz, Ar*H*), 5.16 (1H, sept., ^3J = 6.5 Hz, C*H*$(CH_3)_2$), 2.34 (3H, s, ArCH_3), and 1.24 (d, 6H, ^3J = 6.5 Hz, $(CH_3)_2$); ^{13}C NMR [91 MHz, 80 °C, $(CD_3)_2SO$] 179.8 (quat.), 172.1 (quat.), 164.2 (quat.), 153.4 (quat.), 147.2 (quat.), 146.0 (quat.), 144.8 (quat.), 142.6 (quat.), 134.2 (CH), 133.1 (CH), 132.8 (quat.), 131.0 (quat.), 129.6 (2C, CH), 128.1 (2C, CH), 126.0 (quat.), 125.4 (CH), 123.1 (CH), 122.2 (CH), 118.6 (CH), 117.7 (quat.), 117.1 (CH), 105.7 (quat.), 50.9 (CH), 21.4 (CH_3) and 21.1 (2C, CH_3); *m/z* (ESI-) 751 $[M-H]^-$ (40 %), 375 $[M-2H]^{2-}$ (100); HPLC RT, 10.3 min; λ_{max} (H_2O) 542 nm. Three quaternary resonances are not apparent in the ^{13}C NMR spectrum.

2-(*N'*-{8-[4-(*N'*-Benzoyl-*N*-isopropylhydrazino)-6-oxo-1,6-dihydro-[1,3,5]triazin-2-ylamino]-1-oxo-3,6-disulfo-1*H*-naphthalen-2-ylidene}-hydrazino)-benzoic acid

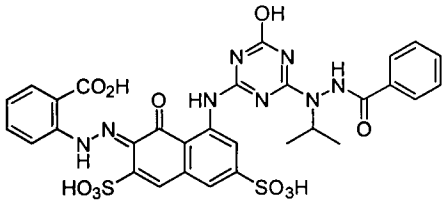

96c

2-(*N'*-{8-[4-(*N'*-Benzoyl-*N*-isopropylhydrazino)-6-oxo-1,6-dihydro-[1,3,5]triazin-2-ylamino]-1-oxo-3,6-disulfo-1*H*-naphthalen-2-ylidene}-hydrazino)-benzoic acid was prepared from S178095 monoazo (4.87 g, 6.00 mmol), cyanuric chloride (1.11 g, 6.00 mmol) and benzoic acid isopropylhydrazide (1.11 g, 6.00 mmol) ^{1}H NMR [360 MHz, 80 °C, $(CD_3)_2SO$] 9.26 (1H, s, Ar*H*), 8.42 (1H, d, ^{3}J = 7.4 Hz, Ar*H*), 8.03 (1H, d, ^{3}J = 7.4 Hz, Ar*H*), 7.63 – 7.36 (8H, m, Ar*H*), 7.15 (1H, t, ^{3}J = 7.5 Hz, Ar*H*), 5.25 (1H, sept., ^{3}J = 6.3 Hz, C*H*$(CH_3)_2$) 1.27 (6H, d, ^{3}J = 6.3 Hz, $(CH_3)_2$CH); ^{13}C NMR [91 MHz, 80 °C, $(CD_3)_2SO$] 180.1 (quat.), 170.6 (quat.), 168.6 (quat.), 164.8 (quat.), 157.9 (quat.), 157.7 (quat.), 154.4 (quat.), 146.2 (quat.), 145.5 (quat.), 138.4 (quat.), 132.7 (CH), 132.6 (CH), 132.5 (quat.), 131.4 (CH), 130.5 (quat.), 129.5 (2C, CH), 129.4 (2C, CH), 125.3 (CH), 122.0 (CH), 119.9 (CH), 118.8 (CH), 117.0 (CH), 51.1 (CH), and 21.3 (2C, CH_3); *m/z* (ESI-) 737 $[M-H]^-$ (18 %), 368 $[M-2H]^{2-}$ (100); HPLC RT, 10.2 min; λ_{max} (H_2O) 542 nm. Three quaternary resonances are not apparent in the ^{13}C NMR spectrum.

2-[*N'*-(8-{4-[*N'*-(4-Chlorobenzoyl)-*N*-isopropylhydrazino]-6-oxo-1,6-dihydro-[1,3,5]triazin-2-ylamino}-1-oxo-3,6-disulfo-1*H*-naphthalen-2-ylidene)-hydrazino]-benzoic acid

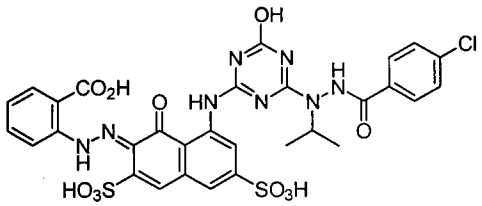

96d

2-[*N'*-(8-{4-[*N'*-(4-Chlorobenzoyl)-*N*-isopropylhydrazino]-6-oxo-1,6-dihydro-[1,3,5]triazin-2-ylamino}-1-oxo-3,6-disulfo-1*H*-naphthalen-2-ylidene)-hydrazino]-benzoic acid was prepared from S178095 monoazo (12.92 g, 10.0 mmol), cyanuric

chloride (1.82 g, 10.0 mmol) and 4-chlorobenzoic acid isopropylhydrazide (2.08 g, 9.80 mmol) ^{1}H NMR [360 MHz, 80 °C, $(CD_3)_2SO$] 9.24 (1H, s, Ar*H*), 8.38 (1H, d, ^3J = 9.7 Hz, Ar*H*), 8.08 (2H, d, ^3J = 7.8 Hz, Ar*H*), 8.04 (1H, d, ^3J = 8.4 Hz, Ar*H*), 7.68 – 7.47 (3H, m, Ar*H*), 7.43 (1H, t, ^3J = 7.0 Hz, Ar*H*), 7.18 (2H, d, ^3J = 7.8 Hz, Ar*H*), 5.22 (1H, sept, ^3J = 6.4 Hz, C*H*$(CH_3)_2$), and 1.27 (6H, d, ^3J = 6.4 Hz, CH$(CH_3)_2$); ^{13}C NMR [91 MHz, 80 °C, $(CD_3)_2SO$] 179.0 (quat.), 170.5 (quat.), 166.9 (quat.), 164.9 (quat.), 164.0 (quat.), 163.4 (quat.), 152.9 (quat.), 144.3 (quat.), 144.1 (quat.), 137.4 (quat.), 136.9 (quat.), 132.6 (quat.), 131.8 (CH), 131.1 (CH), 130.4 (2C, CH), 129.5 (quat.), 128.7 (2C, CH), 126.7 (quat.), 124.8 (CH), 121.5 (CH), 119.3 (CH), 117.5 (CH), 117.3 (quat.), 116.1 (CH), 50.3 (CH), and 20.3 (2C, CH_3); *m/z* (ESI-) 771 [M-H]$^-$ (100 %), 793 [M+Na-2H]$^-$ (80); HPLC RT, 10.4 min; λ_{max} (H_2O) 542 nm. A single quaternary resonance is not apparent in the ^{13}C NMR spectrum.

2-[*N'*-(8-{4-[*N'*-(4-Methoxybenzoyl)-*N,N'*-dimethylhydrazino]-6-oxo-1,6-dihydro-[1,3,5]triazin-2-ylamino}-1-oxo-3,6-disulfo-1*H*-naphthalen-2-ylidene)-hydrazino]-benzoic acid

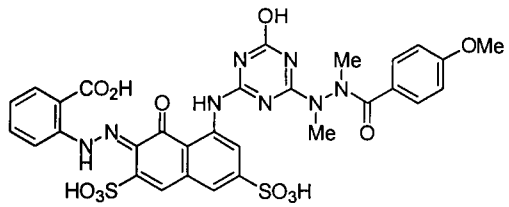

97a

2-[*N'*-(8-{4-[*N'*-(4-Methoxybenzoyl)-*N,N'*-dimethylhydrazino]-6-oxo-1,6-dihydro-[1,3,5]triazin-2-ylamino}-1-oxo-3,6-disulfo-1*H*-naphthalen-2-ylidene)-hydrazino]-benzoic acid was prepared from S178095 monoazo (4.88 g, 6.00 mmol), cyanuric chloride (1.09 g, 6.00 mmol) and 4-methoxybenzoic acid *N,N'*-dimethylhydrazide (1.16 g, 6.00 mmol) ^{1}H NMR [360 MHz, 80 °C, $(CD_3)_2SO$] 8.89 (1H, s, Ar*H*), 8.41 (1H, d, ^3J = 8.0 Hz, Ar*H*), 8.07 (2H, d, ^3J = 7.1 Hz, Ar*H*), 7.63 (2H, d, ^3J = 7.7 Hz, Ar*H*), 7.51 (1H, s, Ar*H*), 7.49 (1H, s, Ar*H*), 7.42 (1H, t, ^3J = 7.2 Hz, Ar*H*), 7.24 (1H, t, ^3J = 7.4 Hz, Ar*H*), 6.89 (1H, d, ^3J = 7.7 Hz, Ar*H*), 3.78 (3H, s, ArOCH_3), 3.33 (3H, br. s, NCH_3) and 2.43 (3H, br. s, N'CH_3); ^{13}C NMR [91 MHz, 80 °C, $(CD_3)_2SO$]; *m/z* (ESI-) 753 [M-H]$^-$ (64 %), 775 [M+Na-2H]$^-$; HPLC RT, 9.4 min; λ_{max} (H_2O) 542 nm.

2-(*N'*-{8-[4-(*N'*-Benzoyl-*N,N'*-dimethylhydrazino)-6-oxo-1,6-dihydro-[1,3,5]triazin-2-ylamino]-1-oxo-3,6-disulfo-1*H*-naphthalen-2-ylidene}-hydrazino)-benzoic acid

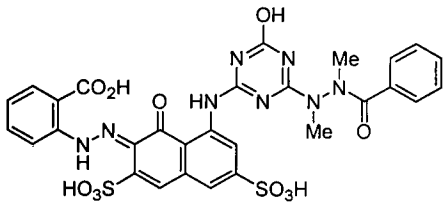

97c

2-(*N'*-{8-[4-(*N'*-Benzoyl-*N,N'*-dimethylhydrazino)-6-oxo-1,6-dihydro-[1,3,5]triazin-2-ylamino]-1-oxo-3,6-disulfo-1*H*-naphthalen-2-ylidene}-hydrazino)-benzoic acid was prepared from S178095 monoazo (4.87 g, 6.00 mmol), cyanuric chloride (1.11 g, 6.00 mmol) and benzoic acid *N,N'*-dimethylhydrazide (0.98 g, 6.00 mmol) ^{1}H NMR [360 MHz, 80 °C, $(CD_3)_2SO$] 8.88 (1H, s, Ar*H*), 8.45 (1H, d, ^{3}J = 8.2 Hz, Ar*H*), 8.18 (1H, d, ^{3}J = 7.3 Hz, Ar*H*), 7.58 – 7.29 (8H, m, Ar*H*), 7.21 (1H, t, ^{3}J = 7.1 Hz, Ar*H*), 3.18 (3H, s, NCH_3) and 2.71 (3H, s, N'CH_3); ^{13}C NMR [75 MHz, 80 °C, D_2O + $(CD_3)_2SO$] 181.0 (quat.), 174.8 (quat.), 168.4 (quat.), 162.4 (quat.), 159.0 (quat.), 150.5 (quat.), 144.7 (quat.), 143.9 (quat.), 142.5 (quat.), 139.4 (quat.), 137.0 (quat.), 134.6 (CH), 133.4 (CH), 133.2 (CH), 130.9 (2C, CH), 129.4 (2C, CH), 128.6 (CH), 127.2 (quat.), 126.8 (CH), 125.4 (CH), 123.9 (quat.), 121.7 (quat.), 119.4 (CH), 118.9 (CH), 41.7 (CH_3), and 35.8 (CH_3); *m/z* (ESI-) 723 $[M-H]^-$ (30 %), 361 $[M-2H]^{2-}$ (100) ; HPLC RT, 10.3 min; λ_{max} (H_2O) 542 nm.

(2-Methoxynaphthalen-1-yl)phenyldiazene

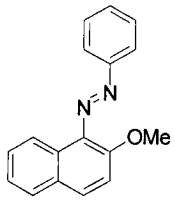

135

To a stirred solution of 1-phenylazonapthalene-2-ol (5.0 g, 20 mmol) in anhydrous DMF (300 cm^3) was added anhydrous potassium carbonate (11 g, 80 mmol) and methyl iodide (56 g, 0.44 mol). The reaction mixture was stirred for 120 h before being concentrated under reduced pressure to a volume of ca. 50 cm^3 and diluted with deionised water (300 cm^3), which was then washed with diethyl ether (3 × 300 cm^3). The combined organic layers were washed with water (3 × 300 cm^3) before being dried over Na_2SO_4 and concentrated under reduced pressure to yield **x** as a red oil as a mixture of *cis*- and *trans*-isomers (5.15 g, 98% yield). The oil crystallised on prolonged standing to yield the *trans* isomer. R_f 0.54 (4:1 EtOAc:Hexane); m.p. 51 – 53 °C; ^{1}H NMR (250 MHz, $CDCl_3$) 8.37 (1H, dd, ^3J = 8.6 Hz, ^4J = 0.7 Hz, Ar*H*), 8.03 (2H, m, Ar*H*), 7.89 (1H, d, ^3J = 9.0 Hz, Ar*H*), 7.84 (1H, d, ^3J = 8.1 Hz, Ar*H*), 7.55 (4H, m, Ar*H*), 7.48 – 7.41 (2H, m, Ar*H*) and 4.00 (3H, s, OCH_3); ^{13}C NMR (63 MHz, $CDCl_3$) 153.4 (quat.), 148.3 (quat.), 136.5 (quat.), 132.4(quat.), 130.9 (CH), 129.0 (2C, CH), 128.4 (quat.), 127.9 (CH), 127.7 (CH), 124.4 (CH), 123.2 (CH), 122.7 (2C, CH), 114.5 (CH) and 57.3 (CH_3); *m/z* (ESI+) 263 $[M+H]^+$.

Reaction of naphthalene-1-ol with benzenediazonium chloride

To a stirred, cooled (~ 5 °C) solution of aniline (5.0 g, 54 mmol) in $HCl_{(aq)}$ (32 cm^3, 18 % w/v) was added a solution of sodium nitrite (4.0 g, 56 mmol, 1.1 eq.) in deionised water (20 cm^3). Naphthalen-1-ol (7.8 g, 54 mmol) was dissolved in $NaOH_{(aq.)}$ (45 cm^3, 10% w/w) and cooled to ~ 5 °C and added slowly to the diazonium salt with stirring. The reaction was stirred for 30 min and the product recovered by continous extraction overnight (DCM/H_2O). The organics were concentrated under reduced pressure and a portion of the product (0.50 g) was purified by dry-flash chromatography to yield 2-phenylazonaphthalen-1-ol (0.10 g) and 4-phenylazonaphthalen-1-ol (0.082 g).

2-Phenylazonaphthalen-1-ol

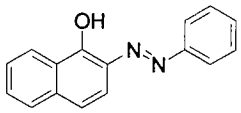

11

R_f 0.88 (4:1 EtOAc:Hexane); ^1H NMR (360 MHz, $CDCl_3$) 8.44 (1H, d, ^3J 8.2 Hz, Ar*H*), 7.66 – 7.58 (4H, m, Ar*H*), 7.50 – 7.44 (3H, m Ar*H*), 7.29 – 7.23 (2H, m Ar*H*) and 7.03 (1H, d, ^3J 9.2 Hz, Ar*H*); ^{13}C NMR (63 MHz, $CDCl_3$); ^{13}C NMR (91 MHz, $CDCl_3$) 174.3 (quat.), 143.1 (quat.), 137.1 (quat.), 132.7 (quat.), 132.3 (CH), 130.2 (quat.), 129.5 (2C, CH), 128.6 (CH), 127.5 (CH), 126.7 (CH), 126.6 (CH), 126.2 (CH), 121.0 (CH), 117.5 (2C, CH); *m/z* (ESI+) 249 $[M+H]^+$.

4-Phenylazonaphthalen-1-ol

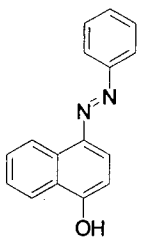

9

^1H NMR (360 MHz, $CDCl_3$) 8.80 (1H, d, ^3J 8.4 Hz, Ar*H*), 8.17 (1H, d, ^3J 8.4 Hz, Ar*H*), 7.84 (1H, d, ^3J 7.5 Hz, Ar*H*), 7.74 (1H, d, ^3J 8.4 Hz, Ar*H*), 7.57 – 7.18 (6H, m, Ar*H*) and 6.87 (1H, d, ^3J 8.4 Hz, Ar*H*); ^{13}C NMR (91 MHz, $CDCl_3$) 158.8 (quat.),

154.2 (quat.), 141.4 (quat.), 134.2 (quat.), 131.2 (CH), 130.2 (2C, CH), 128.5 (CH), 126.3 (CH), 123.9 (CH), 127.2 (quat.), 123.7 (2C, CH), 115.9 (CH), 114.7 (CH) and 109.5 (CH); *m/z* (ESI+) 249 $[M+H]^+$.

(1-Methoxynaphthalen-2-yl)-phenyldiazene

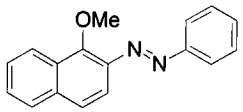

136

To a stirred solution of 2-phenylazonaphthalene-1-ol (0.05 g, 0.2 mmol) in DMF (2 cm^3) was added anhydrous potassium carbonate (0.06 g, 0.4 mmol, 2 eq.) and methyl iodide (0.15 g, 1.0 mmol, 5 eq.). The reaction mixture was stirred for 0.5 h before being diluted with deionised water (10 cm^3), which was then washed with diethyl ether (3 × 10 cm^3). The organics were combined and washed with water (3 × 10 cm^3) before being dried over Na_2SO_4 and concentrated under reduced pressure to yield **x** (0.05 g, 0.2 mmol, 94%). R_f 0.82 (4:1 EtOAc:Hexane); ^1H NMR (360 MHz, $CDCl_3$) 8.44 (1H, m, Ar*H*), 8.02 – 7.97 (3H, m, Ar*H*), 7.85 (1H, m, Ar*H*), 7.61 – 7.53 (5H, m, Ar*H*), 7.49 (1H, m, Ar*H*) and 4.42 (3H, s, ArOCH_3); ^{13}C NMR (90 MHz, $CDCl_3$) 155.9 (quat.), 152.9 (quat.), 139.7 (quat.), 135.9 (quat.), 130.6 (CH), 129.0 (2C, CH), 128.8 (quat.), 128.0 (CH), 127.7 (CH), 126.3 (CH), 123.6 (CH), 123.3 (CH), 122.8 (2C, CH), 115.3 (CH) and 65.0 (CH_3); ν_{max} (KBr disc) 2933, 2848, 1572, 1207, 1091, 817; *m/z* (ESI+) 263 $[M+H]^+$.

(4-Methoxynaphthalen-1-yl)-phenyldiazene

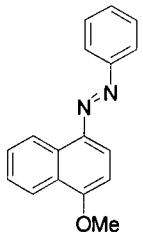

158

To a stirred solution of 1-phenylazonaphthalene-4-ol (0.05 g, 0.2 mmol) in DMF (5 cm^3) was added anhydrous potassium carbonate (0.06 g, 0.4 mmol, 2 eq.) and methyl iodide (0.15 g, 1.0 mmol, 5 eq.). The reaction mixture was stirred for 2 h before being diluted with deionised water (10 cm^3), which was then washed with diethyl ether (3 × 10 cm^3). The organics were combined and washed with water (3 × 10 cm^3) before being dried over Na_2SO_4 and concentrated under reduced pressure to yield **x** (0.05 g, 0.2 mmol, 91%). ^1H NMR (250 MHz, $CDCl_3$); 8.61 (1H, d, ^3J 8.2 Hz, Ar*H*), 8.01 (1H, d, ^3J 8.1 Hz, Ar*H*), 7.84 (2H, d, ^3J 7.5 Hz, Ar*H*), 7.68 (1H, d, ^3J 8.2 Hz, Ar*H*), 7.47 – 7.32 (5H, m, Ar*H*) and 6.84 (1H, d, ^3J 8.1 Hz, Ar*H*); ^{13}C NMR (91 MHz, $CDCl_3$) 157.4 (quat.), 153.3 (quat.), 143.4 (quat.), 131.1 (quat.), 132.4 (CH), 129.4 (2C, CH), 127.5 (CH), 126.2 (CH), 123.9 (CH), 127.2 (quat.), 123.1 (2C, CH), 118.1 (CH), 118.2 (CH), 104.9 (CH) and 56.1 (CH_3); *m/z* (ESI+) 263 $[M+H]^+$.

2-Hydroxy-4-(methyl-phenylhydrazono)-4H-naphthalen-1-one

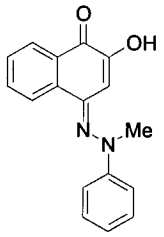

144

Method A:

To a stirred solution of 1,2-naphthoquinone-4-sulfonic acid (0.20 g, 0.84 mmol) in aqueous acetic acid (15 cm^3, 20 % v/v) was added *N*-methyl-*N*-phenylhydrazine (0.10 g, 0.84 mmol, 1.0 eq.). The solution was stirred for 1 h to yield the title compound as a red precipitate, collected by suction filtration (0.19 g, 1.1 mmol, 81%).

Method B:

To a stirred suspension of 1,2-naphthoquinone (0.20 g, 1.3 mmol) in aqueous acetic acid (15 cm^3, 20 % v/v) was added *N*-methyl-*N*-phenylhydrazine (0.16 g, 1.3 mmol). The solution was stirred for 1 h to yield the title compound as a red precipitate, collected by suction filtration (0.21 g, 0.76 mmol, 58%).

R_f 0.46 (4:1 EtOAc:Hexane); m.p. 137 – 139 °C; ^{1}H NMR (250 MHz, $CDCl_3$) 8.55 (1H, d, ^3J = 7.6 Hz, Ar*H*), 8.27 (1H, dd, ^3J = 7.8 and 1.1 Hz, Ar*H*), 7.69 (1H, dt, ^3J = 8.3 and 1.3 Hz, Ar*H*), 7.44 (1H, s, Ar*H*), 7.42 (1H, s, Ar*H*), 7.15 – 7.12 (2H, m, Ar*H*), 7.05 (1H, s, Ar*H*) and 3.81 (3H, s, NCH_3); ^{13}C NMR (63 MHz, $CDCl_3$) 179.3 (quat.), 149.3 (quat.), 148.6, (quat.), 137.5 (quat.), 136.5 (quat.), 132.2 (CH), 129.1 (2C, CH), 128.3 (quat.), 128.0 (CH), 125.7 (CH), 124.3 (CH), 122.8 (CH), 116.6 (2C, CH), 103.7 (CH), and 45.1 (CH_3); *m/z* (ESI+) 279 $[M+H]^+$; HRMS (EI) found 278.1056, $C_{17}H_{14}N_2O_2$.requires 278.1055

Reaction of 1,4-naphthoquinone with *N*-methyl-*N*-phenylhydrazine

To a stirred suspension of 1,4-naphthoquinone (0.20 g, 1.3 mmol) in aqueous acetic acid (20 cm^3, 20 % v/v) was added *N*-methyl-*N*-phenylhydrazine (0.16 g, 1.3 mmol, 1 eq.). The red precipitate was collected by suction filtration and dried in a desiccator before being purified by dry-flash chromatography.

4-(Methyl-phenyl-hydrazono)-*4H*-naphthalen-1-one

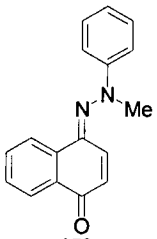

159

R_f 0.22 (4:1 EtOAc:Hexane); ^{1}H NMR (250 MHz, $CDCl_3$) 8.43 (1H, ddd, ^3J 8.1 ^4J 1.2 ^5J 0.6, Ar*H*), 8.23 (1H, ddd, ^3J 8.1 ^4J 1.2 ^5J 0.6, Ar*H*), 7.65 (1H, ddd, ^3J 8.3 ^4J 7.1 ^5J 1.5, Ar*H*), 7.60 (1H, d, ^3J 10.5, Ar*H*) 7.69 – 7.41 (5H, m, Ar*H*), 7.18 (1H, m, Ar*H*), 6.62 (1H, d, ^3J 10.5, Ar*H*) and 3.90 (3H, s, ArCH_3); ^{13}C NMR (63 MHz, $CDCl_3$) 184.6 (quat.), 149.0 (quat.), 136.6 (quat.), 134.5 (quat.), 131.8 (CH), 130.6 (quat.), 129.3 (2C, CH), 129.0 (CH), 127.8 (CH), 127.2 (CH), 125.8 (CH), 123.8 (2C, CH), 117.3 (2C, CH) and 45.7 (CH_3); ν_{max} (KBr disc) 2916, 2849, 1631, 1595, 1457, 756; *m/z* (ESI+) 263 $[M+H]^+$.

4-Hydroxy-2-(methyl-phenyl-hydrazono)-2H-naphthalen-1-one

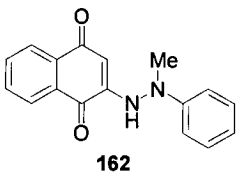

162

R_f 0.48 (4:1 EtOAc:Hexane); m.p. 126 – 128 °C; ^{1}H NMR (250 MHz, $CDCl_3$) 8.10 (1H, dd, ^3J 7.9 ^4J 1.4, Ar*H*), 8.07 (1H, dd, ^3J 7.9, ^4J 1.4, Ar*H*), 7.77 (1H, dt, ^3J 7.5, ^4J 1.4, Ar*H*), 7.66 (1H, dt, ^3J 7.5, ^4J 1.4, Ar*H*) 7.35 – 7.24 (2H, m, Ar*H*), 6.98 – 6.86 (3H, m, Ar*H*), 6.12 (1H, s, Ar*H*) and 3.19 (3H, s, NCH_3); ^{13}C NMR (63 MHz, $CDCl_3$) 183.4 (quat.), 181.9 (quat.), 148.5 (quat.), 146.3 (quat.), 134.6 (CH), 133.1

(quat.), 132.1 (CH), 130.7 (quat.), 129.2 (2C, CH), 126.1 (CH), 125.8 (CH), 120.6 (CH) 113.5 (2C, CH), 103.1 (CH) and 39.8 (CH_3); *m/z* (ESI+) 279 $[M+H]^+$; HRMS (EI) found 278.1055, $C_{17}H_{14}N_2O_2$.requires 278.1055

Solution Ozonolyses

Solution ozonolysis of the "simple" phenylazonaphthols was performed in IPA solvent with an ozone concentration of ~3 mM. Detailed discussion of the conditions is given in Appendix 7.3. The reaction was monitored by HPLC using the following conditions:

Column: Waters Spherisorb (15 cm × 4.6 mm internal diameter, 5 μ)

Eluent A: H_2O (1 % Ammonium Acetate)

Eluent B: 9:1 MeCN:H_2O (1 % Ammonium Acetate)

Monitoring Wavelength: 254 nm

Gradient Table:

Time / min	% B	Flow / $cm^3 min^{-1}$
0	5	1.0
3	5	1.0
10	60	1.0
13	60	1.0
15	5	1.0
20	5	1.0

Ozonolysis of **10**

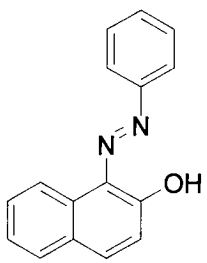

To a saturated solution of ozone in IPA (50 cm^3) was added **10** (0.005 g, 0.02 mmol) in IPA (5 cm^3). The solution was subjected to a continuous stream of ozone for 30 min. The reaction was monitored by HPLC at timed intervals. The reaction was

adjudged complete when the solution appeared to have lost all colour to the naked eye.

Ozonolysis of **11**

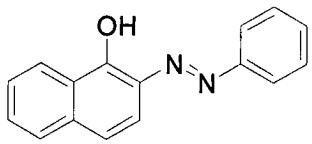

To a saturated solution of ozone in IPA (50 cm^3) was added **11** (0.005 g, 0.02 mmol) in IPA (5 cm^3). The solution was subjected to a continuous stream of ozone for 30 min. The reaction was monitored by HPLC at timed intervals. The reaction was adjudged complete when the solution appeared to have lost all colour to the naked eye.

Ozonolysis of **9**

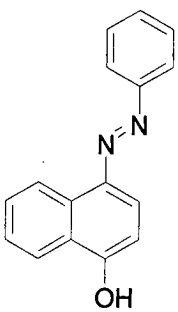

To a saturated solution of ozone in IPA (50 cm^3) was added **9** (0.005 g, 0.02 mmol) in IPA (5 cm^3). The solution was subjected to a continuous stream of ozone for 30 min. The reaction was monitored by HPLC at timed intervals. The reaction was adjudged complete when the solution appeared to have lost all colour to the naked eye.

Ozonolysis of **137**

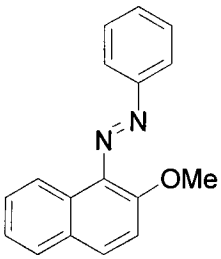

To a saturated solution of ozone in IPA (50 cm^3) was added **137** (0.005 g, 0.02 mmol) in IPA (5 cm^3). The solution was subjected to a continuous stream of ozone for 120 min. The reaction was monitored by HPLC at timed intervals. The reaction was adjudged complete when the solution appeared to have lost all colour to the naked eye.

Ozonolysis of **138**

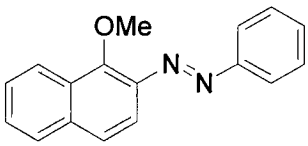

To a saturated solution of ozone in IPA (50 cm^3) was added **138** (0.005 g, 0.02 mmol) in IPA (5 cm^3). The solution was subjected to a continuous stream of ozone for 120 min. The reaction was monitored by HPLC at timed intervals. The reaction was adjudged complete when the solution appeared to have lost all colour to the naked eye.

Ozonolysis of **158**

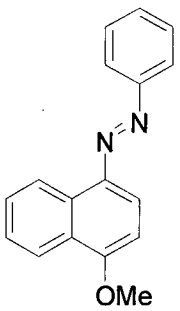

To a saturated solution of ozone in IPA (50 cm^3) was added **158** (0.005 g, 0.02 mmol) in IPA (5 cm^3). The solution was subjected to a continuous stream of ozone for 120 min. The reaction was monitored by HPLC at timed intervals. The reaction

was adjudged complete when the solution appeared to have lost all colour to the naked eye.

Ozonolysis of **159**

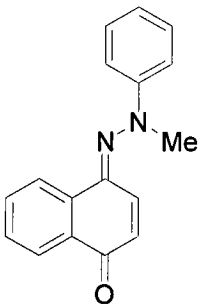

To a saturated solution of ozone in IPA (50 cm^3) was added **159** (0.005 g, 0.02 mmol) in IPA (5 cm^3). The solution was subjected to a continuous stream of ozone for 5 min. The reaction was monitored by HPLC at timed intervals. The reaction was adjudged complete when the solution appeared to have lost all colour to the naked eye.

7 Appendices

7.1 X-ray Crystal Structure of 67d

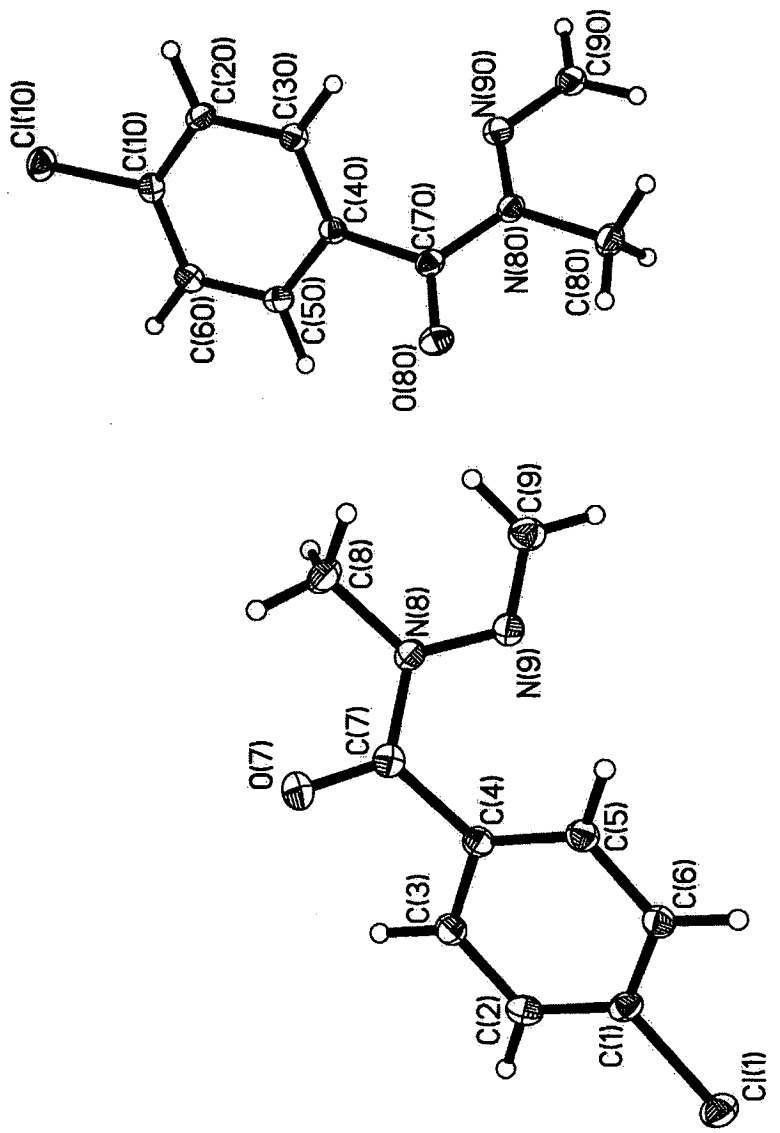

Crystal data and structure refinement for **67d:**

A. CRYSTAL DATA

Empirical formula	C9 H9 Cl1 N2 O1
Formula weight	196.64
Wavelength	0.71073 A
Temperature	150 K
Crystal system	Monoclinic
Space group	P 21/c
Unit cell dimensions	a = 24.2273(8) A α = 90 deg. b = 3.84280(10) A β = 116.801(2) deg. c = 21.9106(7) A γ = 90 deg.
Volume	1820.76(10) A^3
No. of reflections for cell	6575 (5 < theta < 58 deg.)
Z	8
Density (calculated)	1.435 Mg^{-1} m^3
Absorption coefficient	0.377 mm^{-1}
F(000)	816

B. DATA COLLECTION

Crystal description	colourless block
Crystal size	0.35 x 0.28 x 0.24 mm
Instrument	Bruker SMART
θ range for data collection	0.942 to 29.821 °.
Index ranges	-33<=h<=28, -5<=k<=4, -29<=l<=29
Reflections collected	18423
Independent reflections	4754 [R(int) = 0.038]
Scan type	\f & \w scans
Absorption correction	Semi-empirical from equivalents (Tmin= 0.67, Tmax=0.91)

C. SOLUTION AND REFINEMENT.

Solution	direct (SIR92 (Altomare et al., 1994))
Refinement type	Full-matrix least-squares on F^2
Program used for refinement	CRYSTALS
Hydrogen atom placement	geom
Hydrogen atom treatment	noref

Data	3188
Restraints	0
Parameters	235
Goodness-of-fit on F^2	1.0852
Conventional R [$F>4\sigma(F)$]	R1 = 0.0325 [3188 data]
Rw	0.0366
Final maximum δ/σ	0.000897
Weighting scheme	Sheldrick Weights
Largest diff. peak and hole	0.30 and -0.17 $e.A^{-3}$

Table 2. Atomic coordinates (x 10^4) and equivalent isotropic displacement parameters (A^2 x 10^3) for **67d**. U(eq) is defined as one third of the trace of the orthogonalized Uij tensor.

	x	y	z	U (eq.)
Cl(1)	880(1)	3824(2)	2128(1)	36
Cl(10)	-5906(1)	-6445(2)	-3763(1)	35
C(1)	116(1)	4359(6)	1503(1)	27
C(2)	-352(1)	3226(7)	1646(1)	29
C(3)	-961(1)	3676(6)	1157(1)	27
C(4)	-1088(1)	5149(6)	527(1)	25
C(5)	-608(1)	6263(6)	391(1)	27
C(6)	4(1)	5879(6)	888(1)	27
C(7)	-1761(1)	5729(6)	50(1)	27
C(8)	-2642(1)	5019(7)	-1071(1)	35
C(9)	-1803(1)	1775(8)	-1414(1)	35
C(10)	-5148(1)	-5685(6)	-3625(1)	25
C(20)	-5037(1)	-4095(6)	-4124(1)	27
C(30)	-4428(1)	-3556(6)	-4006(1)	25
C(40)	-3941(1)	-4581(6)	-3388(1)	23
C(50)	-4068(1)	-6127(6)	-2890(1)	27
C(60)	-4669(1)	-6729(7)	-3004(1)	27
C(70)	-3275(1)	-3822(6)	-3197(1)	25
C(80)	-2384(1)	-4199(7)	-3439(1)	32
C(90)	-3193(1)	-7606(7)	-4608(1)	32
N(8)	-1988(1)	4576(5)	-609(1)	27
N(9)	-1594(1)	2787(5)	-797(1)	27
N(80)	-3036(1)	-4856(5)	-3624(1)	25
N(90)	-3410(1)	-6743(5)	-4199(1)	28
O(7)	-2094(1)	7173(5)	256(1)	38
O(80)	-2954(1)	-2337(5)	-2655(1)	35

Table 3. Bond lengths [Å] and angles [deg] for **67d**.

Cl(1)-C(1)	1.747(2)
Cl(10)-C(10)	1.746(2)
C(1)-C(2)	1.377(4)
C(1)-C(6)	1.379(3)
C(2)-C(3)	1.388(3)
C(2)-H(21)	1.002
C(3)-C(4)	1.392(3)
C(3)-H(31)	1.001
C(4)-C(5)	1.393(3)
C(4)-C(7)	1.504(3)
C(5)-C(6)	1.397(3)
C(5)-H(51)	1
C(6)-H(61)	1
C(7)-N(8)	1.368(3)
C(7)-O(7)	1.221(3)
C(8)-N(8)	1.455(3)
C(8)-H(81)	1
C(8)-H(82)	1
C(8)-H(83)	1
C(9)-N(9)	1.272(3)
C(9)-H(91)	1.004
C(9)-H(92)	0.999
C(10)-C(20)	1.382(3)
C(10)-C(60)	1.390(3)
C(20)-C(30)	1.393(3)
C(20)-H(201)	0.999
C(30)-C(40)	1.393(3)
C(30)-H(301)	0.999
C(40)-C(50)	1.393(3)
C(40)-C(70)	1.501(3)

C(50)-C(60)	1.382(3)
C(50)-H(501)	1
C(60)-H(601)	0.999
C(70)-N(80)	1.365(3)
C(70)-O(80)	1.227(3)
C(80)-N(80)	1.464(3)
C(80)-H(801)	1
C(80)-H(802)	1
C(80)-H(803)	1
C(90)-N(90)	1.272(3)
C(90)-H(901)	1
C(90)-H(902)	1.001
N(8)-N(9)	1.380(3)
N(80)-N(90)	1.380(3)
Cl(1)-C(1)-C(2)	118.38(19)
Cl(1)-C(1)-C(6)	119.14(18)
C(2)-C(1)-C(6)	122.5(2)
C(1)-C(2)-C(3)	118.8(2)
C(1)-C(2)-H(21)	120.7
C(3)-C(2)-H(21)	120.4
C(2)-C(3)-C(4)	120.0(2)
C(2)-C(3)-H(31)	120.1
C(4)-C(3)-H(31)	119.9
C(3)-C(4)-C(5)	120.3(2)
C(3)-C(4)-C(7)	115.8(2)
C(5)-C(4)-C(7)	123.7(2)
C(4)-C(5)-C(6)	119.7(2)
C(4)-C(5)-H(51)	120.2
C(6)-C(5)-H(51)	120
C(5)-C(6)-C(1)	118.6(2)
C(5)-C(6)-H(61)	120.5
C(1)-C(6)-H(61)	120.9

C(4)-C(7)-N(8)	118.63(19)
C(4)-C(7)-O(7)	120.1(2)
N(8)-C(7)-O(7)	121.3(2)
N(8)-C(8)-H(81)	109.5
N(8)-C(8)-H(82)	109.5
H(81)-C(8)-H(82)	109.5
N(8)-C(8)-H(83)	109.5
H(81)-C(8)-H(83)	109.5
H(82)-C(8)-H(83)	109.5
N(9)-C(9)-H(91)	120
N(9)-C(9)-H(92)	120.3
H(91)-C(9)-H(92)	119.7
Cl(10)-C(10)-C(20)	120.12(17)
Cl(10)-C(10)-C(60)	117.95(18)
C(20)-C(10)-C(60)	121.9(2)
C(10)-C(20)-C(30)	119.1(2)
C(10)-C(20)-H(201)	120.4
C(30)-C(20)-H(201)	120.5
C(20)-C(30)-C(40)	120.0(2)
C(20)-C(30)-H(301)	119.9
C(40)-C(30)-H(301)	120.1
C(30)-C(40)-C(50)	119.5(2)
C(30)-C(40)-C(70)	123.3(2)
C(50)-C(40)-C(70)	116.95(19)
C(40)-C(50)-C(60)	121.1(2)
C(40)-C(50)-H(501)	119.4
C(60)-C(50)-H(501)	119.4
C(10)-C(60)-C(50)	118.3(2)
C(10)-C(60)-H(601)	120.9
C(50)-C(60)-H(601)	120.8
C(40)-C(70)-N(80)	119.20(18)
C(40)-C(70)-O(80)	119.6(2)

N(80)-C(70)-O(80)	121.15(19)
N(80)-C(80)-H(801)	109.5
N(80)-C(80)-H(802)	109.5
H(801)-C(80)-H(802)	109.5
N(80)-C(80)-H(803)	109.5
H(801)-C(80)-H(803)	109.5
H(802)-C(80)-H(803)	109.5
N(90)-C(90)-H(901)	120.1
N(90)-C(90)-H(902)	120
H(901)-C(90)-H(902)	119.9
C(8)-N(8)-C(7)	119.4(2)
C(8)-N(8)-N(9)	122.22(19)
C(7)-N(8)-N(9)	118.23(17)
N(8)-N(9)-C(9)	118.2(2)
C(80)-N(80)-C(70)	119.92(18)
C(80)-N(80)-N(90)	121.79(19)
C(70)-N(80)-N(90)	118.10(18)
N(80)-N(90)-C(90)	118.0(2)

Table 4. Anisotropic displacement parameters ($A^2 \times 10^3$) for **67d**. The anisotropic displacement factor exponent takes the form: $-2\ pi^2\ [\ h^2\ a^{*2}\ U11 + ... + 2\ h\ k\ a^*\ b^*\ U12\ ]$

	U11	U22	U33	U23	U13	U12
Cl(1)	28(1)	42(1)	31(1)	0(1)	6(1)	5(1)
Cl(10)	25(1)	40(1)	41(1)	-3(1)	15(1)	-5(1)
C(1)	24(1)	24(1)	27(1)	-6(1)	6(1)	2(1)
C(2)	37(1)	26(1)	23(1)	1(1)	12(1)	0(1)
C(3)	29(1)	28(1)	26(1)	-2(1)	14(1)	-2(1)
C(4)	26(1)	23(1)	25(1)	-5(1)	11(1)	0(1)
C(5)	28(1)	27(1)	25(1)	-2(1)	12(1)	-1(1)
C(6)	28(1)	28(1)	28(1)	-5(1)	14(1)	-2(1)

C(7)	27(1)	24(1)	29(1)	2(1)	14(1)	0(1)
C(8)	22(1)	43(1)	33(1)	6(1)	7(1)	1(1)
C(9)	36(1)	36(1)	31(1)	-4(1)	13(1)	-6(1)
C(10)	23(1)	24(1)	29(1)	-6(1)	13(1)	-3(1)
C(20)	23(1)	28(1)	24(1)	0(1)	6(1)	3(1)
C(30)	26(1)	26(1)	24(1)	0(1)	11(1)	1(1)
C(40)	24(1)	23(1)	22(1)	-3(1)	10(1)	-1(1)
C(50)	28(1)	28(1)	22(1)	0(1)	9(1)	1(1)
C(60)	31(1)	26(1)	27(1)	-2(1)	15(1)	-2(1)
C(70)	23(1)	25(1)	24(1)	4(1)	8(1)	1(1)
C(80)	23(1)	38(2)	35(1)	4(1)	12(1)	-1(1)
C(90)	31(1)	35(1)	29(1)	2(1)	13(1)	7(1)
N(8)	22(1)	30(1)	26(1)	1(1)	9(1)	0(1)
N(9)	27(1)	26(1)	29(1)	-2(1)	13(1)	-1(1)
N(80)	21(1)	28(1)	25(1)	1(1)	8(1)	-2(1)
N(90)	28(1)	28(1)	26(1)	0(1)	11(1)	2(1)
O(7)	32(1)	48(1)	38(1)	-6(1)	19(1)	4(1)
O(80)	28(1)	44(1)	27(1)	-8(1)	7(1)	-7(1)

Table 5. Hydrogen coordinates (x 10^4) and isotropic displacement parameters (A^2 x 10^3) for **67d**.

H(21)	-257	2098	2095	34
H(31)	-1308	2945	1257	33
H(51)	-699	7327	-62	31
H(61)	353	6682	798	33
H(81)	-2843	6384	-837	39
H(82)	-2688	6292	-1490	39
H(83)	-2843	2684	-1204	39
H(91)	-2243	2280	-1748	41
H(92)	-1531	470	-1567	41
H(201)	-5388	-3343	-4564	29

H(301)	-4341	-2433	-4365	30
H(501)	-3718	-6803	-2442	31
H(601)	-4758	-7892	-2650	33
H(801)	-2195	-2795	-3009	38
H(802)	-2352	-2887	-3816	38
H(803)	-2160	-6465	-3365	38
H(901)	-2763	-6910	-4510	38
H(902)	-3452	-8975	-5030	38

7.2 Degradation data obtained at Avecia (Blackley)

CSL TEST DATA

DYE LOADING 3.5%

INK pH 8.5 - 9.5

INK VEHICLE 7.5% GLYCEROL;
7.5% ETHYLENE GLYCOL;
7.5% UREA;
1% SURFYNOL 465;
REMAINDER dH2O (CANON)

COLOUR MEASUREMENTS GRETAG MACBETH - NO FILTER (U)
ILLUMINANT - D50
OBSERVER - 2°
DENSITY - ANSI A

PROTOCOL CANON II (CANON i950)

DYE	SUBSTRATE	TEST	DEPTH %	ROD	L	A	B	C	H	DE	% ROD LOSS
94C	PR101 MKII	INITIAL	100	2.13	44	81	12	82	8		
94C	PR101 MKII	INITIAL	50	1.41	54	79	-15	80	349		
94C	PR101 MKII	LF 100H	50	0.85	65	61	-12	63	349	21	40
94C	PR101 MKII	OF 1PPM/24H	50	0.79	66	57	-9	58	351	26	44
94C	PRINTASIA PHOTO	INITIAL	100	2.18	42	79	13	80	9		
94C	PRINTASIA PHOTO	INITIAL	50	1.48	50	76	-11	77	352		
94C	PRINTASIA PHOTO	LF 100H	50	0.86	62	58	-10	58	350	22	42
94C	HP PRINTING PAPER	INITIAL	100	1.29	44	61	-4	61	356		
94C	HP PRINTING PAPER	INITIAL	50	1.03	51	58	-14	60	346		
94C	HP PREMIUM PLUS MKII	INITIAL	100	2.45	44	81	18	83	12		
94C	HP PREMIUM PLUS MKII	INITIAL	50	1.48	54	78	-6	78	355		
94C	HP PREMIUM PLUS MKII	LF 4 YR	50	0.95	61	63	-8	63	353	17	36
94C	SEC PREMIUM PHOTO	INITIAL	100	2.11	42	80	1	80	1		
94C	SEC PREMIUM PHOTO	INITIAL	50	1.21	55	73	-19	76	345		
94C	SEC PREMIUM PHOTO	LF 4 YR	50	0.83	64	59	-11	60	349	19	31
94C	SEC PREMIUM PHOTO	OF 1PPM/24H	50	0.89	60	59	-7	59	353	20	26
97C	PR101 MKII	INITIAL	100	2.06	47	81	23	84	16		
97C	PR101 MKII	INITIAL	50	1.39	56	78	-4	78	357		
97C	PR101 MKII	LF 100H	50	0.58	72	47	-7	48	352	35	58
97C	PR101 MKII	OF	50	0.89	64	63	-2	63	358	18	36

		1PPM/24H									
97C	PRINTASIA PHOTO	INITIAL	100	2.21	43	80	17	82	12		
97C	PRINTASIA PHOTO	INITIAL	50	1.52	52	78	-7	79	355		
97C	PRINTASIA PHOTO	LF 100H	50	0.9	61	60	-10	61	351	**21**	**41**
97C	HP PRINTING PAPER	INITIAL	100	1.25	50	67	9	68	7		
97C	HP PRINTING PAPER	INITIAL	50	0.99	57	62	0	62	360		
97C	HP PREMIUM PLUS MKII	INITIAL	100	2.44	46	82	26	86	18		
97C	HP PREMIUM PLUS MKII	INITIAL	50	1.48	55	78	1	78	1		
97C	HP PREMIUM PLUS MKII	LF 4 YR	50	0.91	63	61	-1	61	359	**18**	**39**
97C	SEC PREMIUM PHOTO	INITIAL	100	2.01	48	80	28	84	19		
97C	SEC PREMIUM PHOTO	INITIAL	50	1.14	59	71	4	71	3		
97C	SEC PREMIUM PHOTO	LF 4 YR	50	0.74	67	55	-3	55	356	**20**	**35**
97C	SEC PREMIUM PHOTO	OF 1PPM/24H	50	0.88	63	59	14	60	13	**16**	**23**
96C	PR101 MKII	INITIAL	100	2.08	48	82	18	84	12		
96C	PR101 MKII	INITIAL	50	1.35	57	78	-9	78	353		
96C	PR101 MKII	LF 100H	50	0.78	67	59	-11	60	349	**21**	**42**
96C	PR101 MKII	OF 1PPM/24H	50	0.85	66	62	-8	63	352	**18**	**37**
96C	PRINTASIA PHOTO	INITIAL	100	2.16	44	80	14	81	10		
96C	PRINTASIA PHOTO	INITIAL	50	1.36	53	75	-10	76	353		
96C	PRINTASIA PHOTO	LF 100H	50	0.83	63	57	-10	58	350	**20**	**39**
96C	HP PRINTING PAPER	INITIAL	100	1.28	50	68	6	68	5		
96C	HP PRINTING PAPER	INITIAL	50	1.02	56	64	-5	64	356		
96C	HP PREMIUM PLUS MKII	INITIAL	100	2.39	46	82	20	84	14		
96C	HP PREMIUM PLUS MKII	INITIAL	50	1.42	55	78	-5	78	357		
96C	HP PREMIUM PLUS MKII	LF 4 YR	50	0.84	64	59	-6	59	354	**21**	**41**
96C	SEC PREMIUM PHOTO	INITIAL	100	2.04	48	81	22	83	15		
96C	SEC PREMIUM PHOTO	INITIAL	50	1.01	61	66	2	66	2		
96C	SEC PREMIUM PHOTO	LF 4 YR	50	0.74	67	55	-8	56	352	**16**	**27**
96C	SEC PREMIUM PHOTO	OF 1PPM/24H	50	0.74	66	51	14	53	15	**19**	**27**
96B	PR101 MKII	INITIAL	100	2.1	45	81	16	82	11		
96B	PR101 MKII	INITIAL	50	1.39	56	78	-10	79	352		
96B	PR101 MKII	LF 100H	50	0.69	70	54	-10	55	349	**28**	**50**
96B	PR101 MKII	OF 1PPM/24H	50	0.76	68	58	-9	59	351	**24**	**45**
96B	PRINTASIA PHOTO	INITIAL	100	2.16	42	78	14	80	10		
96B	PRINTASIA PHOTO	INITIAL	50	1.4	52	75	-10	75	352		
96B	PRINTASIA PHOTO	LF 100H	50	0.78	64	52	-11	53	348	**25**	**44**
96B	HP PRINTING PAPER	INITIAL	100	1.29	48	66	4	66	4		
96B	HP PRINTING PAPER	INITIAL	50	1.03	55	63	-5	63	355		
96B	HP PREMIUM PLUS MKII	INITIAL	100	2.39	43	80	18	82	13		
96B	HP PREMIUM PLUS MKII	INITIAL	50	1.44	53	77	-6	77	356		

96B	HP PREMIUM PLUS MKII	LF 4 YR	50	0.74	66	52	-7	52	352	**28**	**49**
96B	SEC PREMIUM PHOTO	INITIAL	100	2.09	46	79	20	82	14		
96B	SEC PREMIUM PHOTO	INITIAL	50	1.05	59	67	-3	67	358		
96B	SEC PREMIUM PHOTO	LF 4 YR	50	0.68	69	51	-8	52	351	**19**	**35**
96B	SEC PREMIUM PHOTO	OF 1PPM/24H	50	0.68	68	48	11	49	13	**25**	**35**
97A	PR101 MKII	INITIAL	100	2.04	47	81	18	83	13		
97A	PR101 MKII	INITIAL	50	1.27	57	76	-8	77	354		
97A	PR101 MKII	LF 100H	50	0.7	69	55	-11	56	349	**25**	**45**
97A	PR101 MKII	OF 1PPM/24H	50	0.76	67	57	-5	58	355	**21**	**40**
97A	PRINTASIA PHOTO	INITIAL	100	2.18	43	80	11	81	8		
97A	PRINTASIA PHOTO	INITIAL	50	1.36	53	75	-12	76	351		
97A	PRINTASIA PHOTO	LF 100H	50	0.82	63	56	-11	57	349	**21**	**40**
97A	HP PRINTING PAPER	INITIAL	100	1.25	49	66	4	66	4		
97A	HP PRINTING PAPER	INITIAL	50	0.99	57	63	-5	63	355		
97A	HP PREMIUM PLUS MKII	INITIAL	100	2.42	46	82	18	84	13		
97A	HP PREMIUM PLUS MKII	INITIAL	50	1.41	55	77	-5	77	356		
97A	HP PREMIUM PLUS MKII	LF 4 YR	50	0.81	64	57	-4	57	356	**22**	**43**
97A	SEC PREMIUM PHOTO	INITIAL	100	2.03	47	81	17	82	12		
97A	SEC PREMIUM PHOTO	INITIAL	50	1.12	59	71	-5	71	356		
97A	SEC PREMIUM PHOTO	LF 4 YR	50	0.66	69	50	-6	50	354	**23**	**41**
97A	SEC PREMIUM PHOTO	OF 1PPM/24H	50	0.82	64	57	6	57	6	**19**	**27**
96A	PR101 MKII	INITIAL	100	2.07	48	82	17	84	12		
96A	PR101 MKII	INITIAL	50	1.4	57	79	-10	80	353		
96A	PR101 MKII	LF 100H	50	0.71	70	56	-12	57	348	**26**	**49**
96A	PR101 MKII	OF 1PPM/24H	50	0.78	68	59	-10	60	351	**23**	**44**
96A	PRINTASIA PHOTO	INITIAL	100	2.16	44	81	13	82	9		
96A	PRINTASIA PHOTO	INITIAL	50	1.41	53	76	-10	77	353		
96A	PRINTASIA PHOTO	LF 100H	50	0.86	63	59	-10	59	350	**20**	**39**
96A	HP PRINTING PAPER	INITIAL	100	1.28	50	68	5	68	4		
96A	HP PRINTING PAPER	INITIAL	50	1	57	64	-7	65	354		
96A	HP PREMIUM PLUS MKII	INITIAL	100	2.42	46	82	19	85	13		
96A	HP PREMIUM PLUS MKII	INITIAL	50	1.46	55	78	-6	78	356		
96A	HP PREMIUM PLUS MKII	LF 4 YR	50	0.8	65	57	-5	57	355	**23**	**45**
96A	SEC PREMIUM PHOTO	INITIAL	100	2.08	48	81	18	84	13		
96A	SEC PREMIUM PHOTO	INITIAL	50	1.09	60	69	-2	69	358		
96A	SEC PREMIUM PHOTO	LF 4 YR	50	0.74	67	55	-8	56	352	**17**	**32**
96A	SEC PREMIUM PHOTO	OF 1PPM/24H	50	0.77	65	53	12	55	13	**22**	**29**
CRI	PR101 MKII	INITIAL	100	2.11	47	84	-5	84	357		
CRI	PR101 MKII	INITIAL	50	1.22	59	75	-21	78	345		

CRI	PR101 MKII	LF 100H	50	0.52	75	43	-8	43	350	38	57
CRI	PR101 MKII	OF 1PPM/24H	50	0.81	67	59	-11	60	350	20	34
CRI	PRINTASIA PHOTO	INITIAL	100	2.07	45	80	-2	80	358		
CRI	PRINTASIA PHOTO	INITIAL	50	1.23	56	72	-18	74	346		
CRI	PRINTASIA PHOTO	LF 100H	50	0.67	67	46	-11	47	346	29	46
CRI	HP PRINTING PAPER	INITIAL	100	1.19	50	64	-7	64	354		
CRI	HP PRINTING PAPER	INITIAL	50	0.97	57	62	-17	64	345		
CRI	HP PREMIUM PLUS MKII	INITIAL	100	2.4	44	82	2	82	2		
CRI	HP PREMIUM PLUS MKII	INITIAL	50	1.38	55	76	-15	77	349		
CRI	HP PREMIUM PLUS MKII	LF 4 YR	50	0.8	65	54	-12	55	348	24	42
CRI	SEC PREMIUM PHOTO	INITIAL	100	2.09	46	83	-4	83	357		
CRI	SEC PREMIUM PHOTO	INITIAL	50	1.26	58	75	-22	78	344		
CRI	SEC PREMIUM PHOTO	LF 4 YR	50	0.71	70	52	-16	54	343	26	44
CRI	SEC PREMIUM PHOTO	OF 1PPM/24H	50	0.99	63	65	-13	66	349	14	21

CSL TEST DATA

DYE LOADING 3.5%

INK pH 8.5 - 9.5

INK VEHICLE 7.5% GLYCEROL;
7.5% ETHYLENE GLYCOL;
7.5% UREA;
1% SURFYNOL 465;
REMAINDER dH2O (CANON)

COLOUR MEASUREMENTS GRETAG MACBETH - NO FILTER (U)
ILLUMINANT - D50
OBSERVER - 2°
DENSITY - ANSI A

PROTOCOL CANON (CANON S800)

DYE	SUBSTRATE	TEST	Depth %	ROD	L	A	B	C	H	DE	ROD LOSS %
94F	PR101 MKII	INITIAL	100	2.17	47	83	12	84	8		
94F	PR101 MKII	INITIAL	50	1.65	53	82	-8	82	354		
94F	PR101 MKII	LF 100H	50	1.02	62	68	-11	69	351	16	38
94F	PR101 MKII	OF 1PPM/24H	50	1.01	62	67	-9	68	353	17	39
94F	PRINTASIA PHOTO	INITIAL	100	2.21	44	80	10	81	7		
94F	PRINTASIA PHOTO	INITIAL	50	1.66	50	79	-8	79	354		
94F	PRINTASIA PHOTO	LF 100H	50	1.01	58	63	-9	64	352	18	39

94F	PRINTASIA PHOTO	OF 1PPM/24H	50	1.62	49	78	-9	79	353	**2**	**2**
94F	ILFORD INSTANT DRY	INITIAL	100	2.06	46	81	14	83	10		
94F	ILFORD INSTANT DRY	INITIAL	50	1.62	53	81	-7	81	355		
94F	ILFORD INSTANT DRY	LF 100H	50	1.05	61	69	-11	70	351	**15**	**35**
94F	ILFORD INSTANT DRY	OF 1PPM/24H	50	1.29	56	74	-1	74	359	**10**	**20**
94F	SEC PREMIUM PHOTO	INITIAL	100	2.07	46	83	3	83	2		
94F	SEC PREMIUM PHOTO	INITIAL	50	1.43	53	79	-15	81	349		
94F	SEC PREMIUM PHOTO	LF 100H	50	1.01	59	66	-12	67	349	**15**	**29**
94F	SEC PREMIUM PHOTO	OF 1PPM/24H	50	1.02	59	64	0	64	360	**22**	**29**
94F	HP PRINTING PAPER	INITIAL	100	1.34	46	67	0	67	0		
94F	HP PRINTING PAPER	INITIAL	50	1.11	52	65	-9	66	352		
94F	HP PRINTING PAPER	LF 100H	50	0.71	63	46	-7	46	352	**22**	**36**
94F	HP PRINTING PAPER	OF 1PPM/24H	50	1.11	53	65	-9	66	352	**0**	**0**
94F	HP PREMIUM PLUS MKII	INITIAL	100	2.31	46	82	13	83	9		
94F	HP PREMIUM PLUS MKII	INITIAL	50	1.68	52	81	-4	81	357		
94F	HP PREMIUM PLUS MKII	LF 100H	50	1.09	58	67	-7	68	354	**15**	**35**
94F	HP PREMIUM PLUS MKII	OF 1PPM/24H	50	1.64	53	80	-4	80	357	**1**	**2**
94F	HR 2	INITIAL	100	2.14	43	81	3	81	2		
94F	HR 2	INITIAL	50	1.44	52	78	-12	79	351		
94F	HR 2	LF 100H	50	0.77	64	54	-7	55	352	**27**	**47**
94F	HR 2	OF 1PPM/24H	50	1.28	53	73	-9	73	353	**6**	**11**
95d	PR101 MKII	INITIAL	100	2.11	49	83	10	84	7		
95d	PR101 MKII	INITIAL	50	1.47	56	80	-8	81	354		
95d	PR101 MKII	LF 100H	50	0.9	65	64	-11	65	350	**18**	**39**
95d	PR101 MKII	OF 1PPM/24H	50	0.98	63	67	-9	68	353	**15**	**33**
95d	PRINTASIA PHOTO	INITIAL	100	2.21	45	82	6	82	4		
95d	PRINTASIA PHOTO	INITIAL	50	1.46	52	77	-10	78	353		
95d	PRINTASIA PHOTO	LF 100H	50	0.81	63	56	-11	57	349	**24**	**45**
95d	PRINTASIA PHOTO	OF 1PPM/24H	50	1.44	52	77	-9	77	353	**0**	**1**
95d	ILFORD INSTANT DRY	INITIAL	100	1.98	49	81	19	83	13		
95d	ILFORD INSTANT DRY	INITIAL	50	1.4	57	78	-1	78	359		
95d	ILFORD INSTANT DRY	LF 100H	50	0.85	66	63	-11	63	350	**20**	**39**
95d	ILFORD INSTANT DRY	OF 1PPM/24H	50	1.14	60	71	4	71	3	**8**	**19**
95d	SEC PREMIUM PHOTO	INITIAL	100	2.03	48	82	8	83	5		
95d	SEC PREMIUM PHOTO	INITIAL	50	1.29	56	76	-9	76	353		
95d	SEC PREMIUM PHOTO	LF 100H	50	0.77	66	56	-8	56	352	**22**	**40**
95d	SEC PREMIUM PHOTO	OF 1PPM/24H	50	0.96	61	62	2	62	2	**18**	**26**
95d	HP PRINTING PAPER	INITIAL	100	1.3	49	69	3	69	2		

95d	HP PRINTING PAPER	INITIAL	50	1.04	56	65	-7	65	354		
95d	HP PRINTING PAPER	LF 100H	50	0.51	72	38	-6	39	351	31	51
95d	HP PRINTING PAPER	OF 1PPM/24H	50	1.03	56	65	-6	65	355	1	1
95d	HP PREMIUM PLUS MKII	INITIAL	100	2.31	48	83	12	84	8		
95d	HP PREMIUM PLUS MKII	INITIAL	50	1.4	55	77	-4	77	357		
95d	HP PREMIUM PLUS MKII	LF 100H	50	0.88	63	61	-7	61	354	18	37
95d	HP PREMIUM PLUS MKII	OF 1PPM/24H	50	1.43	55	77	-3	78	358	1	-2
95d	HR 2	INITIAL	100	1.82	50	79	21	81	15		
95d	HR 2	INITIAL	50	1.09	60	69	5	69	4		
95d	HR 2	LF 100H	50	0.66	69	49	-3	49	356	23	39
95d	HR 2	OF 1PPM/24H	50	1.00	61	65	8	65	7	6	8
95A	PR101 MKII	INITIAL	100	2.04	50	83	10	84	7		
95A	PR101 MKII	INITIAL	50	1.33	58	78	-8	78	354		
95A	PR101 MKII	LF 100H	50	0.8	67	60	-10	61	350	20	40
95A	PR101 MKII	OF 1PPM/24H	50	0.93	64	65	-7	66	354	14	30
95A	PRINTASIA PHOTO	INITIAL	100	2.09	46	81	5	82	4		
95A	PRINTASIA PHOTO	INITIAL	50	1.33	54	75	-9	75	353		
95A	PRINTASIA PHOTO	LF 100H	50	0.77	65	55	-10	56	349	23	42
95A	PRINTASIA PHOTO	OF 1PPM/24H	50	1.30	54	74	-9	75	353	1	2
95A	ILFORD INSTANT DRY	INITIAL	100	1.93	50	81	19	83	13		
95A	ILFORD INSTANT DRY	INITIAL	50	1.26	58	75	0	75	360		
95A	ILFORD INSTANT DRY	LF 100H	50	0.76	68	58	-10	59	350	22	40
95A	ILFORD INSTANT DRY	OF 1PPM/24H	50	1.07	61	69	4	69	3	8	15
95A	SEC PREMIUM PHOTO	INITIAL	100	1.95	50	81	14	83	10		
95A	SEC PREMIUM PHOTO	INITIAL	50	1.12	60	71	-2	71	358		
95A	SEC PREMIUM PHOTO	LF 100H	50	0.62	70	48	-5	48	354	26	45
95A	SEC PREMIUM PHOTO	OF 1PPM/24H	50	0.85	64	59	8	59	8	17	24
95A	HP PRINTING PAPER	INITIAL	100	1.27	50	69	4	69	3		
95A	HP PRINTING PAPER	INITIAL	50	1.01	57	64	-5	64	355		
95A	HP PRINTING PAPER	LF 100H	50	0.47	74	35	-5	36	352	33	53
95A	HP PRINTING PAPER	OF 1PPM/24H	50	1.00	57	64	-5	64	356	1	1
95A	HP PREMIUM PLUS MKII	INITIAL	100	2.13	49	82	14	83	9		
95A	HP PREMIUM PLUS MKII	INITIAL	50	1.31	57	75	-2	75	358		
95A	HP PREMIUM PLUS MKII	LF 100H	50	0.8	65	57	-6	57	355	20	39
95A	HP PREMIUM PLUS MKII	OF 1PPM/24H	50	1.31	57	75	-2	75	358	0	0
95A	HR 2	INITIAL	100	1.75	51	78	22	81	16		
95A	HR 2	INITIAL	50	1	62	66	6	67	5		
95A	HR 2	LF 100H	50	0.47	75	37	-1	37	359	33	53
95A	HR 2	OF 1PPM/24H	50	0.92	62	62	9	63	8	6	8
95C	PR101 MKII	INITIAL	100	2.07	49	83	13	84	9		
95C	PR101 MKII	INITIAL	50	1.49	56	80	-6	80	356		

95C	PR101 MKII	LF 100H	50	0.9	65	64	-10	65	351	19	40
95C	PR101 MKII	OF 1PPM/24H	50	1.00	62	68	-6	68	355	14	33
95C	PRINTASIA PHOTO	INITIAL	100	2.24	45	82	7	82	5		
95C	PRINTASIA PHOTO	INITIAL	50	1.57	52	79	-9	79	354		
95C	PRINTASIA PHOTO	LF 100H	50	0.82	63	57	-10	58	350	25	48
95C	PRINTASIA PHOTO	OF 1PPM/24H	50	1.54	52	78	-9	79	354	1	2
95C	ILFORD INSTANT DRY	INITIAL	100	1.94	49	80	21	83	15		
95C	ILFORD INSTANT DRY	INITIAL	50	1.4	57	77	2	77	1		
95C	ILFORD INSTANT DRY	LF 100H	50	0.89	65	64	-9	65	352	19	36
95C	ILFORD INSTANT DRY	OF 1PPM/24H	50	1.14	60	70	7	71	6	9	19
95C	SEC PREMIUM PHOTO	INITIAL	100	2	49	81	15	82	10		
95C	SEC PREMIUM PHOTO	INITIAL	50	1.27	57	75	-2	75	359		
95C	SEC PREMIUM PHOTO	LF 100H	50	0.72	67	54	-5	54	355	23	43
95C	SEC PREMIUM PHOTO	OF 1PPM/24H	50	0.91	62	60	10	61	10	19	28
95C	HP PRINTING PAPER	INITIAL	100	1.3	49	69	4	69	3		
95C	HP PRINTING PAPER	INITIAL	50	1.06	55	65	-5	66	355		
95C	HP PRINTING PAPER	LF 100H	50	0.53	71	39	-5	39	352	31	50
95C	HP PRINTING PAPER	OF 1PPM/24H	50	1.05	56	65	-4	65	357	2	1
95C	HP PREMIUM PLUS MKII	INITIAL	100	2.36	48	83	14	84	10		
95C	HP PREMIUM PLUS MKII	INITIAL	50	1.56	54	79	-2	79	358		
95C	HP PREMIUM PLUS MKII	LF 100H	50	0.91	63	62	-6	62	354	20	42
95C	HP PREMIUM PLUS MKII	OF 1PPM/24H	50	1.56	55	79	-2	79	359	0	0
95C	HR 2	INITIAL	100	1.79	50	77	24	81	17		
95C	HR 2	INITIAL	50	1.11	59	69	7	69	6		
95C	HR 2	LF 100H	50	0.61	70	47	-1	47	359	26	45
95C	HR 2	OF 1PPM/24H	50	1.00	61	64	12	66	10	7	10
95B	PR101 MKII	INITIAL	100	2.1	49	83	12	84	8		
95B	PR101 MKII	INITIAL	50	1.49	56	80	-7	81	355		
95B	PR101 MKII	LF 100H	50	0.87	66	63	-11	64	351	20	42
95B	PR101 MKII	OF 1PPM/24H	50	1.00	63	68	-7	68	354	14	33
95B	PRINTASIA PHOTO	INITIAL	100	2.24	45	82	7	82	5		
95B	PRINTASIA PHOTO	INITIAL	50	1.54	52	78	-8	79	354		
95B	PRINTASIA PHOTO	LF 100H	50	0.8	64	56	-10	57	349	26	48
95B	PRINTASIA PHOTO	OF 1PPM/24H	50	1.51	52	78	-8	78	354	0	2
95B	ILFORD INSTANT DRY	INITIAL	100	1.96	50	81	20	83	14		
95B	ILFORD INSTANT DRY	INITIAL	50	1.4	57	77	1	77	1		
95B	ILFORD INSTANT DRY	LF 100H	50	0.85	67	63	-10	63	351	21	39
95B	ILFORD INSTANT DRY	OF 1PPM/24H	50	1.14	60	71	5	71	4	8	19
95B	SEC PREMIUM PHOTO	INITIAL	100	2.03	50	82	15	83	11		

95B	SEC PREMIUM PHOTO	INITIAL	50	1.29	58	76	-2	76	358		
95B	SEC PREMIUM PHOTO	LF 100H	50	0.68	69	52	-6	52	353	26	47
95B	SEC PREMIUM PHOTO	OF 1PPM/24H	50	0.91	63	61	10	62	9	19	29
95B	HP PRINTING PAPER	INITIAL	100	1.29	50	69	4	69	4		
95B	HP PRINTING PAPER	INITIAL	50	1.04	56	65	-5	65	356		
95B	HP PRINTING PAPER	LF 100H	50	0.48	74	35	-5	36	352	34	54
95B	HP PRINTING PAPER	OF 1PPM/24H	50	1.03	57	65	-4	65	357	1	1
95B	HP PREMIUM PLUS MKII	INITIAL	100	2.33	48	82	16	84	11		
95B	HP PREMIUM PLUS MKII	INITIAL	50	1.52	55	79	-1	79	359		
95B	HP PREMIUM PLUS MKII	LF 100H	50	0.89	63	61	-6	62	355	20	41
95B	HP PREMIUM PLUS MKII	OF 1PPM/24H	50	1.54	55	79	-1	79	359	0	-1
95B	HR 2	INITIAL	100	1.65	51	76	28	81	20		
95B	HR 2	INITIAL	50	1.03	61	67	10	67	9		
95B	HR 2	LF 100H	50	0.51	74	40	-2	40	357	32	50
95B	HR 2	OF 1PPM/24H	50	0.96	62	63	13	65	12	5	7
95E	PR101 MKII	INITIAL	100	2.1	48	82	9	83	7		
95E	PR101 MKII	INITIAL	50	1.48	55	80	-9	80	354		
95E	PR101 MKII	LF 100H	50	0.73	68	56	-9	57	351	27	51
95E	PR101 MKII	OF 1PPM/24H	50	0.97	63	66	-7	67	354	16	34
95E	PRINTASIA PHOTO	INITIAL	100	2.25	44	81	5	81	4		
95E	PRINTASIA PHOTO	INITIAL	50	1.56	51	78	-10	79	353		
95E	PRINTASIA PHOTO	LF 100H	50	0.8	63	54	-9	55	351	26	49
95E	PRINTASIA PHOTO	OF 1PPM/24H	50	1.52	51	77	-10	78	353	1	3
95E	ILFORD INSTANT DRY	INITIAL	100	1.99	48	80	17	82	12		
95E	ILFORD INSTANT DRY	INITIAL	50	1.43	56	78	-2	78	359		
95E	ILFORD INSTANT DRY	LF 100H	50	0.81	66	59	-8	60	352	22	43
95E	ILFORD INSTANT DRY	OF 1PPM/24H	50	1.15	59	71	3	71	2	9	20
95E	SEC PREMIUM PHOTO	INITIAL	100	2.02	47	80	8	81	6		
95E	SEC PREMIUM PHOTO	INITIAL	50	1.32	55	75	-8	75	354		
95E	SEC PREMIUM PHOTO	LF 100H	50	0.66	69	49	-4	49	355	30	50
95E	SEC PREMIUM PHOTO	OF 1PPM/24H	50	0.94	61	61	5	61	4	20	29
95E	HP PRINTING PAPER	INITIAL	100	1.29	49	67	1	67	1		
95E	HP PRINTING PAPER	INITIAL	50	1.07	55	65	-7	65	354		
95E	HP PRINTING PAPER	LF 100H	50	0.54	70	37	-4	37	354	32	50
95E	HP PRINTING PAPER	OF 1PPM/24H	50	1.05	55	64	-6	65	354	1	2
95E	HP PREMIUM PLUS MKII	INITIAL	100	2.35	47	82	12	83	8		
95E	HP PREMIUM PLUS MKII	INITIAL	50	1.55	54	79	-5	79	357		
95E	HP PREMIUM PLUS MKII	LF 100H	50	0.9	62	60	-5	60	355	21	42

95E	HP PREMIUM PLUS MKII	OF 1PPM/24H	50	1.56	54	79	-4	79	357	1	-1
95E	HR 2	INITIAL	100	1.87	48	79	16	80	12		
95E	HR 2	INITIAL	50	1.18	57	71	1	71	1		
95E	HR 2	LF 100H	50	0.47	75	36	-2	36	357	39	60
95E	HR 2	OF 1PPM/24H	50	1.08	59	67	5	67	4	6	8
CRI	PR101 MKII	INITIAL	100	2.11	48	84	-5	84	357		
CRI	PR101 MKII	INITIAL	50	1.41	57	78	-17	80	348		
CRI	PR101 MKII	LF 100H	50	0.71	70	54	-8	54	352	29	50
CRI	PR101 MKII	OF 1PPM/24H	50	1.04	62	68	-12	69	350	13	26
CRI	PRINTASIA PHOTO	INITIAL	100	2.13	45	81	-5	81	356		
CRI	PRINTASIA PHOTO	INITIAL	50	1.4	53	75	-17	77	347		
CRI	PRINTASIA PHOTO	LF 100H	50	0.65	67	45	-9	45	349	35	54
CRI	PRINTASIA PHOTO	OF 1PPM/24H	50	1.40	53	75	-16	77	348	1	0
CRI	ILFORD INSTANT DRY	INITIAL	100	1.98	47	82	-4	82	357		
CRI	ILFORD INSTANT DRY	INITIAL	50	1.4	56	77	-17	79	347		
CRI	ILFORD INSTANT DRY	LF 100H	50	0.82	68	58	-11	59	350	23	41
CRI	ILFORD INSTANT DRY	OF 1PPM/24H	50	1.23	58	73	-12	74	350	7	12
CRI	SEC PREMIUM PHOTO	INITIAL	100	2.1	48	84	-8	84	355		
CRI	SEC PREMIUM PHOTO	INITIAL	50	1.4	56	78	-20	80	346		
CRI	SEC PREMIUM PHOTO	LF 100H	50	0.85	67	59	-15	61	345	22	39
CRI	SEC PREMIUM PHOTO	OF 1PPM/24H	50	1.19	59	71	-13	72	350	10	15
CRI	HP PRINTING PAPER	INITIAL	100	1.23	50	66	-8	66	353		
CRI	HP PRINTING PAPER	INITIAL	50	1.01	56	63	-16	65	346		
CRI	HP PRINTING PAPER	LF 100H	50	0.34	80	24	-2	25	355	47	66
CRI	HP PRINTING PAPER	OF 1PPM/24H	50	1.00	56	62	-15	64	346	1	1
CRI	HP PREMIUM PLUS MKII	INITIAL	100	2.18	46	82	-2	82	359		
CRI	HP PREMIUM PLUS MKII	INITIAL	50	1.46	54	77	-14	78	350		
CRI	HP PREMIUM PLUS MKII	LF 100H	50	0.91	62	59	-11	60	349	20	38
CRI	HP PREMIUM PLUS MKII	OF 1PPM/24H	50	1.44	55	77	-13	78	350	1	1
CRI	HR 2	INITIAL	100	2.08	47	83	-7	83	355		
CRI	HR 2	INITIAL	50	1.4	56	78	-19	80	346		
CRI	HR 2	LF 100H	50	0.67	72	50	-9	51	349	34	52
CRI	HR 2	OF 1PPM/24H	50	1.24	58	73	-14	74	349	8	11

NMR data for 139

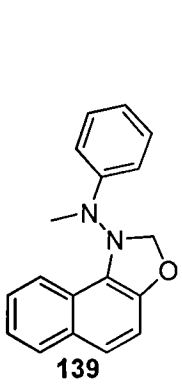

139

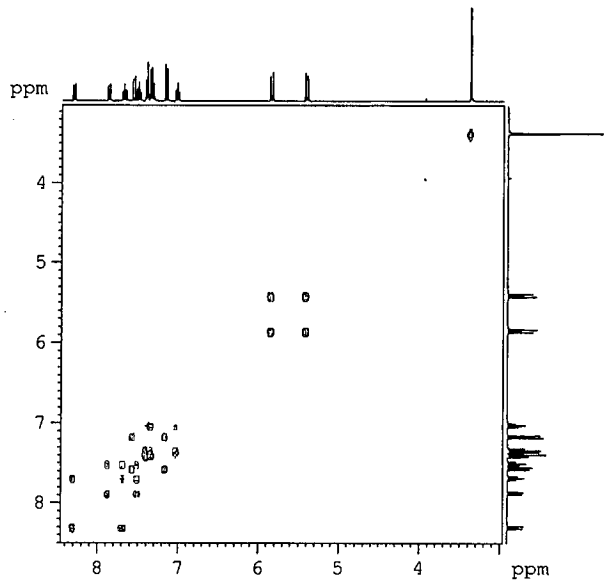

[^{1}H, ^{1}H] COSY

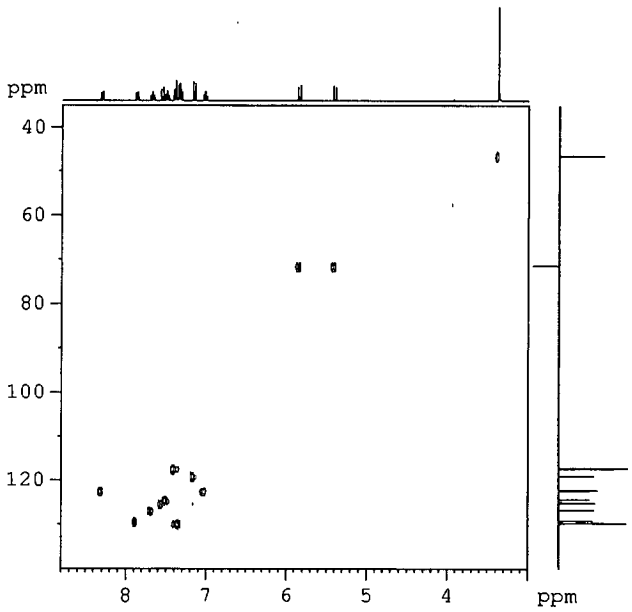

[^{1}H, ^{13}C] HSQC

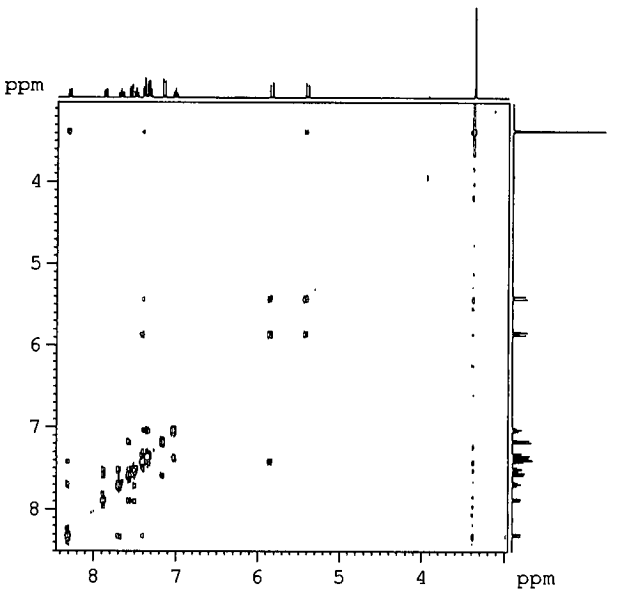

[^{1}H, ^{1}H] NOESY

7.3 Ozone Generation

Ozone was generated using an Argentox GLX ozone generator. This generates ozone from a stream of air or pure oxygen in an electric spark chamber. Ozone concentration can be controlled by adjusting the input gas flow-rate or the spark voltage. Pure oxygen was used in all ozonolysis experiments as the use of air can also lead to the generation of reactive NO_x gases, which could also react with azo dyes.

Ozone was generated at a voltage of 135 V, with a current of 0.22 A. The inlet oxygen flow rate was ~240 cm^3 min^{-1}, measured and controlled using a using a Platon A1HD rotameter.

7.4 Ozone Reactor Design

Commercial gas reactors are available; however they are expensive and often overly complicated for the requirements of this project. As a proof-of-concept experiment a simple ozone reaction vessel, such as has been used previously in the Hulme group, was used. This consisted of a two-necked flask in which a thermometer adaptor fitted with a Pasteur pipette was placed in the side-arm (Figure 7.1 A). The tip of the pipette was drawn out in a flame in order to produce a fine capillary. This allowed a fine stream of bubbles to be passed into the ozonolysis chamber. Although this design was effective, the capillary was fragile and the solution required external stirring in order to give satisfactory mixing.

A modified cold-trap gave a more robust system (Figure 7.1 B). The central finger was fitted with a porosity 3 glass frit, giving a fine stream of bubbles through the ozonolysis solution. External stirring was still required, however.

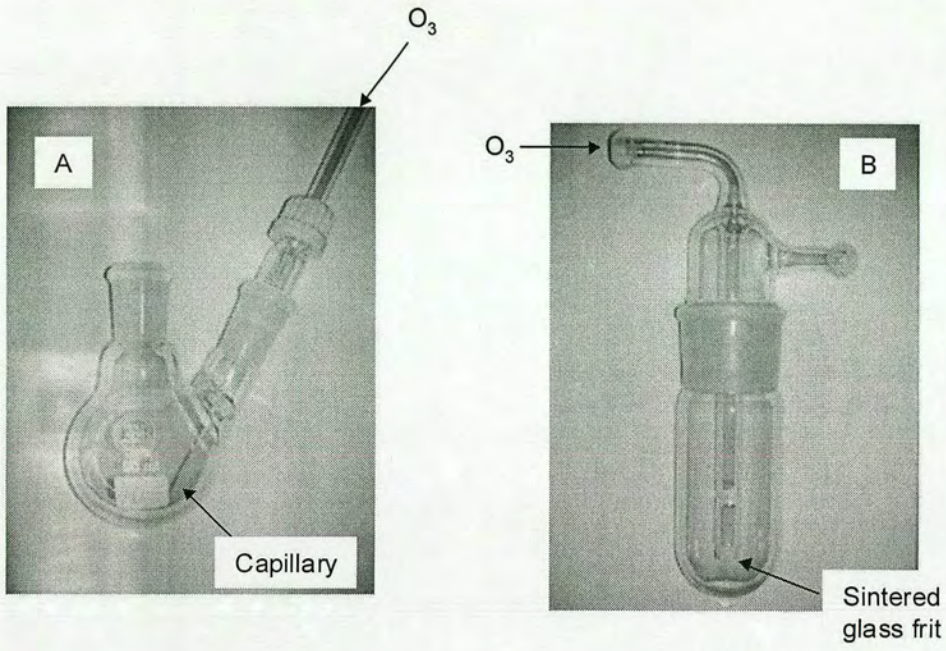

Figure 7.1

The final design used a glass column fitted with a sintered glass frit at the base. Ozone is passed through the bottom of the chamber *via* a sidearm. The solution is prevented from passing through the frit when there is no ozone flow by a tap in the arm (Figure 7.2). This design allows a large volume of ozone to pass through the solution, the agitation of the gas negates the need to provide external mixing.

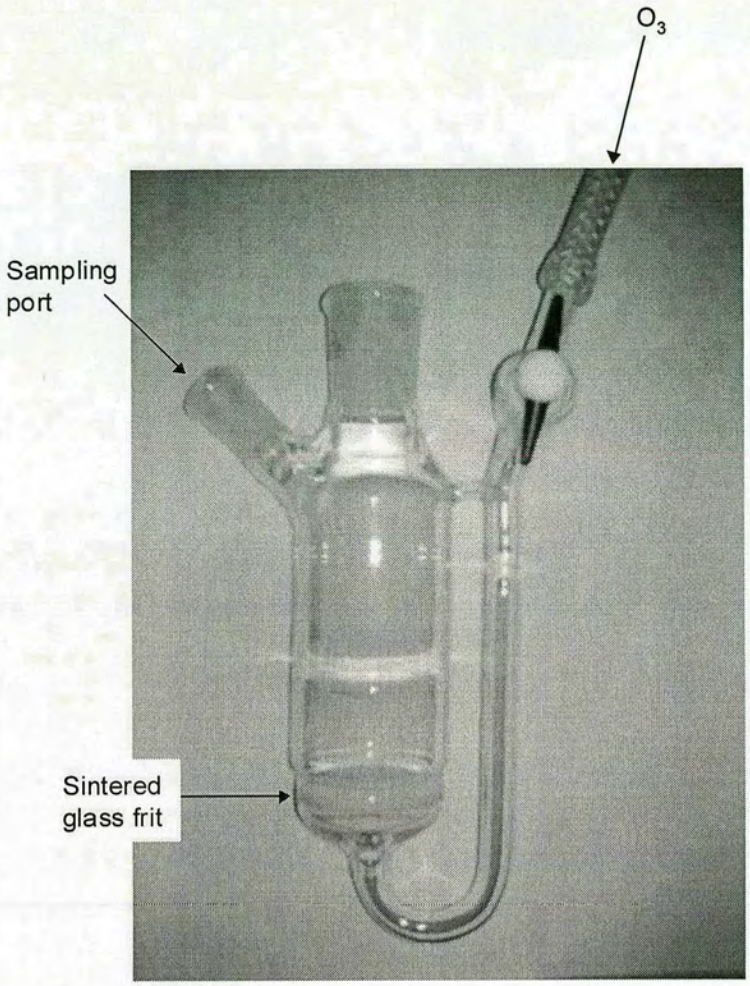

Figure 7.2

7.5 ESI-MS conditions

Dye analysis, ESI-

Performed on Masslynx Platform instrument

Sample introduced by infusion pump in 0.01 % aqueous TFA.

Capillary Voltage: 2.70 kV

Cone Voltage: 60 - 75 kV

Source Block Temperature: 140 °C

Desolvation Temperature: 140 °C

Hydrazide analysis, ESI+

Performed on Masslynx Platform instrument

Sample introduced by HPLC injection, 1:1:1 MeOH:MeCN:H_2O

Capillary Voltage: 2.70 kV

Cone Voltage: 25 kV

Source Block Temperature: 110 °C

Desolvation Temperature: 110 °C

7.6 Variable Temperature NMR

Variable temperature NMR experiments were performed on a Bruker DPX360 spectrometer. Sub-ambient temperatures were achieved by cooling the probe with the burn-off from a liquid nitrogen Dewar, heating was *via* the internal heating element of the spectrometer. NMR spectra were obtained over the temperature range + 213 K to + 333 K in 10 K intervals. Around the coalescence temperature spectra were recorded at 2 K intervals. The measured temperature was corrected according to a previously obtained temperature profile chart. The probe was re-tuned at each temperature recorded; otherwise poorly resolved spectra were obtained

1 L. Rayleigh, *Proc. London Math. Soc.*, 1878, **4**, 13.

2 P. Gregory, *Proc. RMS*, 2001, **36**, 232.

3 P. Gregory, *Chem. Br.*, 2000, **36**, 39.

4 H. P. Le, *J. Imag. Sci. Tech.*, 1998, **42**, 49.

5 R. Elmquist, US Patent No. 2566443, 1951.

6 R. G. Sweet, *Rev. Sci. Instrum.*, 1965, **36**, 131.

7 C. H. Hertz, US Patent No. 3416153, 1968.

8 S. I. Zoltan, US Patent No. 3683212, 1972.

9 P. Gregory in High Technology Applications of Organic Colourants, p. 197, Plenum Press, New York, 1991.

10 I. Endo, Y. Sato, S. Saito, T. Nagakari, and S. Ohno, GB Patent No. 2007162, 1979.

11 R. W. Kenyon in Chemistry and Technology of Printing and Imaging Systems, p. 151, ed. P. Gregory, Blackie, Glasgow, 1996.

12 W. R. Cox, T. Chen, D. J. Hayes, and M. E. Grove, proceedings of SPIE MOEMS & Miniaturized Systems, San Francisco, 2001.

13 M. B. Lyne, *J. Imaging Technol.*, 1986, **12**, 80.

14 R. W. Kenyon in Chemistry and Technology of Printing and Imaging Systems, p. 158, ed. P. Gregory, Blackie, Glasgow, 1996.

15 M. T. Nowak, European Patent No. 206286, 1986.

16 T. M. Cooke, A. C. R. Lin, and A. R. Merrit, US Patent No. 4484948, 1984.

17 T. M. Cooke, A. C. R. Lin, and A. R. Merrit, European Patent No. 181198, 1986.

18 R. M. Christie, in Colour Chemistry 'Chapter 10: Functional or "High Technology" Dyes and Pigments', RSC, Cambridge, 2001.

19 K. Suzuki, proceedings of the SPSE Third International Conference on Advances in Non-Impact Printing Technology, San Francisco, 1986.

20 P. F. Gordon and P. Gregory, in Organic Chemistry in Colour, 'Chapter 2: Classification and Synthesis of Dyes', Springer-Verlag, Berlin, 1987.

21 R. M. Christie, in Colour Chemistry, 'Chapter 2: The Physical and Chemical Basis of Colour', RSC, Cambridge, 2001.

22 T. Zincke and H. Bindewald, *Chem. Ber.*, 1884, **17**, 3032.

23 R. Kuhn and F. Bär, *Annalen.*, 1935, 143.

24 S. Kishimoto, S. Kitahara, O. Manabe, and H. Hiyama, *J. Org. Chem.*, 1978, **43**, 3882.

25 O. N. Witt, *Chem. Ber*, 1876, **9**, 522.

26 W. Dilthey and R. Wizinger, *J. Prakt. Chem.*, 1928, **118**, 321.

27 K. A. Bello and J. Griffiths, *J. Chem. Soc., Chem. Comm.*, 1986, 1639.

28 T. A. Baker and G. I. Gellene, *J. Comp. Chem.*, 2000, **21**, 943.

29 T. Hihara, Y. Okada, and Z. Morita, *Dyes Pigments*, 2004, **61**, 199.

30 B. Li, W. Miao, Q. Meng, and L. Cheng, *Dyes Pigments*, 2004, **62**, 299.

31 N. Ohta, *J. Appl. Photogr. Engr.*, 1976, **2**, 75.

32 X-Rite Inc., *A Guide to Understanding Colour Communication*, 2000.

33 Gretag Macbeth, *Fundamentals of Colour and Appearance*, 1998.

34 X-Rite Inc., *The Colour Guide and Glossary*, 1998.

35 P. F. Gordon and P. Gregory, in Organic Chemistry in Colour, 'Chapter 6: Applications and Fastness Properties of Dyes', Springer-Verlag, Berlin, 1987.

36 G. S. Egerton and A. G. Morgan, *J. Soc. Dyers Colour.*, 1970, **86**, 242.

37 D. Brownlie, *J. Soc. Dyers Colour.*, 1902, **18**, 288.

38 Z. Csepregi, P. Aranyosi, I. Rusznak, L. Toke, J. Frankl, and A. Vig, *Dyes Pigments*, 1998, **37**, 1.

39 J. S. P. Blumberger, *Chem. Weekblad*, 1931, **28**, 310.

40 N. S. Allen, *Rev. Prog. Color.*, 1987, **17**, 61.

41 W. Meuly, *Helv. Chim. Act.*, 1923, **6**, 931.

42 R. L. M. Allen, in Studies in Modern Chemistry: Colour Chemistry, 'Chapter 2', Nelson, London, 1971.

43 H. Oda, *Dyes Pigments*, 2001, **48**, 151.

44 W. W. Lebensaft and V. S. Salvin, *Tex. Chem. Color.*, 1972, **4**.

45 V. S. Salvin, *Tex. Chem. Color.*, 1974, **6**.

46 J. C. Haylock and J. L. Rush, *Tex. Res. J.*, 1976.

47 NEGTAP, *Transboundary Air Pollution*, 2001.

48 SEPA, *State of the Environment Report*, 1999.

49 Personal communication, Dr Paul Wight, Avecia (Blackley), 2001.

50 P. R. Gogate and A. B. Pandit, *Adv. Environ. Res.*, 2004, **8**, 501.

51 M. Matsui, *Dyes Pigments*, 1984, **5**, 321.

52 A. Schöfer and A. Schwan, *J. Prakt. Chem*, 1850, **51**, 185.

53 H. Paulsen and D. Stoye, in The Chemistry of Amides, 'Chapter 10: The Chemistry of Hydrazides', ed. S. Patai, Interscience, London, 1970.

54 W. Baker, C. N. Haksar, and J. F. W. McOmie, *J. Chem. Soc.*, 1950, 170.

55 J. Gante, *Synthesis*, 1989, **6**, 405.

56 F. Stieber, U. Grether, and H. Waldmann, *Chem.-Eur. J.*, 2003, **9**, 3270.

57 U. Kraatz, W. Kraemer, W. Adersch, A. Turberg, and N. Mencke, German Patent No. DE19530079, 1997.

58 R. Skoda-Foldes, Z. Szarka, L. Kollar, Z. Dinya, J. Horvath, and Z. Tuba, *J. Org. Chem.*, 1999, **64**, 2134.

59 S. G. Kücükgüzel, S. Rollas, I. Kücükgüzel, and M. Kiraz, *Eur. J. Med. Chem.*, 1999, **34**, 1093.

60 E. Licandro and D. Perdicchia, *Eur. J. Org. Chem.*, 2004, 665.

61 P. A. S. Smith, *Org. Reactions*, 1946, **3**, 366.

62 E. C. Kornfeld, E. J. Fornefeld, G. B. Kline, M. J. Mann, D. E. Morrison, R. G. Jones, and R. B. Woodward, *J. Am. Chem. Soc.*, 1956, **78**, 3087.

63 O. L. Salerni, B. E. Smart, A. Post, and C. C. Cheng, *J. Chem. Soc. C.*, 1968, 1399.

64 R. L. Hinman, *J. Am. Chem. Soc.*, 1956, **78**, 2463.

65 R. L. Hinman and D. Fulton, *J. Am. Chem. Soc.*, 1958, **80**, 1895.

66 A. Benderly and S. Stavchansky, *Tetrahedron Lett.*, 1988, **29**, 739.

67 R. F. Smith, *J. Org. Chem.*, 1968, **33**, 851.

68 R. L. Hinman, *J. Am. Chem. Soc.*, 1956, **78**, 1645.

69 S. G. Cohen and J. Nicholson, *J. Org. Chem.*, 1965, **30**, 1162.

70 P. Hope and L. A. Wiles, *J. Chem. Soc. C.*, 1967, 2636.

71 W. J. Theuer and J. A. Moore, *J. Org. Chem.*, 1964, **29**, 3734.

72 F. E. Condon, *J. Org. Chem.*, 1972, **37**, 3608.

73 A. A. Khatib and H. H. Sisler, *Inorg. Chem.*, 1990, **29**, 309.

74 D. Perdicchia, E. Licandro, S. Maiorana, C. Baldoli, and C. Giannini, *Tetrahedron*, 2003, **59**, 7733.

75 M. A. Herrero, J. Wannberg, and M. Larhed, *Synlett*, 2004, **13**, 2335.

76 M. R. Netherton and G. C. Fu, *Org. Lett.*, 2001, **3**, 4295.

77 W. A. Herrmann, V. P. W. Bohm, and C.-P. Reisinger, *J. Organometallic Chem.*, 1999, **576**, 23.

78 A. Basha, M. Lipton, and S. M. Weinreb, *Org. Synth.*, 1979, **59**, 49.

79 J. I. Levin, E. Turos, and S. M. Weinreb, *Synth. Commun.*, 1982, **12**, 989.

80 A. Basha, M. Lipton, and S. M. Weinreb, *Tetrahedron Lett.*, 1977, **48**, 4171.

81 F. E. Condon, *J. Org. Chem.*, 1972, **37**, 3615.

82 H. Dyker, J. Scherkenbeck, D. Gondol, A. Goehrt, and A. Harder, *J. Org. Chem.*, 2001, **66**, 3760.

83 Curtius and Hartmann, *Chem. Ber*, 1912, **45**, 1055.

84 J. Buckingham, *Quart. Rev.*, 1969, **63**, 37.

85 S. Hammerum, *Tetrahedron Lett.*, 1972, **10**, 949.

86 R. J. W. Cremlyn, B. B. Dewhurst, and D. H. Wakeford, *J. Chem. Soc. C.*, 1971, 3011.

87 J. L. McVeigh and J. D. Rose, *J. Chem. Soc.*, 1945, 713.

88 W. G. Finnegan, R. A. Henry, and G. B. L. Smith, *J. Am. Chem. Soc.*, 1952, **74**, 2981.

89 R. Phillips and J. F. Williams, *J. Am. Chem. Soc.*, 1928, **50**, 2465.

90 W. F. Whitmore, A. J. Revukas, and G. B. L. Smith, *J. Am. Chem. Soc.*, 1935, **57**, 706.

91 N. J. Leonard and J. H. Boyer, *J. Org. Chem.*, 1950, **15**, 42.

92 P. C. Guha and S. C. De, *J. Chem. Soc.*, 1924, **125**, 1217.

93 C. V. Romana and A. Vasella, *Helv. Chim. Act.*, 2000, **83**, 1599.

94 M. B. Hursthouse, M. E. Light, and R. C. F. Jone, Cambridge Crystallographic Database, 2003.

95 R. L. Augustine, in Heterogeneous Catalysis for the Synthetic Chemist, 'Chapter 17: Hydrogenation IV: Aromatic Compounds', Marcel-Dekker, New York, 1995.

96 S. Patai, in The Chemistry of the C=N Bond, Interscience, London, 1970.

97 S. Kobayashi and H. Ishitani, *Chem. Rev.*, 1999, **99**, 1069.

98 S. A. Galema, *Chem. Soc. Rev.*, 1997, **26**, 233.

99 H. H. Fox, *J. Org. Chem.*, 1958, **23**, 468.

100 K. Manabe, H. Oyamada, K. Sugita, and S. Kobayashi, *J. Org. Chem.*, 1999, **64**, 8054.

101 A. D. Bain, *Progress in Nuclear Magnetic Resonance Spectroscopy*, 2003, **43**, 63.

102 J. B. Lambert, H. F. Shurvell, D. A. Lightner, and D. A. Cooks, in Organic Structural Spectroscopy, Prentice Hall, New Jersey, 1998.

103 H. Shanan-Atidi and K. H. Bar-Eli, *J. Phys. Chem.*, 1970, **74**, 961.

104 W. E. Stewart and T. H. Siddall, *Chem. Rev.*, 1970, **70**, 517.

105 J. Riand, M. T. Chenon, and N. Lumbrosobader, *J. Chem. Soc., Perkin Trans. 2*, 1987, **11**, 1551.

106 ICI, UK Patent No. 797946, 1958.

107 ICI, UK Patent No. 798121, 1958.

108 W. E. Stephen, *Chimia*, 1965, **19**, 261.

109 Personal Communication, C. Boyle, Avecia (Grangemouth), 2001.

110 With thanks to Dr. L. Monahan, Avecia (Grangemouth), 2001.

111 Personal Communication, C. Boyle, Avecia (Grangemouth), 2001.

112 Personal Communication, Dr. P. Wight, Avecia (Blackley), 2001.

113 P. Bamfield, in Chromic Phenomena - Technological Applications of Colour Chemistry, RSC, Cambridge, 2001.

114 With thanks to Dr. P. Wight, Avecia (Blackley), 2001.

115 A. B. Baylis and M. E. D. Hillman, German Patent No. 2155113, 1972.

116 D. Basavaiah, A. J. Rao, and T. Satyanarayana, *Chem. Rev.*, 2003, **103**, 811.

117 H. Wilhelm, proceedings of IS&T 12th International Symposium on Photofinishing Technology, p. 32, 2002.

118 R. Steiger and P.-A. Brugger, proceedings of IS&T NIP14: International Conference on Digital Printing Technologies, 1998, p. 114.

119 R. Fernandez, A. Ferrete, J. M. Llera, A. Magriz, E. Martin-Zamora, E. Diez, and J. M. Lassaletta, *Chem.-Eur. J.*, 2004, **10**, 737.

120 P. S. Bailey, in Ozonation in Organic Chemistry 2, 'Chapter VII: Ozonation of Nucleophiles', Academic Press, London, 1982.

121 P. S. Bailey, in Ozonation in Organic Chemistry 2, 'Introduction', Academic Press, London, 1982.

122 A. Nemes, I. Fabian, and G. Gordon, *Ozone-Sci. Eng.*, 2000, **22**, 287.

123 Y. Ku, W. J. Su, and Y. S. Shen, *Ind. Eng. Chem. Res.*, 1996, **35**, 3369.

124 H. Y. Shu and C. R. Huang, *Chemosphere*, 1995, **31**, 3813.

125 W. Chu and C. W. Ma, *Wat. Res.*, 2000, **34**, 3153.

126 F. M. Saunders, J. P. Gould, and C. R. Southerland, *Wat. Res.*, 1983, **17**, 1407.

127 P. Ball and C. H. Nicholls, *Dyes Pigments*, 1982, **3**, 5.

128 D. Hadzi, *J. Chem. Soc.*, 1956, 2143.

129 J. N. Ospenson, *Acta Chem. Scand.*, 1951, **5**, 491.

130 M. Matsui, Y. Iwata, T. Kato, and K. Shibata, *Dyes Pigments*, 1988, **9**, 109.

131 R. E. Miller, *J. Org. Chem.*, 1961, **26**, 2327.

132 P. S. Bailey, in Ozonation in Organic Chemistry 2, 'Chapter VIII: Ozonation of Hetero Multiple Bonds', Academic Press, London, 1982.

133 M. Matsui, K. Kobayashi, K. Shibata, and Y. Takase, *J. Soc. Dyers Colour.*, 1981, **97**, 210.

134 T. Veysoglu, L. A. Mitscher, and J. K. Swayze, *Synthesis*, 1980, 807.

135 M. Matsui, N. Midzui, K. Shibata, and H. Muramatsu, *Dyes Pigments*, 1992, **20**, 67.

136 C. G. Namboodri, W. S. Perkins, and W. K. Walsh, *Am. Dyest. Rep.*, 1994, **83**, 17.

137 C. G. Namboodri, W. S. Perkins, and W. K. Walsh, *Am. Dyest. Rep.*, 1994, **83**, 17.

138 M. Matsui, A. Konda, and K. Shibata, *Bull. Chem. Soc. Jpn.*, 1985, **58**, 2829.

139 A. Burawoy, A. G. Salem, and A. R. Thompson, *J. Chem. Soc.*, 1952, 4793.

140 M. Matsui, S. Kawamura, K. Shibata, H. Muramatsu, M. Mitani, H. Sawada, and M. Nakayama, *J. Fluor. Chem.*, 1992, **57**, 209.

141 A. Burawoy and A. R. Thompson, *J. Chem. Soc.*, 1953, 1443.

142 J. Kelemen, S. Moss, H. Sauter, and T. Winkler, *Dyes Pigments*, 1982, **3**, 27.

143 J. Griffiths, *J. Soc. Dyers Colour.*, 1972, **88**, 106.

144 E. Hofer and H. Uffmann, *Tetrahedron Lett.*, 1971, **35**, 3241.

145 L. Antonov and S. Stoyanov, *Dyes Pigments*, 1995, **28**, 31.

146 L. Antonov, S. Stoyanov, and T. Stoyanova, *Dyes Pigments*, 1995, **27**, 133.

147 S. Stoyanov and L. Antonov, *Dyes Pigments*, 1989, **10**, 33.

148 M. Koch, A. Yediler, D. Lienert, G. Insel, and A. Kettrup, *Chemosphere*, 2002, **46**, 109.

149 S. Liakou, M. Kornaros, and G. Lyberatos, *Water Sci. Technol.*, 1997, **36**, 155.

150 S. G. de Moraes, R. S. Freire, and N. Duran, *Chemosphere*, 2000, **40**, 369.

151 J. L. Sotelo, F. J. Beltran, J. Beltranheredia, and J. M. Encinar, *Ozone-Sci. Eng.*, 1989, **11**, 391.

152 R. E. Erickson, P. S. Bailey, A. H. Riebel, and A. M. Reader, *Annalen*, 1962, **653**, 129.

153 P. Griess, *J. Chem. Soc.*, 1867, 36.

154 C. Liebermann, *Chem. Ber.*, 1883, 2858.

155 J. T. Hewitt and H. A. Phillips, *J. Chem. Soc.*, 1901, **79**, 160.

156 F. Charrier, *Gazz. Chim. Ital.*, 1912, **2**, 123.

157 A. I. Vogel, in Textbook of Practical Organic Chemistry, ed. S. F. Furniss, A. J. Hannaford, P. W. G. Smith, and A. R. Tatchell, 5th Ed. p. 941, Longman Group, Harlow, 1989.

158 L. A. Fedorov, *Usp. Khim.*, 1988, **57**, 1643.

159 J. Smith, *J. Chem. Soc.*, 1908, **93**, 845.

160 Y. A. Ibrahim, N. A. Al-Awadi, and K. Kual, *Tetrahedron*, 2003, **59**, 5425.

161 G. R. Hodges, J. R. L. Smith, and J. Oakes, *J. Chem. Soc., Perkin Trans. 2*, 1998, **3**, 617.

162 L. Abate, M. L. Longo, E. Maccarone, and M. Torre, *J. Chem. Soc.,Perkin Trans. 2*, 1980, **4**, 628.

163 H. Zollinger, in Azo and Diazo Chemistry, 1st Ed., p. 322, Interscience, New York, 1961.

164 N. V. Sidgewick, in The Organic Chemistry of Nitrogen, 3rd Ed., p. 980, Clarendon Press, Oxford, 1966.

165 R. G. Pearson, *J. Am. Chem. Soc.*, 1963, **85**, 3533.

166 S. Woodward, *Tetrahedron*, 2002, **58**, 1017.

167 J. E. Baldwin, *J. Chem. Soc., Chem. Comm.*, 1976, **18**, 734.

168 T. Purdie and J. C. Irvine, *J. Chem. Soc.*, 1903, **83**, 1021.

169 L. Antonov, S. Kawauchi, M. Satoh, and J. Komiyama, *Dyes Pigments*, 1998, **38**, 157.

170 E. Bergmann and A. Weizmann, *J. Chem. Soc., T. Faraday Soc.*, 1936, **32**, 1327.

171 Personal Communication, Dr. P. Wight and C. Foster, Avecia (Blackley), 2003.

172 Balasubramaniyan V., *Chem. Rev.*, 1966, **66**, 567.

173 I. D. Biggs and J. M. Tedder, *Tetrahedron*, 1978, **34**, 1377.

174 A. A. Kutyrev, *Tetrahedron*, 1991, **47**, 8043.

175 O. A. Garibyan, G. U. Palikyan, and S. O. Badanyan, *Z. Org. Khim.*, 2000, **36**, 1462.

176 B. E. Zaitsev, E. D. Sycheva, G. V. Sheban, E. S. Lisitsyna, T. A. Mikhailova, G. N. Rodionova, and K. M. Dyumaev, *Z. Org. Khim.*, 1987, **23**, 1743.

177 M. H. Davey, V. Y. Lee, R. D. Miller, and T. J. Marks, *J. Org. Chem.*, 1999, **64**, 4976.

178 J. H. Boyer, in The Chemistry of the Nitro and Nitroso Groups, Part 1, ed. H. Feuer, p. 278, Interscience, New York, 1969.

179 E. Toja, D. Selva, and P. Schiatti, *J. Med. Chem.*, 1984, **27**, 610.

180 P. Bortolus, S. Monti, A. Albini, E. Fasani, and S. Pietra, *J. Org. Chem.*, 1989, **54**, 534.

181 K. J. Morgan, *J. Chem. Soc.*, 1961, 2151.

182 G. M. Badger and R. G. Buttery, *J. Chem. Soc.*, 1956, 614.

183 W. McPherson, *Am. Chem. J.*, 1899, **22**, 376.

184 Millefiori.S, Zuccarel.F, Millefiori.A, and F. Guerrera, *Tetrahedron*, 1974, **30**, 735.

185 S. A. A. Osman, A. A. Abdalla, and M. O. Alaib, *J. Pharm. Sci.*, 1983, **72**, 63.

186 S. Ledakowicz, R. Maciejewska, J. Perkowski, and A. Bin, *Water Sci. Technol.*, 2001, **44**, 47.

187 C. Picard, A. Larbot, J. Sarrazin, P. Janknecht, and P. Wilderer, *Ann. Chim.-Sci. Mat.*, 2001, **26**, 13.

188 P. Janknecht, P. A. Wilderer, C. Picard, and A. Larbot, *Sep. Purif. Technol.*, 2001, **25**, 341.

189 Sigma Aldrich, catalogue number Z21,445.

190 L. Forni, D. Bahnemann, and E. J. Hart, *J. Phys. Chem.*, 1982, **86**, 255.

191 E. J. Hart, K. Sehested, and J. Holcman, *Analytical Chemistry*, 1983, **55**, 46.

192 M. L. Kilpatrick and C. D. Herrick, *J. Am. Chem. Soc.*, 1965, **78**, 1784.

193 A. R. McCarthy, W. D. Ollis, and C. A. Ramsden, *J. Chem. Soc., Perkin Trans. 1*, 1974, 627.

194 M. J. V. J. de Oliveira Baptista, *J. Chem. Soc., Perkin Trans. 1*, 1977, 1477.

195 T. V. Troepolinskaya, R. A. Sitdikov, Z. S. Titova, A. P. Stolyarov, and Y. P. Kitaev, *Bull. Acad. Sci. USSR Div. Chem. Sci (Engl. Trans.)*, 1980, **29**, 903.

196 J. L. Cavill, J. Peters, and N. Thomkinson, *Chem. Comm.*, 2003, **6**, 728.

197 Freifelder, *J. Org. Chem.*, 1961, **26**, 383.

198 B. T. Gillis and R. E. Kadunce, *J. Org. Chem.*, 1967, **32**, 91.

199 H. W. Heine, *J. Org. Chem.*, 1976, **41**, 3229.

200 I.O. Kalikhman, O.B. Bannikova, L.I. Volkova, R.G. Sultangareev, V.A. Lopyrev, *Bull. Acad. Sci. USSR Div. Chem. Sci. (Engl. Transl.)*, 1981, **6**, 1268.